AGRICULTURAL UNIVERSITY OF ATHENS
DEPARTMENT OF FOOD SCIENCE & HUMAN NUTRITION
LABORATORY OF FOOD MICROBIOLOGY & BIOTECHNOLOGY

PhD Dissertation

Implementation of rapid methods of analysis and model development in quality assessment of raw and processed poultry meat

Evgenia D. Spyrelli

Supervisor:
Efstathios Z. Panagou, Professor AUA

Members of Supervising Board:
Efstathios Z. Panagou, Professor AUA
George-John E. Nychas, Professor AUA
Kostas Koutsoumanis, Professor AUTh

ATHENS
2022

AGRICULTURAL UNIVERSITY OF ATHENS
DEPARTMENT OF FOOD SCIENCE & HUMAN NUTRITION
LABORATORY OF FOOD MICROBIOLOGY & BIOTECHNOLOGY

PhD Dissertation

Implementation of rapid methods of analysis and model development in quality assessment of raw and processed poultry meat

«Εφαρμογή σύγχρονων ταχέων αναλύσεων και ανάπτυξη μοντέλων εκτίμησης της αλλοίωσης νωπού και επεξεργασμένου κρέατος πουλερικών»

Evgenia D. Spyrelli

Thesis committee:
Efstathios Z. Panagou, Professor AUA
George-John E. Nychas, Professor AUA
Kostas Koutsoumanis, Professor AUTh
Christos Pappas, Associate Professor AUA
Vasilis Valdramidis, Associate Professor NKUA
Alexandra Lianou, Assistant Professor, University of Patras
Agapi Doulgeraki, Assistant Researcher ITAP, HAO– DEMETER

Implementation of rapid methods of analysis and model development in quality assessment of raw and processed poultry meat

Department of Food Science & Human Nutrition
Laboratory of Food Microbiology & Biotechnology

Abstract

Non-invasive rapid methods have been introduced over the years in the assessment of food quality and they have been well established in the food industry in the context of technological evolution as consumers' demands for high quality and safety foods constantly increases. In the present thesis, rapid spectroscopic and biomimetic sensors have been investigated for their potential to accurately assess quality in different poultry products (chicken breast and thigh fillets, chicken marinated souvlaki and chicken burger). Multispectral Imaging (MSI), Fourier Transform Infrared spectroscopy (FT-IR) and electronic nose (E-nose) were employed (individually and in combination) in tandem with multivariate data analysis for the assessment of the microbiological quality and the spoilage level in chicken samples, as well as in the determination of the "time from slaughter". For this purpose, different batches of chicken samples were subjected to storage experiments including both isothermal and dynamic temperature conditions and analyzed microbiologically to determine the population dynamics of the indigenous microbiota. In parallel, spectroscopic data were acquired through MSI and FT-IR instrumental analysis, whereas the volatile fingerprint of samples during storage was recorded by means of an E-nose. Regression and classification (linear and nonlinear) models assessing poultry meat quality were developed and validated with data from independent experiments (different batch/season of slaughter, dynamic temperature conditions of storage or different analysts). Moreover, ensemble methods and data fusion were performed to the existing data in an attempt to enhance the predictive performance of the developed models. Furthermore, the safety of poultry meat with special focus on *Campylobacter* spp. presence and survival in stored marinated chicken at refrigeration temperatures was explored via predictive modeling and molecular analysis.

In **chapter 2**, MSI analysis was implemented on an industrial scale in chicken products for the assessment of their quality. For this purpose, chicken breast fillets, thigh

fillets, marinated souvlaki and burger were analyzed microbiologically for the enumeration of TVCs and *Pseudomonas* spp., while MSI spectral data were acquired at the same time points as for microbiological analysis. Partial Least Squares Regression (PLS-R) models were developed based on MSI data for the determination of the "time from slaughter" parameter for each product type. Results showed that PLS-R models could predict accurately the time from slaughter in all products with the chicken thigh model providing the lowest RMSE value (0.160), followed by the chicken burger model (RMSE= 0.285).

In **chapter 3**, FT-IR and MSI spectroscopic methods were evaluated for their efficacy to assess spoilage on the surface of chicken breast fillets in tandem with multivariate data analysis. Briefly, stored samples of chicken breast fillets at isothermal conditions (0, 5, 10, 15 ^{o}C) were analyzed microbiologically for the enumeration of TVCs and *Pseudomonas* spp. and also by FT-IR and MSI sensors. Multivariate data analysis was performed via two software platforms (a commercial software and a publicly available developed platform) by applying several machine learning models for the estimation of TVCs and *Pseudomonas* spp. population of the surface of the samples. The performance of the obtained models was assessed by intra batch and independent batch testing. PLS-R models from the commercial software predicted TVCs with RMSE values of 1.359 and 1.029 log CFU/cm^2 for MSI and FT-IR analysis, respectively. Moreover, RMSE values for *Pseudomonas* spp. model were 1.574 log CFU/cm^2 for MSI data and 1.078 log CFU/cm^2 for FT-IR data. From the implementation of the in-house sorfML platform, ANN models developed with MSI data provided the lowest RMSE values (0.717 log CFU/cm^2) for intra-batch testing, while least-angle regression (lars) models developed with FT-IR data demonstrated RSME values of 0.904 and 0.851 log CFU/cm^2 in intra-batch and independent batch testing, respectively.

In **chapter 4**, FT-IR and MSI spectral data were employed in combination with machine learning classification models for the evaluation of spoilage in chicken breast fillets. In this context, chicken breast samples were subjected to storage experiments using eight isothermal (0, 5, 10, 15, 20, 25, 30, 35 ^{o}C) and two dynamic temperature profiles for up to 480 h. At pre-determined intervals, samples were analyzed microbiologically for the enumeration of TVCs, while in parallel MSI and FT-IR instrumental analysis was

performed. In addition, sensory analysis was undertaken by 14- member untrained panel for the assessment of fresh and spoiled samples. Based on the outcome of sensory analysis (threshold of spoilage: TVCs = 6.2 log CFU/cm^2), samples were divided in two quality classes, namely fresh and spoiled. Eight machine learning models (single-based and ensemble) were developed with MSI and FT-IR spectral data for the detection of spoilage, whereas their performance was validated by an independent data set from the two dynamic temperature profiles. MSI analysis and subspace ensemble provided the highest overall accuracy (64.8 %), while this combination demonstrated also acceptable values of specificity and sensitivity (69.7 %). On the contrary, FT-IR spectral data presented slightly better performance with Partial Least Squares-Discriminant Analysis (PLS-DA), as the samples were classified correctly with an overall accuracy of 67.6 %.

In **chapter 5**, FT-IR and MSI rapid techniques were employed for the assessment of the microbiological quality in chicken thigh fillets via qualitative and quantitative machine learning models. For this purpose, chicken thigh fillets were stored at eight isothermal (0, 5, 10, 15, 20, 25, 30, 35 ^{o}C) and two dynamic temperature profiles and analyzed microbiologically for the determination of TVCs and *Pseudomonas* spp., whereas MSI and FT-IR spectral data were acquired at the same time points. Samples were also evaluated by a sensory panel which established a TVC spoilage threshold at 6.99 log CFU/cm^2. PLS-R models were implemented for the estimation of TVCs and *Pseudomonas* spp. counts on chicken's surface. Moreover, classification models (LDA, QDA, SVMs, QSVMs) were developed for the discrimination of samples in two quality classes (fresh vs. spoiled). PLS-R models coupled to MSI data predicted TVCs and *Pseudomonas* spp. counts satisfactorily, with RMSE values of 0.987 and 1.215 log CFU/cm^2, respectively. SVM model developed with MSI data exhibited the highest performance with an overall accuracy of 94.4%, while in the case of FT-IR, acceptable classification was obtained with the QDA model (overall accuracy 71.4%).

In **chapter 6**, FT-IR, MSI and E-nose have been explored individually and in combination via data fusion for their efficacy in the evaluation of quality in marinated chicken souvlaki. In brief, chicken marinated souvlaki samples were subjected to storage experiments at both isothermal and dynamic temperature conditions. During storage,

microbiological analyses were performed for the determination of the population dynamics of TVCs and *Pseudomonas* spp. in parallel with FT-IR, MSI and E-nose analyses. PLS-R and SVM-R models were developed and validated for the estimation of TVCs on chicken marinated souvlaki. Furthermore, three classification models (LDA, LSVM and QSVM) were investigated for the classification of stored samples in 2 and 3 quality classes (fresh vs spoiled; fresh, semi-fresh and spoiled). The developed models were externally validated with data obtained by six different analysts and three different batches of marinated souvlaki. The PLS-R models developed on MSI and FT-IR/MSI spectral data provided the best predictions of TVCs, with RMSE values of 0.998 and 0.983 log CFU/g, respectively. Moreover, for SVM models developed on MSI and FT-IR/MSI data, the population of TVCs was efficiently predicted with RMSE being 0.973 and 0.999 log CFU/g, respectively. For the classification models with 3 quality classes, the overall accuracy was calculated below 60 % in all cases. On the contrary, for the 2-class models, FT-IR/MSI spectral data analyzed by CSVM model exhibited overall accuracy of 87.5 %, followed by MSI data analyzed by LSVM model providing overall accuracy of 80 %. Finally, middle level data fusion of FT-IR to MSI was proven as a promising alternative for the assessment of quality in this poultry product.

In **chapter 7**, the survival of *Campylobacter* spp. was investigated after inoculation of six strains (four *Campylobacter coli* strains and two *Campylobacter jejuni* strains) in chicken marinated souvlaki. Moreover, the microbial growth of the indigenous microbiota of the inoculated and non-inoculated chicken marinated souvlaki was examined. Inoculated and non-inoculated chicken marinated souvlaki samples were stored at three different isothermal conditions (0, 5, and 10 ^{o}C) and a dynamic temperature profile. At predetermined intervals, inoculated and non-inoculated samples were microbiologically analyzed for the enumeration of TVCs, *Pseudomonas* spp., anaerobic bacteria and *Campylobacter* spp. A one-step modelling approach was employed for chicken marinated souvlaki (inoculated and non-inoculated) for the determination of the kinetic parameters of growth for TVCs and *Pseudomonas* spp. Model validation was performed with an independent dataset derived from a dynamic temperature profile storage experiment. Further on, survival models predicting *Campylobacter* spp. counts during low storage temperatures were developed and assessed. Molecular analysis via Random amplified

polymorphic DNA PCR (RAPD-PCR) was conducted with isolates obtained from three time points during the experiments. The developed models for TVCs and *Pseudomonas* spp. in inoculated and non-inoculated samples exhibited RMSE values lower than 0.941 log CFU/g. *Campylobacter* spp. survived despite the barrier of the low storage temperature where a decline of 1.5 log CFU/g was observed. From the survival models, the highest accuracy was provided by the Weibull model at 5 ^{o}C with RSME values of 0.112 log CFU/g. Molecular results confirmed that both *C. coli* and *C. jejuni* strains could survive during low temperature storage experiments with the exception of 5 ^{o}C, where only *C. coli* could be retrieved.

Scientific area: Food microbiology

Keywords: poultry products; spectroscopic methods; microbiological quality; biomimetic sensors; multivariate data analysis; data fusion; safety

This research has been co-financed by the European Union and Greek national funds through the Operational Program Competitiveness, Entrepreneurship and Innovation, under the call RESEARCH – CREATE – INNOVATE (project code: T1EDK-04344)

Εφαρμογή σύγχρονων ταχέων αναλύσεων και ανάπτυξη μοντέλων εκτίμησης της αλλοίωσης νωπού και επεξεργασμένου κρέατος πουλερικών

Τμήμα Επιστήμης Τροφίμων και Διατροφής του Ανθρώπου
Εργαστήριο Μικροβιολογίας και Βιοτεχνολογίας Τροφίμων

Περίληψη

Η ραγδαία αύξηση της τεχνολογίας και η απαίτηση των καταναλωτών για ποιοτικά και ασφαλή τρόφιμα έχει οδηγήσει τα τελευταία χρόνια στην ανάπτυξη και εφαρμογή ταχέων σύγχρονων αναλυτικών μεθόδων που έχουν ως στόχο της έγκαιρη ανίχνευση της υποβάθμισης της ποιότητας στα τρόφιμα. Στην παρούσα διατριβή μελετήθηκε η αποτελεσματικότητα των ταχέων, μη επεμβατικών τεχνικών της φασματοσκοπίας υπέρυθρου με μετασχηματισμό Fourier (FT-IR), της πολυφασματικής απεικόνισης (MSI) και της ηλεκτρονικής μύτης (E-nose) στην εκτίμηση της ποιότητας σε διάφορα προϊόντα κοτόπουλου. Οι τεχνικές αυτές εφαρμόστηκαν σε συντηρημένα δείγματα από φιλέτο στήθος κοτόπουλου, φιλέτο μπούτι κοτόπουλου, μαριναρισμένο κοτόπουλο και μπιφτέκι κοτόπουλου, και σε συνδυασμό με πολυμεταβλητή ανάλυση δεδομένων (multivariate data analysis) αναπτύχθηκαν και επικυρώθηκαν μοντέλα εκτίμησης του μικροβιακού πληθυσμού, της ποιότητας καθώς και του χρόνου από την σφαγή στα εν λόγω δείγματα. Ποσοτικά και ποιοτικά (γραμμικά και μη γραμμικά) μοντέλα αναπτύχθηκαν μετά από τη συσχέτιση των μικροβιολογικών, οργανοληπτικών και των δεδομένων που προήλθαν από τους αισθητήρες. Η επικύρωση των εν λόγω μοντέλων, πραγματοποιήθηκε με δεδομένα που συλλέχθηκαν από ανεξάρτητα πειράματα συντήρησης προϊόντων κοτόπουλου σε ενδιάμεσες θερμοκρασιακές συνθήκες ή σε δυναμικά χρονο- θερμοκρασιακά προφίλ, όπου η περίοδος σφαγής, η παρτίδα καθώς και ο αναλυτής διέφεραν. Πέρα από την ανάπτυξη και επικύρωση μεμονωμένων μοντέλων ανά αισθητήρα διερευνήθηκε επίσης και η επίδοση μοντέλων που είτε συνδύαζαν διαφορετικούς αλγόριθμους εκμάθησης (ενοποίηση, ensemble), είτε βασίζονταν στη συγχώνευση των δεδομένων από διαφορετικούς αισθητήρες (συγχώνευση δεδομένων, data fusion) για τη ανάπτυξη ενός ενιαίου μοντέλου πρόβλεψης της ποιότητας. Επιπλέον, εκτός από την εκτίμηση της ποιότητας στα προϊόντα κοτόπουλου εξετάστηκε και η συμπεριφορά του παθογόνου μικροοργανισμού *Campylobacter* spp. σε δείγματα μαριναρισμένου σουβλάκι κοτόπουλου που συντηρήθηκε υπό ψύξη.

Ειδικότερα, στο **κεφάλαιο 2**, η μέθοδος της πολυφασματικής απεικόνισης (Multispectral imaging, MSI) εφαρμόστηκε σε βιομηχανικές εγκαταστάσεις, παράλληλα με τη γραμμή παραγωγής σε τέσσερα είδη από προϊόντα κοτόπουλου: φιλέτο στήθος κοτόπουλου, φιλέτο μπούτι κοτόπουλου, μαριναρισμένο σουβλάκι κοτόπουλου και μπιφτέκι κοτόπουλου. Δείγματα από διαφορετικές παρτίδες παραγωγής αναλύθηκαν μικροβιολογικά ενώ παράλληλα ελήφθησαν φασματοσκοπικά δεδομένα με τη χρήση του εγκατεστημένου στην παραγωγή οργάνου πολυφασματικής απεικόνισης. Τα μικροβιολογικά αποτελέσματα συσχετίστηκαν με τα αντίστοιχα φασματοσκοπικά δεδομένα για την ανάπτυξη μοντέλου εκτίμησης του χρόνου από την σφαγή (time to slaughter) μέσω της γραμμικής παλινδρόμησης με τη μέθοδο μερικών ελαχίστων τετραγώνων (Partial-least Squares Regression, PLS-R). Η επίδοση των ανεπτυγμένων μοντέλων ήταν υψηλή σε όλες τις κατηγορίες προϊόντων, με τα μοντέλα εκτίμησης του χρόνου από τη σφαγή για το φιλέτο μπούτι κοτόπουλου και το μπιφτέκι κοτόπουλου να παρουσιάζουν την μικρότερη ρίζα μέσου τετραγωνικού σφάλματος (Root Mean Squared Error, RMSE) κατά την επικύρωση, με τιμή ίση με 0,160 και 0,285 αντιστοίχως.

Στο **κεφάλαιο 3**, εξετάστηκε η αποτελεσματικότητα των μεθόδων FT-IR και MSI για την ανάπτυξη μοντέλων εκτίμησης της μικροβιακής αλλοίωσης στην επιφάνεια φιλέτου από στήθος κοτόπουλου. Για το σκοπό αυτό, δείγματα συντηρήθηκαν σε τέσσερις ισοθερμοκρασιακές συνθήκες (0, 5, 10, 15 ^{o}C) και ανά τακτά χρονικά διαστήματα αναλύονταν για την εκτίμηση του μικροβιολογικού τους φορτίου (Ολική Μεσόφιλη Χλωρίδα, ΟΜΧ και *Pseudomonas* spp.), ενώ παράλληλα στα ίδια χρονικά σημεία ελήφθησαν φάσματα FT-IR και MSI. Από τα αποτελέσματα των αναλύσεων αυτών αναπτύχθηκαν μοντέλα (γραμμικά και μη γραμμικά) για την εκτίμηση του πληθυσμού της ΟΜΧ και του βακτηρίου *Pseudomonas* spp. με τη χρήση ενός εμπορικού λογισμικού προγράμματος ανάλυσης δεδομένων καθώς επίσης και με τη χρήση μίας διαδικτυακής πλατφόρμας επεξεργασίας δεδομένων. Η επικύρωση των μοντέλων πραγματοποιήθηκε με τον διαχωρισμό των φασματοσκοπικών δεδομένων σε αναλογία 70/30 (ανάπτυξη/επικύρωση), ενώ επιπλέον πραγματοποιήθηκε και εξωτερική επικύρωση (πρόβλεψη) με διαφορετική παρτίδα δειγμάτων κοτόπουλου. Κατά την εφαρμογή του εμπορικού προγράμματος ανάλυσης δεδομένων, η εκτίμηση της ΟΜΧ μέσω του μοντέλου PLS-R παρουσίασε τιμή RMSE κατά την πρόβλεψη ίση με 1,359 και 1,029 log CFU/cm^2,

για τα δεδομένα της MSI και της FT-IR ανάλυσης αντιστοίχως. Για την εκτίμηση των βακτηρίων του γένους *Pseudomonas* μέσω των φασματοσκοπικών δεδομένων της MSI, η τιμή RMSE της πρόβλεψης ήταν ίση με 1,574 log CFU/cm^2, ενώ μέσω της ανάλυσης FT-IR η αντίστοιχη τιμή RMSE υπολογίστηκε σε 1,078 log CFU/cm^2. Σε ότι αφορά στα μοντέλα που προέκυψαν μέσω της διαδικτυακής πλατφόρμας sorfML, το μοντέλο που παρουσίασε τη μικρότερη τιμή RMSE κατά την πρόβλεψη (0,717 log CFU/cm^2) ήταν αυτό που αναπτύχθηκε με τη χρήση τεχνητών νευρωνικών δικτύων (Artificial Neural Networks, ANN) μέσω των δεδομένων της πολυφασματικής απεικόνισης (MSI) και την επικύρωση με δείγματα από την ίδια παρτίδα. Αντιθέτως, το μοντέλο least-angle regression (lars) προσαρμόστηκε καλύτερα στα φασματοσκοπικά δεδομένα από την ανάλυση FT-IR) εμφανίζοντας τιμές RMSE ίσες με 0,904 και 0,851 log CFU/cm^2 κατά την επικύρωση με δείγματα από την ίδια και διαφορετική παρτίδα αντιστοίχως.

Στο **κεφάλαιο 4**, εφαρμόστηκαν οι ταχείες μέθοδοι FT-IR και MSI σε περισσότερα δείγματα και παρτίδες φιλέτου από στήθος κοτόπουλου για την ανάπτυξη ποιοτικών μοντέλων εκτίμησης της αλλοίωσης των δειγμάτων. Όμοια με την πειραματική διαδικασία του κεφαλαίου 3, δείγματα φιλέτου από στήθος κοτόπουλου συντηρήθηκαν σε οχτώ ισοθερμοκρασιακές συνθήκες συντήρησης και δύο δυναμικά χρονο-θερμοκρασιακά προφίλ. Κατά τη δειγματοληψία, τα δείγματα αναλύονταν μικροβιολογικά, φασματοσκοπικά (FT-IR και MSI) ενώ παράλληλα πραγματοποιήθηκε οργανοληπτική αξιολόγηση των δειγμάτων από ομάδα 14 ατόμων για την εκτίμηση του βαθμού αλλοίωσής τους (φρέσκο και αλλοιωμένο). Με βάση τα αποτελέσματα του οργανοληπτικού ελέγχου ορίστηκε το όριο μικροβιολογικής αλλοίωσης και τα δείγματα χωρίστηκαν σε δύο κατηγορίες ποιότητας (φρέσκο και αλλοιωμένο). Εν συνεχεία, οκτώ μοντέλα μηχανικής μάθησης (μεμονωμένα και συνδυασμοί τους) αναπτύχθηκαν για κάθε κατηγορία φασματοσκοπικής μεθόδου και επικυρώθηκαν με δεδομένα από ανεξάρτητα πειράματα συντήρησης σε δυναμικά θερμοκρασιακά προφίλ. Ο συνδυασμός της πολυφασματικής απεικόνισης (MSI) με το ενοποιημένο μοντέλο subspace παρουσίασε το μεγαλύτερο ποσοστό συνολικής ακρίβειας (64,8 %). Αντιστοίχως, αποδεκτή ήταν και η επίδοση κατά την εφαρμογή του μοντέλου της διακριτικής ανάλυσης με τη μέθοδο μερικών ελαχίστων τετραγώνων (Partial Least Squares- Discriminant Analysis, PLS-DA) στα δεδομένα από τη φασματοσκοπία FT-IR, όπου το ποσοστό της συνολικής ακρίβειας ανήλθε σε 67,6 %.

Στο **κεφάλαιο 5**, φιλέτο από μπούτι κοτόπουλου αναλύθηκε με όμοια πειραματική διαδικασία με τα **κεφάλαια 3** και **4**, ωστόσο τα φασματοσκοπικά δεδομένα FT-IR και MSI αξιοποιήθηκαν για την ανάπτυξη ποσοτικών και ποιοτικών μοντέλων εκτίμησης της μικροβιακής ποιότητας στην επιφάνεια του φιλέτου από μπούτι κοτόπουλο. Επίσης, όπως και στο κεφάλαιο 4, κατά τη δειγματοληψία πραγματοποιήθηκε και οργανοληπτική αξιολόγηση των δειγμάτων κατά συντήρηση, τα αποτελέσματα της οποίας καθόρισαν ως όριο μικροβιακής αλλοίωσης στο συγκεκριμένο προϊόν την τιμή 6,99 log CFU/cm^2 για την OMX. PLS-R μοντέλα εφαρμόστηκαν στα φασματοσκοπικά δεδομένα από τις τεχνικές FT-IR και MSI για τον ποσοτικό προσδιορισμό της OMX και του βακτηρίου *Pseudomonas* spp. Επιπρόσθετα, αναπτύχθηκαν ποιοτικά μοντέλα (Linear Discriminant Analysis, LDA; Quadratic Discriminant Analysis, QDA; Support Vector Machines, SVM; Quadratic Support Vector Machines, QSVM) για τον διαχωρισμό των δειγμάτων σε δύο κατηγορίες ποιότητας (φρέσκο και αλλοιωμένο) με βάση το όριο που προσδιορίστηκε από την οργανοληπτική αξιολόγηση των δειγμάτων. Η εκτίμηση του πληθυσμού της OMX και των βακτηριών του γένους *Pseudomonas* μέσω της τεχνικής MSI και του μοντέλου PLS-R ήταν ικανοποιητική, με τιμές RMSE κατά την επικύρωση 0,987 και 1,215 log CFU/cm^2 αντιστοίχως. Η εφαρμογή του μοντέλου SVM στα φασματοσκοπικά δεδομένα της τεχνικής MSI παρουσίασε την καλύτερη επίδοση με ποσοστό συνολικής ακρίβειας κατάταξης των δειγμάτων στις δύο κατηγορίες ποιότητας που ανήλθε σε 94,4%. Ικανοποιητική κρίθηκε επίσης η χρήση του μοντέλου QDA στα φασματοσκοπικά δεδομένα της τεχνικής FT-IR, με ποσοστό συνολικής ακρίβειας κατά την ταξινόμηση των δειγμάτων σε κλάσεις ποιότητας ίσο με 71,4%.

Στο **κεφάλαιο 6**, εκτός από την εφαρμογή των φασματοσκοπικών μεθόδων FT-IR και MSI, εξετάστηκε και η αποτελεσματικότητα της ηλεκτρονικής μύτης (E-nose) στην εκτίμηση της ποιότητας δειγμάτων από μαριναρισμένο σουβλάκι κοτόπουλο. Για τον σκοπό αυτό, τα δείγματα συντηρήθηκαν σε τρία ισοθερμοκρασιακά και σε ένα δυναμικά χρονο-θερμοκρασιακό προφίλ ψύξης. Ανά τακτά χρονικά διαστήματα, τα συντηρημένα δείγματα αναλύονταν μικροβιολογικά για την απαρίθμηση της OMX και του βακτηρίου *Pseudomonas* spp., ενώ παράλληλα ελήφθησαν φασματοσκοπικά δεδομένα (FT-IR και MSI) και ταυτόχρονα πραγματοποιήθηκε καταγραφή του πτητικού αποτυπώματος των δειγμάτων μέσω της ηλεκτρονικής μύτης (E-nose). Μοντέλα PLS-R and SVM-R

αναπτύχθηκαν και επικυρώθηκαν για τον προσδιορισμό της ΟΜΧ στα μαριναρισμένα δείγματα, για κάθε όργανο ξεχωριστά καθώς και συνδυαστικά. Επιπλέον, διερευνήθηκε η δυνατότητα ταξινόμησης των δειγμάτων σε τρεις (φρέσκο, αποδεκτό, αλλοιωμένο) ή δυο (φρέσκο, αλλοιωμένο) κατηγορίες ποιότητας, με την εφαρμογή ποιοτικών μοντέλων (LDA, LSVM, CSVM) που αναπτύχθηκαν είτε με τα δεδομένα του κάθε οργάνου ξεχωριστά είτε συνδυαστικά. Η επικύρωση όλων των μοντέλων πραγματοποιήθηκε με δεδομένα από ανεξάρτητα πειράματα συντήρησης των δειγμάτων κοτόπουλου από τρεις διαφορετικές παρτίδες που ελήφθησαν από διαφορετικό αναλυτή (έξι αναλυτές συνολικά). Σε ότι αφορά στα μοντέλα PLS-R για την εκτίμηση της ΟΜΧ, η χρήση φασματοσκοπικών δεδομένων από την τεχνική MSI παρουσίασε την καλύτερη επίδοση με τιμή RMSE κατά την πρόβλεψη ίση με 0,998 log CFU/g, ενώ ο συνδυασμός δεδομένων από δύο φασματοσκοπικές μεθόδους FT-IR/MSI παρουσίασε επίσης καλή επίδοση με τιμή RMSE κατά την πρόβλεψη ίση με 0,983 log CFU/g. Ομοίως, τα μοντέλα SVM που αναπτύχθηκαν με τα φασματοσκοπικά δεδομένα της πολυφασματικής απεικόνισης (MSI) και του συνδυασμού FT-IR/MSI παρουσίασαν ικανοποιητική επίδοση με τιμές RMSE κατά την πρόβλεψη ίσες με 0,973 και 0,999 log CFU/g, αντιστοίχως. Κατά την επικύρωση των ποιοτικών μοντέλων κατηγοριοποίησης των δειγμάτων σε τρεις κλάσεις, η συνολική ακρίβεια ήταν μικρότερη από 60 %, για όλες τις εξεταζόμενες περιπτώσεις. Αντιθέτως, για τα μοντέλα των δυο κλάσεων, το μοντέλο CSVM που αναπτύχθηκε με τα δεδομένα που προήλθαν από το συνδυασμό των τεχνικών FT-IR/MSI εμφάνισε ποσοστό συνολικής ακρίβειας κατάταξης των δειγμάτων στις δύο κλάσεις 87,5 %, ενώ η ανάπτυξη του μοντέλου LSVM με τα δεδομένα της τεχνικής MSI παρουσίασε ποσοστό ταξινόμησης των δειγμάτων στη σωστή τους κλάση 80 % στο στάδιο της πρόβλεψης. Η συνδυαστική χρήση των φασματοσκοπικών δεδομένων των μεθόδων FT-IR και MSI αποδείχθηκε ως μία αποτελεσματική εναλλακτική λύση για την εκτίμηση της ποιότητας στο συγκεκριμένο προϊόν.

Στο **κεφάλαιο 7**, μελετήθηκε η ασφάλεια ενός επεξεργασμένου προϊόντος κοτόπουλου σχετικά με τον παθογόνο μικροοργανισμό του γένους *Campylobacter* που συναντάται συχνά στο κοτόπουλο. Για τον σκοπό αυτό, δείγματα από μαριναρισμένο σουβλάκι κοτόπουλο εμβολιάστηκαν με έξι στελέχη *Campylobacter* (τέσσερα στελέχη *C. coli* και δύο στελέχη *C. jejuni*) και μελετήθηκε η συμπεριφορά του εν λόγω μικροοργανισμού καθώς και της αυτόχθονος μικροχλωρίδας του προϊόντος κατά την

συντήρησή του σε θερμοκρασίες ψύξης (τρείς ισοθερμοκρασιακές συνθήκες και μία δυναμικά μεταβαλλόμενη θερμοκρασιακή συνθήκη). Παράλληλα, μελετήθηκε η συμπεριφορά της αλλοιογόνου μικροχλωρίδας σε μη εμβολιασμένα με το παθογόνο βακτήριο δείγματα του ίδιου προϊόντος. Πρωτογενή και δευτερογενή μοντέλα της αύξησης της ΟΜΧ και του βακτηρίου *Pseudomonas* spp. σε σχέση με την θερμοκρασία συντήρησης αναπτύχθηκαν και επικυρώθηκαν για τα ενοφθαλμισμένα και μη δείγματα. Επιπλέον, πρωτογενή μοντέλα επιβίωσης του *Campylobacter* spp. αναπτύχθηκαν με τα δεδομένα από τα τρία ισοθερμοκρασιακά προφίλ συντήρησης. Τέλος, η επιβίωση των στελεχών του παθογόνου βακτηρίου σε κάθε θερμοκρασιακή συνθήκη πραγματοποιήθηκε με τη χρήση της μοριακής μεθόδου Random amplified polymorphic DNA PCR (RAPD-PCR) σε απομονώσεις που πραγματοποιήθηκαν στο αρχικό, ενδιάμεσο και τελικό στάδιο κατά τη διάρκεια συντήρησης των δειγμάτων. Τα πρωτογενή μοντέλα για την εκτίμηση της κινητικής συμπεριφοράς της ΟΜΧ και του βακτηρίου *Pseudomonas* spp. εμφάνισαν τιμές RMSE μικρότερες από 0,941 log CFU/g για τα ενοφθαλμισμένα και μη δείγματα. Από τα μοντέλα επιβίωσης των στελεχών *Campylobacter* spp., το μοντέλο Weibull που αναπτύχθηκε με τα δεδομένα από τη θερμοκρασία 5 ^{o}C παρουσίασε ικανοποιητική επίδοση, με τιμή RMSE ίση με 0,112 log CFU/g. Τέλος, τα αποτελέσματα των μοριακών αναλύσεων έδειξαν ότι τα είδη *C. coli* και *C. jejuni* επιβίωσαν κατά την ψύξη του μαριναρισμένου κοτόπουλου, με μοναδική εξαίρεση τη θερμοκρασία 5 ^{o}C, όπου μόνο το είδος *C. coli* ήταν ανιχνεύσιμο.

Επιστημονική περιοχή: Μικροβιολογία Τροφίμων

Λέξεις-κλειδιά: προϊόντα πουλερικών, φασματοσκοπικές μέθοδοι ανάλυσης, μικροβιακή αλλοίωση, βιομιμητικοί αισθητήρες, πολυμεταβλητή ανάλυση δεδομένων, ασφάλεια πουλερικών

Acknowledgements

I would like to express my gratitude and thanks to Professor George-John Nychas who guided me, supported me and gave me the opportunity to work in the Laboratory of Microbiology and Biotechnology in Foods (LMBF) in the framework of the QAPP project. I would like to thank my supervisor Professor Efstathios Panagou for his guidance, suggestions and support during this PhD study and my MSc thesis as well. It was an opportunity to have him as a Professor during my MSc thesis, while our collaboration and discussions defined my PhD research. Also, I would like to thank Professor Kostas Koutsoumanis for his advice and collaboration during these three years.

I am thankful to Associate Professor Christos Pappas and Associate Professor Vasileios Valdramidis for dedicating time for my thesis. Moreover, I would like to express my thanks to Assistant Professor Alexandra Lianou with whom I had the chance to collaborate (through my Master thesis and the first two years of my PhD thesis) and who was always there for advice and mental support. Sincere thanks have to be given to the Assistant Researcher Dr. Agapi Doulgeraki for her collaboration and advice.

I would like to thank the personnel of Institute of Technology of Agricultural products, Hellenic Agricultural Organization – DIMITRA who welcomed and assisted me in the first month of my PhD study and especially Research Director and Deputy Director Dr. Chyssoula Tassou and Assistant Researcher Dr. Anthoula Argyri. I would like to thank Dr. Anastasia Lytou, Dr. Panagiotis Tsakanikas, Dr. Alexandros Kanapitsas, Dr. Athina Grounta and Dr. Dimitra Dourou for their collaboration through QAPP project and my PhD thesis.

I am thankful to the members of the Laboratory of Microbiology and Biotechnology in Foods for their collaboration and constant assistance all these years. I am grateful and thankful to Eirini Sxoina, Dr. Evita Manthou, Stamatoula Bonatsou, Aikaterini Tzamourani and Dr. Lemonia-Christina Fengou for their advice, assistance, discussions, and support but most importantly for their friendship. At this point, I would like to express my thanks to the students I collaborated with and especially to Christina Papachristou, Rania

Raftopoulou, Ariadni Kourkouli, Vasileios Skarpelos, Kalypso Voudouki and Maria Choulioumi.

Last but not least, I would like to express my gratitude and thanks to my parents for all their love, caring, patience, support and understanding all these years. I would like also to thank my sister, my family and my friends who have always been by my side supporting and encouraging me.

«Με την άδειά μου, η παρούσα εργασία ελέγχθηκε από την Εξεταστική Επιτροπή μέσα από λογισμικό ανίχνευσης λογοκλοπής που διαθέτει το ΓΠΑ και διασταυρώθηκε η εγκυρότητα και η πρωτοτυπία της»

Table of contents

List of Tables

List of Figures

List of Abbreviations

TVCs	Total Viable Counts
MSI	Multispectral Imaging
HSI	Hyperspectral Imaging
FT-IR	Fourier Transformed infrared spectroscopy
NIR	Near Infrared spectroscopy
PCA	Principal Component Analysis
PLS-R	Partial Least Squares Regression
SVM-R	Support Vector Machines Regression
SVM	Support Vector Machines
LSVM	Support Vector Machines with linear kernel function
QSVM	Support Vector Machines with quadratic kernel function
CSVM	Support Vector Machines with cubic kernel function
LDA	Linear Discriminant Analysis
QDA	Quadratic Discriminant Analysis
DFA	Discriminant Factor Analysis
ANNs	Artificial Neural Networks
Nnets	Artificial Neural Networks
BPPN	Back propagation neural networks
LOOCV	Leave-one-out-cross validation
FCV	Full cross validation
CV	Cross validation
k-CV	k- fold cross validation
lars	least-angle regression
RMSE	Root Mean Squared Error
R2	Coefficient of determination
r	correlation coefficient
λ	lag phase (h)
μ_{max}	specific growth rate (h-1)
MAE	mean absolute error
se(fit)	standard error of fitting
A_f	Accuracy factor
B_f	Bias factor

Chapter 1: Introduction

In the last decades, the continuous evolution and implementation of technologies in time-temperature indicators (TTIs), smart sensors (package level freshness visibility), smart labels (QR codes) and integrated software systems have enriched consumers' knowledge and awareness in food quality and safety (Sanz-Valero et al., 2016; Bouzembrak et al., 2019; Li & Messer, 2019; Dey et al., 2021; Kumar et al., 2021). Consumers' demands for high quality and safety in food with nutritional and healthy benefits have been increased. Moreover, the recall and withdrawing of food products due to poor quality aspects or to foodborne pathogens have forced the authorities and the producers to establish the guidelines for the quality and safety assessment of foods through the farm to table chain (EC regulation 852/2004, EC regulation 2073/2005). In order to meet consumer's demand which has been constantly evolving and expanding as quality food standards rise, the industries have invested in the development and continuous improvement of techniques assessing foods quality and shelf- life (Chen, 2015; Verdouw et al., 2016). Furthermore, real-time monitoring of temperature and other important factors influencing foods quality and safety at the retail's points and consumer fridges have been employed for the avoidance of food recalls and food loss and waste (Kouma & Liu, 2011).

1.1 Quality and Safety in foods

According to FAO, the food loss index was worldly estimated at 13.80 % until 2016, including post-harvest losses (FAO, 2019), indicating that both food loss and waste should be reduced by half in 2030 globally (UNEP, 2021; FAO, 2022). Quantitative and qualitative food loss and waste are a result of industries inability to properly estimate foods deterioration from intrinsic and extrinsic factors during production, packaging, storage and distribution, as well as of retailers, food services and consumers unawareness concerning the optimum conditions of storage and cooking. Food rejection is strongly linked with spoilage which is defined as the process of physical, chemical and sensory (off-flavours, off-odours, appearance, texture) changes in a food product that characterize it unacceptable from the consumers point of view (Koutsoumanis, 2009; Macé et al., 2013; Lianou et al., 2016). More than 25% of global food waste at post-harvest or post slaughter processes is attributed to the microbial activity in the food matrix. Nevertheless, microbiological spoilage in foods has been described by many researches as the most responsible cause of

deterioration in food quality during storage (Gram et al., 2002; Iulietto et al., 2015; Remenant et al., 2015; Koutsoumanis et al., 2021).

1.1.1 Quality and Safety in poultry

Poultry meat is popular among consumers as it contains high percentages of protein, vitamins, minerals and essential polyunsaturated fatty acids (PUFAs), especially the omega (n)-3 fatty acids (Lin et al., 2011). Moreover, it has an affordable price and it is recommended to populations which exclude beef or pork meat for religious reasons (FAO, 2022). Taking into account these benefits, as well as the fact that the poultry sector is fast growing and the most flexible of all livestock sectors, it is forecasted that poultry production will expand by 1.8 Mt annually by 2025 (Souza et al., 2018; FAO, 2022). However, due to its nutritional content and intrinsic factors (pH, water activity, initial microbiota and redox potential) poultry products are susceptible to microbial spoilage and pathogens survival or growth (Baston & Barna, 2010; Dawson et al., 2013; Iulietto et al., 2015). The sensorial attributes that signify poultry's spoilage are the presence of slime on some parts or on all the surface of chicken, the development of off-odours (slight sulphurous or ammoniacal, rancid, acid, putrid), the deterioration in colour (light cream and grey or greening) and loss in muscles elasticity (no return) (Baston & Barna, 2010; Baston et al., 2010; Dawson et al., 2013; Chmiel, M. and Słowiński, 2018). During microbial spoilage and more specifically during the proteolytic activity of the indigenous microbiota on chicken, the off odours from the produced volatile molecules of sulphure- and ammonia-based compounds are traceable (Nychas & Tassou, 1997; Nychas et al., 2008; Alexandrakis et al., 2012). Extended presence of slime on the surface of chicken is related to *Pseudomonas* spp. biofilm formation on chilled meat (Wickramasinghe et al., 2019, 2020).

1.1.2 Spoilage microorganisms in poultry

The indigenous microbial groups associated with spoilage in poultry products are *Pseudomonas* spp. (*Pseudomonas fragi*, *Pseudomonas lundensis*, and *Pseudomonas fluorescens*), Enterobacteriaceae (*Hafnia* spp., *Serratia* spp., *Rahnella* spp.), *Enterococcus* spp., *Lactobacillus* spp., *Brochothrix thermosphacta* and *Shewanella* spp. (Gram et al., 2002; Lee et al., 2017; Lindblad, 2007; Säde et al., 2013). These microorganisms can be

transmitted to the sterile chicken carcasses during slaughtering process from contaminated areas in the slaughterhouse (i.e., air, water bath, low hygiene in employees, equipment, surfaces, chilling) (Tompkin, 1994; Geornaras et al., 1999; Rouger et al., 2017). Each one from the abovementioned microorganisms could grow and dominate over the other depending on the conditions of storage and packaging in chicken products (Smolander et al., 2004; Doulgeraki et al., 2012; Holl et al., 2016). Storage of chicken meat in low temperatures at aerobic conditions favors the growth of *Pseudomonas* spp. which is reported in the literature as the main spoilage microorganism during raw or processed poultry meat (marinated) storage in aerobic conditions (Liang et al., 2012; Morales et al., 2016). Moreover, a detailed description of *Pseudomonas* spp. growth behavior at chill temperatures (1-10 ^{o}C) and aerobic conditions of storage in poultry is presented by EFSA panel on Biological Hazards (EFSA Panel on Biological Hazards (BIOHAZ), 2016). On the contrary, modified atmosphere packaging (vacuum, N_2/CO_2, O_2/CO_2) favored the dominance of anaerobic and facultative anaerobic microorganisms such as LAB and *Brochothrix thermosphacta* during spoilage in poultry products (Björkroth, 2005; Balamatsia et al., 2007; Patsias et al., 2008; Franqueza & Barreto, 2011; Silva et al., 2018).

1.1.3 Pathogen microorganisms in poultry

Regarding safety in chicken and the presence of pathogenic microorganisms causing severe diseases, the most commonly isolated foodborne pathogens from chicken products are *Campylobacter* spp. and *Salmonella* spp. (EFSA/ECDC, 2021). The former microorganism has been reported as the cause of campylobacteriosis which has been the most frequent disease with food etiology since 2005 around the globe (Gharst et al., 2013; WHO, 2013; Repérant et al., 2016). *Campylobacter* spp. has been isolated from poultry plants and poultry products as this pathogen can survive under low temperature storage and acid conditions (Björkroth, 2005; Silva et al., 2011; Yun et al., 2016; Lanzl et al., 2020). For this reason, a modification of the EU 2073/2005 regulation was necessary for the detection of *Campylobacter* spp. in poultry meat after slaughter procedure (via ISO 10272-2) and the upper limit concerning the safety of the inspected meat was defined at 1,000 CFU/g. Likewise, *Salmonella* spp. has been transmitted through chicken meat consumption to humans and 91,857 incidences of salmonellosis have been reported in the EU in 2018 (EFSA/ECDC, 2019). Therefore, in the EU 2073/2005 regulation on the microbiological

criteria of foodstuffs, the guidelines regarding this pathogen have been established in order to diminish salmonellosis originated from chicken meat consumption (EN/ISO 6579). Nevertheless, CAC/GL 78-2011 provides the guidelines for the control of both pathogens in chicken meat from primary production to consumption (CAC, 2011).

1.2 Process Analytical Technologies (PAT)

Poultry's vulnerability to spoilage, consumers' demand for qualitative food and the vast economic losses for the food industry due to food loss and waste necessitated for the adaptation of alternative methods assessing in real-time the spoilage in poultry meat. In the last decade, PAT concept has been implemented in the pharmaceutical as well as in the food industry (on-, in- and at- line) as an efficient suggestion for the evaluation of quality and freshness in meat (van den Berg et al., 2013; Cullen et al., 2014). Rapid analytical techniques (as smart sensors) could be associated with microbiological, chemical, molecular and sensory data via multivariate data analysis for the development of predictive models (food matrix specific models) assessing products' quality. Afterwards, these rapid analytical techniques could be embodied in the production line and continuously updated with data sets for the detection of spoilage during meat processing, packaging or/and storage (Nychas et al., 2016). The implementation of PAT could be beneficial for all stakeholders in the food chain. From the producers' point of view, this approach could facilitate the release time of a product, permit on-site inspections, allow continuous assurance of product quality and shelf-life avoiding recalls or complains from costumers. Similarly, retailers could check their supplier easily and rapidly and monitor in real- time the quality in stored food products (Gomes & Leta, 2012; Dey et al., 2021). Concerning the consumers, they could be alerted if the quality of a product deteriorates during refrigerated storage and thus, minimize or prevent food waste (Kamble et al., 2019).

1.2.1 Noninvasive methods applied in Food Science

In recent years, a variety of sensors have been developed, applied and evaluated for their potential to rapidly assess freshness in meat and poultry products. In order to be considered as an alternative for PAT application, a sensor should assess rapidly and efficiently the critical control parameter of interest without destruction of the product (van den Berg et al., 2013). Spectroscopic methods (FT-IR, NIR and RAMAN), hyperspectral

(HSI) or multispectral imaging (MSI) and biomimetic sensors (electronic nose, E-nose; electronic tongue, E-tongue) have been proposed (individually or in combination) as reliable, non-invasive methods for the evaluation of quality in meat and poultry products (Ghasemi-Varnamkhasti, 2010; Argyri et al., 2013; Pu et al., 2015; Ye et al., 2016; Falkovskaya & Gowen, 2020). In addition, these techniques are environmentally friendly, cost-effective and easy to be implemented by non-skilled personnel compared to the conventional, time consuming and expensive microbiological, chemical and molecular methods of analysis (Nychas et al., 2016; Khulal et al., 2017).

1.2.2 Multispectral Imaging (MSI)

Multispectral imaging combines spectroscopy (in the visual and near-infrared region, NIR) with computer vision for the acquisition of spectral and spatial data providing information on the metabolites on the surface of the examined food. This analysis combines fast image acquisition and processing methods and it has lower cost compared to hyperspectral imaging. Moreover, MSI does not require sample pre-treatment, it is simple to apply and hence it is appropriate for online monitoring during food production (Kutsanedzie at al., 2019). This novel technique has been employed in the evaluation of quality and the identification of defects, contaminants or adulteration in a variety of poultry products. Specifically, MSI has been applied in the range of 400 to 1700 nm (visual and NIR region) for the development and validation of quantitative or qualitative models predicting the bacterial populations of Total Viable Counts (TVCs) and *Pseudomonas* spp. on chicken meat during spoilage (Feng & Sun, 2013a, 2013b; Ye et al., 2016). Furthermore, this nondestructive technique could successfully identify fecal contaminants in poultry line and the presence of tumors on the surface of chicken breast (Yang et al., 2006; Nakariyakul & Casasent, 2009). MSI analysis could also efficiently detect the adulteration/food fraud of minced beef with chicken meat as well as food fraud in minced pork adulterated with chicken (Kamruzzaman et al., 2021; Fengou et al., 2021).

1.2.3 Fourier Transformed Infrared Spectroscopy (FT-IR)

Fourier Transform Infrared spectroscopy is a vibrational spectroscopy analysis adapted from the relationship of the interactions of infrared radiation (IR) to matter, where Fourier transformation is performed via an interferometer by multiplexing the wavelengths

in one measurement. When IR radiation passes through sample surface and the crystal, each specific vibrational mode absorbs IR at its characteristic frequency, so that each molecule will have its own distinct peak combination providing a unique molecular fingerprint of the sample (Gromski et al., 2015; Candoğan et al., 2021). In the literature, FT-IR sensors emitting mostly in the mid-infrared (MIR) region (400-4000 cm^{-1}) have been proposed as nondestructive methods assessing spoilage in meat and poultry (Ellis et al., 2002; Argyri et al., 2013; Ropodi et al., 2018; Alamprese et al., 2016; Candoğan et al., 2021). Briefly, this spectroscopic method has been recommended as an effective method for the differentiation of intact chicken breast muscle during spoilage by Alexandrakis et al. (2012). Likewise, in other studies the time of storage as well as the spoilage microbiota was assessed via FT-IR models in chicken breast fillets stored under aerobic conditions (Ellis et al., 2002; Sahar & Dufour, 2014; Vasconcelos et al., 2014; Rahman et al., 2018). An attempt to discriminate beef from chicken samples and beef-chicken mixtures at different percentages with FT-IR measurements was undertaken successfully by Keshavarzi et al. (2020), whereas in a recent work successful clustering of chicken meat from other raw food matrices stored at different temperature and packaging conditions was reported (Tsakanikas et al., 2020). Furthermore, FT-IR spectroscopy has been satisfactorily employed for the detection of adulteration in beef with chicken and/or turkey meat and reversibly (Alamprese et al., 2013; Alamprese et al., 2016; Deniz et al., 2018). In addition, this rapid technique could efficiently classify fresh from frozen/thawed chicken meat according to Grunert et al. (2016). Regarding safety in chicken meat, FT-IR models exhibited good prediction of *Salmonella* spp. as well as of the indigenous spoilage microorganisms in inoculated and non-inoculated chicken liver samples (Dourou et al., 2021). The potential of FT-IR in tandem with multivariate analysis to separate frozen chicken salami samples inoculated with *L. monocytogenes, E. coli. P. ludensis* and *S.* Enteritidis as well as spiked with *P. ludensis, S.* Enteritidis and untreated ones has been discussed by Grewal et al. (2015).

1.2.4 Electronic nose (E-nose)

The electronic nose (E-nose) is a biomimetic sensor imitating the olfactory system of humans. An E-nose instrument consists of an array of electronic chemical sensors with cross-sensitivity, partial specificity and an appropriate pattern recognition system, capable

for the identification of simple or complex odor via volatiles (Ghasemi-Varnamkhasti et al., 2010; Loutfi et., 2015; Di Rosa et al. et al., 2017). Until now, mostly metal-oxide sensors (n-type and p-type semiconductors) as SnO_2, ZnO, Fe_2O_3, WO_3, CuO, NiO and CoO have been employed for the recognition of H_2, CH_4, CO, C_2H_5 or H_2S, O_2, NO_2 and Cl_2 gases, respectively in food matrices (Baldwin et al., 2011; Lin et al., 2014; Haddi et al., 2015; Handa & Singh, 2018). Different combinations of these metal-oxide sensors have been assembled in sensing systems and tested for their accuracy in the recognition of quality in meat and poultry products (Balasubramanian et al., 2004; Ghasemi-Varnamkhasti et al., 2009; Wang et al., 2012; Papadopoulou et al., 2013; Estellez-Lopez et al., 2017; Shi et al., 2017). E-nose implementation has been suggested for the estimation of chicken fat (Rajamaki et al., 2006; Song et al., 2013). In another application, E-nose could accurately determine the level of TVCs on stored chicken (Timsorn et al., 2016). Moreover, the effect of the season of the year on different batches of chicken and beef meat were efficiently discriminated whereas the sensory attributes corresponding to these batches were predicted via E-nose data acquisition (Tian et al., 2014). Recently, E-nose in tandem with dispersive liquid–liquid microextraction–gas chromatography–mass spectrometry (DLLME-GC-MS) has been evaluated for the determination of the biogenic amine index in fresh chicken breast muscles (Wojnowski et al., 2019).

1.3 Machine Learning

An important and challenging decision in the development of predictive models with data originating from sensors is the selection of the most appropriate machine learning algorithm. Unsupervised pattern recognition techniques should be firstly applied to the data set of interest in order to comprehend the relationship between observations and the trend in the data subspace (Brereton & Loyd, 2014; Gromski et al., 2015). Supervised machine learning methods could be implemented in a data set containing independent and their corresponding dependent variables for the development of quantitative or qualitative models assessing a continuous (Regression models) or a categorical (Classification models) output (target) variable. The application of the abovementioned techniques in food science for the rapid estimation of quality in meat and poultry have been discussed by many researchers and a plethora of pertinent websites (e.g., sorfML, Metaboanalyst) or software

(R, MatLab, Python, The Unscrambler) have been developed for this purpose (Ropodi et al., 2016; Kumar & Karne, 2017; Candoğan et al., 2021).

1.3.1 Unsupervised machine learning methods for pattern recognition

Principal component analysis (PCA) and cluster analysis (CA) are two unsupervised methods capable of pattern recognition among data which are frequently employed in exploratory data analysis (Beruetta et al., 2007). PCA aims at the reduction of data dimensionality by transforming the original variables into new uncorrelated variables called Principal Components (PCs), containing linear combinations of the original data. The PCs graphically define (as vectors) the new subspace where its orthogonal axes represent the directions of greatest variance in the data. In general, the PCs contributing mostly to the visualization of the new subspace with percentages more than 95 % are the ones describing successfully the original data set. The new observation values located in this subspace are called PC scores. The obtained PCA scores could be further utilized as input variables to other more complex classification or prediction models through data fusion (Di Rosa et al., 2017). Concerning Cluster analysis, observations are grouped in a hierarchical dendrogram based on the distance (Euclidean, Manhattan or other) between them and an agglomerative distance model (Ropodi et al., 2016).

1.3.2 Supervised machine learning methods

Partial Least Squares-Regression (PLS-R) is a supervised predictive model widely employed in food science and chemistry for the development and validation of quantitative models. Through this analysis, a matrix of independent (X) variables (instruments/sensors data) is linearly correlated to a dependent numerical variable. Similar to PCA, PLS-R also represents geometrically the data set in a new sub-space (reduction of dimensionality) via linear combinations of the original variables. This method can be applied to collinear data with many X-variables (Wold et al., 2001). Optimized and validated PLS-R models using spectral or E-nose features have been proposed for the determination of microbial populations (spoilage or pathogens), chemical compounds as well as different batches/seasons in red meat and poultry (Kamruzzaman et al., 2013; Fengou et al., 2019; Rahman et al., 2018).

Support Vector Machines-Regression (SVM-R) is a merging of Support Vector Machines classification approach to linear or non-linear models, where the model's response is a continuous variable. SVM-R separates the data set in a hyperplane defined by linear or nonlinear kernels (functions) by optimizing the maximum margin within them (Cortes & Vapnik, 1995). This approach is efficient with high dimensionally inputs and nonlinear relationships; however high computational time and difficulty in the final SVM outcome could occur due to the nature of programming (quadratic programming and nonlinear equation sets) (Balabin & Lomakina, 2011). SVM-R models coupled with data sets derived from rapid sensors have been recommended for the estimation of meat microbiota as well as for the enumeration of pathogens and the discrimination of different raw food matrices (Wang et al., 2012; Papadopoulou et al., 2013; Estelez-López et al., 2017; Fengou et al., 2020; Tsakanikas et al., 2020; Dourou et al., 2021). SVMs are also frequently used as a classification algorithm for the separation of samples in classes. The appropriate choice of kernel function (linear, LSVM; polynomial SVMs of degree d as quadratic or cubic, QSVM, CSVM; radial basis function, RBF) is a challenging task when a SVMs model is developed and optimized (Luts et al., 2010). SVMs have been employed to spectral data for the assessment of quality and authenticity in meat products providing robust models (Ropodi et al., 2016; Jaafreh et al., 2019; Jiménez-Carvelo 2019; Fengou et al., 2021a, 2021b; Tsakanikas et al., 2020).

Regarding classification models, Linear Discriminant Analysis (LDA) arranges the samples in sub-groups via a linear function of variables (canonical variables, CV) determined by the maximum distance between groups and the minimum distance of samples within each group. Likewise, in Quadratic discriminant analysis (QDA) the same rationale is followed with the exception that the relationship between X and Y variables is described by a quadratic function. Both discriminant methods assume a multivariate normal distribution in each sub-group while in QDA the covariance for each group differs. One disadvantage in these classification methods is that overfitting could be evident if the variables present high collinearly. Moreover, LDA could not be capable to separate samples if non-Gaussian distribution is observed on groups (Grouven et al., 1996; Kim et al., 2011; Kumar & Karne, 2017). Over the years, LDA has been undertaken with spectral data derived from stored meat for quality assessment and adulteration detection

(Balasubramanian et al., 2004, 2005; Chen et al., 2011; Restaino et al., 2011; Alamprese et al., 2013; Arredondo et al., 2014; Ropodi et al., 2015).

Artificial Neural Networks (ANNs) are deep learning algorithms simulating the human neural system and they have been implemented for the development of regression and classification models. ANNs contain a network of interconnected nodes divided in three main layers, namely the input layer, the hidden layer and the output layer. Independent variables are inserted in the input layer which is mainly used for the summation of the input variables. The signals proceed to the next layer (hidden) where a transfer function (linear, sigmoidal) processes the signal/variable and transfers it to the following layer. The output layer of an ANN results in the calculation of the dependent variable which could be continuous or categorical (Jain et al., 1996; Marini, 2009). This analysis has been applied in tandem with signals from biomimetic sensors as well as with spectroscopic data for the assessment of meat quality exhibiting successful performance (Balasubramanian et al., 2009; Ghasemi-Varnamkhasti et al., 2009; Chen et al., 2014; Li et al., 2014; Timsorn et al., 2016).

1.3.3 Ensemble approach

In the last decades, ensemble learning methods have gained popularity among the single machine learning models as the collaboration of multiple algorithms can significantly enhance the performance of a model. Ensemble methods employ multiple well-known algorithms, by creating smaller subsets of the initial data set, training different classifiers with these partitions and combining their outputs. They have demonstrated improved performance compared to the outcome from their single base learners (Polikar, 2006). The efficiency of these techniques has been investigated in many scientific fields such as face and emotion recognition, text classification, medical diagnosis and financial forecasting (Pintelas & Livieris 2020). Furthermore, boosting, bagging (Panov & Džeroski, 2007; Seiffert et al., 2008), random forest (Jimenez-Carvelo et al., 2019) and random subset-based strategy (Sun & Zang, 2006; Rokach, 2010) have been employed for the development of reliable classification models in foods such as beef fillets (Mohareb et al., 2016), minced meat, green olives, beer and oil (Kucheryavskiy, 2018).

1.3.4 Data Fusion

Another state-of-the-art data manipulation technique that can be employed to enhance model performance is data fusion. In data fusion, signals/features from different sensors are conjoined (low- level fusion, mid- level fusion and high-level fusion) in order to describe more accurately phenomena with high complexity. For low-level fusion, features from different sensors are combined and machine learning model is fitted to the revised data set. In mid-level fusion, features of each sensor are modified via an unsupervised method (PCA or HCA) and the outcome of this analysis is utilized for the performance of a supervised regression or classification model. In high-level fusion, a machine learning technique is implemented to each sensor features individually and the results are embodied in a new data set in which a machine learning method is performed (Borràs et al., 2015; Di Rosa et al. et al., 2017). Data fusion has been familiar to human neural system which combines multiple senses and signals for the assessment of food safety and suitability for consumption for centuries. Taking into account the nature of food matrix (physical, biological and chemical properties) and the multiple processes occurring through meat spoilage, a combination of sensor features could frame both internal (metabolites, chemical compounds) and external (color, smell, texture, tenderness) alterations and thus could identify more accurately quality defects and contaminants in food (Huang et al., 2014; Kutsanedzie at al., 2019; Weng et al., 2020; Chung & Yoon, 2021).

1.3.5 Multivariate data analysis applied to poultry products

Exploratory and supervised data analysis via the above-mentioned models and their combinations or fusion have been employed for the assessment of meat quality and specifically of poultry products. In **Table 1.1** a summary of the existing literature is provided for poultry products, with main focus on spectroscopic and biomimetic sensors coupled with exploratory methods (PCA, HCA), regression (PLS-R, SVM-R) and linear/nonlinear classification models (SVM, PLS-DA, OPA, DA, LDA, DFA, SIMCA, ANNs and BPNN). It is worth mentioning that recent studies have been relied mostly on the combination of different machine learning approaches in an attempt to develop the optimum model for quality evaluation in poultry (Khulal et al., 2017; Tsakanikas et al., 2020; Weng et al., 2020).

Table 1.1: Spectroscopic and biomimetic sensors implementation in tandem with machine learning methods for the assessment of quality and adulteration in poultry products.

Sensor	Product	Purpose	Data analysis method	Reference
HSI	Chicken breast fillets	Determination of TVCs	PLS-R	Feng & Sun, 2013a
HSI	Chicken breast fillets	Determination of *Pseudomonas* spp. counts	PLS-R	Feng & Sun, 2013b
HSI	Chicken breast fillets	Determination of TVCs via TBFI	PLS-R	Ye et al., 2016
HSI	Beef adulterated with chicken	Determination of adulteration with chicken %	PLS-R	Kamruzzaman et al., 2016
MSI	Pork adulterated with chicken	Classification of samples based on the % adulteration with chicken	SVM classification (RBF kernel function)	Fengou et al., 2021a
MSI	Chicken breast, thigh, marinated souvlaki and burger	Determination of time from slaughter	PLS-R	Spyrelli et al., 2020
FT-IR and NIR	Chicken breast fillets	Detection of spoilage	PCA, PLS-DA, OPA	Alexandrakis et al., 2012
FT-IR	Chicken breast fillets	a) Determination of TVCs, *Pseudomonas* spp., *Enterobacteriaceae and Brochothrix thermosphacta*; b) Discrimination of samples based on the day of storage	PLS-R, PLS-DA	Sahar & Dufour, 2014
FT-IR	Chicken breast fillets	Determination of TVCs	PLS-R	Ellis et al., 2002
FT-IR	Chicken breast fillets	TVC, lactic acid bacteria (LAB), *Pseudomonas spp.,Brochothrix thermosphacta, Enterobacteriaceae* counts and pH	PCA, DA, PLS-R	Vasconcelos et al., 2014
FT-IR	Chicken breast fillets	Determination of total plate count (TPC), *Entetobacteriaceae* count, pH, CTn (Color transmittance number) color analysis, TVBN, (total volatile basic nitrogen) contents, and shear force	PCA, PLS-R	Rahman et al., 2018
FT-IR	Beef fillets, chicken thigh fillets, mixed samples of chicken and beef	Discrimination between beef and chicken meat and quantification of chicken in beef meat mixture	PCA, PLS-R, ANNs	Keshavarzi et al., 2020

FT-IR	Chicken marinated breast	Classification of seven different types of food	PCA, PLS-R, SVM classification	Tsakanikas et al., 2020
UV–vis, NIR and MIR	Beef and turkey minced meat mixtures	Detection of minced beef adulteration with turkey meat	PCA, PLS-R, LDA, low fusion for a PLS-R model combined with UV-vis, NIR and FT-IR data	Alamprese et al., 2013
FT-NIR	Beef bottom round minced meat and turkey breast minced meat mixtures	Identification and quantification of turkey meat adulteration in fresh, frozen-thawed and cooked minced beef	PCA, PLS-R, PLS-DA	Alamprese et al., 2016
FT-IR	Beef, chicken, and turkey minced meat mixtures	Differentiation of beef mixtures adulterated with chicken or turkey meat	PCA, HCA	Deniz et al., 2018
FT-IR	Fresh and frozen/thawed chicken	Differentiation of fresh and frozen/thawed chicken	HCA, ANNs classification	Grunert et al., 2016
FT-IR	Spiked chicken salami with 4 specific microorganisms	Detection of *Salmonella enteritidis, Pseudomonas ludensis, Listeria monocytogenes* and *Escherichia coli*	PCA, SIMCA, PLS-DA, PLS-R for pathogens levels	Grewal et al., 2015
FT-IR	Inoculated and no inoculated chicken liver	Estimation of total viable count, *Pseudomonas spp., B. thermosphacta, LAB, Enterobacteriaceae,* and *Salmonella* on chicken liver	SVM-R	Dourou et al., 2021
E-nose	Modified atmosphere packaged poultry meat	Determination of the microbiota, sensory attributes and dimethyl sulphide and hydrogen sulphide concentrations (GC and HS-GC/MS results)	PCA, PLS-R	Rajamäki et al., 2006
E-nose	Sliced chicken breast	Estimation of TVCs on chicken meat	PCA, BPNN	Timsorn et al., 2016
E-nose	Chicken meat	Discrimination of chicken seasonings based on sensory attributes and quantitative estimation of sensory characteristics	PCA, DFA, CA, PLS-R	Tian et al., 2014
E-nose	Chicken breast	Estimation of the Biogenic Amines Index of Poultry	BPNN	Wojnowski et al., 2019
E-nose, CV, AT sensory	Chicken breast	Evaluation of freshness in chicken	Mid- fusion: PCA, SVM	Weng et al., 2020

			(RBF) classification for storage time, PCA and PLS-R for TVB-N	
Olfactory/E-Nose system based on Colorimetric sensors, HIS	Chicken breast fillets	Determination of TVB-N with multiple level data fusion	Multiple level data fusion: PCA in each sensor and in TVB-N values and after BP-ANN for TVB-N estimation	Khulal et al., 2017

1.4 Objectives

In the present thesis, the main objective was the development and validation of predictive models assessing poultry's quality with independent data obtained by non-destructive spectroscopic and biomimetic sensors (MSI, FTIR, E-nose), at- line or off- line in raw and stored (isothermal conditions and dynamic temperature profile) chicken products. Different batches of many seasons of the year were used through the experimental procedure in an attempt to include many different scenarios in this project.

In this context, in **Chapter 2**, MSI was explored as an alternative for the assessment of the quality in four poultry products on an industrial scale. In brief, chicken breast fillets, thigh fillets, marinated souvlaki and burger were analyzed microbiologically for the enumeration of TVCs and *Pseudomonas* spp. while MSI measurements were acquired at-line. Partial Least Squares Regression (PLS-R) models were developed based on MSI data for the prediction of "time from slaughter" parameter for each product type.

The efficacy of FT-IR and MSI in tandem with multivariate data analysis for the assessment of spoilage on the surface of chicken fillets was investigated in Chapters 3, 4 and 5, as follows:

In **Chapter 3**, two independent storage experiments of chicken breast fillets were executed at 0, 5, 10, and 15 ^{o}C until 480 h. At pre-determined intervals, samples were subjected to microbiological analysis for the enumeration of TVCs and *Pseudomonas* spp. and in parallel FT-IR and MSI spectral data were obtained from sensors. Two software platforms (a commercial and a publicly available developed platform) were employed for the development of nine linear and no linear models for the determination of the TVCs and *Pseudomonas spp*. counts on the surface of the samples. Models' prediction skills were assessed by intra batch and independent batch testing.

In **Chapter 4**, chicken breast samples were stored for up to 480 h at eight isothermal conditions (0, 5, 10, 15, 20, 25, 30, and 35 ^{o}C) and two dynamic temperature profiles (winter and summer transportation scenarios). Microbiological analysis for the enumeration of TVCs was undertaken at certain intervals, whereas MSI and FT-IR analyses were conducted. Samples were subjected to sensory analysis by 14 individuals for the

evaluation of fresh and spoiled samples. Eight machine learning models (single-based and ensemble) were investigated for their classification skills with their performance being validated by an independent data set from the dynamic temperature profiles.

In **Chapter 5**, spoilage experiments were performed to chicken thigh fillets at eight isothermal and two dynamic temperature profiles. Samples were analyzed microbiologically (TVCs and *Pseudomonas* spp.), sensory analysis was undertaken by a panel, while simultaneously MSI and FT-IR spectra were acquired. PLS-R models were implemented for the estimation of TVCs and *Pseudomonas* spp. counts on chicken's surface. Four classification models (LDA, QDA, LSVM, QSVM) were employed for the discrimination of fresh from spoiled samples.

In **Chapter 6**, FT-IR, MSI and E-nose have been examined (individually and combined) as a potential for the quality assessment in chicken product via data fusion. Chicken marinated souvlaki samples were subjected to storage experiments (0, 5, 10 ^{o}C and a dynamic temperature profile: 12 h at 0 ^{o}C, 8 h at 5 ^{o}C and 4 h at 10 ^{o}C) at aerobic conditions. Samples were microbiologically analyzed for the enumeration of TVCs and *Pseudomonas* spp. while in parallel, FT-IR, MSI and E-nose data were acquired. Quantitative linear and no linear (PLS-R, SVM-R) models (for each sensor and combined) were developed and validated for the determination of TVCs on chicken marinated souvlaki. In addition, three classification models (LDA, LSVM, CVM) were optimized and evaluated for the separation of samples in 2 (fresh or spoiled) and 3 (fresh, semi- fresh and spoiled) quality classes for each case of sensor individually and in combination. Model performance was assessed with data obtained by six different analysts and three different batches.

Further on, taking into account the safety in poultry products and the increased reports for *Campylobacter* spp. in poultry, in **Chapter 7**, *Campylobacter* spp. behavior (six different *Campylobacter* strains, belonging to the genera *C. jejuni* and *C.coli*) in inoculated chicken marinated souvlaki under different storage temperatures was investigated via survival models, as well as the indigenous microbiota's growth behavior of the inoculated and non-inoculated chicken marinated souvlaki.

Chapter 2: Implementation of Multispectral Imaging (MSI) for Microbiological Quality Assessment of Poultry Products

Published as:

Spyrelli, E.D., Doulgeraki, A.I., Argyri, A.A., Tassou, C.C., Panagou, E.Z., Nychas, G.J.E. 2020. Implementation of Multispectral Imaging (MSI) for Microbiological Quality Assessment of Poultry Products. *Microorganisms*, 8, 552.

Abstract

The objective of this research was to investigate on an industrial scale the potential of multispectral imaging (MSI) in the assessment of the quality of different poultry products. Samples of chicken breast fillets, thigh fillets, marinated souvlaki and burger were subjected to MSI analysis during production together with microbiological analysis for the enumeration of Total Viable Counts (TVCs) and *Pseudomonas* spp. Partial Least Squares Regression (PLS-R) models were developed based on the spectral data acquired to predict the "time from slaughter" parameter for each product type. Results showed that PLS-R models could predict effectively the time from slaughter in all products, while the food matrix and variations within and between batches were identified as significant factors affecting the performance of the models. The chicken thigh model showed the lowest RMSE value (0.160) and an acceptable correlation coefficient (r = 0.859), followed by the chicken burger model where RMSE and r values were 0.285 and 0.778, respectively. Additionally, for the chicken breast fillet model the calculated r and RMSE values were 0.886 and 0.383 respectively, whereas for chicken marinated souvlaki, the respective values were 0.934 and 0.348. Further improvement of the provided models is recommended in order to develop efficient models estimating time from slaughter.

2.1 Introduction

In the last decade, meat consumption has rapidly increased while demand for high-quality meat is expected to continue augmenting as the world population rises. Chicken meat products account for 37% of global meat production due to their low-fat content, affordable price and exclusion of beef and/or pork meat for religious purposes (FAO, 2022). However, raw poultry products are susceptible to deterioration (short shelf life) and to unpleasant organoleptic attributes during spoilage (Baston & Barna, 2010; Dawson et al., 2013). These facts in tandem with consumers' demand for fresh meat has led to the development of alternative approaches, such as Process Analytical Technology (PAT), that are considered efficient in predicting quality and freshness in meat products during production (Kamruzzaman et al., 2015; Nychas et al., 2016).

PAT is a promising approach for the assessment of products' quality and it is currently implemented not only in the pharmaceutical industry (Chen et al., 2011) but also in the food industry (van den Berg et al., 2013; Cullen et al., 2014). The main concept of PAT is the combination of multivariate data derived through real-time (in-, on-, at- line) analytical methods to multivariate data analysis for continuous feedback and information build-up (Grassi et al., 2018). As analytical techniques of PAT are considered among others spectroscopic methods such as vibrational spectroscopy (FT-IR, NIR, Raman) (Cai et al., 2011; Teena et al., 2013; Alamprese et al., 2016), hyperspectral and multispectral imaging (Qin et al., 2013; Liu et al., 2014; Xiong et al., 2015) and biomimetic sensors (e-nose, e-tongue) (Ghasemi-Varnamkhasti et al., 2010; Huffman et al., 2017). Moreover, this innovative approach coupled to microbiological analysis, quality factors and machine learning tools, can permit the understanding of the process, the identification of Critical Control Points (CCPs) and finally the application of a knowledge base to control the process (Vasconcelos et al., 2014; Estelles-Lopez et al., 2017; Tsakanikas et al., 2018).

According to PAT approach, a potential analysis and sensor have to be able to estimate successfully and rapidly the critical control parameter of interest without the destruction of the product (van den Berg et al., 2013). These requirements are fulfilled in the case of multispectral imaging (Feng et al., 2018) that combines an optical technique (visible and NIR region) to computer vision in an attempt to obtain spectral and spatial data for the metabolites on the surface of the examined sample. The main advantage over hyperspectral

analysis is the fast image acquisition and the usage of simple algorithms for image processing (ROI region) and decision-making (Qin et al., 2013; Tsakanikas et al., 2016).

In recent years, many researchers have recommended this nondestructive method and several machine learning algorithms for the rapid assessment of meat quality (Panagou et al. 2014; Pu et al., 2015; Nychas et al., 2016). Specifically, for poultry products qualitative models were constructed for the classification of intact chicken breast fillets based on three quality grades using hyperspectral analysis (Yang et al., 2018). Quantitative and/or qualitative models in the region of visible and near-infrared (400–1700 nm), were able to detect the bacterial population (TVCs, *Pseudomonas* spp. and *Enterobacteriaceae*) during spoilage of chicken meat (Feng & Sun, 2013a, 2013b; Feng et al., 2013; Ye et al., 2016). Other studies involving multispectral imaging were associated with the adulteration of minced beef with chicken meat (Kamruzzaman et al., 2016), the presence of fecal contaminants in a poultry line (Yang et al., 2005; Cho et al., 2006), defects (Park et al., 2006; Yang et al., 2006; Chao et al., 2007) and tumors on the surface of chicken breasts (Barni et al., 1997; Nakariyakul & Casasent, 2009).

So far there are limited studies on the implementation of spectroscopic methods during processing at meat industries (Dixit et al., 2017) and the majority is focused on the determination of fat and fatty acids in pork and chicken breast fillets with near-infrared sensors (i Furnols & Gispert, 2009; De Marchi et al., 2012; Sørensen et al., 2012; Prieto et al., 2017). Hence, the aim of this research was to investigate the potential of multispectral imaging, applied in a poultry processing industry, to determine the time from slaughter of four different poultry products and develop PLS-R models assessing the time from slaughter directly from spectral data.

2.2 Materials and Methods

2.2.1 Experimental design

Multispectral Imaging (MSI) was performed at-line in a Greek poultry industry on four different poultry products: a) chicken breast fillets (n = 104, batches = 5), b) chicken thigh fillets (n = 97, batches = 5), c) chicken burger (n = 131, batches = 3), and d) marinated chicken souvlaki (n = 144, batches = 4). At regular intervals, samples from each batch were analyzed microbiologically for the enumeration of Total Viable Counts (TVCs) and

Pseudomonas spp. in parallel with MSI spectral data acquisition. In addition, samples from each product were stored at 4 °C for 216 h (9 days), since this time period is defined by the industry as the shelf-life of the product. In parallel to the spectral acquisition, the microbiological analysis was performed simultaneously with the other batches.

Sample origins were extensive farming facilities where animals (*Gallus domesticus*: Ross strain) were fed from the company with a customized diet. Feeding consisted of grain, wheat, maize, soya bean oil and meat and premix for broilers (vitamin and mineral supplement). Chickens were slaughtered after 3 months of age and production was conducted according to the regulations of the EU 823/2004, 824/2004, 834/2004 and 543/2008.

2.2.2 Microbiological analysis

From each sample, 10 g were added aseptically to 90 ml of sterile quarter strength Ringer's solution (Lab M Limited, Lancashire, United Kingdom) in a stomacher bag (Seward Medical, London, UK) and homogenized in a stomacher device (Lab Blender 400, Seward Medical, London, UK) for 60 s at room temperature. For the enumeration of Total Viable Counts (TVC) and the dominant spoilage microorganism *Pseudomonas* spp., serial decimal dilutions were prepared in the same diluent and spread on the following media: a) tryptic glucose yeast agar (Plate Count Agar, Biolife, Milan, Italy) for TVCs incubated at 25 °C for 72 h, and b) *Pseudomonas* Agar Base with selective supplement cephalothin-fucidin-cetrimide (LabM Limited, Lancashire, UK) for *Pseudomonas* spp., incubated at 25 °C for 48 h. After incubation, colonies were enumerated and microbial counts were logarithmically transformed (log CFU/g). Poultry samples with TVC counts exceeding 7.0 log CFU/g were considered spoiled as reported elsewhere (Raab et al., 2008; Souza et al., 2018; Baltic et al., 2019).

2.2.3 Spectra Acquisition

MSI analysis was performed using a Videometer-Lab instrument (Videometer A/S, Videometer, 2019, Herlev, Denmark) which was installed in close proximity to the production line (at-line measurement) with the possibility of sample conditioning (Porep et al., 2015). Videometer-Lab captures surface reflectance of samples in 18 different wavelengths (405–970 nm), namely: 405, 435, 450, 470, 505, 525, 570, 590, 630, 645, 660,

700, 850, 870, 890, 910, 940 and 970 nm. Surface reflectance is recorded by a standard monochrome charged coupled device chip (CCD). The object of interest is placed at the center of an Ulbricht sphere, which has a matte white coating inside and light-emitting diodes (LEDs) with narrow-band spectral radiation positioned side by side at spheres rim. The purpose of the coating is to ensure a diffused and spatially homogenous reflectance of the sample. During instrument performance, the diodes are turned on successively leading to a monochrome image with 32-bit floating-point accuracy for each wavelength. The final outcome of MSI analysis is a data cube of spatial and spectral data for each sample of size m × n × 18 (where m × n is the image size in pixels) (Dissing et al., 2013; Tsakanikas et al., 2015).

A critical point before MSI application is the assurance that the range of LEDs intensity is stable while phenomena such as shadows and object's disfiguration are avoided (Daugaard et al., 2010; Panagou et al., 2014). Therefore, a light set up procedure in which the acquisition captured at zero time of the experiment (auto light) is recalled and light-emitting diodes (LEDs) intensities are stabilized. Subsequently, geometric and radiometric calibration is undertaken in the Region of Interest (ROI) area with the aim of prototype target.

In order to exclude non-informative areas such as Petri dish surface, fat, connective tissue etc., a pre-process step is required. The segmentation of ROI on the sample from no relevant areas and the implementation of Canonical Discriminant Analysis (CDA) areas is conducted via Videometer-Lab version 2.12.39 (Videometer A/S, Herlev, Denmark). Also known as Fisher (Fisher's discriminant analysis), CDA separates pixels to different classes, based on ROI, through the following Equation 2.1 (Duda et al., 2000; Carstensen et al., 2003):

$$R(a) = \frac{a^T \Sigma_S a}{a^T \Sigma_N a} \quad 2.1$$

where Σs is the distribution between classes and Σ_N is the distribution within a class.

2.2.4 Data Pre-Processing and Model Development

For the development of models estimating the time from slaughter, Partial Least Squares Regression (PLS-R) (Wold et al., 2001; Xiaobo et al., 2010) was chosen, where

spectral data were the independent variables (n = 36) and time from slaughter (t_s) was the dependent variable. Time from slaughter is considered as the time elapsed from slaughter until the MSI measurement. For each poultry model, a two-stage model development approach was followed: (a) calibration and full cross-validation (using leave one out cross-validation) for model optimization and (b) external validation with samples from different batches. More specifically, for chicken breast fillets, calibration was performed using a dataset from three independent batches (n= 82) and external validation was undertaken with two other batches (n = 22). Similarly, the PLS-R model for chicken thigh fillets was constructed using a training dataset from three batches (n = 67), whereas two other batches (n = 30) were used to assess the prediction performance of the model. Concerning the chicken burger, two batches (n = 87) were used in model training and one batch (n = 44) in prediction. Finally, for marinated chicken souvlaki, the dataset consisted of two batches (n = 91) for training and two different batches (n = 43) for external validation.

Prior to analysis, spectral data for each type of poultry product were pre-processed by different transformation techniques in an attempt to reduce random or systematic variations (Brereton & Lloyd, 2014; Tsakanikas et al., 2016). Reducing the total volume of data results in effective multispectral imaging systems and image acquisition with relatively low spatial resolutions in a few important wavelengths (Qin et al., 2013). Standard Normal Variate transformation (SNV) Equation 2.2 was applied in the case of chicken thigh and burger in order to avoid collinear and "noisy" data areas (Bi et al., 2016). In contrast, spectral data from chicken breast and marinated souvlaki were pre-processed with baseline offset treatment (Rinnan et al., 2009; Engel et al., 2013) Equation 2.3. Regarding time from slaughter (y variable), a logarithmic transformation was considered necessary due to large differences in the intensities of the raw data (Berrueta et al., 2007). Data pre-treatment, model development and validation were implemented using the Unscrambler© v.9.7 software (CAMO Software AS, Oslo, Norway).

$$s_I^{SNV} = \frac{S_I - \text{mean}(S)}{\text{stdev}(S)} \qquad 2.2$$

where S refers to pixel-wise spectra, S_i is the "old" information contained in a specific wavelength and Si^{SNV} is the "new-transformed" information contained in a specific wavelength (Tsakanikas et al., 2016).

$$S(x) = x - \min(x) \quad (2.3)$$

where S denotes pixel-wise spectra for one sample, x is information contained at a specific wavelength, and min(x) is the minimum variable in the x dataset.

2.3 Results

2.3.1 Microbiological Analysis

The range of the microbial population of TVC and *Pseudomonas* spp. for the different batches of poultry products and storage time is illustrated in **Figure 2.1.** Additionally, the spread of TVCs for fresh and spoiled samples is provided for each product case. More specifically, for chicken breast fillets, the initial number of TVCs and *Pseudomonas* spp. was 5.2 (±0.6) and 4.9 (±0.82) log CFU/g respectively, whereas in spoiled samples the respective values were 8.4 (±0.46) and 8.3 (±0.47) log CFU/g. Additionally, for chicken thigh fillets, samples were considered fresh with TVCs and *Pseudomonas* spp. counts at 5 (±0.83) and 4.5 (±0.98) log CFU/g. Spoiled chicken thigh samples had TVCs and *Pseudomonas* spp. values at 7.9 (±0.50) and 7.8 (±0.49) log CFU/g, respectively.

For chicken burger samples, TVCs and *Pseudomonas* spp. counts in fresh samples were 5.5 (±0.36) and 4.8 (±0.75) log CFU/g, respectively, while in spoiled samples the respective counts were 10.7 (±1.9) and 7.8 (±0.25) log CFU/g. Finally, marinated chicken souvlaki fresh samples had TVCs and *Pseudomonas* spp. counts at 4.6 (±0.50) and 3.6 (±0.71) log CFU/g, respectively. In contrast, TVCs and *Pseudomonas* spp. values for spoiled samples were 7.9 (±0.95) and 7.5 (±1.00) log CFU/g, respectively.

Results from storage experiments at 4 °C showed that chicken breast fillets were determined as spoiled beyond 168 h of storage (TVCs > 7 log CFU/g) with TVCs value at 7.76 log CFU/g and *Pseudomonas* spp. counts at 7.6 log CFU/g. For chicken thigh fillets, samples were characterized as fresh until 120 h when TVCs and *Pseudomonas* spp. counts were 7.5 log CFU/g and 7.5 log CFU/g, respectively. TVCs and *Pseudomonas* spp. counts were 8.8 log CFU/g and 7.7 log CFU/g in spoiled chicken burger samples (storage time 216 h). Moreover, chicken marinated souvlaki was defined as spoiled after 168 h of storage in which TVCs were 7.3 log CFU/g and *Pseudomonas* spp. counts were 6.8 log CFU/g.

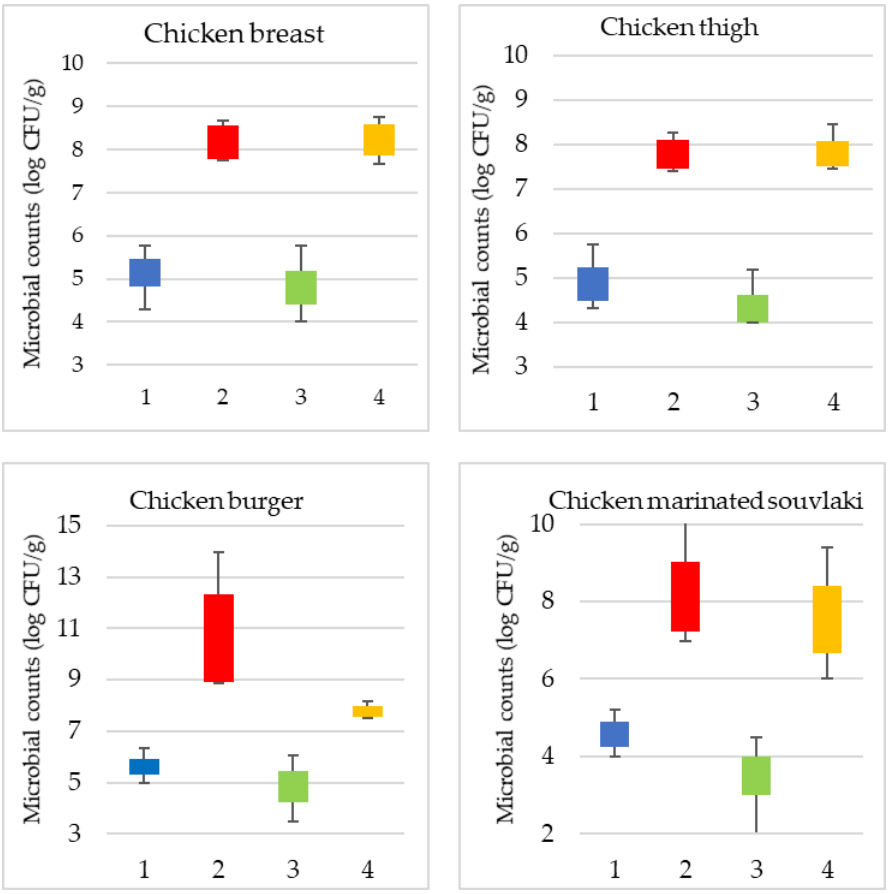

Figure 2.1: Boxplots for microbial counts (log CFU/g) of TVCs (1: blue,2: red) and *Pseudomonas* spp. (3: green,4: orange) in fresh (1: blue,3: green) and spoiled (2: red,4: orange) samples of each product.

2.3.2 Spectral Measurements

For the development of PLS-R models, each wavelength contributed differently to each category of poultry product, despite the fact that all these products have the same basic ingredient (i.e., poultry meat). This is demonstrated in **Figure 2.2** where differences could be observed in the spectra among different product types during storage at 4 °C, based mostly on their nutrition composition difference (Cozzolino et al., 2004; Kamruzzaman et al., 2013).

The same figure (**Figure 2.2**) confirms also the ability of this spectroscopic method to detect and/or separate spoiled from fresh samples for each of the four products. For instance, in the case of chicken breast, wavelengths with variations in reflectance for fresh and spoiled samples were located in the areas of 470–570 nm and 590–970 nm, respectively. Wavelength range from 660 to 970 nm seemed to affect the estimation of

spoilage for chicken thigh. Similarly, for marinated chicken souvlaki reflectance measurements at wavelengths above 570 nm deviated between fresh and spoiled samples, whereas for the chicken burger wavelengths of 850–970 nm were noticed as different.

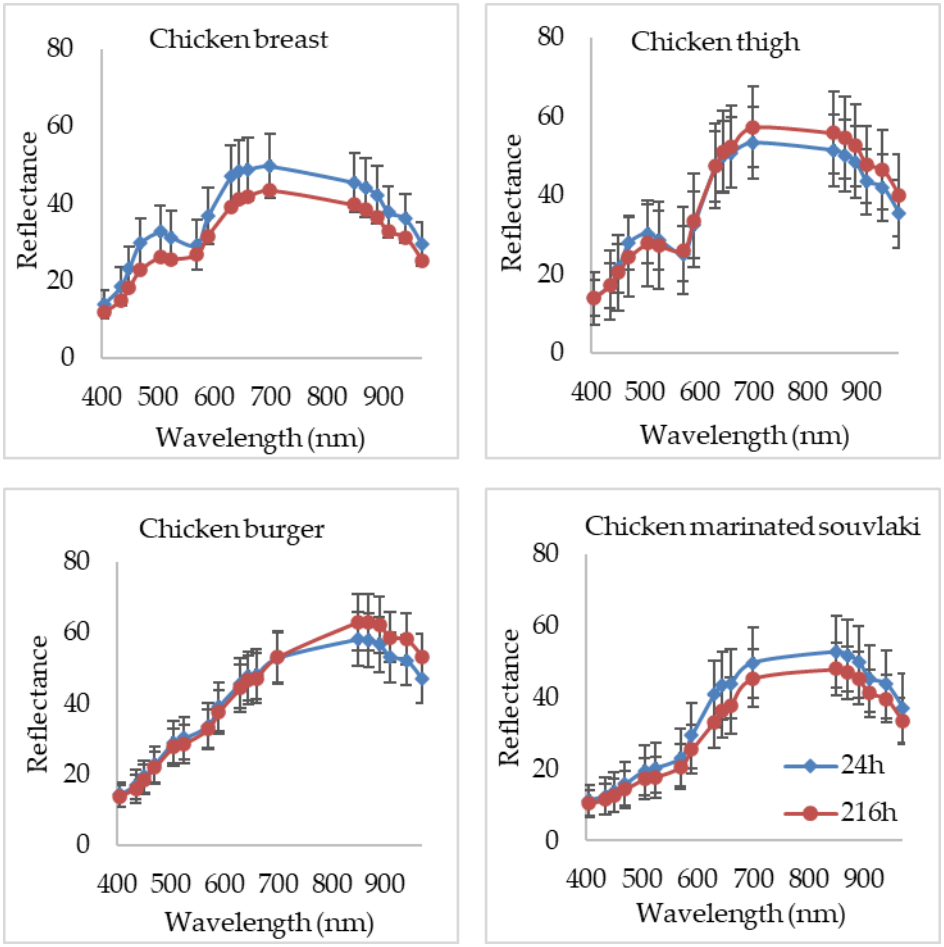

Figure 2.2: Spectra from MSI analysis (405–970 nm) for each poultry product at 24 h (blue line) and 216 h (red line) of storage at 4 °C.

2.3.3. PLS-R Model Performance

PLS-R models assessing the time from slaughter showed satisfactory performance for each category of poultry product as inferred both graphically (**Figure 2.3**) and computationally based on performance indices such as slope, offset, correlation coefficient (r) and root mean squared error (RMSE) (**Table 2.1**).

For chicken breast fillets, time from slaughter was estimated quite accurately despite the variations between batches, with r and RMSE values for the prediction dataset of 0.886 and 0.383, respectively. Differences between batches and ingredients (spices, herbs and

sauce) used in marinated chicken souvlaki did not affect the prediction performance of the PLS-R model, with r and RMSE values of 0.934 and 0.348, respectively. Even though chicken thigh muscle has a more complex texture, with a higher percentage of fat and connective fat tissue (Lin et al., 2011; Amorim et al., 2016), no differences were observed between batches and subsequently, external validation was performed satisfactorily with r and RMSE values of 0.859 and 0.160, respectively. Similarly, the presence of vegetables (peppers, onions and herbs) and spices in the homogeneous mixture of chicken burgers was not an obstacle for the external validation, where r and RMSE values were 0.778 and 0.285, respectively. The above-mentioned RMSE values of prediction indicate satisfactory accuracy of the models used to assess the observed data (Sant'Ana et al., 2012; Feng et al., 2013).

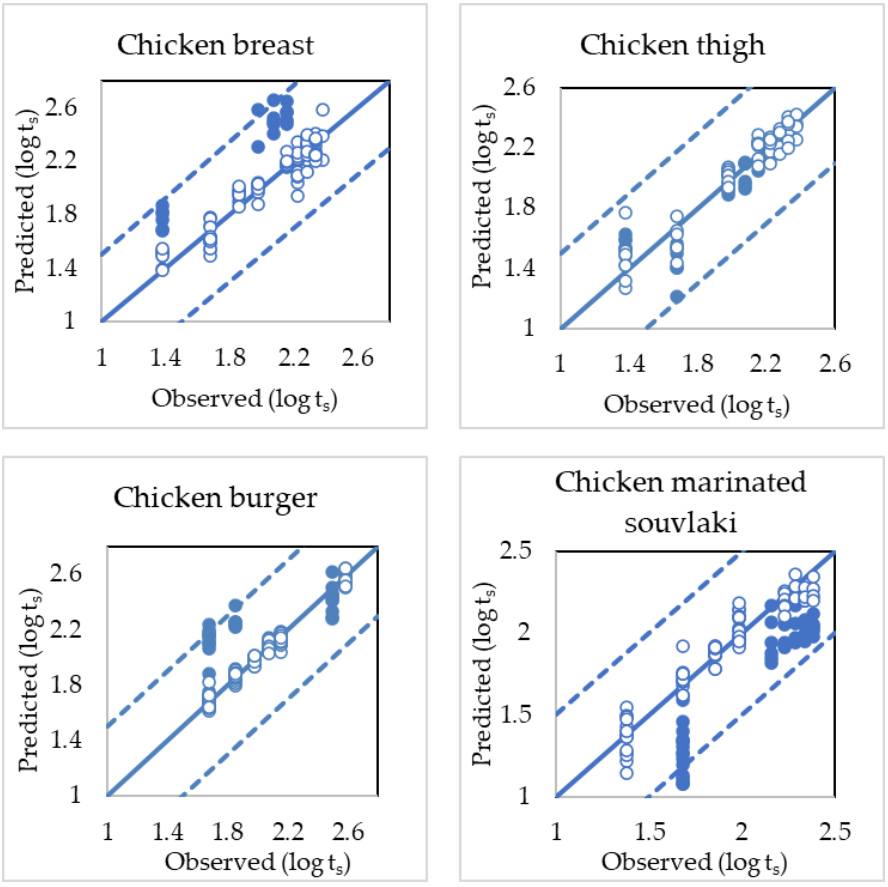

Figure 2.3: Comparison of observed (open symbols) and predicted (solid symbols) values of time from slaughter (log ts) after the development of the PLS-R model. Solid line depicts the line of equity (y = x) and dashed lines are ± 1.6 log ts (i.e., 48 h after slaughter).

Table 2.1: Performance indices (slope, offset, r and RMSE) for PLS-R model development and validation for each poultry product.

Poultry Product	Stage of Modelling	N_o of Samples	Slope	Offset	r (Correlation Coefficient)	RMSE
Chicken Breast	Calibration	82	0.933	0.138	0.966	0.076
	FCV[1]	82	0.916	0.173	0.953	0.091
	Prediction	22	1.150	0.055	0.886	0.383
Chicken Thigh	Calibration	67	0.953	0.097	0.976	0.065
	FCV	67	0.933	0.136	0.957	0.088
	Prediction	30	0.854	0.243	0.859	0.160
Chicken Burger	Calibration	87	0.982	0.035	0.991	0.033
	FCV	87	0.968	0.063	0.987	0.040
	Prediction	44	0.513	1.172	0.778	0.285
Chicken Marinated Souvlaki	Calibration	91	0.962	0.073	0.981	0.067
	FCV	91	0.954	0.092	0.964	0.093
	Prediction	43	1.183	0.650	0.934	0.348

[1]FCV: Full cross-validation.

The important wavelengths (mean values and standard deviations) reflecting the characteristics of spectral data for each poultry product were obtained based on the beta regression coefficients (**Figures 2.4–2.7**).

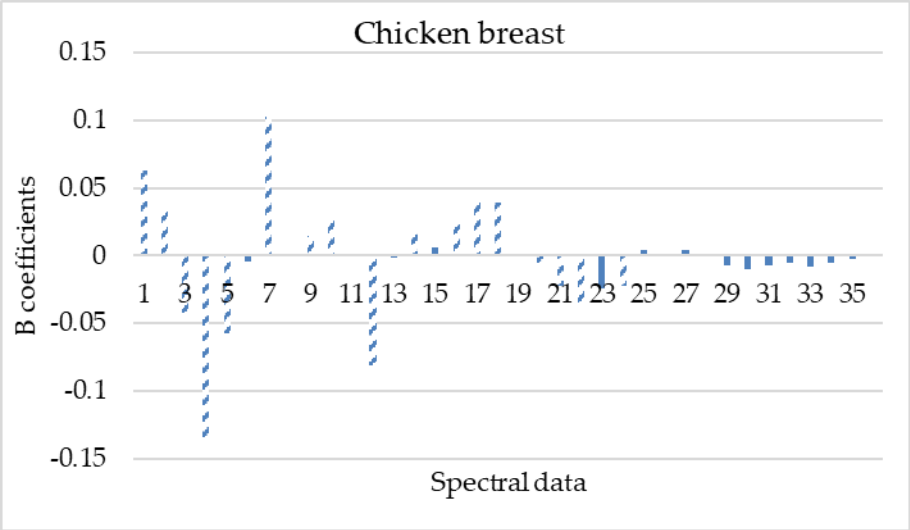

Figure 2.4: Spectral data (mean and standard deviation) influence (b coefficients) on PLS-R model construction for chicken breast samples. Dashed bars represent data that influenced more the model (1,19: 405 nm; 2, 20: 435 nm; 3, 21: 450 nm; 4, 22: 470 nm; 5, 23: 505 nm; 6, 24: 525 nm; 7, 25: 570 nm; 8, 26: 590 nm; 9, 27: 630 nm; 10, 28: 645 nm; 11, 29: 660 nm; 12, 30: 700 nm; 13, 31: 850 nm; 14, 32: 870 nm; 15, 33: 890 nm; 16, 34: 910 nm; 17, 35: 940 nm and 18, 36: 970 nm).

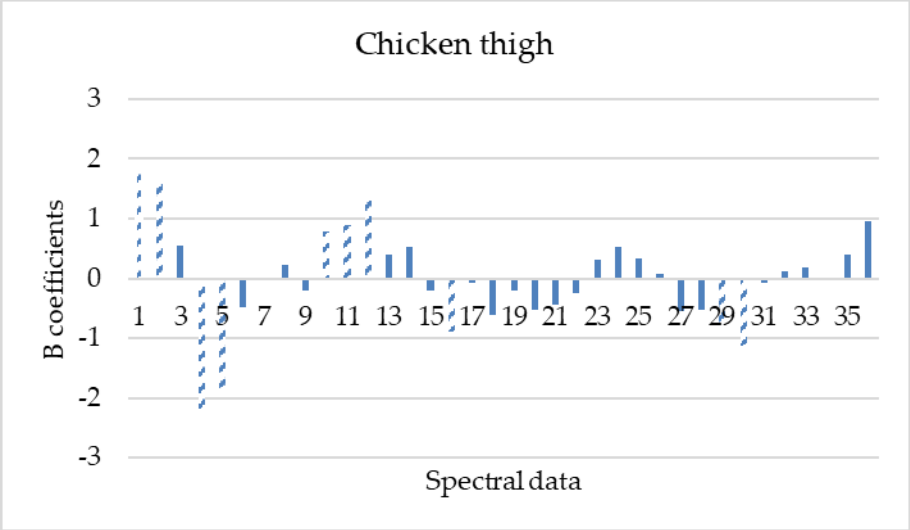

Figure 2.5: Spectral data (mean and standard deviation) influence (b coefficients) to PLS-R model construction for chicken thigh samples. Dashed bars represent data that influenced more the model (1, 19: 405 nm; 2, 20: 435 nm; 3, 21: 450 nm; 4, 22: 470 nm; 5, 23: 505 nm; 6, 24: 525 nm; 7, 25: 570 nm; 8, 26: 590 nm; 9, 27: 630 nm; 10, 28: 645 nm; 11, 29: 660 nm; 12, 30: 700 nm; 13, 31: 850 nm; 14, 32: 870 nm; 15, 33: 890 nm; 16, 34: 910 nm; 17, 35: 940 nm and 18, 36: 970 nm).

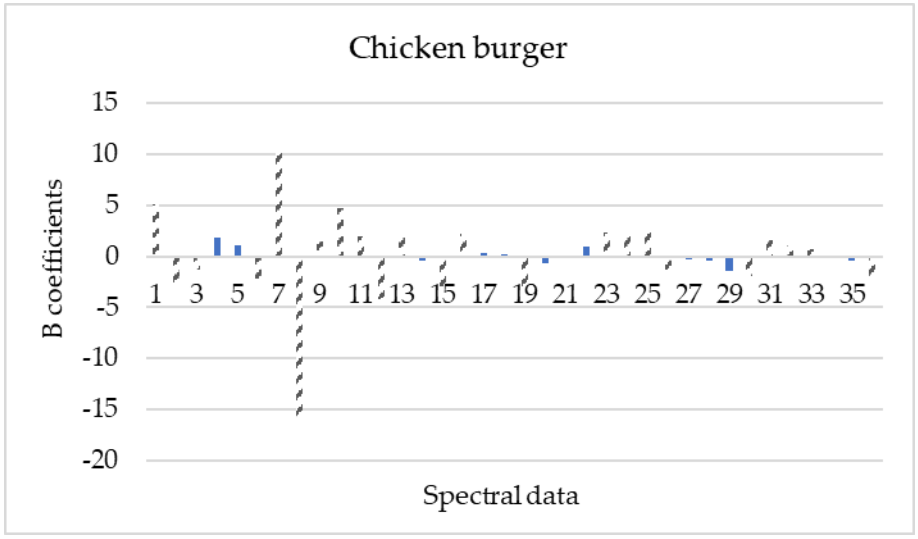

Figure 2.6: Spectral data (mean and standard deviation) influence (b coefficients) to PLS-R model construction for chicken burger samples. Dashed bars represent data that influenced more the model (1, 19: 405 nm; 2, 20: 435 nm; 3, 21: 450 nm; 4, 22: 470 nm; 5, 23: 505 nm; 6, 24: 525 nm; 7, 25: 570 nm; 8, 26: 590 nm; 9, 27: 630 nm; 10, 28: 645 nm; 11, 29: 660 nm; 12, 30: 700 nm; 13, 31: 850 nm; 14, 32: 870 nm; 15, 33: 890 nm; 16, 34: 910 nm; 17, 35: 940 nm and 18, 36: 970 nm).

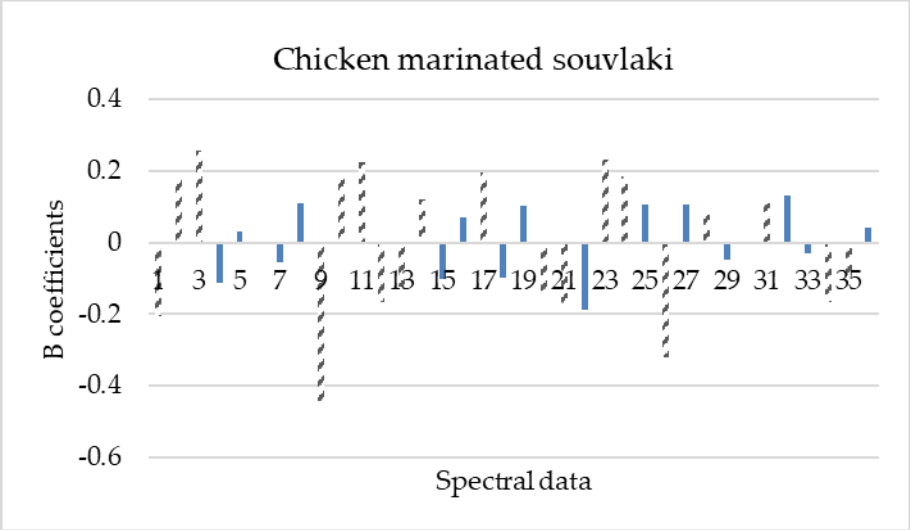

Figure 2.7: Spectral data (mean and standard deviation) influence (b coefficients) to PLS-R model construction for chicken marinated souvlaki samples. Dashed bars represent data that influenced more the model (1, 19: 405 nm; 2, 20: 435 nm; 3, 21: 450 nm; 4, 22: 470 nm; 5, 23: 505 nm; 6, 24: 525 nm; 7, 25: 570 nm; 8, 26: 590 nm; 9, 27: 630 nm; 10, 28: 645 nm; 11, 29: 660 nm; 12, 30: 700 nm; 13, 31: 850 nm; 14, 32: 870 nm; 15, 33: 890 nm; 16, 34: 910 nm; 17, 35: 940 nm and 18, 36: 970 nm).

Based on these beta regression coefficients, equations were constructed for the assessment of time from slaughter for each product (equations 2.4–2.7).

$$\mathbf{Y_{ts,chicken\ breast}} = 2.016 + 0.063\ X_{mean,405\ nm} + 0.033\ X_{mean,435\ nm} - 0.042\ X_{mean,450\ nm} - 0.134\ X_{mean,470\ nm} - 0.057\ X_{mean,505\ nm} + 0.103\ X_{mean,570\ nm} + 0.015\ X_{mean,630\ nm} + 0.027\ X_{mean,645\ nm} - 0.081\ X_{mean,700\ nm} + 0.012\ X_{mean,870\ nm} + 0.023\ X_{mean,910\ nm} + 0.040\ X_{mean,940\ nm} + 0.039\ X_{mean,\ 970\ nm} - 0.022\ X_{SD,450\ nm} - 3.505\ X_{SD,470\ nm} - 2.462\ X_{SD,505\ nm} - 0.023\ X_{SD,525\ nm} \quad (2.1)$$

$$\mathbf{Y_{ts,chicken\ thigh}} = -1.287 + 1.823\ X_{mean,405\ nm} + 1.596\ X_{mean,\ 435\ nm} - 2.277\ X_{mean,\ 470\ nm} - 1.835\ X_{mean,505\ nm} + 0.774\ X_{mean,645\ nm} + 0.901\ X_{mean,\ 660\ nm} + 1.407\ X_{mean,\ 700\ nm} - 0.888\ X_{mean,\ 910\ nm} - 0.754\ X_{SD,\ 660\ nm} - 1.135\ X_{SD,\ 700\ nm} \quad (2.2)$$

$$\mathbf{Y_{ts,chicken\ burger}} = 3.042 + 5.092\ X_{mean,405\ nm} - 2.948\ X_{mean,435\ nm} - 1.332\ X_{mean,450\ nm} - 2.205\ X_{mean,525\ nm} + 10.153\ X_{mean,570\ nm} - 15.754\ X_{mean,590\ nm} + 1.397\ X_{mean,630\ nm} + 4.716\ X_{mean,645\ nm} + 1.982\ X_{mean,660\ nm} - 4.230\ X_{mean,700\ nm} + 2.344\ X_{mean,850\ nm} - 2.989\ X_{mean,890\ nm} + 2.237\ X_{mean,910\ nm} - 3.283\ X_{SD,405\ nm} + 2.382\ X_{SD,505\ nm} + 2.161\ X_{SD,525\ nm} + 2.304\ X_{SD,570\ nm} - 1.799\ X_{SD,590\ nm} - 1.402\ X_{SD,660\ nm} - 1.874\ X_{SD,700\ nm} + 1.558\ X_{SD,850\ nm} + 1.112\ X_{SD,870\ nm} - 2.188\ X_{SD,970\ nm} \quad (2.3)$$

$$\mathbf{Y_{ts,chicken\ marinated\ souvlaki}} = 3.071 - 0.205\ X_{mean,405\ nm} + 0.180\ X_{mean,435\ nm} + 0.255\ X_{mean,450\ nm} - 0.442\ X_{mean,630\ nm} + 0.189\ X_{mean,645\ nm} + 0.223\ X_{mean,660\ nm} - 0.168\ X_{mean,700\ nm} - 0.122\ X_{mean,850\ nm} + 0.119\ X_{mean,870\ nm} + 0.196\ X_{mean,940\ nm} - 0.150\ X_{SD,435\ nm} - 0.185\ X_{SD,450\ nm} + 0.232\ X_{SD,505\ nm} + 0.184\ X_{SD,525\ nm} - 0.319\ X_{SD,590\ nm} + 0.091\ X_{SD,645\ nm} + 0.131\ X_{SD,870\ nm} - 0.165\ X_{SD,910\ nm} - 9.849\ X_{SD,940\ nm} \quad (2.4)$$

2.4. Discussion

Microbiological analysis demonstrated variations between batches for each category of poultry product even though the examined samples were obtained by the same farming conditions, slaughter process and production. For chicken breast and thigh samples, differences occurred at the initial microbial load (TVCs and *Pseudomonas* spp.) based mostly on animal strain and fat content (Amorim et al., 2016). Furthermore, in the case of processed poultry products, the presence of additional ingredients such as vegetables and herbs seemed to influence the initial and final load of microorganisms.

MSI acquisition showed variations in reflectance at many wavelengths between the four poultry products due to their differences in the food matrix (chicken breast and chicken thigh) and the supplementary ingredients used in the production process of different chicken products (i.e., burger and marinated souvlaki). Moreover, spectra figures for fresh and spoiled samples (**Figure 2.2**) provided by MSI application indicated reflectance differences at several wavelengths, which are firmly linked to biochemical alterations and metabolic compounds produced by the spoilage microbiota on the surface of meat and poultry products. More specifically, reflectance at 570–700 nm is related to respiratory pigments such as myoglobin (570 nm), oxymyoglobin (590 nm) and metmyoglobin (630 nm) (Cozzolino & Murray, 2004; Panagou et al., 2014; Pu et al., 2015). In the NIR region, absorption bands at 910 nm are linked to denaturation of proteins (Kamruzzaman et al., 2013; Ropodi et al., 2018) while at 750 and 970 nm, O-H second overtones are related to the moisture content in the samples (Xiaobo et al., 2010; Feng & Sun, 2013a; Dixit et al., 2017). In addition, absorption bands observed in the NIR region (928 and 940 nm) are correlated to the presence of fatty acids and fat within the sample matrix (Alomar et al., 2003; Kamruzzaman et al., 2013; Liu et al., 2014).

PLS-R models predicted satisfactorily the time from slaughter for each poultry product (**Table 2.1**) where the chicken thigh model showed the lowest value of RMSE followed by the chicken burger model. RMSE and r values of prediction were in the range of 0.160–0.348 and 0.778–0.943 respectively, for all PLS-R models. Model performance was gradually deteriorated from the calibration to the prediction stage. As illustrated in **Figure 2.3**, batches used in external validation differed from the calibration dataset in all products

and especially in the case of the chicken breast. These findings indicate the importance of performing validation with independent datasets (distinct batches) and to include as much variability as possible in the developed model (Boulesteix et al., 2006; Ropodi et al., 2016; Ropodi et al., 2018). Additionally, the developed model addressed for at-line implementation must be validated by an independent dataset in order to construct an accurate and robust model (Wold et al., 2001; Pu et al., 2015). Despite this variation in batches, both calibration and prediction datasets in **Figure 2.3** are situated within the limit area of ±1.6 log t_s resulting in acceptable PLS-R models. For chicken marinated souvlaki and burger models, variations between batches and higher RMSE values could be explained due to different types of ingredients such as spices, chopped vegetables and marinade employed in the production process.

Beta regression coefficients revealed the influence of each wavelength on the assessment of time from slaughter for each poultry product. According to **Figures 2.4–2.7**, wavelengths with high positive or negative values have an important contribution to the model and convey useful information. The comparison of these findings with the raw spectra shown in **Figure 2.2** confirms the significant role of reflectance bands in the range 570–700 nm and 700–970 nm for the development of PLS-R models (Park et al., 2002; Dixit et al., 2017). As mentioned above, absorption bands at NIR region of 910 nm seemed to be associated with proteins, which are in abundance in chicken meat, especially in chicken breast (Lin et al., 2011). The influence of muscle pigments and water content on the classification of chicken breast fillets was also highlighted by Yang et al. (2018) where samples were successfully classified in different quality grades (Yang et al., 2018).

Chapter 3: Spoilage assessment of chicken breast fillets by means of Fourier Transform Infrared spectroscopy (FT-IR) and Multispectral Image analysis (MSI)

Published as:

Spyrelli, E.D., Ozcan, O., Mohareb, F., Panagou, E.Z. and Nychas, G.J.E., 2021. Spoilage assessment of chicken breast fillets by means of fourier transform infrared spectroscopy and multispectral image analysis. Current Research in Food Science, 4, 121-131.

Abstract

The aim of this study was the evaluation of Fourier transform infrared spectroscopy (FT-IR) and multispectral image analysis (MSI) as efficient spectroscopic methods in tandem with multivariate data analysis and machine learning for the assessment of spoilage on the surface of chicken breast fillets.

For this purpose, two independent storage experiments of chicken breast fillets (n=215) were conducted at 0, 5, 10, and 15 ^{o}C for up to 480 h. During storage, samples were analyzed microbiologically for the enumeration of Total Viable Counts (TVCs) and *Pseudomonas* spp. In addition, FT-IR and MSI spectral data were collected at the same time intervals as for microbiological analyses. Multivariate data analysis was performed using two software platforms (a commercial and a publicly available developed platform) comprising several machine learning algorithms for the estimation of the TVCs and *Pseudomonas* spp. population of the surface of the samples. The performance of the developed models was evaluated by intra batch and independent batch testing. PLS-R models from the commercial software predicted TVCs with Root mean squared error of prediction (RMSE) values of 1.359 and 1.029 log CFU/cm^2 for MSI and FT-IR analysis, respectively. Moreover, RMSE values for *Pseudomonas* spp. model were 1.574 log CFU/cm^2 for MSI data and 1.078 log CFU/cm^2 for FT-IR data. From the implementation of the in-house sorfML platform, artificial neural networks (ANNs) and least-angle regression (lars) were the most accurate models with the best performance in terms of RMSE values. ANN models developed on MSI data demonstrated the lowest RMSE values (0.717 log CFU/cm^2) for intra-batch testing, while lars outperformed ANNs on independent

batch testing with RSME of 1.252 log CFU/cm^2. Furthermore, lars models excelled with the FT-IR data with RSME of 0.904 and 0.851 log CFU/cm^2 in intra-batch and independent batch testing, respectively. These findings suggested that FT-IR analysis is more efficient than MSI to predict the microbiological quality on the surface of chicken breast fillets.

3.1 Introduction

According to the Food and Agriculture Organization (FAO, 2019) around 14 % of the world's food is lost after harvest and before reaching the retail level, including on-farm activities, storage and transportation. A key to the reduction of food loss and waste is to improve the efficiency of the food system by monitoring each production stage carefully (FAO, 2019). At the same time, consumers' awareness and demand for high quality and safe food has been continuously arising, especially in the case of meat products. Poultry meat and more specifically chicken breast is one of the most preferable products due to its high protein content and low price (FAO, 2022). However, its susceptibility to spoilage (Dawson et al., 2013; Rouger, et al., 2017; Silva et al. 2018) necessitates the rapid quality assessment during production, transportation or retailing in order to avoid further food waste.

An alternative approach for rapid quality assessment, feasible by technology and science evolution, is the implementation of spectroscopic methods such as vibrational spectroscopy (FT-IR, NIR, Raman) (Argyri et al., 2013; Alamprese, Amigo, Casiraghi & Engelsen, 2016; Grassi & Alamprese, 2018), hyperspectral and multispectral imaging (Liu et al., 2014; Qin et al., 2013) and biomimetic sensors (e-nose, e-tongue) (Loutfi et al., 2015; Wojnowski et al., 2017). These nondestructive methods can be combined with microbiological, sensory and multivariate data analysis for the development of models evaluating meat quality. In addition, the developed models accompanied by their datasets could be uploaded and maintained in cloud data repositories, updated constantly with new data in order to be consultative to food industries (Nychas et al., 2016; Tsakanikas et al., 2020).

In the last decade, the performance of instruments based on light emission interaction with the surface according to its chemical and physical properties (Hyper and Multispectral Imaging) or vibrational spectroscopy (FT-IR) has been investigated in the evaluation of quality characteristics of various food commodities (Prieto et al., 2009; Xiong et al., 2015). Both spectroscopic methods have been proven promising and effective for the development of predictive models assessing the quality and microbiological load in many meat products (Pu et al., 2015). Specifically, for poultry products qualitative models have been constructed and evaluated for the classification of intact chicken breast fillets based on hyperspectral analysis (Yang et al., 2018). Moreover, qualitative as well as quantitative models developed on spectral data (400–1100 nm) could determine bacterial counts during spoilage of chicken meat (Feng & Sun, 2013a; Feng et al., 2013). Likewise, Alexandrakis et al. (2012) proposed FT-IR as effective method for the discrimination of intact chicken breast muscle during spoilage. The potential of FT-IR to accurately detect spoilage bacteria on the surface of chicken meat has been also confirmed by Ellis et al. (2002).

An important and challenging decision in the development of predictive models with spectral data is the performance of the optimum machine learning algorithm resulting in efficient models that describe more accurately the dynamics of microorganisms during spoilage. Until now, many algorithms have been employed in the rapid assessment of meat quality through several software applications (Chen et al., 2011; Kamruzzaman et al., 2015). SorfML is a publicly available Web platform that has the flexibility to provide rapid screening of experimental data by allowing the development and validation of a variety of linear and non-linear algorithms (Estelles-Lopez et al., 2017; Manthou et al., 2020). This leverage allows user to investigate data's tendency, exclude models with poor performance and compare the most accurate ones. Additionally, it enables the comparison of different sensors' performance in order to facilitate the selection of the most reliable analysis/sensor for food quality assessment.

The aim of this research was (i) to develop models derived from different analytical instruments (FT-IR and MSI) assessing the microbiological quality of chicken breast fillets during storage at isothermal conditions, (ii) to assess the performance of different machine learning algorithms and analytical platforms, based on a commercial software and a

publicly available Web platform, to monitor the population dynamics of spoilage microorganisms during storage, and (iii) to infer on the potential and limitations of each analytical tool.

3.2 Materials and Methods

3.2.1 Experimental design

Chicken breast fillets (*ca*. 245-280 g per fillet) were obtained from a Greek poultry industry and transported under refrigeration immediately to the laboratory. The samples were supplied by the industry in plastic packages (width: 25 cm, thickness: 90 μm, permeability of ca. 25, 90, 6 $cm^3\ m^{-2}day^{-1}bar^{-1}$ at 20 °C and 50 % RH for CO_2, O_2 and N_2, respectively) and stored aerobically at four isothermal conditions (0, 5, 10, 15 ^oC) for up to 480 h depending on storage temperature. At regular time intervals, spectral data (FT-IR and MSI) were collected from the surface of chicken meat samples and correlated with microbiological data. Two independent experiments were undertaken with two different chicken meat batches and duplicate samples were analyzed from each sampling point and storage temperature. Storage of samples was terminated at 480 h at 0 ^oC while for the highest storage temperature (15 °C) the duration of the experiments was 168 h. All samples originated from Ross strains broilers with the same feeding, farming and slaughtering conditions. Feeding was customized by the company and comprised of grain, wheat, maize, soya bean oil and meat and premix for broilers (vitamin and mineral supplement). Chickens were slaughtered after 3 months of age and all stages of production were in compliance with EU regulations (823/2004, 824/2004, 834/2004 and 543/2008).

3.2.2 Microbiological analysis

A slice of 20 cm^2 (maximum thickness 2 mm) from the surface of chicken breast fillet was removed aseptically using a sterile stainless steel cork borer (2.5 cm in diameter), scalpel and forceps, added to 100 ml of sterile quarter strength Ringer's solution (Lab M Limited, Lancashire, United Kingdom) and homogenized in a Stomacher device (Lab Blender 400, Seward Medical, United Kingdom) for 120 s at room temperature. Serial decimal dilutions were prepared in the same medium and 1.0 or 0.1 ml of the appropriate dilutions were spread or poured on the following media: a) Tryptic glucose yeast agar (Plate Count Agar, Biolife, Milan, Italy) for the enumeration of Total Viable Counts

(TVCs) incubated at 25 ^{o}C for 72 h; b) Pseudomonas Agar Base with selective supplement cephalothin-fucidin-cetrimide (LabM Limited, Lancashire, United Kingdom) for the enumeration of *Pseudomonas* spp. after incubation at 25 ^{o}C for 48 h. After incubation, typical colonies for each microbial group were enumerated and colony counts were logarithmically transformed and expressed as log CFU/cm^2. Further on, the primary model of Baranyi and Roberts (1994) was fitted to the growth data of TVCs and *Pseudomonas* spp. to determine the kinetic parameters of microbial growth (maximum specific growth rate and lag phase duration).

3.2.3 Gas composition

Prior to microbiological analysis, the gas composition in the headspace of the packages was analyzed using a Dansensor CheckMate 9900 gas analyzer (PBI-Dansensor A/S, Ringsted, Denmark) to monitor the changes in the concentration (%) of O_2 and CO_2 during storage.

3.2.4 Spectra acquisition

3.2.4.1 Multispectral imaging

MSI spectra were captivated via Videometer-Lab instrument (Videometer A/S, Herlev, Denmark) which frames surface reflectance of samples from 18 different monochromatic wavelengths (405–970 nm), namely: 405, 435, 450, 470, 505, 525, 570, 590, 630, 645, 660, 700, 850, 870, 890, 910, 940 and 970 nm. The organology of this sensor and the image acquisition is thoroughly described in previous publications (Dissing et al., 2013; Fengou et al., 2019). The result of the measurement is a data cube comprised of spatial and spectral data for each sample of size m×n×18 (where m×n is the image size in pixels) (Tsakanikas et al., 2015). Furthermore, a segmentation process is required for the selection of the Region of interest (ROI) on the samples surface. This process is accomplished by Canonical Discriminant Analysis (CDA) and it is implemented by Videometer-Lab version 2.12.39 software (Videometer A/S, Herlev, Denmark).

3.2.4.2 FT-IR spectroscopy

FT-IR measurements were performed using a ZnSe 45 HATR (Horizontal Attenuated Total Reflectance) crystal (PIKE Technologies, Madison, Wisconsin, United

States), and a FT-IR-6200 JASCO spectrometer (Jasco Corp., Tokyo, Japan). The measurement crystal shows a refractive index of 2.4 and a depth of penetration of 2.0 μm at 1000 cm^{-1}. Spectra were obtained at the wavenumber range of 4000 to 400 cm^{-1} using Spectra Manager Code of Federal Regulations (CFR) software version 2 (Jasco Corp., Tokyo, Japan), by accumulating 100 scans with a resolution of 4 cm^{-1} and a total integration time of 2 min.

3.2.5 Data analysis

3.2.5.1 PLS-R unscrambler

For the development of PLS-R models assessing TVCs and *Pseudomonas* spp. counts the statistical software The Unscrambler © ver.9.7 (CAMO Software AS, Oslo, Norway) was used. Prior to analysis, MSI data were pretreated by Standard Normal Variate (SNV) transformation for the exclusion of collinear and "noisy" data (Bi et al., 2016). Likewise, FT-IR spectral data were subjected to Savinsky- Golay pre-treatment (second polynomial order, 1st derivative, 9-point window) (independent variables = 829) to minimize baseline shifts and noise (Rinnan et al., 2009; Alamprese et al., 2016). Additionally, wavenumbers in the range of 900–2000 cm^{-1} were utilized for the analysis as suggested by other researchers (Argyri et al., 2013; Ropodi et al., 2018). Calibration and full cross validation (leave-one-out cross validation) were conducted using one batch (n = 115) and prediction was implemented by the second batch (n = 99). Independent variables for PLS-R models were the spectral data acquired by MSI and FT-IR and TVCs and *Pseudomonas* spp. counts were considered as dependent variables.

3.2.5.2 Using SorfML for model development and validation

An alternative approach was investigated by the implementation of the sorfML software (www.sorfml.com), in which nine algorithms were considered for the prediction of TVCs counts, namely Partial-least squares (pls) (Geladi & Kowalski, 1986); Support vector machine with linear kernel (svmLinear) (Cortes & Vapnik, 1995); Support vector machine with radial basis function kernel (svmRadial); Random forests (rf) (Breiman, 2001); K-nearest neighbours (knn) (Cover and Hart, 1967); Principal component regression (pcr) (Jolliffe, 1982); Least-angle regression (lars) (Loubes & Massart, 2004); Ridge regression (ridge) (Hoerl & Kennard, 1970); Artificial neural networks (nnet) (Jain

et al., 1996). Spectral data were mean-centered and standardized prior to analysis. This modification allows every variable equal opportunity to influence the final statistical model (Verboven et al., 2012). FT-IR spectral data set was constricted from 800 to 4000 cm^{-1}.

Another point of attention in the sorfML software analysis was the splitting procedure of the data sets, which consisted of two phases (**Figure 3.1**). In the first one, the dataset (one batch) was separated randomly into training and testing sets with a 70%–30% split. Each machine learning algorithm was applied to the training set using repeated k-fold cross validation (k = 10, repeats = 3) and grid search to obtain best performing models with the optimal parameters. After model development, prediction was undertaken by the test set to assess overall performance which is firmly depended on the random training/test split undertaken. In order to provide an appropriate and unbiased outcome, Monte Carlo cross validation was implemented (k = 100) for a number of times with different training and test splits, and giving an average of the performance of all iterations (Xu and Liang, 2001). In the second phase, one batch was trained with k-fold cross validation (k = 10, repeats = 3) and the best model was validated on the other batch (B1 on B2: B1 as training set and B2 as testing one; B2 on B1: B2 as training set and B1 as testing one).

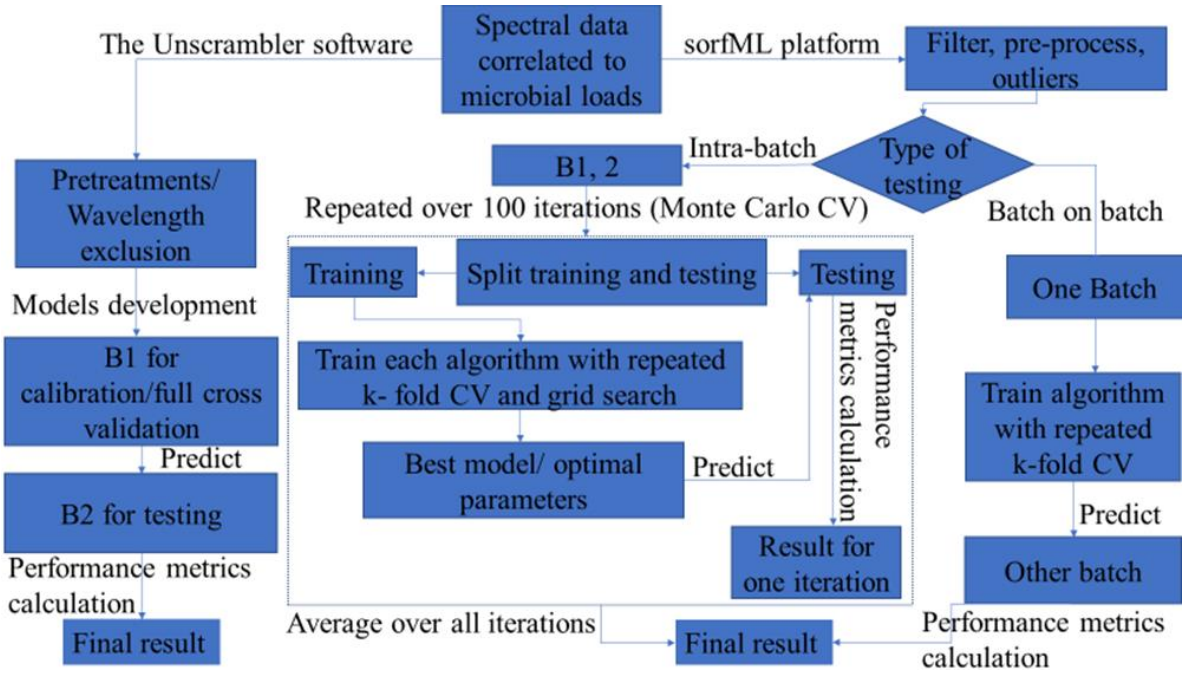

Figure 3.1: Flowchart describing model's development and validation though The Unscrambler and sorfML via data processing stage.

3.2.6 Model performance indices

The assessment of model performance was based on the calculation of the root mean squared error (RMSE) (Sant'Ana et al., 2012; Feng et al., 2013), mean absolute error (MAE) (Sang et al., 2008), coefficient of determination (R^2) (Asuero et al., 2006) and accuracy index. Unlike classification models, accuracy in the case of quantitative models could be defined as TVC predictions within 1 log CFU/cm^2 off the actual (observed) values (Estelles-Lopez et al., 2017). Supplementary to these metrics, r (correlation coefficient) was computationally calculated via the Unscrambler software. Even though the above-mentioned performance metrics were calculated, models' accuracy on prediction was assessed based on RMSE values.

3.3 Results

3.3.1 Microbiological analysis

The microbial population of TVCs and *Pseudomonas* spp. on the surface of chicken breast fillets for each storage condition is presented in **Figure 3.2**. The initial load of TVCs was 3.3 and 2.9 log CFU/cm^2 in B1 and B2, respectively. Likewise, *Pseudomonas* spp. was enumerated at the beginning of storage at 2.0 and 2.1 log CFU/cm^2 for B1 and B2, respectively. Storage temperature seemed to significantly influence the growth of chicken's microbiota as inferred by the respective kinetic parameters for TVCs and *Pseudomonas* spp. as derived by the primary growth model of Baranyi and Roberts (1994) (Appendix I, **Table 3A**). Specifically, the lag phase duration and μ_{max} of *Pseudomonas* spp. of chicken samples stored at 0 ^{o}C were 72.2 h and 0.036 h^{-1}, respectively. On the contrary, samples stored at 15 ^{o}C exhibited μ_{max} and lag phase duration of *Pseudomonas* spp. at 0.241 h^{-1} and 8.8 h, respectively.

TVCs and *Pseudomonas* spp. counts in B1 and B2 presented variations during storage at 0 and 5 ^{o}C but always within the range of ± 1 log unit. At the end of storage, TVCs and *Pseudomonas* spp. counts on samples from B1 were 6.2 and 5.7 log CFU/cm^2, respectively. Similarly, for B2 samples the level of final TVCs and *Pseudomonas* spp. counts was 6.3 and 5.5 log CFU/cm^2, respectively. For B1 at 5 ^{o}C the number of TVCs and *Pseudomonas* spp. after a period of 360 h was 6.8 and 6.6 log CFU/cm^2, respectively, while for B2 at the same storage conditions, TVCs and *Pseudomonas* spp. counts were 7.6 and

6.2 log CFU/cm^2, respectively. This difference in microbial counts was expected as samples of B1 and B2 were collected with an interval of 4 months (winter- spring) to take into account seasonal variation. It is also worth noting that in all storage conditions, the final number of TVCs ranged between 6.2-7.6 log CFU/cm^2, unlike other studies reporting spoilage level of poultry meat at 7.0-8.0 log CFU/cm^2 (Rouger et al., 2017). The lower TVCs values during spoilage of poultry meat observed in this work could be attributed to the non-permeable film used by the poultry company as packaging material. Indeed, the percentage of CO_2 inside the packages at the end of storage was 14.3 % and 47.5 % for samples stored at 0^o C and 15^o C, respectively (Appendix I, **Figure 3A**).

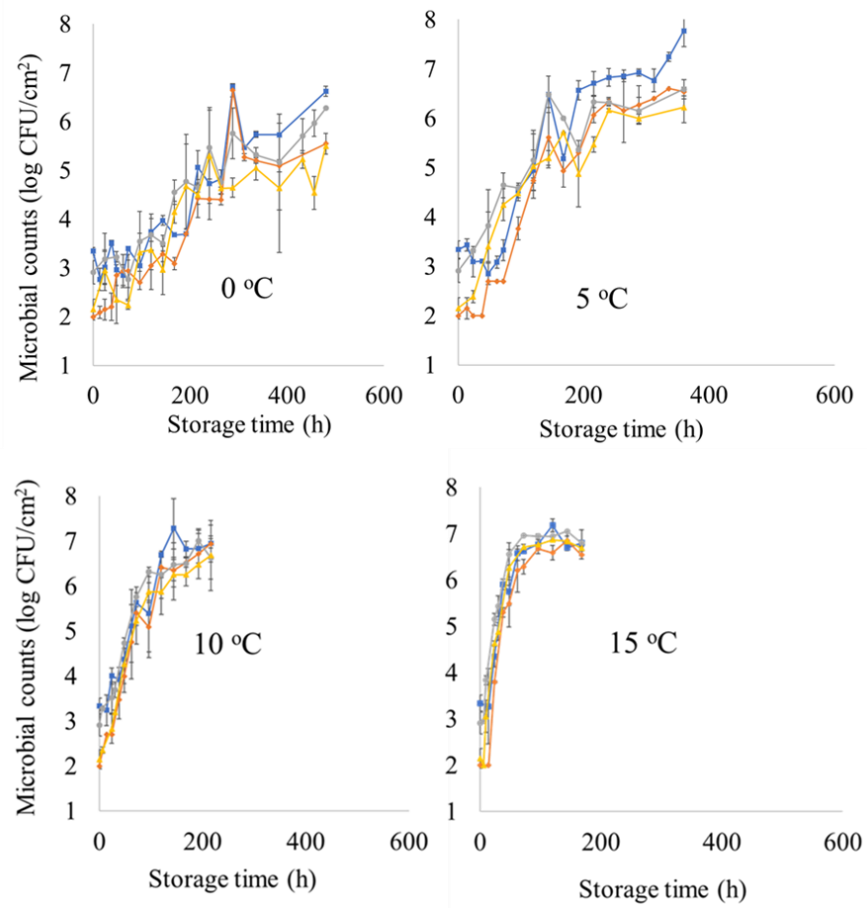

Figure 3.2: Microbial counts of TVCs (batch 1: blue line), *Pseudomonas* spp. (batch 1: orange line), TVCs (batch 2: grey line) and) and *Pseudomonas* spp. (batch 2: yellow line) on the surface of chicken breast fillet samples stored at 0, 5, 10 and 15 °C.

3.3.2 Spectral measurements

Typical MSI and FT-IR spectra of fresh (0 h corresponding to 3.3 log CFU/cm^2) and spoiled (456 h corresponding to 5.9 log CFU/cm^2) chicken breast fillet samples are illustrated in **Figures 3.3, 3.4**, respectively. The comparison of reflectance in MSI spectra between fresh and spoiled samples confirmed the role of myoglobin in meat color assessment (570 to 700 nm). Concerning FT-IR spectra, the contribution of the absorption bands in the range of 1,400-1,800 cm^{-1} for the prediction of the microbial counts on the surface of samples is highlighted in **Figure 3.4**. The absorbance in this region is mainly related to the metabolic fingerprint of samples which is derived from the metabolic activity of microorganisms during spoilage procedure (Alexandrakis et al., 2012).

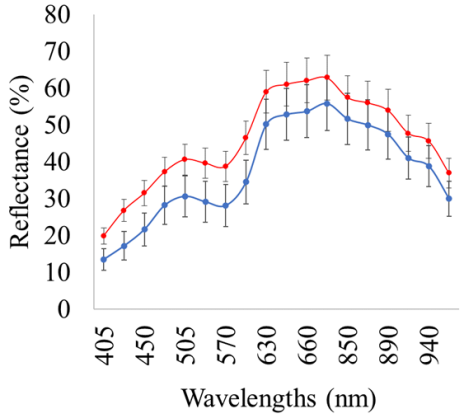

Figure 3.3: Spectrum of fresh (blue line, storage time: 0 h) and spoiled (red line, storage time: 456 h) chicken breast fillet samples stored at 0 ºC from MSI spectra (wavelengths: 405- 970 nm).

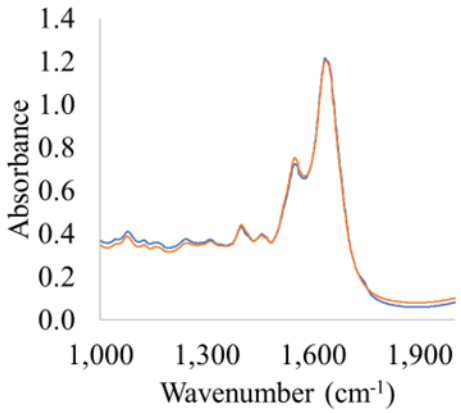

Figure 3.4: Spectrum of fresh (blue line, storage time: 0 h) and spoiled (red line, storage time: 456 h) chicken breast fillet samples stored at 0 ^{o}C from FT-IR measurements (wavelengths: 1,000- 2,000 cm^{-1}).

3.3.3 Models assessing microbial population via MSI analysis

Performance metrics (r, RMSE, MAE, accuracy) as well as linear parameters (slope, offset) are provided in **Table 3.1** for PLS-R model calibration, cross-validation and prediction, estimating the level of TVCs and *Pseudomonas* spp. on the surface of chicken breast fillets via MSI analysis. More specifically, RMSE and r values ranged between 0.752- 1.359 log CFU/cm^2 and 0.604- 0.876, respectively for the estimation of TVCs counts when B1 was used as training set and B2 as testing set. Similar performance was observed for PLS-R model assessing *Pseudomonas* spp. counts. In this case, the values of r increased from 0.665- 0.905, while RMSE exhibited values in the range of 0.724 to 1.574 log CFU/cm^2. Additionally, a graphical approach of these linear models is represented in **Figure 3.5** where predicted vs observed TVCs and *Pseudomonas* spp. counts are illustrated. Beta coefficients of the models are provided in order to comprehend the contribution of specific wavelengths to model development. As demonstrated in **Figure 3.6**, six of the 36 spectral variables were important in model optimization as their beta coefficients significantly differed from those of the other wavelengths. Wavelengths influencing PLS-R model were 630, 645 and 660 nm. Likewise, high values of b coefficients noticed at 850, 890 and 940 nm.

Table 3.1: MSI model performance parameters (slope, offset, Latent variables LVs,) and metrics (r, RMSE, MAE, Accuracy %).

TVCs	N	LVs	slope	offset	Correlation coefficient r	RMSE (log CFU/cm^2)	MAE	% Accuracy
Calibration	115[a]	9	0.768	1.177	0.876	0.752		
FCV	115[a]	9	0.719	1.428	0.807	0.931		
Prediction	100[b]		0.534	3.139	0.604	1.359	1.042	59
***Pseudomonas* spp.**								
Calibration	115[a]	10	0.818	0.817	0.904	0.724		
FCV	115[a]	10	0.766	1.035	0.843	0.920		
Prediction	100[b]		0.597	2.930	0.664	1.574	1.276	51

[a] data set from batch 1; [b] data set from batch 2; LVs: Latent variables; FCV: Full-cross validation

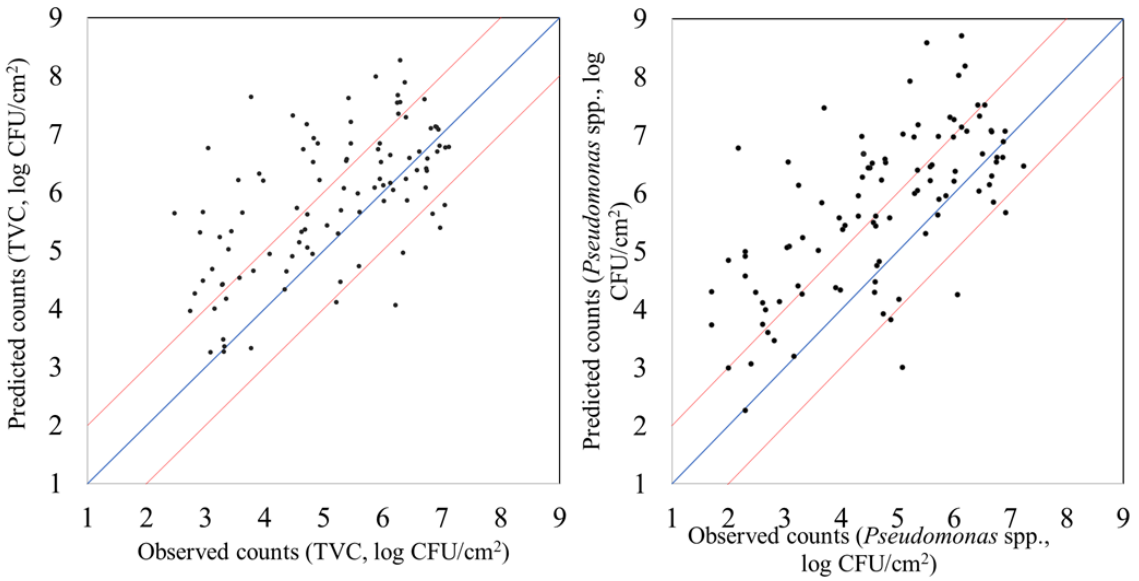

Figure 3.5: Predicted versus observed TVCs and *Pseudomonas* spp. counts after MSI models validation. Blue line depictures the line of equity (y=x) and red lines indicate ± 1 log unit area.

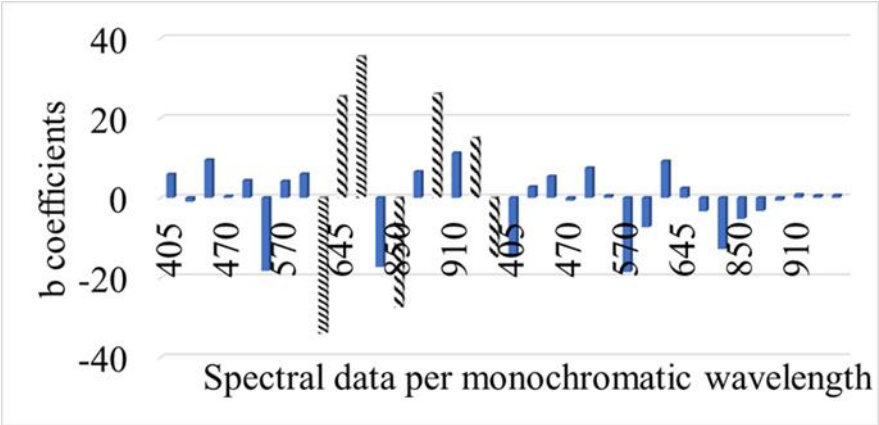

Figure 3.6: b coefficients of PLS-R model for MSI analysis per monochromatic wavelength from 405 to 970 nm. Dashed bars represent data per wavelength that influenced more model's performance.

Results for MSI spectral data after the implementation of 9 algorithms via sorfML platform consisting of internal testing on B1 and B2, averaged over 100 iterations (Monte Carlo cross validation) are shown in **Figure 3.7**. RMSE values ranged from 0.717 to 1.387 log CFU/cm^2, MAE from 0.554 to 1.158, R^2 from -12.064 to 0.725 and accuracy from 43.5 % to 84.1 %. The highest performance was achieved with nnet with RMSE value of 0.717 log CFU/cm^2 on B1 and 0.752 log CFU/cm^2 on B2 . Additionally, other machine learning algorithms such as ridge, lars, pcr, pls and svmLinear performed equally well with RMSE values below 0.78 log CFU/cm^2.

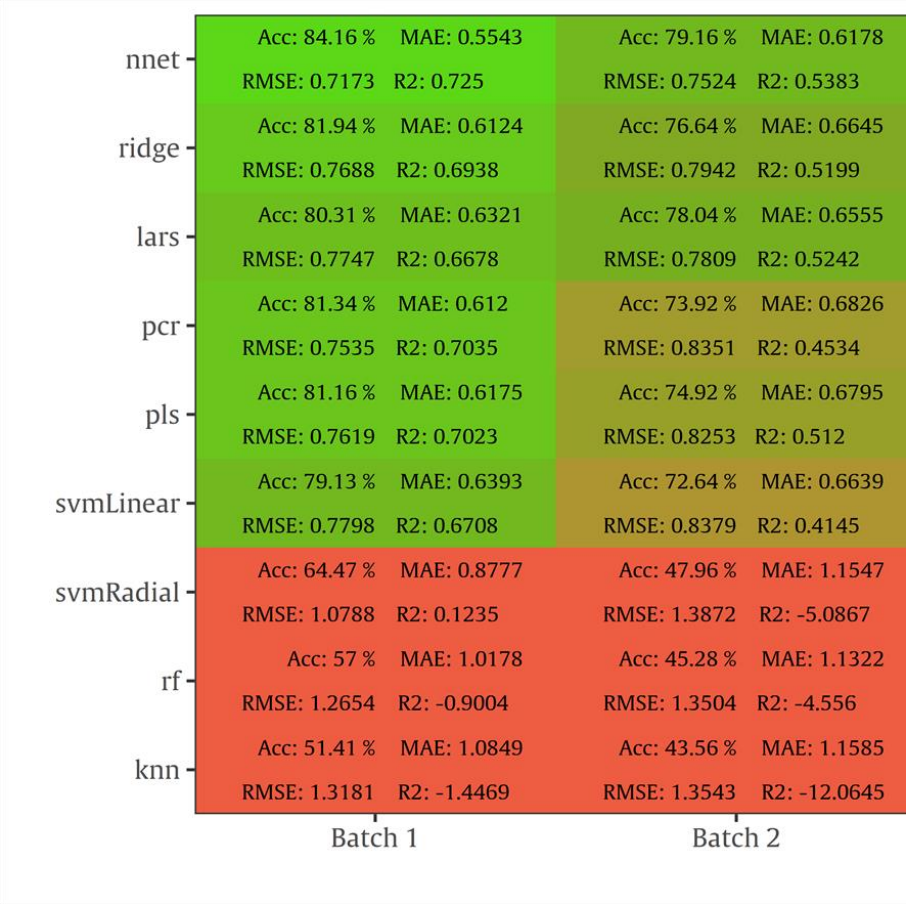

Figure 3.7: Performance metrics (Accuracy, MAE, RMSE, R^2) of MSI models with intra-batch validation.

Following the same approach, results for batch-on-batch are provided in **Figure 3.8**. A less satisfactory performance can be observed compared to intra-batch testing, with RMSE values ranging from 1.252 to 1.995 log CFU/cm^2, MAE from 0.993 to 1.710, R^2 from -23.368 to 0.246 and accuracy from 27 to 56 %. More specifically, the models developed on B1, predicted TVC population from B2 with around 0.3 higher performance on RMSE values. In contrast to intra- batch case, the highest performance was accomplished by lars with RMSE of 1.252 log CFU/cm^2. Model's optimization with B1 exhibited low values of RMSE (1.251 versus 1.544 log CFU/cm^2 for lars model). However, in the case of B2 as a calibration data set, R^2 values presented improved values, especially when lars, pls and ridge algorithms were applied.

Figure 3.8: Performance metrics (Accuracy, MAE, RMSE, R^2) of MSI models with batch-on-batch validation. Model B1 on B2 was developed via batch 1 and tested via batch 2. The reversed procedure was followed for B2 on B1.

3.3.4 Models assessing microbial population via FT- IR analysis

The findings of models predicting TVCs and *Pseudomonas* spp. counts with FT-IR measurements are shown in **Figure 3.9- 3.12**. Performance metrics for PLS-R models are also provided in **Table 3.2** for calibration, cross- validation and prediction procedures where B1 was used for model development and B2 for testing. For the estimation of TVCs on chicken breast, RMSE and r demonstrated values 0.739- 1.029 log CFU/cm^2 and 0.679-0.882, respectively. PLS-R model for *Pseudomonas* spp. via FT-IR exhibited r values of 0.739-0.916 and RMSE values were from 0.683 to 1.077 log CFU/cm^2. The influence of each spectral variable is illustrated in **Figure 3.10** in terms of beta coefficients of the PLS-

R models per wavenumber. The main region between 1,004 to 1,222 cm^{-1} contained interesting information and therefore had great impact on model development. Absorption bands of 1,230-1,403 cm^{-1} were considered as important for the prediction of TVCs and *Pseudomonas* spp. Beta coefficients of 1,432- 1,498 cm^{-1} as well as 1,549- 1,584 cm^{-1} and 1,658- 1,704 cm^{-1} had impact on model construction.

Table 3.2: FT-IR model performance parameters (slope, offset, Latent variables LVs,) and metrics (r, RMSE, MAE, Accuracy %).

TVCs	N	LVs	slope	offset	Correlation coefficient r	RMSE (log CFU/cm²)	MAE	% Accuracy
Calibration	115[a]	5	0.777	1.128	0.882	0.739		
FCV	115[a]	5	0.654	1.805	0.778	0.989		
Prediction	99[b]		0.493	2.883	0.679	1.029	0.861	65
***Pseudomonas* spp.**								
Calibration	115[a]	5	0.839	0.723	0.916	0.683		
FCV	115[a]	5	0.669	1.528	0.749	1.155		
Prediction	99[b]		0.682	1.767	0.739	1.077	0.894	65

[a] data set from batch 1; [b] data set from batch 2; LVs: Latent variables; FCV: Full-cross validation

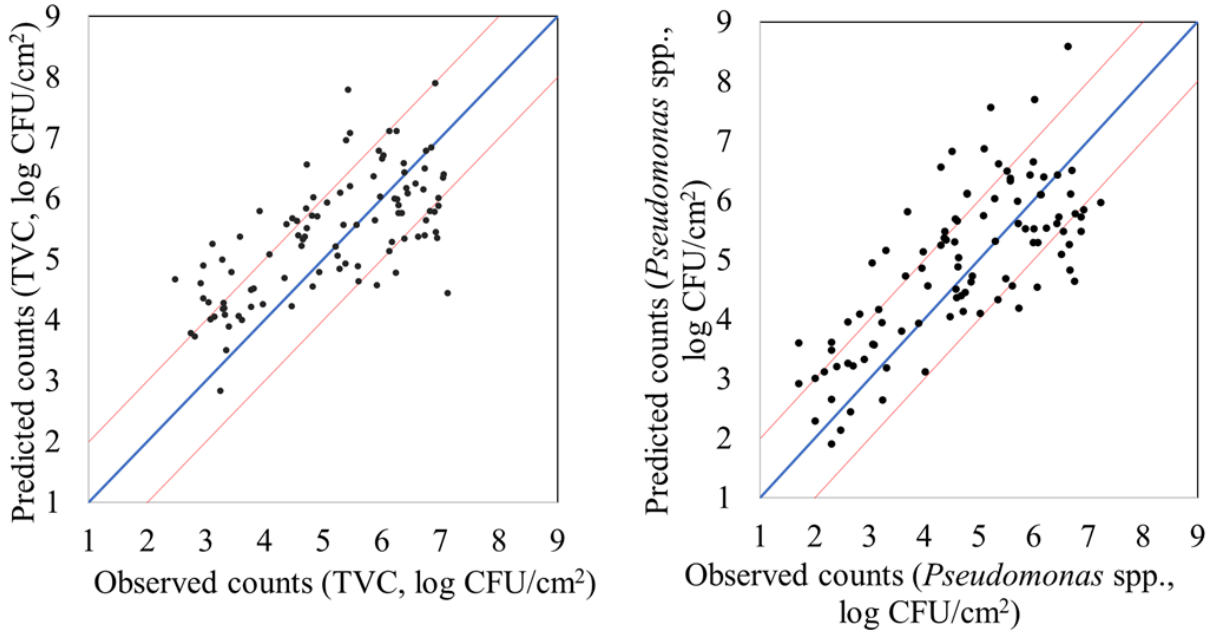

Figure 3.9: Predicted versus observed TVCs and Pseudomonas spp. counts after FT-IR models validation. Blue line depictures the line of equity (y = x) and red lines indicate ± 1 log unit area.

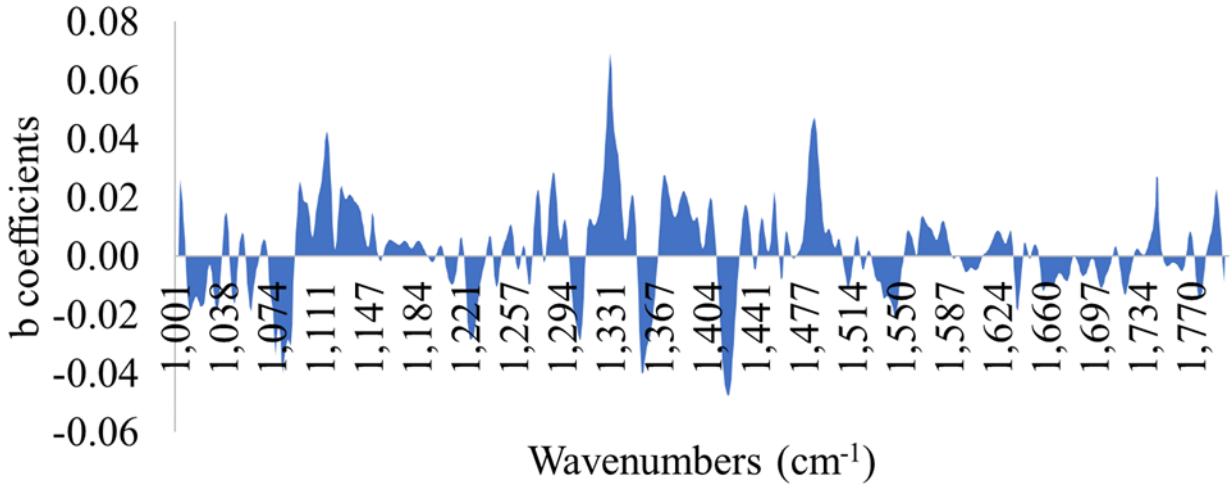

Figure 3.10: b coefficients of PLS-R model for FT-IR analysis for each wavelength within 1,000-1,800 cm^{-1}.

The results for intra batch training for FT-IR data are summarized as a heatmap in **Figure 3.11** containing also the performance metrics for the 9 algorithms. RMSE values ranged from 0.857 to 1.536 log CFU/cm^2, MAE from 0.669 to 1.164, R^2 from -3.129 to 0.546, and accuracy from 50.0 to 75.9 %. As **Figure 3.11** indicates, prediction on B2 was more accurate than B1 based on RMSE values. Nnet exhibited acceptable performance on B1 with 1.047 log CFU/cm^2 for RMSE, while lars and svmLinear algorithms performed better with RMSE being at 0.904 and 0.954 log CFU/cm^2, respectively for B2.

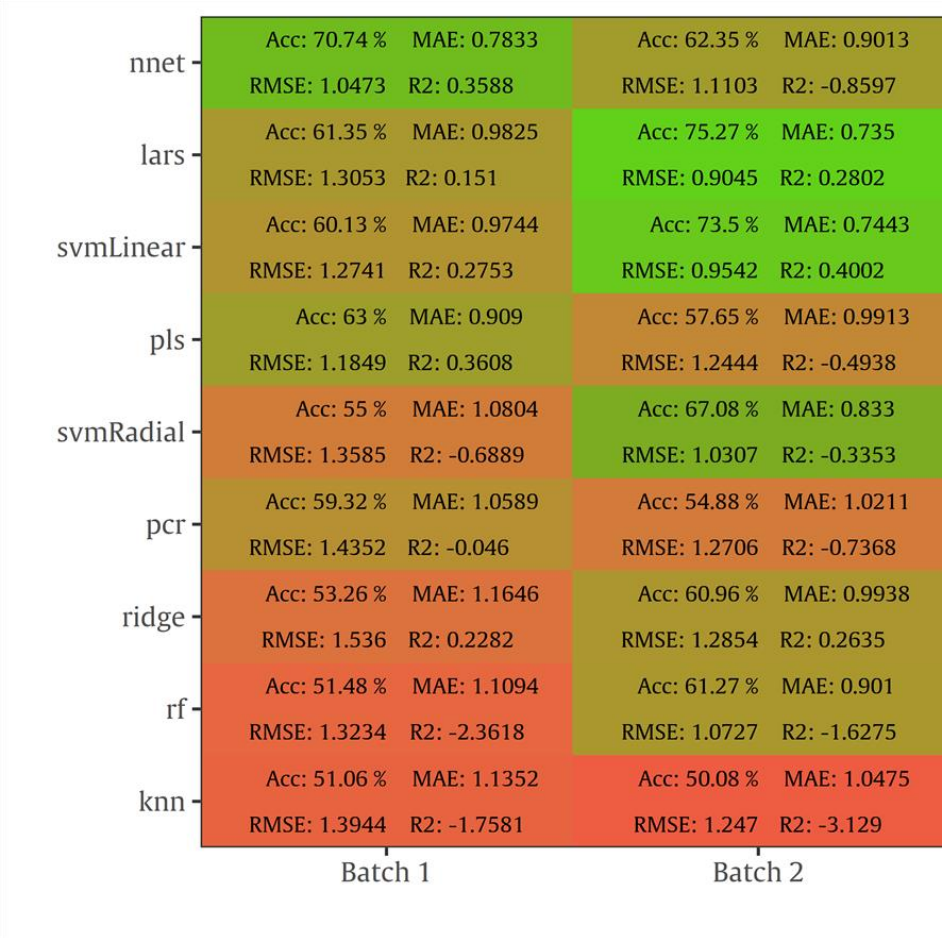

Figure 3.11: Performance metrics (Accuracy, MAE, RMSE, R^2) of FT-IR models with intra-batch validation.

Likewise, batch-on-batch prediction metrics are represented in **Figure 3.12**. In comparison to MSI models, FT-IR models predicted TVCs counts satisfactory when B1 was used as training set. RMSE values ranged from 0.851 to 3.924 log CFU/cm^2 while training model on B1 and validating on B2 outperformed the second model around significantly with 55% lower RMSE. More specifically, nnet accomplished the lowest RMSE (0.851 log CFU/cm^2) and MAE (0.67 log CFU/cm^2) over the other algorithms as well as models trained on B2 and validated on B1.

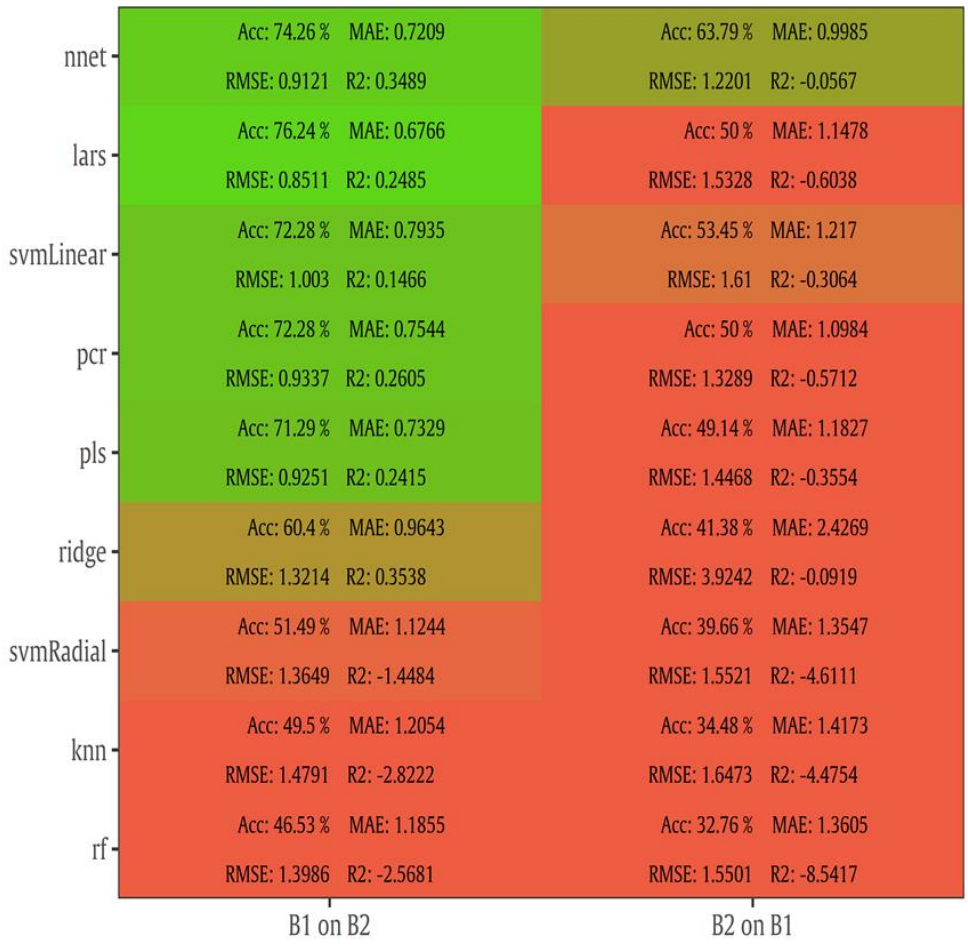

Figure 3.12: Performance metrics (Accuracy, MAE, RMSE, R^2) of FT-IR models with batch-on-batch validation. Model B1 on B2 was developed via batch 1 and tested via batch 2. The reversed procedure was followed for B2 on B1.

3.4 Discussion

The initial population of TVCs and *Pseudomonas* spp. was 3.1 (± 0.29) and 2.1 (± 0.15) log CFU/cm^2, respectively, which is considered low compared to published data where the respective counts for TVCs and *Pseudomonas* spp. were above 5.0 and 3.5 log CFU/cm^2, respectively (EFSA, 2016; Rouger et al, 2017). As presented in **Figure 3.2**, the final population of microbiota was considerably low in the case of samples stored at 0 ^{o}C in comparison to the threshold of spoilage of other meats (*ca.* 7.0-8.0 log CFU/cm^2) (Nychas et al., 2008). Unlike literature (Rouger et al., 2017), *Pseudomonas* spp. counts were enumerated at the final sampling point at 0 ^{o}C below 7 log CFU/cm^2 (Al-Nehlawiet al., 2013), due to the fact that packaging film did not permit diffusion of gases. Therefore,

the produced CO_2 from microbiota's metabolic reactions acted as modified atmosphere packaging (Koutsoumanis et al., 2008, Liang et al., 2012, Holl et al., 2016). The differences between and within batches could be attributed to animals' variations (Marcato et al., 2006), alterations of nutrition (Sakomura et al., 2015) as well as by the time of the year (winter-summer), slaughtering and distributing to retail points (Nychas et al., 2008; Collins et al., 2015). It is worth noting that the 2 analyzed chicken breast fillet samples per sampling point could not be from the same chicken as they were randomly selected.

For MSI spectral data, model performance metrics predicted RMSE from 0.739 to 1.536 log CFU/cm^2. For the prediction of TVCs and *Pseudomonas* spp. counts with PLS-R models, RMSE was 1.359 and 1.574 log CFU/cm^2, respectively. It needs to be noted that all developed models presented the tendency of overestimating the predicted counts. The increased RMSE values could be further improved (reduced) by applying alternative algorithms and sample splitting. Indeed, the assessment of TVCs counts by sorfML platform showed satisfactory results, especially in the case of intra-batch validation and nnet algorithm. In this model, RMSE presented the lowest value (0.717 log CFU/cm^2) while for ridge model RMSE was 0.769 log CFU/cm^2. On the contrary, for batch-on-batch validation, three algorithms were considered acceptable for the evaluation of TVCs, with lars model having RMSE of 1.252 log CFU/cm^2 followed by pls and ringle models with1.319 and 1.262 log CFU/cm^2, respectively.

FT-IR models showed satisfactory prediction of counts, with performance metrics achieving better values than MSI. For PLS-R models, TVCs and *Pseudomonas* spp. counts were predicted with RMSE being 1.029 and 1.078 log CFU/cm^2, respectively. For intra batch testing, nnet algorithm for B1 and lars for B2 were considered effective for the evaluation of TVCs, with lars having lower RMSE (0.905 log CFU/cm^2) than nnet (1.047 log CFU/cm^2). In contrast, in batch-on-batch validation, RMSE value for nnet (B1 on B2: 0.912 log CFU/cm^2) were higher than lars where RMSE had the lowest value (0.851 log CFU/cm^2).

The differentiation of model performance for the 2-sensor analysis highlights the important role of splitting process, data set selection and algorithm during model's optimization. One significant factor for accurate prediction is inter-batch variability.

Moreover, MSI results on intra-batch performance and its low RMSE suggested that this analysis could be applicable for internal validation or quality control in the production line. The latter option has been confirmed via experiments performed in the production line of chicken products at industrial level (Spyrelli et al., 2020). Furthermore, the fundamental role of training and testing data set definition is demonstrated by FT-IR lars model during B1 on B2 validation, which significantly outperformed batch-on-batch performance of MSI (RMSE: 0.851 vs 1.251 log CFU/cm^2). Additionally, several models of FT-IR were able to attain respectable prediction on different data sets.

Another step affecting model's performance is the selection of the appropriate cross-validation procedure. Leave-one out cross validation (LOOCV) implemented for PLS-R models is a variant of *k*-fold cross-validation which removes only one sample at a time from the training set and considers it as a test set. Subsequently, for this case *k* is equal to the number of objects. This method may be useful for small database size presenting the problem of the inability to divide the data set into fairly sized subsets for training and test sets. However, this cross-validation approach can lead to overfit when the sample size is not large enough, and thus, results in high prediction error (Beruetta et al., 2007). In contrast, *k*-fold validation separates training data into *k* random groups, trains the model on *k*-1 groups and evaluates it on the remaining group. This is iterated for each unique group, and for repeated k-fold cross validation, the whole process is repeated for the specified times. Overlapping within training and testing data set was avoided (k=100) with Monte Carlo cross validation by repeating the process outlined above for a number of times with different training and test splits and by averaging the performance of all iterations (Xu & Liang, 2001). Regarding machine learning algorithms implemented for intra- and batch on batch models, artificial neural network (nnet) and least-angle regression (lars) exhibited better performance metrics overall than other models. The former algorithm is considered as a suitable for spectral data sets due to its high tolerance to noisy data. On the other hand, the accuracy of lars might be explained by its ability in dealing with correlated predictors which are abundant in the existing datasets. Moreover, overfitting could be eliminated by reducing predictors range, while simultaneously this reduction could lead to an increasement of the generalising ability of the models (Hesterberg et al., 2008).

The influence of certain wavelengths to MSI model development was documented via b coefficient values for PLS-R models (**Figure 3.6**). Reflectance intensity at 570–700 nm is related to the presence of respiratory pigments such as myoglobin (570 nm), oxymyoglobin (590 nm) and metmyoglobin (630 nm) (Panagou et al., 2014; Pu et al., 2015). Fatty acids and fat within the food matrix were mainly responsible for the intensity at 928 and 940 nm while reflectance at 910 nm is evidence of protein denaturation (Kamruzzaman et al.,2015; Ropodi et al., 2018). Proteins and proteolysis products are in abundance in chicken meat, especially in chicken breast (Lin et al., 2011) and hence absorption band at 910 nm is considered as one of the most significant wavelengths for quality assessment on chicken breast fillets. Moreover, O-H second overtones observed at 750 and 970 nm are related to the moisture content in the raw samples (Dixit et al., 2017; Xiaobo et al., 2010). The influence of muscle pigments and water content on the classification of chicken breast fillets was also highlighted by Yang et al. (2018), where samples were successfully classified in different quality grades.

The b coefficients of PLS-R models (**Figure 3.10**) for FT-IR spectral data revealed the important contribution of certain wavelengths in model development. Absorption bands at 1,011, 1,032 and 1,111-1,143 cm^{-1} were related to polyglycines, polysaccharides (C-O stretch) and amines (NH_2 rock/twist), respectively (Böcker et al., 2007). Specifically, the absorption at 1032 cm^{-1} which corresponds to polysaccharides, could be associated to biofilm formation by *Pseudomonas* spp. on stored chilled meat (Liu et al., 2015; Wickramasinghe et al., 2019; Wickramasinghe et al., 2020). Additionally, high absorption occurred in the regions of 1,222-1,230 cm^{-1}, 1,284-1,289 cm^{-1} and 1,345-1,352 cm^{-1} which are linked to the presence of lipids, nucleic acids (asym PO_2-stretch), amines from free amino acids and amide III (Argyri et al., 2014). The critical role of amides and free amines for the prediction of spoilage in meat is presented via high b coefficients at 1,369-1,426 cm^{-1} and 1,464-1,567 cm^{-1} (Böcker et al., 2007). These outcomes are in compliance to the existing literature where absorption bands of 1,650, 1,550 and 1,400- 1,200 cm^{-1} are linked to amide I, II and III and subsequently to the proteolytic activity of *Pseudomonas* spp. on meat (Nychas & Tassou, 1997; Ellis et al., 2002). Especially for chicken breast analysis via FTIR and NIR spectroscopy, the estimation of spoilage in intact chicken breast muscle was influenced by the absorption bands at 1,080, 1,550 and 1,640 cm^{-1} and the increased

content in free amino acids and peptides as a result of proteolysis during storage maintenance (Alexandrakis et al., 2012). In another study the estimation of microbial spoilage was attempted at 600-1,110 cm^{-1} where the findings indicated the region of 1,000–1,060 cm^{-1} corresponding to protein functional group, such as R-CO-NH_2, R-NH_2,R-CO-NH-R and R-NH-R as the most significant (Lin et al., 2004).

Chapter 4: Implementation of spectroscopic sensors and multivariate data analysis for the assessment of quality on chicken breast fillets

Abstract

Multivariate data analysis and pattern recognition methods coupled with nondestructive spectroscopic techniques have manifested their potential as powerful techniques assessing food quality. In this context, Multispectral Imaging (MSI) and Fourier Transform Infrared Spectroscopy (FT-IR) were employed together with machine learning techniques for the construction of qualitative models evaluating spoilage of chicken breast meat. For this purpose, chicken breast samples (n= 427) were subjected to spoilage experiments for up to 480 h at isothermal conditions (0, 5, 10, 15, 20, 25, 30, and 35 ^{o}C) and dynamic temperature profiles (winter and summer transportation scenarios). The samples were analyzed microbiologically for the determination of Total Viable Counts (TVCs), while in parallel MSI and FT-IR measurements were performed. Moreover, sensory analysis was undertaken by a 14- member untrained sensory panel for the evaluation of fresh and spoiled samples. Based on the sensory results the threshold TVCs value corresponding to the shelf-life of the samples was 6.2 log CFU/cm^2. According to this limit, samples were separated in two classes (fresh and spoiled) that were further correlated to MSI and FT-IR spectra for the development of classification models. Eight machine learning models (single-based and ensemble) were investigated for their efficacy to identify spoilage whereas their performance was validated by an independent data set from the two dynamic temperature profiles. MSI analysis and subspace ensemble exhibited the highest overall accuracy of prediction (64.8 %), while this combination demonstrated also acceptable values of specificity and sensitivity (69.7 %). On the contrary, FT-IR features presented better performance with Partial Least Squares- Discriminant Analysis (PLS-DA), as the samples were classified correctly with an overall accuracy of 67.6 %. However, in all cases of algorithms developed on FT-IR data, the misclassification rate of spoiled samples as fresh was 36.7%. These results suggest that spectroscopic methods and the developed models could be beneficial for the rapid assessment of quality in the poultry industry and simultaneously result in significant reduction in food waste.

4.1 Introduction

The continuous technology evolution and consumers expectation for food of high quality and safety resulted in the development of smart spectroscopic sensors assessing quality and freshness in foods and in particular in meat products (Tsakanikas et al., 2020). Nevertheless, in the last decade food waste increased (FAO, 2021) and the significant economic losses for the meat industry dictated the necessity for alternative rapid methods to assess microbial quality and freshness (Lytou et al., 2016), especially for poultry products (raw or processed) due to their short shelf life. Unlike the conventional methods (e.g., microbiological, chemical, sensory, molecular analysis) which are time consuming and destructive, these smart devices are non- invasive, easily established and applied at-, in- or on-line while they enhance productivity in the meat industry (Sørensen et al., 2012; Dixit et al., 2017; Prieto et al., 2017).

In recent years, many researchers have proposed spectroscopic methods such as Fourier-Transform Infrared spectroscopy (FT-IR), Near Infrared spectroscopy (NIR), Hyperspectral imaging (HSI), and Multispectral imaging (MSI) as alternative approaches for the assessment of quality on a variety of meat products (Panagou et al., 2014; Porep et al., 2015; Alamprese et al., 2016; Xiong et al., 2015). MSI analysis is a combination of spectroscopy (visible and NIR region) to computer vision and it has been recommended for the rapid assessment of meat quality (Pu et al., 2015; Ropodi et al., 2018; Fengou et al., 2019). Specifically, for poultry products qualitative models have been developed for the classification of intact chicken breast fillets based on three quality grades via hyperspectral analysis (Yang et., 2018). Quantitative and/or qualitative models in the visible and near-infrared region (400–1700 nm) have been successfully employed for the assessment of the bacterial population on chicken meat (TVCs and *Pseudomonas* spp.) during spoilage (Feng and Sun, 2013a, b; Ye et al., 2016). In addition, multispectral imaging was suggested for its potential to identify adulteration of minced beef with chicken meat (Kamruzzaman et al., 2016), fecal contaminants in a poultry line (Yang et al., 2005) and tumors on the surface of chicken breasts (Nakariyakul & Casasent, 2009). Moreover, the potential of at-line application of multispectral imaging in a poultry processing industry was investigated, as well as its efficacy to determine the time from slaughter in four different poultry products (Spyrelli et al., 2020).

Regarding the use of FT-IR in food science, there is evidence of its efficiency on the qualitative and quantitative evaluation of meat products (Argyri et al., 2010; Argyri et al., 2013; Ropodi et al., 2018). This vibrational method was proposed by Alexandrakis et al. (2012) as an effective method for the discrimination of intact chicken breast muscle during spoilage. Additionally, FT-IR detected accurately the level of spoilage bacteria on the surface of chicken meat (Ellis et al., 2002). Likewise, this spectroscopic method is documented as promising, real- time method for the evaluation of freshness on stored chicken breast fillets (Vansconcelos et al., 2014). Recently, a workflow has been reported for the recognition of chicken meat among seven raw types of food via FTIR approach despite of variations among batches and storage conditions (temperature, duration, packaging, spoilage levels) (Tsakanikas et al., 2020).

For the accurate and rapid assessment of quality in food matrices and specifically in meat, many researchers employ quantitative and qualitative machine learning algorithms in tandem with spectroscopic methods (Berrueta et al., 2007; Jiménez-Carvelo et al., 2019). Common tools involved in the development of predictive models for spoilage or adulteration assessment in meat are Artificial Neural Networks (ANNs), Partial Least Squares Regression (PLS- R), Partial Least Squares Discriminant Analysis (PLS-DA), Linear Discriminant Analysis (LDA), Support Vector Machines (SVM), Random Forests (RF) and k-Nearest Neighbors (kNN) (Kamruzzaman et al., 2016; Falkovskaya and Gowen, 2020). Nowadays, there are available websites (e.g., sorfML, Metaboanalyst) or softwares (The Unscrambler, R, MatLab, Python) which allow the user to develop, validate and compare simultaneously the above-mentioned algorithms in order to develop the best model describing food spoilage (Ropodi et al., 2016; Jiménez-Carvelo et al., 2019; Fengou et al., 2020; Tsakanikas et al., 2020). For instance, sorfML is an online platform that provides the flexibility to apply different supervised machine learning algorithms simultaneously, while there is also feasibility for the comparison of different sensors performance (Estelles-Lopez et al., 2019; Manthou et al., 2020).

Furthermore, another modeling approach that has recently drawn the attention of data scientists is the construction of ensemble learning methods. Ensemble methods medley multiple well-known algorithms, by creating smaller subsets into the data, training different classifiers with these partitions and combining their outputs, while they have demonstrated

improved performance compared to the outcome from their single base learners (Polikar, 2006). Until now, the implementation of these techniques has been investigated in many scientific fields as face and emotion recognition, text classification, medical diagnosis and financial forecasting (Pintelas & Livieris 2020). In the last decades, boosting, bagging, random forest (Jimenez-Carvelo et al., 2019) and random subset-based strategy (Rokach, 2010) have been employed for the development of reliable classification models in foods such as beef fillets (Mohareb et al., 2016), minced meat, green olives, beer and oil (Kucheryavskiy, 2018).

The aim of this research was the development of individual machine learning classification models and ensemble models coupled to MSI and FT-IR spectral data for the evaluation of chicken breast fillets quality. The models were developed with data obtained from storage experiments of chicken breast fillets at isothermal conditions and validated on two different dynamic temperature profiles simulating temperature alterations during transportation in winter and summer season.

4.2 Materials and Methods

4.2.1 Experimental design

Chicken breast fillets (*ca.* 245- 280 g per fillet) were obtained from a Greek poultry industry and transferred immediately to the laboratory under controlled temperature (1.77 ± 2.70 ^{o}C). Samples were enclosed in plastic packages (length: 25cm, width: 25 cm, thickness: 90 μm, permeability of *ca.* 25, 90, 6 cm^3 $m^{-2}day^{-1}bar^{-1}$(1 bar= 10^5Pa) at 20°C and 50% RH for CO_2, O_2 and N_2, respectively) and stored aerobically at eight isothermal conditions (0, 5, 10, 15, 20, 25, 30, and 35 ^{o}C). Additionally, samples were stored at two dynamic temperature conditions simulating transportation in the winter and summer (summer scenario:12 h at 5 ^{o}C, 8 h at 10 ^{o}C and 4 h at 15 ^{o}C; winter scenario: 12 h at 0 ^{o}C, 8 h at 5 ^{o}C and 4 h at 10 ^{o}C). Samples were placed in high precision (±0.5 ^{o}C) incubation chambers (MIR-153, Sanyo Electric Co., Osaka, Japan) where temperature was recorded every 20 min by means of data loggers (CoxTracer, Belmont, N.C.). At pre- determined intervals, samples were subjected to microbiological analysis and spectral data acquisition by means of MSI and FT-IR. Two independent experiments were undertaken for each storage condition with duplicate samples analyzed per sampling point for isothermal

storage conditions, whereas in the case of dynamic temperature profiles chicken samples were analyzed in triplicate.

Microbiological and sensory data were initially used for the determination of two quality classes, namely fresh and spoiled. Further on, the spectral data from MSI and FT-IR were correlated to the two quality classes and models were developed for the qualitative assessment of spoilage (fresh and spoiled) of chicken breast fillets.

4.2.2 Microbiological analysis

Four slices of 5 cm^2 (total surface: 20 cm^2, maximum thickness: 2 mm) from the surface of chicken breast fillets were removed aseptically, using a sterile stainless steel cork borer (diameter: 2.5 cm), scalpel and forceps, diluted to 100 ml of sterile quarter strength Ringer's solution (Lab M Limited, Lancashire, United Kingdom) and homogenized in a Stomacher device (Lab Blender 400, Seward Medical, United Kingdom) for 120 s at room temperature. The indigenous microbiota on the surface of samples was determined using serial decimal dilutions in the same medium and 0.1 ml was spread on Tryptic glucose yeast agar (Plate Count Agar, Biolife, Milan, Italy) for the enumeration of Total Viable Counts (TVCs) incubated at 25 ^oC for 72 h. TVCs counts were logarithmically transformed and expressed as log CFU/cm^2. Results are presented as average values (± standard deviation) of the 4 samples analyzed at each sampling point. Further on, the primary model of Baranyi and Roberts (1994) was fitted to the growth data of TVCs to determine the kinetic parameters of microbial growth, namely maximum specific growth rate (μ_{max}) and lag phase duration (λ) using Microsoft® Excel Add-in curve-fitting program DMFit, Version 3.5 available at www.combase.cc.

4.2.3 Sensory analysis

In parallel to sampling, samples were placed in sterile petri dishes and were exhibited at room temperature and artificial light for sensory evaluation. Panel of 14 individuals evaluated samples (n= 120) as fresh or spoiled based on odor with a 3point hedonic scale 1- 3, namely: 1=fresh, 2= acceptable, 3= spoiled (Lytou et al., 2016). Sensory evaluation results of odor were correlated with TVCs in order to define the number of TVCs corresponding to spoiled samples (i.e., sensory scores above 2). Based on this TVCs value,

spectral data were coupled to sensory results (class 1: fresh; class 2: spoiled) for the development of classification models assessing spoilage in chicken breast fillets.

4.2.4 Spectra acquisition

MSI spectra were captured using a Videometer-Lab instrument (Videometer A/S, Herlev, Denmark) which frames surface reflectance of samples from 18 different wavelengths (405-970 nm), namely 405, 435, 450, 470, 505, 525, 570, 590, 630, 645, 660, 700, 850, 870, 890, 910, 940, and 970 nm. The organology of this sensor and the image acquisition process are described in detail in previous publications (Dissing et al., 2013, Fengou et al., 2019). The result of the measurement is a data cube comprised of spatial and spectral data for each sample of size m×n×18 (where m×n is the image size in pixels) (Tsakanikas et al., 2015). Furthermore, a segmentation process is required for the isolation of the Region of interest (ROI) on the samples surface. For each image, the mean reflectance spectrum was calculated by taking into account the average value and the standard deviation of the intensity of pixels within the ROI at each wavelength. This process is accomplished by Canonical Discriminant Analysis (CDA) and it is implemented by Videometer-Lab version 2.12.39 software (Videometer A/S, Herlev, Denmark).

FT-IR measurements were performed using a ZnSe 45 HATR (Horizontal Attenuated Total Reflectance) crystal (PIKE Technologies, Madison, Wisconsin, United States) and a FT-IR-6200 JASCO spectrometer (Jasco Corp., Tokyo, Japan). The measurement crystal shows a refractive index of 2.4 and a depth of penetration of 2.0 μm at 1000 cm^{-1}. Spectra were obtained in the wavenumber range of 4000 to 400 cm^{-1} using Spectra Manager Code of Federal Regulations (CFR) software version 2 (Jasco Corp., Tokyo, Japan), by accumulating 100 scans with a resolution of 4 cm^{-1} and a total integration time of 2 min.

4.2.5 Data processing

4.2.5.1 Data pre- processing for MSI and FT-IR analysis

MSI spectral data (n=368) were comprised of 18 mean values and the respective 18 standard deviations of the intensity in pixels. Prior to analysis, the data set was modified by Standard Normal Variance (SNV) transformation for the limitation of collinear and

"noisy" data areas (Bi et al., 2016). The data set from the storage experiments at isothermal conditions (n=368) was used in model calibration, where 222 (60.3%) and 146 (39.7%) of the samples were defined as fresh (Class 1) and spoiled (Class 2), respectively. Model optimization was undertaken with k- validation process (k-fold validation, k=5). The developed models were validated using independent data sets from dynamic temperature conditions simulating transportation scenarios in the winter and summer period (n=71; Class 1: 38 samples (52.5%); Class 2: 33 samples 46.5 %).

Pre-treatment of FT-IR spectral data (n= 829) by Savinsky- Golay (second polynomial order, 1st derivative, 9-point window) was considered necessary for the reduction of baseline shift and noise (Alamprese et al., 2016). Furthermore, wavelengths in the range of 900-2000 cm^{-1} were employed in the analysis as suggested by previous researchers for meat (Ropodi et al., 2018, Fengou et al., 2020). Model's development (calibration and k-cross validation: k- fold, k=5) was conducted by data set from isothermal conditions of storage (n=360), where 219 (60.8 %) were fresh, and 141 (39.2 %) spoiled. Data set from dynamic temperature profiles (n=67) was utilized for validation, with fresh samples being 37 (55.2 %) and spoiled being 30 (44.8 %).

4.2.5.2 Machine learning algorithms and models performance evaluation

The level of spoilage on the surface of chicken breast fillets was assessed by eight algorithms, namely: a) Partial Least Squares-Discriminant Analysis (PLS-DA) (Barker & Rayens, 2003; Indahl et al., 2007) via Unscrambler© ver. 9.7 software (CAMO Software AS, Oslo, Norway); b) Linear Discriminant Analysis (LDA) (Kim et al., 2011); c) Linear Support Vector Machines (LSVM) (Cortes & Vapnik, 1995); d) Quadratic Support Vector Machine, (QSVM) (Osuna et al., 1997); e) *k*-Nearest Neighbor classification **(**fine-KNN) (Cover & Hart, 1967); g) decision tree-simple (Loh, 2011); f) subspace (Ho, 1998); h) rusboosted (Seiffert et al., 2008; Hu et al., 2014) via MATLAB 2012a software (The MathWorks, Inc., Natick, Massachusetts, USA). The last two algorithms are a combination of multiple classifiers in order to achieve high prediction accuracy (Arafat et al., 2019). Further information concerning the parameters and the corresponding function of each model is presented in Appendix I (**Tables 4A** and **4B**).

Model performance was evaluated by the following indices: overall accuracy, overall error, sensitivity, specificity and precision for model k-cross validation and prediction (**Table 4.1**) (Sokolova & Lapalme, 2009; Arafat et al., 2019).

Table 4.1: Performance indices for the assessment of model's performance (Sokolova & Lapalme, 2009; Arafat et al., 2019)

Performance index	Equation
Overall accuracy (%)	$\frac{tp + tn}{tp + fn + fp + tn}$
Overall error (%)	$\frac{fn + fp}{tp + fn + fp + tn}$
Sensitivity (%)	$\frac{tp}{tp + fn}$
Specificity (%)	$\frac{tn}{fp + tn}$
Precision (%)	$\frac{tp}{tp + fp}$

n: number of samples; tp: positive samples classified correctly; tn: negative samples classified correctly; fn: negative samples classified as positive; fp: positive samples classified as negative;

4.3 Results

4.3.1 Microbiological analysis

The loads of TVCs (log CFU/cm^2) of stored chicken breast fillet samples at 0-15 ^{o}C and 20-35 ^{o}C are illustrated in **Figures 4.1** and **4.2**, respectively. Additionally, the microbiological results from the dynamic temperature profiles simulating two scenarios during transportation are provided in **Figures 4.3** and **4.4**. The initial TVCs in chicken samples stored at isothermal conditions ranged from 3.13 (± 0.30) to 3.24 (± 0.31) log CFU/cm^2 (**Figure 4.1-4.2**), while samples from dynamic temperature profiles showed values of 4.41 ± 0.27 log CFU/cm^2 (summer scenario) and 3.89 ± 0.12 log CFU/cm^2 (winter scenario). As demonstrated in **Figures 4.1** and **4.2**, TVCs were influenced by temperature during storage, hence deterioration and eventually spoilage was evident (off-odors, slime production) at different time points. For instance, TVCs approached 7.0 log CFU/cm^2 at 15°C in 120 h (7.06 ± 0.16 log CFU/cm^2), at 10°C in 192 h (6.92 ± 0.27 log CFU/cm^2) and at 5 ^{o}C in 264 h (6.85 ± 0.11 log CFU/cm^2). Similarly, TVCs ranged above 7.0 log CFU/cm^2 at 20°C in 72 h (7.0 ± 0.16 log CFU/cm^2), at 25°C in 56 h (7.49 ± 1.01 log CFU/cm^2), at 30 ^{o}C in 36 h (7.36 ± 1.18 log CFU/cm^2) and at 35 ^{o}C in 28 h (6.61 ± 0.49 log CFU/cm^2). It needs to be noted that the final TVCs value at 0 ^{o}C was 6.24 ± 0.63 log CFU/cm^2 in 288

h and this finding could be attributed to the non-permeable film used by the poultry company as packaging material. Regarding the samples stored at the two different dynamic profiles (**Figures 4.3** and **4.4**), it was noticed that microbial loads reached 7.0 log CFUcm^2 in 144 h (6.90 ± 0.24 log CFU/cm^2) for summer transportation and in 168 h (6.95 ± 0.17 log CFU/cm^2) for winter transportation.

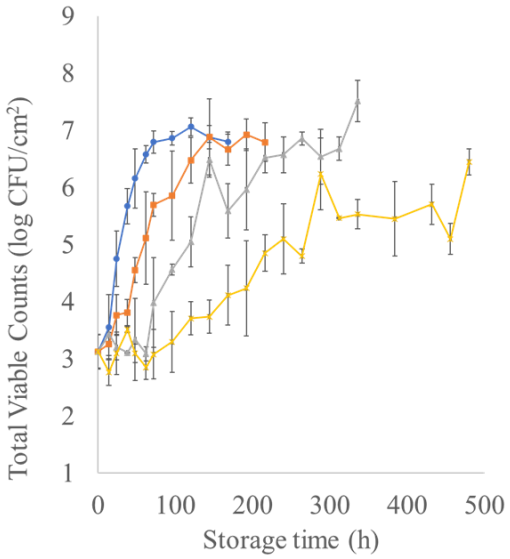

Figure 4.1: Mean (± SD, n=4) TVCs (log CFU/cm^2) in chicken breast samples during storage at 15 (blue line with cycles), 10 (orange line with squares), 5 (grey line with triangles) and 0 ºC (yellow line with stars).

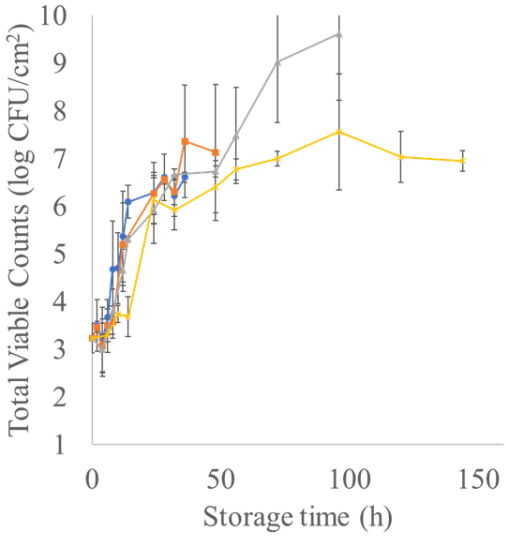

Figure 4.2: Mean (± SD, n=4) TVCs (log CFU/cm^2) in chicken breast samples during storage at 20 (blue line with cycles), 25 (orange line with squares), 30 (grey line with triangles) and 35 ºC (yellow line with stars).

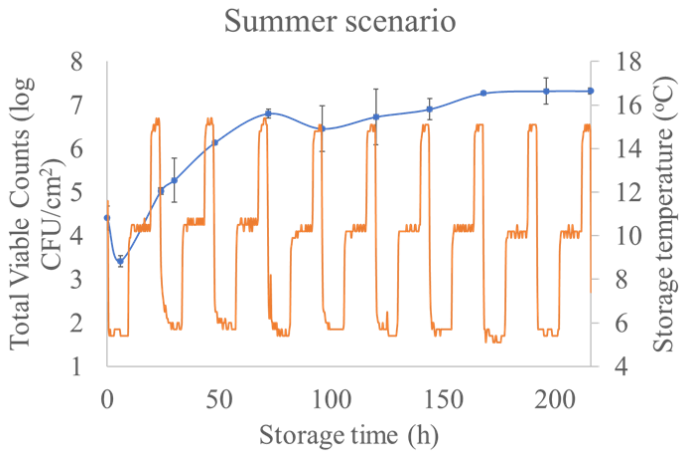

Figure 4.3: Mean (± SD, n=3) TVCs (log CFU/cm^2) in chicken breast samples and recorded temperature (°C) during storage at 1st dynamic temperature profile (summer scenario of transportation:12 h at 5 °C, 8 h at 10 °C and 4 h at 15 °C). Blue line with cycles corresponds to TVCs loads and orange line to temperatures alterations.

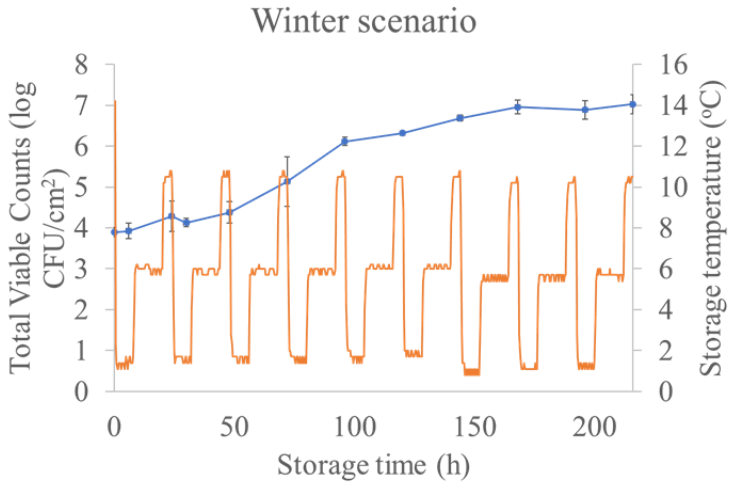

Figure 4.4: Mean (± SD, n=3) TVCs (log CFU/cm^2) in chicken breast samples recorded temperature (°C) during storage at 2nd dynamic temperature profile (winter scenario of transportation:12 h at 0 °C, 8 h at 5 °C and 4 h at 10 °C). Blue line with cycles corresponds to TVCs loads and orange line to temperatures alterations.

The average values of lag phase duration, specific growth rate (μ_{max}), initial (N_0) and maximum (N_{max}) number of TVCs estimated by the Baranyi and Roberts model (1994) are presented in **Table 4.2**. Lag phase values were determined in all cases and were decreased with increasing storage temperature, with maximum and minimum values of 92.6 and 4.7 h at 0 and 35 °C, respectively. On the contrary, the estimated μ_{max} parameter was increased with increasing storage temperature from 0.0382 h^{-1} (0 °C) to 1.5865 h^{-1}(30

^{o}C), whereas above 35 ^{o}C this parameter decreased to 1.329 h^{-1}. The model of Baranyi and Roberts was fitted to the experimental data satisfactorily as can be inferred by the standard error of fit (se(fit)) and the coefficient of determination (R^2) values (**Table 4.2**).

Table 4.2: Estimated kinetic parameters (lag phase, μ_{max}, y_o, y_{max}) and performance indices (standard error of fit: se(fit); R^2) by the implementation of Baranyi and Roberts primary growth model of TVC in chicken breast samples stored at eight isothermal conditions (0, 5, 10, 15, 20, 25, 30 and 35 ^{o}C).

Temperature (^{o}C)	lag (h)	μ_{max} (h^{-1})	N_0 (log CFU/cm^2)	N_{max} (log CFU/cm^2)	se(fit)	R^2
0	92.6±30.59	0.038±0.005	2.7±0.54	5.5±0.73	0.433-0.492	0.826-0.879
5	52.8±4.92	0.057±0.013	3.0±0.29	6.6±0.47	0.426-0.551	0.875-0.937
10	22.7±13.97	0.090±0.005	3.1±032	6.8±0.22	0.279-0.506	0.894-0.964
15	10.2±1.76	0.214±0.096	2.9±0.15	6.8±0.18	0.224-0.545	0.879-0.982
20	8.8±3.29	0.370±0.155	3.3±0.31	6.8±0.27	0.188-0.568	0.873-0.985
25	6.5±2.37	0.296±0.136	3.3±0.42	7.0±0.03	0.400-0.729	0.900-0.943
30	5.8±3.89	1.587±0.301	3.1±0.35	6.3±0.08	0.307-0.544	0.900-0.954
35	4.7±3.27	1.329±0.314	3.3±0.68	6.6±0.26	0.321-0.483	0.928-0.964

4.3.2 Sensory evaluation and shelf-life determination

Sensory results demonstrated that 61.7% of the samples were evaluated as spoiled with average scores above 2 corresponding to TVCs value of 6.2 ± 0.44 log CFU/cm^2. The scores of the judges did not differ significantly ($p< 0.05$). Based on this outcome, two quality classes were developed for chicken breast fillets, namely fresh (TVCs < 6.2 log CFU/cm^2) and spoiled (TVCs ≥ 6.2 log CFU/cm^2) and the spectral data acquired by MSI and FT-IR were associated with these quality classes. SL values followed a similar trend with lag phase and they were decreased with increasing storage temperature. More detailed information of the acceptability limit for each temperature is provided in **Figures 4.5** and **4.6** where sensory results and TVC loads are shown during storage. More specifically, based on the odor of chicken meat samples spoilage was evident in 240 h at 0 ^{o}C (5.9 log CFU/cm^2), 120 h at 5 ^{o}C (6.0 log CFU/cm^2), 96 h at 10 ^{o}C (6.4 log CFU/cm^2) and 48 h at 15 ^{o}C (6.7 log CFU/cm^2), 48 h at 20 ^{o}C (6.7 log CFU/cm^2), 32 h at 25 ^{o}C (log CFU/cm^2), 22 h at 30 ^{o}C, and 6 h at 35 ^{o}C (5.7 log CFU/cm^2).

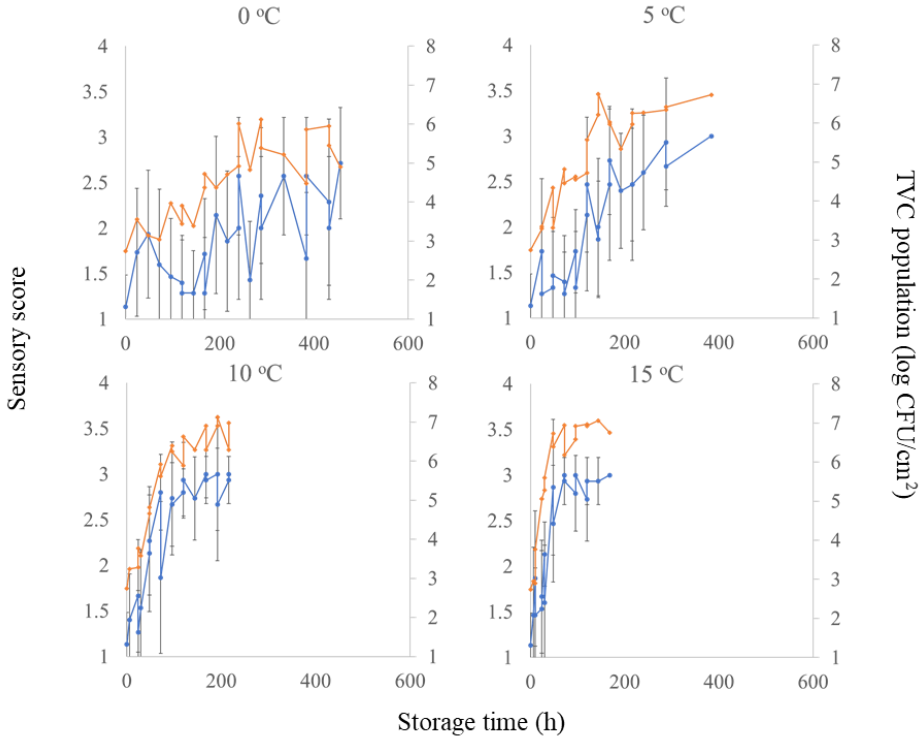

Figure 4.5: Sensory assessment scores (1-3) of odor (orange rhomb) and TVCs population (log CFU/cm^2; blue line with cycles) in chicken samples stored at 0, 5, 10 and 15 ºC.

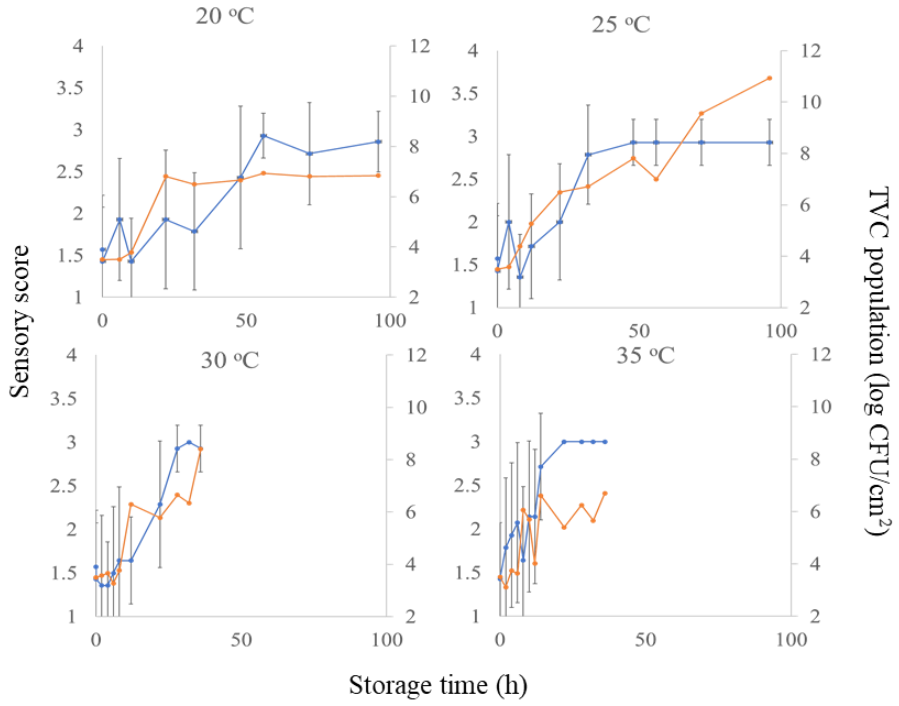

Figure 4.6: Sensory assessment scores of odor (orange rhomb) and TVCs population (log CFU/cm^2; blue line with cycles) in chicken samples stored at 20, 25, 30 and 35 ºC.

4.3.3 Spectra from sensors

Representative spectra of FT-IR and MSI corresponding to fresh (0 h at 0 ºC) and spoiled (278 h at 5 ºC) chicken breast fillet samples are depicted in **Figure 4.7**. Regarding FT-IR (**Figure 4.7A**), the absorption bands showing variations between fresh and spoiled samples were located in the areas of 1,000.87-1,150 cm^{-1} and 1,476.24-1,692.2 cm^{-1}. Specifically, absorption bands at 1,541.81 and 1,629.55 cm^{-1} were attributed to the metabolic products (amide I and II) associated with spoilage microorganisms (Alexandrakis et al., 2012). For MSI spectra (**Figure 4.7B**), reflectance between fresh and spoiled samples differed at 590, 630, 645, 660, 700, 850, 870, 890, 910 and 940 nm, where the region of 570 to 700 nm is related to myoglobin in meat color as described elsewhere (Spyrelli et al., 2020).

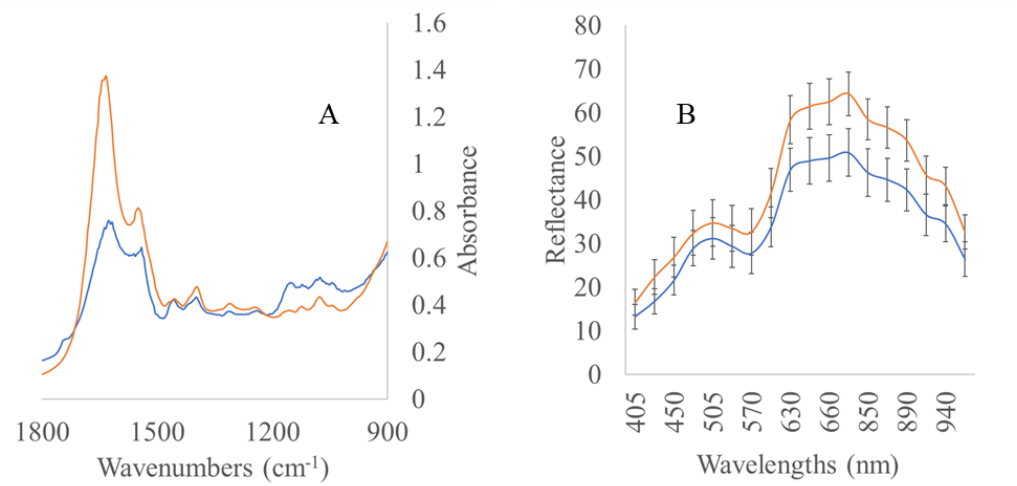

Figure 4.7: Representative spectra of FT-IR (A) and MSI implementation (B) on fresh (0 h at 0 ºC, blue line) and spoiled (278 h at 5 ºC, orange line) chicken breast fillets.

4.3.4 Machine learning for MSI data

The performance of the developed classification models is presented in **Table 4.3**. The overall accuracy showed higher values during CV (62-82.3%) than prediction (49.3-64.8%) and the same trend was observed for the other metrics. The high percentages of specificity in parallel to sensitivity indicated that there is an overestimation of fresh meat samples in all models applied. Subspace ensemble predicted more accurately the quality class of the samples, with overall accuracy in prediction of 64.8%. These values indicated that this model outperformed all the other. Moreover, specificity and sensitivity indexes

for subspace model exhibited satisfactory percentages (specificity: 69.7 %, sensitivity: 69.7 %), unlike all other models where there was an imbalance between the values of these two indexes. Precision was another performance metric showing the highest value (69.7 %) in subspace classification. Other models with acceptable performance where overall accuracy was higher than 50 %, were rusboosted (Overall accuracy: 59.2 %) and LDA (Overall accuracy: 56.3%). The confusion matrices of the three aforementioned models are presented in **Table 4.4**.

Table 4.3: Performance indexes (Overall accuracy, Overall error, Precision, Specificity, Sensitivity) for each supervised classification model derived from MSI data. Provided indexes for internal validation (cross validation: 5-fold validation) and prediction modeling process

Model	Modeling process	Overall Accuracy	Overall Error	Precision	Specificity	Sensitivity
LDA	CV	62.0	38.0	68.8	53.4	67.6
	Prediction	56.3	43.7	59.5	54.5	57.9
LSVM	CV	76.1	23.9	76.4	58.9	87.4
	Prediction	49.3	50.7	15.8	87.9	60.0
QSVM	CV	77.2	22.8	79.2	66.4	84.2
	Prediction	50.7	49.3	15.8	90.9	66.7
FineKNN	CV	64.4	35.6	70.8	56.2	69.8
	Prediction	53.5	46.5	57.9	48.5	56.4
Subspace	CV	77.2	22.8	77.0	59.6	88.7
	Prediction	64.8	35.2	60.5	69.7	69.7
Simple_tree	CV	65.5	34.5	67.0	37.0	84.2
	Prediction	53.5	46.5	63.2	42.4	55.8
rusBoosted	CV	69.0	31.0	73.7	58.9	75.7
	Prediction	59.2	40.8	62.2	57.6	60.5

PLS-DA	CV	82.3	17.7	82.6	53.4	87.3
	Prediction	52.1	47.9	75	52.9	15.8

CV: Cross Validation (k-fold, k=5)

Table 4.4: Confusion matrix of Subspace, rustBoosted and LDA models development and evaluation for MSI data.

Model	Stage	O/P	Fresh	Spoiled	Total number
Subspace	CV	Fresh	197	25	368
		Spoiled	59	87	
	Prediction	Fresh	23	15	71
		Spoiled	10	23	
rusBoosted	CV	Fresh	168	54	368
		Spoiled	60	86	
	Prediction	Fresh	23	15	71
		Spoiled	14	19	
LDA	CV	Fresh	150	72	368
		Spoiled	68	78	
	Prediction	Fresh	22	16	71
		Spoiled	15	18	

4.3.5 Machine learning for FT-IR data

Classification models using FT-IR spectral data identified the quality class of chicken breast fillet samples, with overall accuracy of prediction ranged from 52.2% to 67.6 % according to the model employed (**Table 5.5**). Similar to MSI results, all performance metrics were degraded from CV to prediction procedure. Even though the overall accuracy was considered acceptable, spoiled samples were significantly misclassified as fresh in all models, with specificity values ranging from 10% to 36.7% in the prediction of models. PLS-DA model demonstrated the best combination of performance indexes, with 67.6% overall accuracy of prediction. Furthermore, the model identified accurately (100 %) fresh samples during prediction, precision reached 66.18 % while spoiled samples were underestimated with specificity being only 36.7 %. Among the other classification models,

FineKNN and QSVM presented acceptable values of overall accuracy of prediction with 62.7 % and 61.2 %, respectively. Prediction and sensitivity for these two models indicated percentages greater than 60 %, although specificity was 36.7 and 30 %, respectively (**Table 4.6**).

Table 4.5: Performance indexes (Overall accuracy, Overall error, Precision, Specificity, Sensitivity) for each supervised classification model derived from FT-IR data. Provided indexes for internal validation (cross validation: 5-fold validation) and prediction modeling process.

Models	Modeling process	Overall Accuracy	Overall Error	Precision	Specificity	Sensitivity
LDA	CV	62.5	37.5	70.8	58.2	65.3
	Prediction	58.2	41.8	75.7	36.7	59.6
QSVM	CV	78.6	21.4	82.0	71.6	83.1
	Prediction	61.2	38.8	86.5	30.0	60.4
Simple tree	CV	71.4	28.6	78.2	68.1	73.5
	Prediction	56.7	43.3	94.6	10.0	56.5
rusBoosted trees	CV	73.6	26.4	79.2	68.8	76.7
	Prediction	59.7	40.3	86.5	26.7	59.3
FineKNN	CV	65.8	34.2	72.4	58.2	70.8
	Prediction	62.7	37.3	83.8	36.7	62.0
LSVM	CV	78.3	21.7	77.6	59.6	90.4
	Prediction	52.2	47.8	78.4	20.0	54.7
Subspace	CV	74.4	24.4	79.8	69.5	79.1
	Prediction	56.7	43.3	86.5	20.0	57.1

PLS-DA	CV	71.4	28.6	70	58.2	92.7
	Prediction	67.6	28.4	66.1	36.7	100

Table 4.6: Confusion matrix of PLS- DA, FineKNN and QSVM models development and evaluation for FT-IR data.

Model	Stage	O/P	Fresh	Spoiled	Total number
PLS-DA	CV	Fresh	203	16	360
		Spoiled	87	54	
	Prediction	Fresh	37	0	67
		Spoiled	19	11	
FineKNN	CV	Fresh	155	64	360
		Spoiled	59	82	
	Prediction	Fresh	31	6	67
		Spoiled	19	11	
QSVM	CV	Fresh	182	37	360
		Spoiled	40	101	
	Prediction	Fresh	32	5	67
		Spoiled	21	9	

4.4 Discussion

The microbiological results confirmed the critical role of storage temperature in chicken breast fillet meat and the evolution of TVCs (Alexandrakis et al., 2012; Doulgeraki et al., 2012; Rouger et al., 2017). Low temperatures significantly inhibited chicken's spoilage and in parallel extended the shelf life (Raab et al., 2008), with samples stored at 0 ^{o}C maintaining TVCs below 6 log CFU/cm^2. On the contrary, samples stored at high temperatures demonstrated rapid growth of TVCs and deterioration of the organoleptic characteristics (odor). These findings were in line with Baranyi and Roberts (1994) primary model outcome, where lag phase was prolonged while μ_{max} parameter was decreased in samples stored at low temperatures (**Table 4.2**), similarly to literature (Gospavic et al., 2008; Lytou et al., 2016). The initial microbial load in all batches (isothermal and dynamic

temperature profiles) was in compliance with the existing pool of studies (Rouger et al., 2017; Silva et al., 2008; EFSA, 2016), while the final loads of TVCs approached 7 log CFU/cm^2 at the end of spoilage (above 8-9 log CFU/cm^2) (Nychas et al., 2008). This observation could be linked to the usage of non-permeable film as packaging. This type of packaging film did not allow gases diffusion and hence the produced CO_2 from microbiota's metabolic reactions acted as modified atmosphere packaging, influencing TVC behavior and sensory results (Koutsoumanis et al., 2008; Liang et al., 2012; Holl et al., 2016).

The end of shelf- life (score >2) in samples was established when TVCs reached 6.2 log CFU/cm^2 via sensory outcomes, unlike published studies (Al-Nehlawi, Saldo, Vega & Guri, 2013) due to systematic or random errors during sensory evaluation by the untrained panel (Papadopoulou et al., 2011). The alterations on the behavior of the microbiota in chicken samples due to packaging conditions could mislead panels judgment and subsequently it could affect shelf-life's estimation (Silva et al., 2018). Moreover, differences in microbiota's growth were evident on samples stored at the two dynamic temperature profiles with TVCs in samples stored at summer scenario approaching 7 log CFU/cm^2 a day earlier than in stored samples at winter scenario. This attempt to assimilate temperature during transportation illustrated ones more the impact and the contribution of temperatures alterations to meat quality and safety (Gospavic et al., 2008; Nychas et al., 2008; Lytou et al., 2016).

The performance of MSI models was affected by the ensemble subspace classification model with overall correct classification accuracy of 64.8 %. The catalytic role of the ensemble approach can be exemplified by comparing the overall accuracy of this model to LDA model, where a decrease over 9 % was observed (Polikar, 2006; Sun & Zang, 2007). This outcome verified that ensemble combinations of conventional machine learning methods could improve model's classification performance (Jimenez- Carvelo et al., 2019). For instance, the application of subspace model demonstrated the beneficial role of adding k- nearest neighbors on LDA models and selecting the appropriate number of nearest neighbors in the classifier, as well as the smaller possible number of learners in the ensemble (for this study: k=5, Number of Learners=30) (Kim et al., 2011). Moreover, the

subspace model could classify both fresh and spoiled meat samples with the same percentage (69.7 %), while the LDA model misplaced spoiled samples as fresh with the higher percentage of specificity being at 54.5 %. It is worth noting that it is preferable to classify correctly not only the fresh samples but also the spoiled ones (Sokolova & Lapalme, 2009), especially when it comes to food industries where a recall of a product due to spoilage could result in loss of millions and increase food waste (Nychas et al., 2 016; FAO, 2021).

Unlike MSI data, the combination of algorithms did not seem to ameliorate FT-IR classification models, where PLS-DA exhibited the most satisfactory overall accuracy (67.6 %), followed by FineKNN (62.7%) and QSVM (61.2%). Nevertheless, this outcome confirmed that PLS-DA is a widely and common applied algorithm for classification, especially in food quality and authenticity which can provide accurate prediction of quality (Jimenez- Carvelo et al., 2019). Despite of the highest accuracy and sensitivity in FT-IR models, specificity percentage was not acceptable as its values rated only at 30 %, pointing out the inefficacy of the trained model to detect chicken spoiled samples. Even though this spectroscopic method is proved accurate for the estimation of spoilage in chicken (Ellis et al., 2002; Alexandrakis et al., 2012) and the correct classification of other meat products as beef fillets and minced meat (Ropodi et al., 2018; Fengou et al., 2019), the variability between and within batches based on animal strain, alterations of nutrition (Amorim et al., 2016) or slaughtering and distributing, seemed to influence models' performances.

The developed models for both spectroscopic methods indicated a tendency of classifying spoiled samples as fresh at all stages of model development and prediction. This finding could be attributed to the fact that spoiled samples used for model calibration had lower microbiota on their surface compared to spoiled samples for prediction, due to their different temperatures profile (Gospavic et al., 2008; Ropodi et al., 2018). These temperature alterations in tandem with packaging conditions could have an impact on the metabolic footprint of samples which could differ from those defined as spoiled during model's development (Papadopoulou et al., 2011). However, it was considered more appropriate to validate model's performance with samples stored and distributed at realistic scenarios (Lytou et al., 2016; Lianou et al., 2018). Lastly, it has to be highlighted once

more that the utilization of different batches and microbial quality as prediction data set could be responsible for misclassified samples, due to the significant variability among samples (Ropodi et al., 2018).

Chapter 5: Microbiological quality assessment of chicken thigh fillets using spectroscopic sensors and multivariate data analysis

Published as:

Spyrelli, E.D., Papachristou, C.K., Nychas, G.J.E. and Panagou, E.Z., 2021. Microbiological Quality Assessment of Chicken Thigh Fillets Using Spectroscopic Sensors and Multivariate Data Analysis. Foods, 10(11), 2723.

Abstract

Fourier transform infrared spectroscopy (FT-IR) and multispectral imaging (MSI) were evaluated for the prediction of the microbiological quality of chicken thigh fillets via regression and classification models.

In brief, chicken thigh fillets (n = 402) were subjected to spoilage experiments at eight isothermal and two dynamic temperature profiles. Samples were analyzed microbiologically (total viable counts (TVCs) and *Pseudomonas* spp.), while simultaneously MSI and FT-IR spectra were acquired. The organoleptic quality of the samples was also evaluated by a sensory panel, establishing a TVC spoilage threshold at 6.99 log CFU/cm^2. Partial least squares regression (PLS-R) models were employed in the assessment of TVCs and *Pseudomonas* spp. counts on chicken's surface. Furthermore, classification models (linear discriminant analysis (LDA), quadratic discriminant analysis (QDA), support vector machines (SVMs), and quadratic support vector machines (QSVMs)) were developed to discriminate the samples in two quality classes (fresh vs. spoiled). PLS-R models developed on MSI data predicted TVCs and *Pseudomonas* spp. counts satisfactorily, with root mean squared error (RMSE) values of 0.987 and 1.215 log CFU/cm^2, respectively. SVM model coupled to MSI data exhibited the highest performance with an overall accuracy of 94.4%, while in the case of FT-IR, improved classification was obtained with the QDA model (overall accuracy 71.4%). These results confirm the efficacy of MSI and FT-IR as rapid methods to assess the quality in poultry products.

5.1 Introduction

Food waste amounts to 14% of the worlds' food consumption (FAO, 2022), while meat and specifically poultry production is forecasted to rise at 137 million tones (FAO, 2022). In addition, consumer's awareness and demand for high quality and safety meat and poultry has been continuously increased. For this purpose, non-invasive spectroscopic sensors have been used in the evaluation of the quality and freshness of meat products (Tsakanikas et al., 2020) through the implementation of process analytical technology (PAT) (van den Berg et al., 2013; Cullen et al., 2014). The underlying principle of PAT is to combine spectral data acquired through real-time (in-, on-, at-line) non-destructive analytical techniques with multivariate data analysis for the development of models assessing food quality. These models, along with their datasets, could be uploaded in the cloud, updated regularly with new data in order to be consultative to the food industry (Nychas et al., 2016).

In recent years, multispectral imaging (MSI) and Fourier transform infrared (FT-IR) spectroscopy have been investigated as alternative methods for the evaluation of a variety of meat products (Panagou et al., 2014; Xiong et al., 2015; Alamprese et al., 2016). The former method is a merge of UV and NIR with computer vision, and it has been proposed as an ecological approach for rapid quality evaluation of meat and poultry (Dissing et al., 2013; Pu et al., 2015; Kutsanedzie et al., 2019). Until now, spectral data in the visible and near-infrared region (400–1700 nm) have been employed in the development of quantitative or qualitative models for the determination of the bacterial population (TVCs and *Pseudomonas* spp.) on chicken meat during spoilage (Feng & Sun, 2013a, 2013b; Ye et al., 2016). In the same context, MSI analysis has been proved a solution to the identification of adulteration/food fraud of minced beef with chicken meat (Kamruzzaman et al., 2016), as well as for the detection of food fraud in minced pork adulterated with chicken (Fengou et al., 2021a). Moreover, fecal contaminants in poultry line (Yang et al., 2015) and the presence of tumors on the surface of chicken breasts (Nakariyakul & Casasent, 2009) have been accurately detected via MSI analysis. This innovative method was successfully employed in the at-line estimation of the time from slaughter in four different poultry products (Spyrelli et al., 2020).

Likewise, the potential of FT-IR for the qualitative and quantitative assessment of the microbiological quality of meat products has been explored by other researchers (Ellis et al., 2002; Alexandrakis et al., 2012; Argyri et al., 2013; Grewal et al., 2015; Candŏgan et al., 2021). Especially for poultry, FT-IR was recommended as an effective approach for the differentiation of intact chicken breast muscle during spoilage (Alexandrakis et al., 2012). Additionally, the level of spoilage bacteria on the surface of chicken meat was successfully estimated via FT-IR spectroscopy (Ellis et al., 2002). Further investigation of this promising method for real-time evaluation of the freshness of stored chicken breast fillets was undertaken by Vansconcelos et al. (2014). FT-IR analysis was also proposed as an efficient approach for the categorization of chicken meat among seven raw types of food, irrespective of variations among batches and storage conditions (temperature, storage duration, packaging, spoilage levels) (Tsakanikas et al., 2020).

Spectral data acquired by nondestructive methods such as MSI and FT-IR have been analyzed by a variety of unsupervised and supervised machine learning algorithms for the rapid quality assessment in food matrices including meat (Berrueta et al., 2007; Jiménez-Carvelo et al., 2019; Candŏgan et al., 2021). Partial least squares regression (PLS-R), linear discriminant analysis (LDA), and quadratic discriminant analysis (QDA) have been reported as reliable tools for the development of predictive models for spoilage or adulteration assessment in meat (Friedman et al., 2009; Ropodi et al., 2015; Alamprese et al., 2016; Kumar & Karne, 2017). Moreover, deep learning methodologies such as artificial neural networks (ANNs) and support vector machines (SVMs) (Luts et al., 2010) have been employed, validated, and compared through available websites (e.g., sorfML, Metaboanalyst) or softwares (R, MatLab, Python), in an attempt to provide accurate quantitative and qualitative models for food spoilage assessment (Chen et al., 2011; Ropodi et al., 2016; Estelles-Lopez et al., 2017; Jaafreh et al., 2019; Jiménez-Carvelo et al., 2019; Fengou et al., 2020).

The aim of the present work was to develop and evaluate machine learning regression (PLS-R) and classification models (LDA, QDA, SVMs, QSVMs) based on MSI and FT-IR spectral data for the evaluation of the microbiological quality of chicken thigh fillets. More specifically, PLS-R models were developed for the prediction of the microbiota of

TVCs and *Pseudomonas* spp. on the surface of chicken thigh, whereas LDA, QDA, SVMs, and QSVMs models were employed for the classification of samples in two quality classes (fresh or spoiled) based on the outcome of sensory analysis. The challenging task in this study was not confined in model development, batch variation and different storage temperatures, but it also considered external validation using two different dynamic temperature profiles simulating temperature scenarios during transportation and storage in retail outlets.

5.2 Materials and Methods

5.2.1 Experimental design

Three hundred and thirty (330) chicken thigh fillets (ca. 90–110 g/fillet) enclosed in plastic packages (dimensions = 25 cm (width), 90 μm (thickness), permeability ca. 25, 90, and 6 cm^3 $m^{-2}day^{-1}bar^{-1}$ at 20 °C and 50% RH for CO_2, O_2, and N_2, respectively) were obtained from a poultry industry in Greece and stored aerobically at eight isothermal conditions (0, 5, 10, 15, 20, 25, 30, and 35 °C). Two independent experiments were undertaken at all isothermal conditions using 4 different batches of chicken meat. Moreover, 72 samples were stored at two dynamic temperature profiles (profile 1 = 12 h at 5 °C, 8 h at 10 °C, and 4 h at 15 °C; profile 2 = 12 h at 0 °C, 8 h at 5 °C, and 4 h at 10 °C), simulating temperature scenarios that can be observed during transportation and storage in retail outlets (Vaikousi et al., 2009). At pre-determined time intervals, packages were subjected to microbiological analyses for the enumeration of total viable counts (TVCs) and *Pseudomonas* spp., in parallel with MSI and FT-IR spectral data acquisition. At each sampling point, duplicate packages per isothermal storage condition and triplicate packages from each dynamic temperature profile were subjected to the abovementioned analyses. In addition, chicken samples were subjected to sensory evaluation by a 14-member sensory panel to categorize the samples in two quality classes, namely fresh and spoiled as detailed below. Microbiological counts and sensory scores were correlated with spectral data in order to develop quantitative and qualitative models assessing chicken thigh's microbial loads (TVCs, *Pseudomonas* spp.) as well as their quality class (fresh-spoiled).

5.2.2 Microbiological Analysis and Sensory Evaluation

A total surface of ca. 20 cm^2 (four slices of ca. 5 cm^2 each with a maximum thickness of 2 mm) from chicken thigh fillet was removed aseptically, by means of a sterile stainless steel cork borer (2.5 cm in diameter), scalpel and forceps, added in 100 ml of sterile quarter strength Ringer's solution (Lab M Limited, Lancashire, UK) and homogenized in a Stomacher device (Lab Blender 400, Seward Medical, UK) for 120 s at room temperature (Hutchison et al., 2005). The microbial load on the surface of chicken was enumerated using serial decimal dilutions in the same Ringer's solution and 0.1 ml of the appropriate dilution was spread on the following growth media: (a) Tryptic glucose yeast agar (Plate Count Agar, Biolife, Milan, Italy) for the determination of total viable counts (TVCs) incubated at 25 °C for 72 h; (b) *Pseudomonas* agar base (LAB108 supplemented with selective supplement Cetrimide Fucidin Cephaloridine, Modified C.F.C. X108, LABM) for the determination of presumptive *Pseudomonas* spp. incubated at 25 °C for 48 h. The results were logarithmically transformed and expressed as log CFU/cm^2.

In parallel, sensory evaluation was performed by a 14 member in-house trained sensory panel. For this purpose, samples (n = 103) were placed in sterile petri dishes and scored according to their odor using a 3-point hedonic scale as follows: 1 = fresh, 2 = acceptable, 3 = spoiled (Lytou et al., 2016). Samples with scores < 2 were characterized as fresh (Class 1) whereas samples with scores ≥ 2 as spoiled (Class 2). Finally, the sensory outcome was correlated with spectral data in order to assess the quality class of the samples directly from the acquired MSI and FT-IR spectra.

5.2.3 Spectra Acquisition

Multi-spectral images (MSI) were captured using a Videometer-Lab instrument (Videometer A/S, Herlev, Denmark) that acquires images in 18 different non-uniformly distributed wavelengths from UV (405 nm) to short wave NIR (970 nm), namely, 405, 435, 450, 470, 505, 525, 570, 590, 630, 645, 660, 700, 850, 870, 890, 910, 940, and 970 nm. Detailed information about this spectroscopic sensor is provided elsewhere (Carstensen et al., 2003). Each sample corresponded to spatial and spectral data of size m × n × 18 (where m×n is the image size in pixels) (Tsakanikas et al., 2015). Furthermore, canonical discriminant analysis (CDA) was employed as a supervised transformation building

method to divide the images into regions of interest (ROI) using the Videometer-Lab version 2.12.39 software (Videometer A/S, Herlev, Denmark). The final outcome of this segmentation process for each image was a dataset of spectral data including the average value and the standard deviation of the intensity of the pixels within the ROI at each wavelength.

FT-IR data were obtained using an FT-IR-6200 JASCO spectrometer (Jasco Corp., Tokyo, Japan) and a ZnSe 45 HATR (horizontal attenuated total reflectance) crystal (PIKE Technologies, Madison, Wisconsin, United States) with a refractive index of 2.4 and a depth of penetration of 2.0 μm at 1000 cm^{-1}. Spectra measurements were performed using Spectra Manager Code of Federal Regulations (CFR) software version 2 (Jasco Corp., Tokyo, Japan) in the wavenumber range of 4000–400 cm^{-1}, by accumulating 100 scans with a resolution of 4 cm^{-1} and a total integration time of 2 min.

5.2.4 Data Pre-Processing and Analysis

MSI spectral data were pre-processed by baseline offset treatment (Rinnan et al., 2009; Engel et al., 2013) for the development of PLS-R models in order to reduce random or systematic variations and simultaneously improve image resolution (Qin et al., 2013). Likewise, for the development of the classification models, MSI data were subjected to standard normal variate (SNV) transformation prior to analysis (Tsakanikas et al., 2016). Model training was undertaken with the dataset obtained from the storage experiments at isothermal conditions (n = 330), where 142 (43.1%) and 188 (56.9%) of the samples were defined as fresh (Class 1) and spoiled (Class 2), respectively. Model optimization was based on leave-one-out full-cross validation (LOOCV) process for PLS-R models and k-fold validation (k= 5) for the classification models. Moreover, the efficacy of the developed models to assess the quality of chicken samples was evaluated by external validation using independent datasets from the two dynamic temperature scenarios (n = 72; Class 1 = 36 samples, 50 %; Class 2 = 36 samples, 50%).

FT-IR spectral data were modified by Savitzky-Golay first derivative (second polynomial order, 11-point window) for the development of PLS-R models, while for classification models' spectral data pre-treatment was based on the same model with a 9-point window in order to reduce baseline shift and noise (Alamprese et al., 2016). Spectral

data in the range of 1000 to 2000 cm^{-1} were included in the analysis, since these regions are documented as relevant to meat spoilage (Fengou et al., 2020). FT-IR models were also validated with data sets from dynamic temperature profiles (n = 63), including 30 (47.6 %) fresh and 33 (52.4 %) spoiled samples. The procedure of model training and validation is graphically presented in **Figure 5.1**.

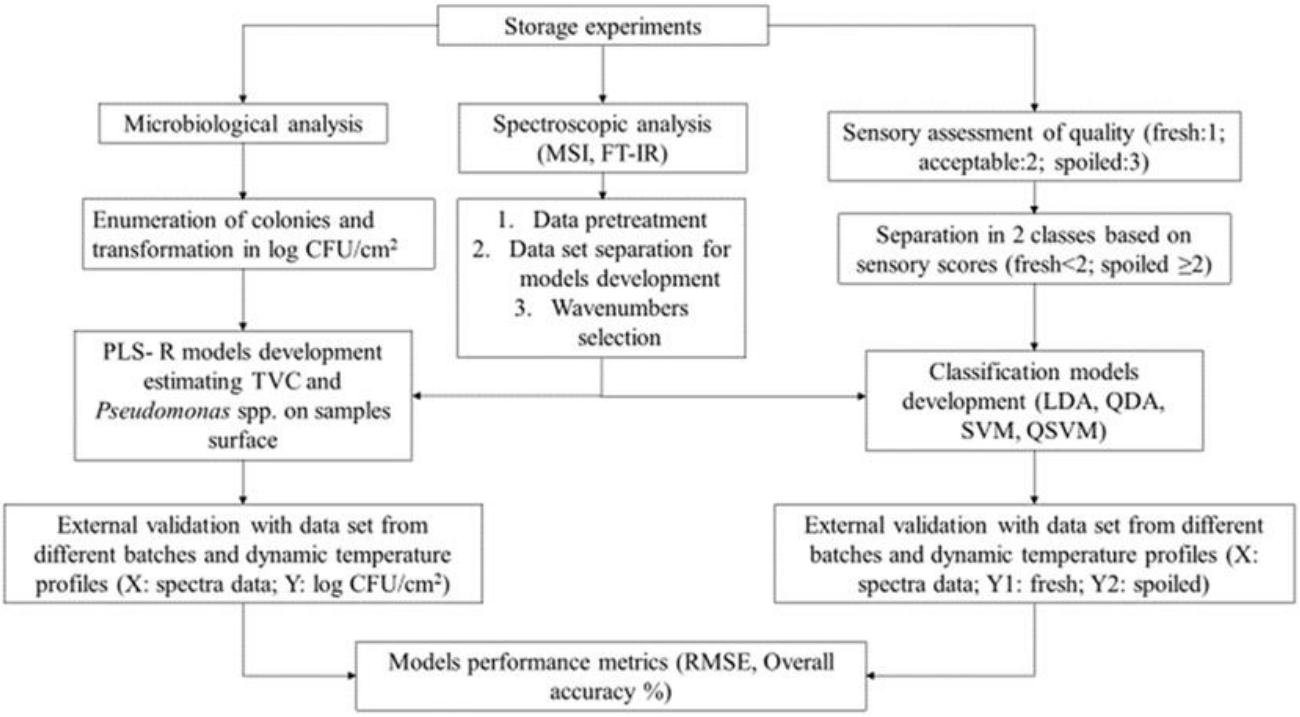

Figure 5.1: Flowchart describing quantitative and qualitative model development and validation.

PLS-R models for the estimation of TVCs and *Pseudomonas* spp. counts on chicken thighs surface were developed and validated by the software Unscrambler © ver. 9.7 (CAMO Software AS, Oslo, Norway). Moreover, linear discriminant analysis (LDA) (Kim et al., 2011), quadratic discriminant analysis (QDA) (Kumar & Karne, 2017), support vector machines (SVMs), and quadratic support vector machines (QSVMs) (Osuna et al., 1997) models were employed for the classification of samples according to their spoilage level using MATLAB 2012a software (The MathWorks, Inc., Natick, MA, USA). The performance of the developed models was evaluated via the following metrics and indexes: root mean squared error (RMSE), correlation coefficient (r), overall accuracy, sensitivity, and specificity (Sokolova & Lapalme, 2009; Márquez et al., 2016).

5.3 Results and Discussion

5.3.1 Microbiological Analysis and Sensory Evaluation

The population dynamics of TVCs and *Pseudomonas* spp. on the surface of chicken thigh fillets stored at isothermal conditions (0, 5, 10, 15, 20, 25, 30, and 35 °C) are presented in **Figure 5.2**. The initial population of TVCs (**Figure 5.2A, B**) and *Pseudomonas* spp. (**Figure 5.2C, D**) was 4.02 (±0.38) and 3.75 (±0.11) log CFU/cm^2, respectively, confirming previous literature findings (Alexandrakis et al., 2012; Doulgeraki et al., 2012; Rouger et al., 2017). As expected, storage temperature significantly influenced microbial growth resulting in sample deterioration and spoilage. For poultry, TVCs values exceeding 7.0 log CFU/cm^2 have been reported by other researchers to signify the end of shelf-life due to spoilage (Dominguez & Schaffner, 2007; Galarz et al., 2016; Rouger et al., 2017). More specifically, in this study TVCs reached values above 7.0 log CFU/cm^2 at 15 °C in 30 h (7.2 ± 0.15 log CFU/cm^2), at 10 °C in 72 h (7.24 ± 0.39 log CFU/cm^2), at 5 °C in 144 h (7.62 ± 0.63 log CFU/cm^2) and at 0 °C in 240 h (7.17 ± 0.42 log CFU/cm^2). *Pseudomonas* spp. counts were similar to TVCs population and spoilage was evident at 15 °C in 48 h (7.3 ± 0.33 log CFU/cm^2), at 10 °C in 72 h (7.06 ± 0.48 log CFU/cm^2), at 5 °C in 120 h (7.22 ± 0.18 log CFU/cm^2), and at 0 °C in 216 h (6.75 ± 0.23 log CFU/cm^2). Furthermore, samples appearance and odor rapidly deteriorated at high storage temperatures and TVCs reached 7.0 log CFU/cm^2 at 20 °C in 32 h (7.36 ± 0.39 log CFU/cm^2), at 25 °C in 24 h (7.78 ± 0.18 log CFU/cm^2), at 30 °C in 24 h (7.95 ± 0.40 log CFU/cm^2), and at 35 °C in 12 h (6.8 ± 0.46 log CFU/cm^2). Similarly, *Pseudomonas* spp. approached 7.0 log CFU/cm^2 at 20 °C in 32 h (6.97 ± 0.39 log CFU/cm^2), at 25 °C in 24 h (6.95 ± 0.36 log CFU/cm^2), at 30 °C in 24 h (6.89 ± 0.68 log CFU/cm^2), and at 35 °C in 24 h (6.69 ± 0.60 log CFU/cm^2).

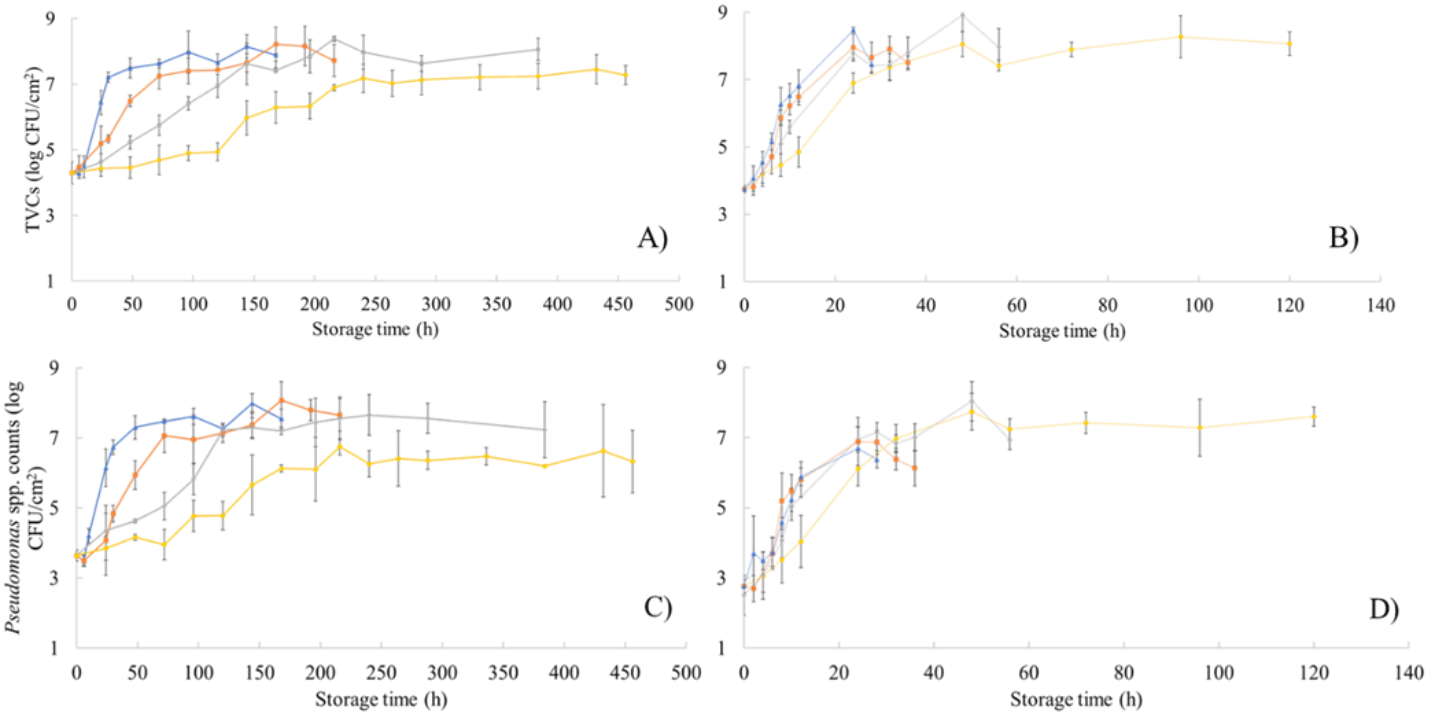

Figure 5.2: Changes in the population (log CFU/cm^2) of total viable counts (TVCs) (**A**, **B**) and *Pseudomonas* spp. (**C**, **D**) in chicken thigh samples during storage at different isothermal conditions (**A**, **C**: 0, 5, 10 and 15 °C); **B**, **D**: 20, 25, 30, and 35 °C). Data points are average values of four replicates of samples ± standard deviation.

Moreover, the microbiological results from the two dynamic temperature profiles are shown in **Figure 5.3**. The initial TVCs and *Pseudomonas* spp. counts were 3.82 ± 0.21 log CFU/cm^2 and 2.51 ± 0.28 log CFU/cm^2, respectively (first dynamic temperature profile, **Figure 5.3A**), and 4.13 ± 0.40 log CFU/cm^2 and 2.87 ± 0.65 log CFU/cm^2, respectively (second dynamic temperature profile, **Figure 5.3B**). Stored samples at these dynamic profiles were considered spoiled in 96 h (TVC = 6.96 ± 0.25 log CFU/cm^2, *Pseudomonas* spp. = 6.19 ± 0.29 log CFU/cm^2) for the first dynamic profile and in 120 h (TVC = 7.08 ± 0.01 log CFU/cm^2, *Pseudomonas* spp. = 7.05 ± 0.03 log CFU/cm^2) for the second dynamic profile. This one-day delay of spoilage could be attributed to the different metabolic footprint of chicken samples due to temperature alterations affecting thus microbial growth (Gospavic et al., 2008; Raab et al., 2008). Statistical analysis for the microbiological results (one-way ANOVA via MATLAB 2012a software (The MathWorks, Inc., Natick, MA, USA)) is available in Appendix I (**Table 5A** and **Table 5B)**.

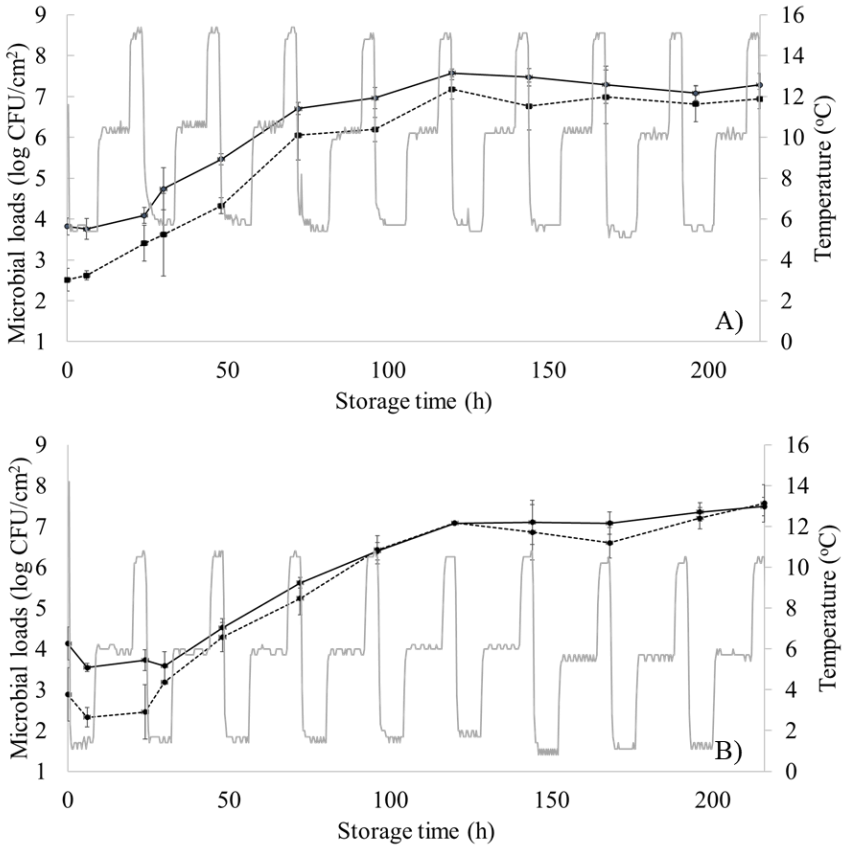

Figure 5.3: Changes in the population (log CFU/cm^2) of total viable counts (TVCs) (solid line) and *Pseudomonas* spp. (dashed line) in chicken thigh samples stored under periodically changing temperature conditions. (**A**) Profile 1 = 12 h at 5 °C, 8 h at 10 °C, and 4 h at 15 °C; (**B**) Profile 2 = 12 h at 0 °C, 8 h at 5 °C, and 4 h at 10 °C. Data points are mean values of triplicate samples ± standard deviation.

More detailed information about chicken thigh fillets spoilage was derived by sensory evaluation, where 56.9% of the samples were scored above 2 and considered spoiled. Samples stored at 0 °C were considered acceptable until 240 h of storage, while samples stored at 30 and 35 °C were evaluated as spoiled after 6 and 12 h, respectively. In addition, deterioration of odor due to spoilage was evident in 96 h at 5 °C, 48 h at 10 °C, and 24 h at 15, 20, and 25 °C. The correlation of sensory scores to samples temperature and TVCs populations is provided at **Table 5.1**. TVCs values above 6.99 log CFU/cm^2 corresponded to samples rated with an average score greater than 2, similarly to other studies where spoilage threshold was established at 7.0 log CFU/cm^2 for poultry (Dominguez & Schaffner, 2007). Based on this criterion, samples were assigned in two

quality classes, namely fresh (score < 2) or spoiled (score ≥ 2), and were further employed in the development of classification models.

Table 5.1: Sensory scores and TVCs counts for chicken thigh samples corresponding to the sensory rejection time at each storage temperature.

Temperature (˚C)	Storage Time (h)	Odor	TVCs (log CFU/cm^2)
0	240	2.5±0.5	6.99
5	96	2.3±0.6	7.08
10	48	2.3±0.5	6.90
15	24	2.1±0.7	7.46
20	24	2.5±0.6	7.40
25	24	2.9±0.8	8.22
30	6	2.1±0.7	5.1
35	12	2.2±0.7	6.84
TVCs average (log CFU/cm^2)	6.99 ± 0.89		

5.3.2 Correlation of Microbiological Data to Spectral Information

PLS-R model parameters (slope and offset) and performance metrics (r, RMSE), for the estimation of the population of TVCs and *Pseudomonas* spp. using MSI spectral data, are presented in **Table 5.2**, for model calibration, full cross validation, and external validation (prediction). For TVCs, the calculated values of RMSE and r during model calibration and cross validation were 0.730 and 0.779 log CFU/cm^2, as well as 0.861 and 0.840, respectively, whereas the respective values for external validation were 0.987 log CFU/cm^2 and 0.895, respectively. The performance of the PLS-R model was also graphically illustrated by the comparison of the observed vs. predicted TVCs (**Figure 5.4A**). Predicted values were mostly located within the area of ±1.0 log CFU/cm^2, which is considered microbiologically acceptable, while an overestimation for low counts (below 4.0 log CFU/cm^2) was evident. Regarding PLS-R model assessing *Pseudomonas* spp. counts via MSI data, RMSE and r values were 0.828 log CFU/cm^2 and 0.853, respectively,

for calibration, while for full cross validation they were 0.886 log CFU/cm^2 and 0.830, respectively. For external validation (prediction) of *Pseudomonas* spp. counts, RMSE and r values were estimated at 1.215 log CFU/cm^2 and 0.904 respectively. Nevertheless, the prediction of *Pseudomonas* spp. counts demonstrated deviations (overestimation) from the ± 1.0 log CFU/cm^2 area, especially for samples with *Pseudomonas* spp. loads lower than 4.0 log CFU/cm^2 (**Figure 5.4B**).

Table 5.2: Performance metrics of the developed PLS-R models estimating TVCs and *Pseudomonas* spp. counts of chicken thigh samples via MSI spectral data analysis.

TVCs	***n***	**LVs**	**slope**	**offset**	**r**	**RMSE**
Calibration	330	10	0.741	1.684	0.861	0.730
Full Cross Validation	330	10	0.726	1.787	0.840	0.779
Prediction	72		0.774	2.023	0.895	0.987
***Pseudomonas* spp.**	***n***	**LVs**	**slope**	**offset**	**r**	**RMSE**
Calibration	330	10	0.727	1.615	0.853	0.828
Full Cross Validation	330	10	0.711	1.714	0.830	0.886
Prediction	72		0.702	2.441	0.904	1.215

n: Number of samples, LVs: Latent variables, r: Correlation coefficient, RMSE: Root mean squared error.

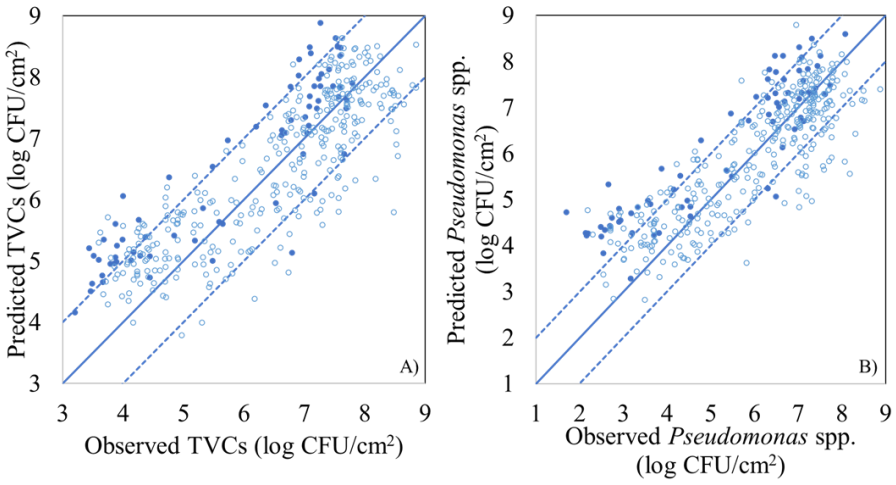

Figure 5.4: Predicted versus observed TVCs (**A**) and *Pseudomonas* spp. (**B**) counts by the PLS-R models, based on MSI data for FCV (open symbols) and prediction (solid symbols). Solid line represents the line of equity (y = x) and dashed lines indicate ± 1.0 log unit area.

The important wavelengths contributing to the prediction of the selected microbial groups were obtained according to PLS-R beta coefficients (B), derived by the Unscrambler software and Marten's Uncertainty test (**Figure 5.5**). The wavelengths 630, 645, 660, 700, and 850 nm were identified as significant (b coefficient greater than 0.2) for determining TVCs counts on the surface of chicken thigh. The significant contribution of the wavelength range 630–700 nm for the determination of meat and poultry spoilage has been reported in previous studies, and could be linked to myoglobin, metmyoglobin, deoxymyoglobin or oxymyoglobin (Pu et al., 2015; Spyrelli et al., 2020). According to the B regression coefficients of the PLS-R models, the quantitative equations for the estimation of TVCs and *Pseudomonas* spp. counts via MSI application could be described as follows:

$$Y_{TVCs} = 5.983 + 0.303 \times X_{mean,405nm} + 0.158 \times X_{mean,450nm} - 0.532 \times X_{mean,470nm} + 0.292 \times X_{mean,525nm} - 0.853 \times X_{mean,630nm} + 0.695 \times X_{mean,645nm} + 0.767 \times X_{mean,660nm} - 0.670 \times X_{mean,700nm} - 0.460 \times X_{mean,850nm} + 0.145 \times X_{mean,890nm} + 0.309 \times X_{mean,910nm} + 0.352 \times X_{mean,940nm} - 0.255 \times X_{mean,970nm} - 0.377 \times X_{SD,435nm} + 0.426 \times X_{SD,470nm} + 0.308 \times X_{SD,505nm} + 0.244 \times X_{SD,525nm} - 0.607 \times X_{SD,590nm} + 0.160 \times X_{SD,645nm} + 0.171 \times X_{SD,660nm} - 0.212 \times X_{SD,850nm} - 0.132 \times X_{SD,870nm} \quad (5.1)$$

$$Y_{Pseudomonas\ spp.\ counts} = 5.416 + 0.204 \times X_{mean,405nm} + 0.308 \times X_{mean,450nm} - 0.745 \times X_{mean,470nm} + 0.326 \times X_{mean,525nm} - 1.020 \times X_{mean,630nm} + 0.802 \times X_{mean,645nm} + 0.885 \times X_{mean,660nm} - 0.766 \times X_{mean,700nm} - 0.500 \times X_{mean,850nm} + 0.332 \times X_{mean,910nm} + 0.422 \times X_{mean,940nm} - 0.344 \times X_{mean,970nm} - 0.602 \times X_{SD,435nm} + 0.501 \times X_{SD,470nm} + 0.367 \times X_{SD,505nm} + 0.272 \times X_{SD,525nm} - 0.679 \times X_{SD,590nm} + 0.244 \times X_{SD,645nm} + 0.222 \times X_{SD,660nm} - 0.321 \times X_{SD,850nm} - 0.204 \times X_{SD,870nm} - 0.133 \times X_{SD,890nm} + 0.159 \times X_{SD,910nm} + 0.177 \times X_{SD,970nm} \quad (5.2)$$

In the above equations, the response variable (Y) can be approximated by a linear combination of the values of the predictors (X) through coefficients called regression or B -coefficients. Specifically, Y is the estimated value for TVCs and *Pseudomonas* spp., respectively, whereas X_{mean} and X_{SD} are the mean intensity and the standard deviation of the pixels at the respective wavelength during MSI acquisition, respectively.

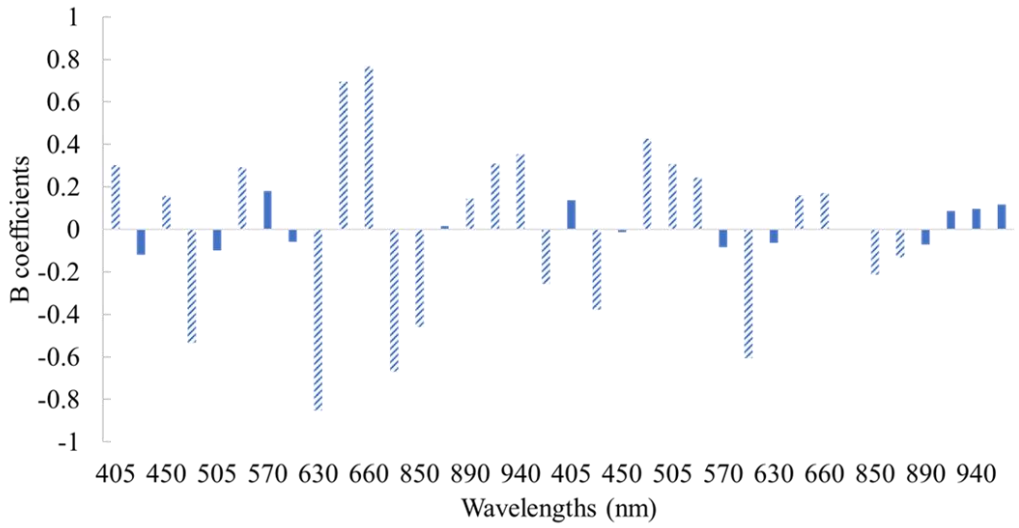

Figure 5.5: Beta (B) coefficient values of the PLS-R model developed on MSI spectral data for chicken thigh fillets. Shaded bars indicate important variables (mean intensity and standard deviation of pixels from each wavelength).

Likewise, model performance for the estimation of TVCs and *Pseudomonas* spp. counts via FT-IR spectral data analysis is presented in **Table 5.3**. For the TVCs prediction model, RMSE and r values for calibration and full cross validation were 0.734 log CFU/cm^2 and 0.856, as well as 0.899 log CFU/cm^2 and 0.781, respectively, while for external validation they were 1.251 log CFU/cm^2 and 0.583, respectively. Similarly, for the prediction of *Pseudomonas* spp. counts via FT-IR analysis, RMSE and r values were 0.838 log CFU/cm^2 and 0.849 for calibration, 1.037 log CFU/cm^2 and 0.762 for full cross validation, and 1.589 log CFU/cm^2 and 0.514 for external validation, respectively. The performance of the PLS-R models was also graphically verified by the comparison of the observed versus predicted counts of TVCs and *Pseudomonas* spp. (**Figure 5.6**), demonstrating an overestimation in the fail-safe zone for samples with TVCs values lower than 4.0 log CFU/cm^2 (**Figure 5.6A**). In contrast, according to **Figure 5.6B**, *Pseudomonas* spp. predicted counts deviated from the acceptable limit of ± 1.0 log CFU/cm^2, presenting both overestimated (for counts < 4.0 log CFU/cm^2) and underestimated (for counts > 7.0 log CFU/cm^2) values. In addition, the influence of each wavenumber in the development of the PLS-R models via FT-IR spectroscopy is highlighted by the beta coefficients (**Figure 5.7**), as well as by the representative spectra acquisition for fresh (0 h at 0 °C) and spoiled (366 h at 0 °C) samples (**Figure 5.8**). Four main regions demonstrated high impact on

model development, namely: region A (1,720–1,790 cm^{-1}); region B (1,630–1,690 cm^{-1}); region C (1,500–1,550 cm^{-1}) and region D (1,300–1,100 cm^{-1}). It is well established that these absorption regions are related to the proteolytic activity of microbiota and the formation of biofilms, and more specifically of *Pseudomonas* spp. during spoilage of chicken breast (Ellis et al., 2002; Alexandrakis et al., 2012; Grewal et al., 2015; Wickramasinghe et al., 2020).

Table 5.3: Performance metrics of the developed PLS-R models estimating TVCs and *Pseudomonas* spp. counts of chicken thigh samples via FT-IR spectral data analysis.

TVCs	***n***	**LVs**	**Slope**	**Offset**	**r**	**RMSE**
Calibration	328	10	0.732	1.747	0.856	0.734
Full Cross Validation	328	10	0.678	2.115	0.781	0.899
Prediction	63		0.367	4.192	0.583	1.251
***Pseudomonas* spp.**	***n***	**LVs**	**slope**	**offset**	**r**	**RMSE**
Calibration	328	10	0.719	1.669	0.849	0.838
Full Cross Validation	328	10	0.660	2.033	0.762	1.037
Prediction	63		0.282	4.152	0.514	1.589

n: Number of samples, LVs: Latent variables, r: Correlation coefficient, RMSE: Root mean squared error.

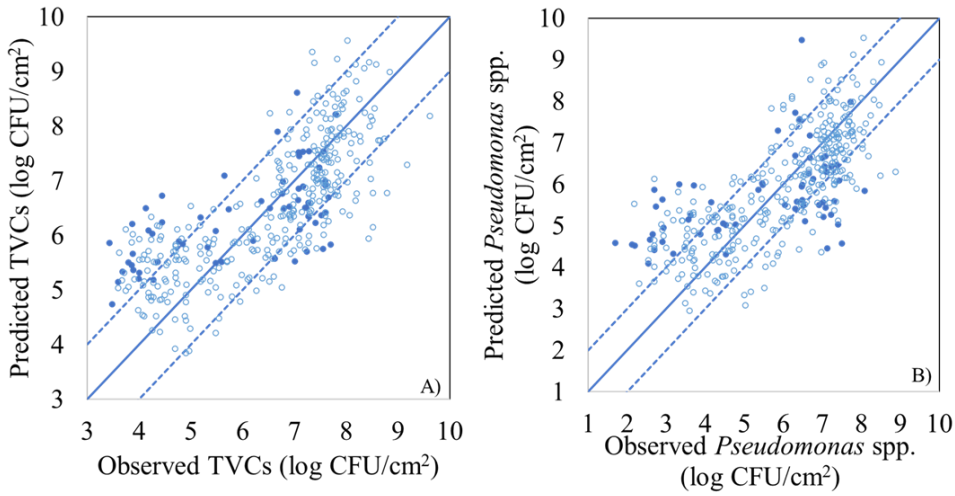

Figure 5.6: Predicted versus observed TVCs (**A**) and *Pseudomonas* spp. counts (**B**) by the PLS-R models, based on FT-IR data for FCV (open symbols) and prediction (solid symbols). Solid line represents the line of equity (y = x) and dashed lines indicate ± 1.0 log unit area.

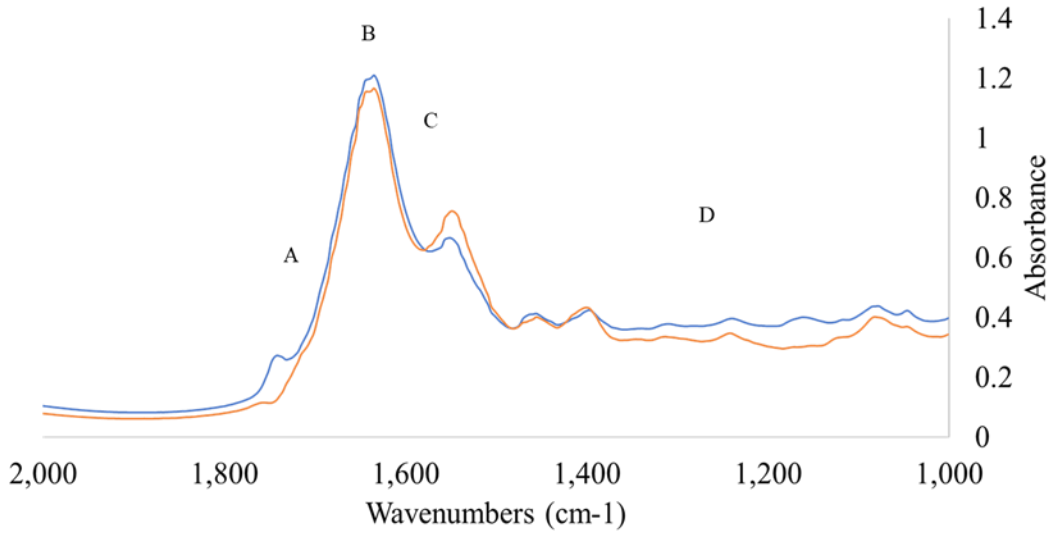

Figure 5.7: Typical FT-IR spectra in the range of 1000–2000 cm^{-1} collected from chicken thigh fillet stored at 0 °C for 0 h (fresh = blue line) and after 366 h (spoiled = orange line).

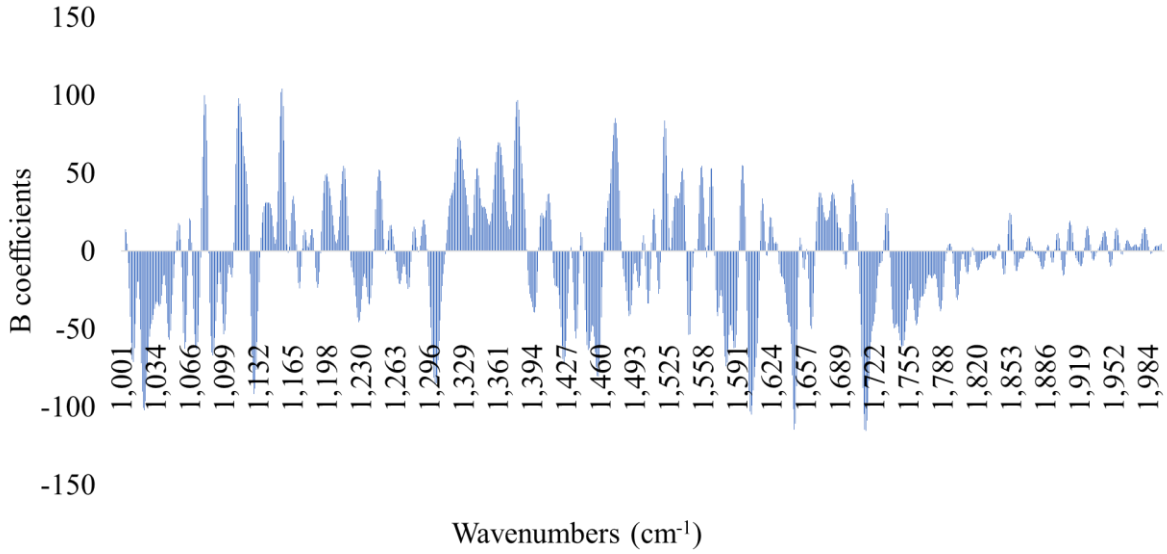

Figure 5.8: Beta (B) coefficients for PLS-R model developed on FT-IR spectral data for chicken thigh fillets.

5.3.3. Classification Models for the Assessment of Spoilage

The performance of the selected models to classify the samples in the respective quality classes (fresh or spoiled) through MSI spectral data is demonstrated by the confusion matrix (**Table 5.4**) for LDA, QDA, SVM, and QSVM. For the LDA model, 219 out of 330 samples and 49 out of 72 samples were correctly classified in both quality classes during model development (FCV) and prediction, respectively, providing overall accuracy

of 66.4% and 68.1%. During FCV process, sensitivity and specificity were 59.4% and 73.3%, respectively, whereas for model prediction the calculated sensitivity and specificity were 76.0% and 63.8%, respectively. For QDA model, 214 out of 330 samples (overall accuracy 64.8%) and 50 out of 72 samples (overall accuracy 69.4%) were classified in the correct class for model FCV and prediction, respectively. Moreover, sensitivity and specificity were estimated at 57.6% and 72.8%, respectively, for model FCV and at 73.3% and 66.7%, respectively, for the model prediction. It is notable that improved results were obtained by the application of SVM model where 301 out of 330 samples (overall accuracy 91.2%) and 68 out of 72 samples (overall accuracy 94.4%) were correctly classified in the respective quality class during model development (FCV) and prediction, respectively. In addition, for SVM model sensitivity and specificity, percentages exhibited their highest values at 94.4% during external validation. Likewise, for QSVM implementation, 287 from 330 samples and 66 from 72 samples were efficiently identified during model development and prediction, with an overall accuracy of 87.0% and 91.7%, respectively. For this model, sensitivity and specificity percentages were calculated at 83.7% and 89.6% for model FCV, while for external validation the estimated values were 94.1% and 89.5%, respectively.

Table 5.4: Confusion matrix and performance indexes of the developed classification models (LDA, QDA, SVM, QSVM) regarding sensory quality discrimination of chicken thigh samples based on MSI spectral data.

Model	Procedure	O/P	Fresh	Spoiled	Overall	Sensitivity (%)	Specificity (%)
LDA	FCV	Fresh	98	67	330	59.4	73.3
		Spoiled	44	121		73.3	59.4
		Overall accuracy (%)		66.4			
	Prediction	Fresh	19	6	72	76.0	63.8
		Spoiled	17	30		63.8	76.0
		Overall accuracy (%)		68.1			
QDA	**Procedure**	**O/P**	**Fresh**	**Spoiled**	**Overall**	**Sensitivity (%)**	**Specificity (%)**

		Fresh	99	73	330	57.6	72.8
	FCV	Spoiled	43	115		72.8	57.6
		Overall accuracy (%)		64.8			
		Fresh	22	8	72	73.3	66.7
	Prediction	Spoiled	14	28		66.7	73.3
		Overall accuracy (%)		69.4			

	Procedure	**O/P**	**Fresh**	**Spoiled**	**Overall**	**Sensitivity (%)**	**Specificity (%)**
		Fresh	130	17	330	88.4	93.4
	FCV	Spoiled	12	171		93.4	88.4
SVM		Overall accuracy (%)		91.2			
		Fresh	34	2	72	94.4	94.4
	Prediction	Spoiled	2	34		94.4	94.4
		Overall accuracy (%)		94.4			

	Procedure	**O/P**	**Fresh**	**Spoiled**	**Overall**	**Sensitivity (%)**	**Specificity (%)**
		Fresh	123	24	330	83.7	89.6
	FCV	Spoiled	19	164		89.6	83.7
QSVM		Overall accuracy (%)		87.0			
		Fresh	32	2	72	94.1	89.5
	Prediction	Spoiled	4	34		89.5	94.1
		Overall accuracy (%)		91.7			

Regarding FT-IR classification models (**Table 5.5**), the LDA model classified correctly 240 out of 328 samples and 44 out of 63 samples during model FCV and external validation, respectively, with overall accuracy reaching 73.2% and 69.8%, respectively. Sensitivity and specificity percentages were 64.1% and 84.7% for model development, whereas for external validation these performance metrics were 70.4% and 69.4%, respectively. For QDA method, 216 out of 328 samples and 45 out of 63 samples were classified at their proper quality group during FCV and external validation, respectively. QDA model enhanced performance against the remaining three models was underlined by its ability to classify fresh samples from an independent validation data set with sensitivity and specificity values of 70.0% and 72.7%, respectively. For QSVM model, 284 out of 328 samples were correctly classified during model development (overall accuracy 86.6%, sensitivity 82.4%, specificity 90.0%), whereas only 38 from 63 samples were located in their correct class during model prediction (overall accuracy 60.3%, sensitivity 55.8%, specificity 70%). Finally, for SVM model 287 out of 328 samples were accurately classified during model FCV (overall accuracy 87.5%, sensitivity 90.7%, specificity 85.1%), whereas during model prediction 44 out of 63 samples were classified correctly in their respective quality class (overall accuracy 69.8%, sensitivity 63.4%, specificity 81.8%).

Table 5.5: Confusion matrix and performance indexes of the developed classification models (LDA, QDA, SVM, QSVM) regarding sensory quality discrimination of chicken thigh samples based on FT-IR spectral data.

Model	Procedure	O/P	Fresh	Spoiled	Overall	Sensitivity (%)	Specificity (%)
LDA	FCV	Fresh	118	66	328	64.1	84.7
		Spoiled	22	122		84.7	64.1
		Overall accuracy (%)		73.2			
	Prediction	Fresh	19	8	63	70.4	69.4
		Spoiled	11	25		69.4	70.4
		Overall accuracy (%)		69.8			

	Procedure	O/P	Fresh	Spoiled	Overall	Sensitivity (%)	Specificity (%)
QDA	FCV	Fresh	118	87	328	57.6	79.7
		Spoiled	25	98		79.7	57.6
		Overall accuracy (%)		65.9			
	Prediction	Fresh	21	9	63	70.0	72.7
		Spoiled	9	24		72.7	70
		Overall accuracy (%)		71.4			

	Procedure	O/P	Fresh	Spoiled	Overall	Sensitivity (%)	Specificity (%)
SVM	FCV	Fresh	127	13	328	90.7	85.1
		Spoiled	28	160		85.1	90.7
		Overall accuracy (%)		87.5			
	Prediction	Fresh	26	15	63	63.4	81.8
		Spoiled	4	18		81.8	63.4
		Overall accuracy (%)		69.8			

	Procedure	O/P	Fresh	Spoiled	Overall	Sensitivity (%)	Specificity (%)
QSVM	FCV	Fresh	122	26	328	82.4	90.0
		Spoiled	18	162		90	82.4
		Overall accuracy (%)		86.6			
	Prediction	Fresh	24	19	63	55.8	70.0
		Spoiled	6	14		70.0	55.8
		Overall accuracy (%)		60.3			

It needs to be noted that MSI-SVM and FT-IR-QDA combinations could not only efficiently classify samples in their correct quality class, with overall accuracy of 94.4% and 71.4%, respectively, but, simultaneously, the misclassified samples were equally distributed in the safe and in the dangerous side, with specificity reaching 94.4% and 72.7%, respectively. Another interesting finding from MSI-SVM model was the low difference in the overall accuracy percentages (91.2% vs. 94.4%) observed between model FCV and prediction, indicating robust model performance. Furthermore, the same trend was observed for sensitivity and specificity (94.0% in both cases). Previous researchers reported that SVMs could result in the development of robust regression and classification models for poultry products (Kumar & Karne, 2017; Fengou et al., 2021a). SVM and QSVM models were more suitable for MSI spectral data, with SVM linear classifiers presenting the best separation of data's hyperplane (Kumar & Karne, 2017). In contrast, probability parametric LDA and QDA models which assume that each class could be described as a multivariate normal distribution (Friedman et al., 2009; Kumar & Karne, 2017), exhibited better discrimination of classes for FT-IR data. This is in good agreement with other studies, where LDA was proposed as a supervised multivariate classification method in FT-IR spectroscopic analysis of meat samples (Candŏgan et al., 2021). Even though data matrices from MSI and especially FT-IR presented high dimensionality, there was no evident class imbalance according to the prediction performance of all developed models (**Tables 5.4** and **5.5**).

Chapter 6: Assessment of chicken marinated souvlaki microbial spoilage and quality though spectroscopic and biomimetic sensors and data fusion

Abstract

Fourier Transform Infrared spectroscopy (FT-IR), Multispectral Imaging (MSI) and electronic nose (E-nose) have been implemented individually and in combination, in an

attempt to investigate and hence identify the complexity of spoilage phenomenon in poultry. For this purpose, chicken marinated souvlaki samples were subjected to storage experiments (isothermal conditions: 0, 5 and 10 ^{o}C; dynamic temperature condition: 12 h at 0 ^{o}C, 8 h at 5 ^{o}C and 4 h at 10 ^{o}C) under aerobic conditions. At pre-determined intervals samples were microbiologically analyzed for the enumeration of Total Viable Counts (TVCs) and *Pseudomonas* spp., while in parallel FT-IR, MSI and E-nose measurements were acquired. The microbiological results of *Pseudomonas* spp. were fitted to predictive growth models (two-step and one-step modeling) in order to investigate the impact of temperature on the population dynamics of *Pseudomonas* spp. on this marinated product. Quantitative models of Partial Least Squares- Regression (PLS-R) and Support Vector Machines-Regression (SVM-R) (for each sensor separately and in combination) were developed and validated for the estimation of TVCs on chicken marinated souvlaki. Furthermore, classification models of Linear Discriminant Analysis (LDA), Linear-Support Vector Machines (LSVM) and Cubic Support Vector Machines (CSVM), classifying samples in 2 (fresh or spoiled) and 3 (fresh, semi- fresh and spoiled) quality classes were optimized and evaluated. Model performance was assessed with data obtained by six different analysts and three different batches of marinated souvlaki. The results from the predictive growth models demonstrated that both modeling approaches could predict accurately the growth behavior of *Pseudomonas* spp. (RMSE< 0.341 log CFU/g). Concerning the estimation of TVCs via PLS-R model, the most efficient prediction was obtained with MSI spectral data (RMSE: 0.998 log CFU/g) as well as with combined data from FT-IR/MSI (RMSE: 0.983 log CFU/g). From the developed SVM models, those derived from MSI and FT-IR/MSI data accurately estimated TVCs with RMSE values of 0.973 and 0.999 log CFU/g, respectively. For the 3-classes models, MSI data coupled to LSVM model as well as combined MSI/E-nose data analyzed by LDA model exhibited overall accuracy percentages below 60 %. On the contrary, for the 2-classes models, combined data from FT-IR/MSI instruments analyzed by CSVM algorithm provided overall accuracy of 87.5 %, followed by MSI spectral data analyzed by LSVM with overall accuracy of 80 %. The abovementioned findings highlighted the efficacy of those non-invasive rapid methods individually and in combination for the assessment of spoilage on chicken marinated products regardless of the impact of the analyst, season or batch.

6.1 Introduction

Spectroscopic methods as Fourier Transform Infrared spectroscopy (FT-IR) and Multispectral Imaging (MSI) have been investigated in tandem with regression and classification algorithms for their effectiveness in quality assessment of meat and poultry (Berrueta et al., 2007; Kamruzzaman et al., 2016; Candŏgan et al., 2021). FT-IR vibrational spectroscopy has been recommended as an efficient solution for the discrimination of intact chicken breast muscle during spoilage via Partial Least Squares- Discriminant analysis (PLS-DA) and Outer Product Analysis (OPA) (Alexandrakis et al., 2012). PLS-R coupled to FT-IR successfully detected the microbial loads of chicken breast (Ellis et al., 2002; Vanconcelos et al., 2014). Furthermore, FT-IR analysis was proved an appropriate tool for the identification of chicken meat among other raw types of food by PLS-R and Support Vector Machines (SVMs) classification based on FT-IR data (Tsakanikas et al., 2020). Regarding MSI analysis, it has been proposed as a reliable method in tandem with PLS-R model development for the estimation of microbial groups associated with spoilage of chicken meat (Feng & Sun, 2013a, b; Ye et al., 2016). Likewise, MSI analysis and PLS-R implementation predicted accurately the time from slaughter in four poultry products (Spyrelli et al., 2020). Nevertheless, this non-destructive method has been suggested as an alternative for the detection of food fraud in minced pork adulterated with chicken (Fengou et al., 2021a). Both MSI and FTIR analysis have been investigated for their ability to feasibly predict TVCs and *Pseudomonas* spp. on the surface of stored chicken thigh fillets while they could accurately classify chicken samples in 2 quality classes (Spyrelli et al., 2021).

Another important indicator related to microbiological spoilage in food is the volatile profile associated with the metabolic activity of the microbiota (Ghasemi-Varnamkhasti et al., 2009). The electronic nose (E-nose) is a biomimetic technology describing the olfactory system of humans and it comprises an array of electronic chemical sensors recording odors via volatiles (Ghasemi-Varnamkhasti et al., 2009; Shi et al., 2019; Song et al., 2013). The main advantage of this method over spectroscopic methods is the low number of derived results which are more convenient for multivariate data analysis due to the reduced noise in the data set (Loutfi et., 2015; Di Rosa et al. et al., 2017). This environmentally friendly approach has been examined for its efficacy to assess quality and microbial spoilage in red

meat and poultry using a variety of regression and discrimination models (Ghasemi-Varnamkhasti et al., 2010; Kutsanedzie at al., 2019; Wojnowski et al, 2019). E-nose and PLS-R implementation has been proposed for the estimation of chicken fat (Rajamäki et al., 2006; Song et al., 2013). Moreover, E-nose has been successfully employed in combination with SVM-R model for the prediction of TVCs on chilled pork (Wang et al., 2012) and on the indigenous microbiota of beef fillets (Papadopoulou et al., 2013). Apart from the development of SVM models, E-nose signals have been used in the development of back propagation neural networks (BPNN) predicting TVCs on chicken (Timsorn et al., 2016), as well as in the implementation of a variety of machine learning models for the determination of microbial groups in minced meat (Estelez-Lopez et al., 2017). In addition, E-nose data analyzed with LDA and BP-ANN models were evaluated for their potential to detect pork freshness via the volatile colorific fingerprint obtained during spoilage of pork samples (Li et al., 2014).

However, each of these rapid and non-invasive methods has its own advantages, weaknesses and limitations concerning the monitoring and controlling procedures of quality and safety in the meat industry (Di Rosa et al. et al., 2017). Taking into consideration the complexity of the food matrix during meat spoilage in terms of physical, biological and chemical properties, a combination of sensor features could capture more effectively both internal (metabolites, chemical compounds) and external (color, smell, texture, tenderness) alterations and thus identify more accurately quality defects in food (Huang et al., 2014; Kutsanedzie at al., 2019). In this context, data fusion from different sensors has been recently investigated for its synergistic role to the improvement of model classification and/or prediction potential (Borràs et al., 2015). For meat products, low and mid fusion has been employed as two different data merge techniques for the development of models predicting quality, freshness, microbial loads (Huang et al., 2014; Liu et al., 2014) and adulteration (Alamprese et al., 2013). Classification models generated with E-nose, Computer vision (CV) and artificial tactile (AT) data demonstrated accurate predictions of pork and chicken freshness (Weng et al., 2020). The ensemble of spectral, texture and color features via a classification model of k-mean-BFF was proven efficient for the quality assessment in chicken meat (Suxia, 2018), whereas the combination of E-Nose (colorimetric sensors array) and hyperspectral imaging successfully estimated

chicken meat quality and freshness (Khulal et al., 2017). In addition, data fusion of two spectral methods namely V-NIR and SWIR was suggested as feasible solution for the tracing of foreign materials (FMs) on the surface of chicken breast fillets (Chung & Yoon, 2021).

The aim of this study was the development of quantitative and qualitative models rapidly assessing spoilage on chicken marinated souvlaki via MSI, FT-IR and E-nose measurements both individually and in combination (mid-fusion). PLS-R and SVM-R models were developed for the determination of TVCs on chicken marinated souvlaki. Further on, LDA, LSVM and CSVM classification models were developed on sensors data (both individually and in combination) for the detection of three and two quality classes, respectively. Model performance assessment with data from independent batches and analysts confirmed the efficacy of nondestructive techniques and their feasibility to be performed even by untrained personnel

6.2 Materials and Methods

6.2.1 Experimental design

Chicken marinated souvlaki (n= 209, *ca* 48.89 ± 1.3 g) samples were transferred from a Greek poultry industry to the laboratory (within 24 h from slaughter and marinade process), placed in styrofoam trays (two portions per tray) and wrapped with cling film. After packaging, samples were stored aerobically at three isothermal conditions, namely 0, 5, and 10 ^{o}C (two independent experiments) and one dynamic temperature profile (12 h at 0 ^{o}C, 8 h at 5 ^{o}C and 4 h at 10 ^{o}C) in high precision (± 0.5 ^{o}C) incubation chambers (MIR-153, Sanyo Electric Co., Osaka, Japan), where temperature was monitored every 20 min by data loggers (CoxTracer, Belmont, N.C.). At predetermined intervals, samples were analyzed microbiologically (enumeration of TVCs and *Pseudomonas* spp.) while simultaneously FT-IR, MSI and E-nose data were acquired. At each sampling point, duplicate samples stored at the same isothermal condition (n= 2×2) and triplicate samples stored at the dynamic temperature profile (n= 3) were subjected to the above-mentioned analyses. The microbiological results were expressed as log CFU/g and were used for the development of primary and secondary predictive models (two-step and one-step modelling approach) for *Pseudomonas* spp. Further on, quantitative and qualitative models

assessing microbial spoilage and quality on chicken marinated souvlaki were developed and validated. PLS-R and SVM-R models were employed for the estimation of TVCs for each sensor separately. Moreover, mid-level fusion (pre- processing of data via Principal Component Analysis, PCA and afterwards employment of PLS-R) was performed for the evaluation of the combined use of MSI, FT-IR and e-nose sensors for TVCs assessment. In the same context, classification models of Linear Discriminant Analysis (LDA), Linear Support Vector Machines (LSMV) and Cubic Support Vector Machines (CSVM) were evaluated for their efficacy to identify 3 and 2 spoilage classes via MSI, FT-IR and E-nose data (in combination and separately).

Validation storage experiments at aerobic isothermal conditions (0, 4, 5, 8 and 10 ^{o}C) were undertaken by different analysts (n= 6) with three different chicken marinated souvlaki batches. MSI, FT-IR and E-nose measurements were collected and correlated to the respective TVCs results. Quantitative and qualitative developed models were fitted to the obtained experimental data in order to evaluate their performance.

6.2.2 Microbiological analysis

A portion of 25 g of chicken marinated souvlaki (chicken thigh fillet, sodium chloride, sodium acetate, sodium citrate, enzyme tenderizer and ascorbic acid) was transferred aseptically to a stomacher bag containing 225 ml of sterile quarter strength Ringer's solution (Lab M Limited, Lancashire, UK) and was homogenized by a Stomacher device (Lab Blender 400, Seward Medical, UK) for 60 s. From this 1:10 sample solution, serial decimal dilutions were prepared using the same diluent and 0.1 ml of the appropriate dilution was spread to the following media: a) Tryptic glucose yeast agar (Plate Count Agar, Biolife, Milan, Italy) for the enumeration of total viable counts (TVCs) incubated at 25^{o}C for 72 h; and b) Pseudomonas agar base (LAB108 supplemented with selective supplement Cetrimide Fucidin Cephaloridine, Modified C.F.C. X108, LABM) for the determination of the presumptive *Pseudomonas* spp. counts incubated at 25^{o}C for 48 h.

6.2.3 Predictive growth models for TVCs and Pseudomonas spp. in chicken marinated samples

6.2.3.1 Two-step modeling approach

The primary model of Baranyi and Roberts (1994) was was fitted to the observed TVCs and *Pseudomonas* spp. counts at each storage temperature in order to determine the kinetic parameters of microbial growth, namely the maximum specific growth rate (μ_{max}), the lag phase duration (λ), and the maximum population density (y_{end}) via Microsoft® Excel Add-in curve-fitting program DMFit, Version 3.5 (Institute of Food Research, Norwich, UK). Afterwards, the influence of storage temperature on *Pseudomonas* spp. μ_{max} parameter was investigated by fitting Ratkowsky growth-temperature secondary model (Ratkowsky, 1983) to the experimental data (Equation 6.1)

$$\sqrt{\mu_{max}} = b\ (T - T_{min}) \qquad (6.1)$$

Where, b is a regression coefficient that depends on environmental factors and T_{min} is the theoretical minimum temperature for microbial growth.

6.2.3.2 One-step modeling approach

One- step modeling (Huang et al., 2016) was also employed for the determination of the primary and secondary model parameters for *Pseudomonas* spp. on chicken marinated souvlaki. Huang full growth primary model (Huang, 2013) (equations 6.2- 6.4) and the secondary Ratkowsky growth-temperature model (Ratkowsky, 1983) were fitted to the obtained *Pseudomonas* spp. counts (equation 6.1). The two models were simultaneously applied to the experimental data via IPMP-Global Fit software (USDA Agricultural Research Service, Eastern, Regional Research Center, Wyndmoor, PA).

$$\boldsymbol{Y(t) = Y_0 + Y_{max} - ln\ [e^{Y0} + (e^{Ymax} - e^{Y0})\ e^{-\mu max\, B(t)}]} \quad (6.2)$$

$$\boldsymbol{B(t) = t + \frac{1}{4}\, ln \frac{1+e^{-4(t-\lambda)}}{1+e^{4\lambda}}} \quad (6.3)$$

$$\boldsymbol{\lambda = \frac{e^{A}}{\mu max^{m}}} \quad (6.4)$$

where: Y(t) is the base-10 logarithms (log_{10}) of the real time microbial counts (log CFU/g) at the respective storage time t (h), y_o is the initial base-10 logarithms (log_{10}) of the microbial counts (log CFU/g), y_{max} is the final base-10 logarithms (log_{10}) of the microbial

counts (log CFU/g), μmax is the specific growth rate of the microbial group (h^{-1}), b, A and m are regression coefficients, λ is the lag phase (h) and B(t) is the transition function.

External validation for both modeling approaches was undertaken with an experimental dataset of *Pseudomonas* spp. counts (n=33, different batch) from a spoilage experiment on chicken marinated souvlaki at a dynamic temperature profile (12 h at 0 ^{o}C, 8 h at 5 ^{o}C and 4 h at 10 ^{o}C). Model performance evaluation was performed using the bias factor (B_f) and accuracy factor (A_f) indices (Ross, 1996).

6.2.4 Sensors

6.2.4.1 Spectral acquisition

Chicken marinated souvlaki samples were subjected to MSI analysis using the Videometer- Lab instrument (Videometer A/S, Herlev, Denmark) which captures surface reflectance of samples from 18 monochromatic wavelengths (405-970 nm), namely 405, 435, 450, 470, 505, 525, 570, 590, 630, 645, 660, 700, 850, 870, 890, 910, 940, and 970 nm. The description of this sensor as well as the process of image acquisition are thoroughly discussed in previous studies (Dissing et al., 2013). The final outcome of this acquisition is a data cube containing spatial and spectral data for each sample of size m×n×18 (where m×n is the image size in pixels) (Tsakanikas et al., 2015). Prior to data analysis, an extra step is needed where the Region of interest (ROI) on the samples surface is separated from the surrounding area containing non useful information. For each image, the mean reflectance spectrum was estimated by the calculation of the average value and the standard deviation of the intensity of pixels within the ROI at each wavelength. For this purpose, Canonical Discriminant Analysis (CDA) was applied to each sample and for each wavelength individually through Videometer-Lab version 2.12.39 software (Videometer A/S, Herlev, Denmark).

FT-IR analysis was implemented using a ZnSe 45 HATR (Horizontal Attenuated Total Reflectance) crystal (PIKE Technologies, Madison, Wisconsin, United States) and an FT-IR-6200 JASCO spectrometer (Jasco Corp., Tokyo, Japan). The ATR crystal shows a refractive index of 2.4 and a depth of penetration of 2.0 μm at 1000 cm^{-1}. Spectra were obtained in the wavenumber range of 4000 to 400 cm^{-1} using Spectra Manager Code of

Federal Regulations (CFR) software version 2 (Jasco Corp., Tokyo, Japan), by accumulating 100 scans with a resolution of 4 cm^{-1} and a total integration time of 2 min.

6.2.4.2 Electronic nose (E-nose)

The Alpha M.O.S a-FOX sensor array system 3000 (Alpha M.O.S, Toulouse, France) with 12 metal oxide sensors was used in this study. The system consists of a sampling apparatus, an array of sensors, an air generator equipment (F-DGSi, Evri, France) and software (Alpha Soft V12.46) for data recording. The sensor array contains 12 metal oxide sensors divided into T, P and LY types, namely: LY2/LG, LY2/G, LY2/AA, LY2/GH, LY2/gGTL, LY2/gGT, T30/1, P10/1, P10/2, P 40/1, T 70/2 and PA/2 (Lin et al., 2013). Prior to injection, 2 g of sample (2.013 ± 0.002 g) were placed in a 2.5 ml vial, sealed with aluminum caps and heated at 50 ^{o}C for 20 min in a thermoblock 2t static headspace sampler (Teknokroma Analitica S.A., Barcelona, Spain). A volume of 500 μl from the generated headspace was injected to the e-nose with the injection rate being 500 μl/s. Method parameters were defined as follows: a) acquisition duration: 120 s; b) acquisition period: 1 s; c) acquisition time: 800 s; and d) gas flow (air): 150 ml/min. The signal response of each array was expressed in the form of relative resistance changes (Delta R/Ro).

6.2.5 Data processing

MSI spectral data were consisted of 18 mean values and the respective 18 standard deviations of the intensity in pixels for each observation/measurement. Spectral data were preprocessed by Standard Normal Variance (SNV) transformation to remove collinear and "noisy" data (Bi et al., 2016). The same transformation was applied to e-nose data which contained the relative resistance for each sensor. For FT-IR spectral data, the Savinsky-Golay second derivative transformation (second order polynomial, 2^{nd} derivative, 9-point window) was applied on spectra at wavelengths in the range of 900 to 2000 cm^{-1} for the reduction of baseline shift and noise (Alamprese et al., 2016).

Both qualitative and quantitative models were calibrated and optimized (k- fold cross validation, k= 10) with data from the storage experiments at 0, 5, 10 ^{o}C and the dynamic temperature profile (n= 169), while model external validation was performed by independent data (n= 40, 3 batches, 6 analysts) from storage experiments at aerobic

isothermal (0, 4, 5, 8, 10 ^{o}C) conditions. For the development of classification models based on 3 quality classes, discrimination was based on TVC values as follows: a) fresh (class 1: 22.48%): TVCs<6.0 log CFU/g; b) semi-fresh (class 2: 18.93%): 6.0≤TVC<7.0 log CFU/g; and c) spoiled (class 3: 58.58%): TVC≥7.0 log CFU/g. For the 2 quality class classification models, samples were defined as fresh (class 1: 42.01%) and spoiled (class 2: 57.99%) when TVCs were below or above 7.0 log CFU/g, respectively. The developed classification models were evaluated for their performance with data from independent experiments, namely: a) for the 3 class-model (n=40; Class 1: 14 samples (35%); Class 2: 8 samples (20%); Class 3: 18 (45 %)), and b) for the 2 class-model (n=40; Class 1: 22 samples (55 %); Class 2: 18 samples (45 %)).

6.2.6 Model development and performance assessment

For the development of PLS-R models for each sensor individually and in combination was performed using the Unscrambler© ver. 9.7 software (CAMO Software AS, Oslo, Norway). For the single sensor models, the acquired sensor data were correlated to TVCs via the development of PLS-R models. Principal Component Analysis (PCA) was applied to sensors data separately and the derived PCA scores were merged for the development of 2-sensors and 3-sensors PLS-R models (Márquez et al., 2016). Similarly, Support Vector Machines-Regression (SVM-R) was employed for the estimation of TVCs, via MATLAB 2012a software (The MathWorks, Inc., Natick, Massachusetts, USA), where single sensor as well as 2-sensor and 3-sensor models were performed and validated. The performance of the developed PLS-R and SVM-R models was evaluated using the correlation coefficient (r) and Root Mean Squared Error (RMSE: log CFU/g) indices. Furthermore, classification models of LDA, LSVM and CSVM were developed via MATLAB 2012a software and assessed for their accuracy using the following performance metrics: overall accuracy (%), sensitivity (%) and precision (%) (Sokolova & Lapalme, 2009).

6.3 Results

6.3.1 Microbiological results

The population dynamics of TVCs and *Pseudomonas* spp. during aerobic storage at isothermal conditions and the dynamic temperature profile are presented in **Figures 6.1**

and **6.2,** respectively. The initial TVCs and *Pseudomonas* spp. counts in chicken marinated samples stored at isothermal conditions were enumerated at 5.37 (± 0.26) and 5.01 (± 0.01) log CFU/g, respectively, whereas these microbial groups reached 5.26 (±0.06) and 4.43 (±0.10) log CFU/g in samples from the dynamic temperature profile. Storage temperature had a great impact on TVCs and *Pseudomonas* spp. behavior in samples, with chickens' spoilage occurring at different time points. Specifically, TVCs reached the threshold of spoilage (7.0 log CFU/g) (Galarz et al., 2016) at 0°C in 216 h (7.41 ± 0.74 log CFU/g), at 5°C in 72 h (7.07 ± 0.73 log CFU/g) and at 10 ^{o}C in 42 h (7.01 ± 0.6 log CFU/g). The population of TVCs in samples maintained at the dynamic temperature profile followed similar growth behavior with the samples stored at 5 ^{o}C, as their counts reached 6.89 (±0.42) log CFU/g in 96 h. Likewise, *Pseudomonas* spp. counts which are associated to the production of slime and off-odors when they reach 7.0 log CFU/g in meat products (Gospavic et al., 2008; Rouger et al., 2017), reached this limit at 0°C in 216 h (7.06 ± 1.04 log CFU/g), at 5°C in 96 h (6.86 ± 0.76 log CFU/g), at 10 ^{o}C in 48 h (7.61 ± 0.38 log CFU/g) and at the dynamic temperature profile in 120 h (6.46 ± 0.81 log CFU/g).

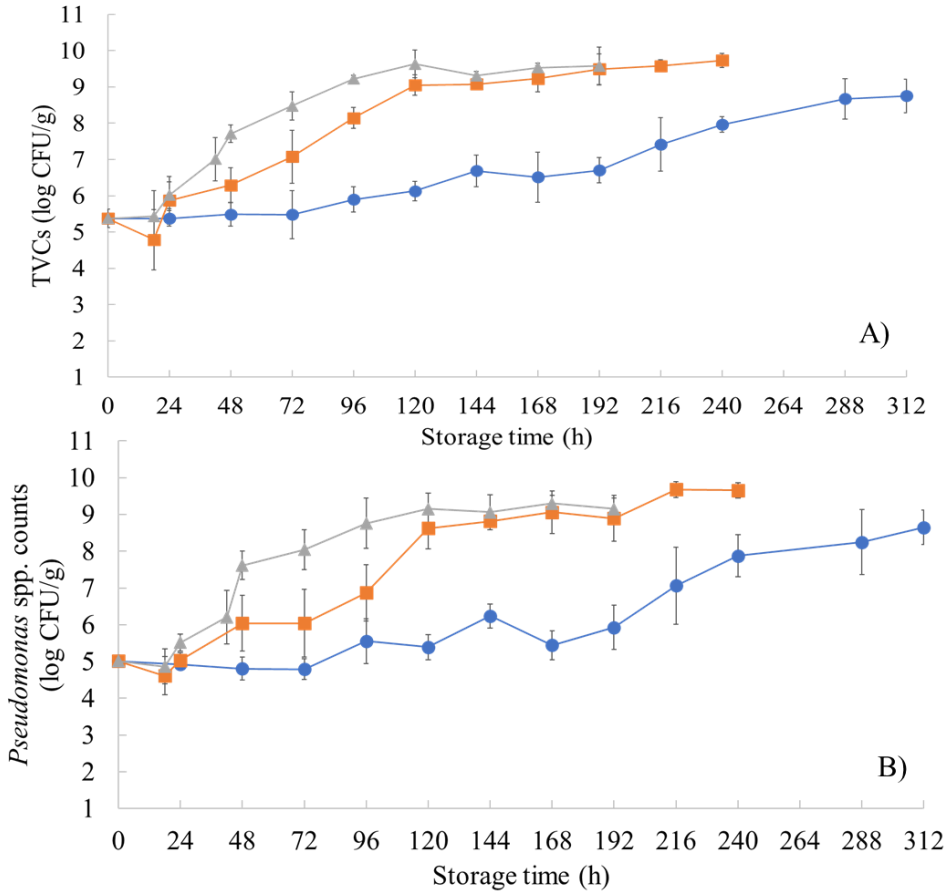

Figure 6.1: Mean (± SD, n=4) TVCs (A) and *Pseudomonas* spp. counts (B) in chicken marinated souvlaki samples during storage at 10 (triangle symbol), 5 (square symbol) and 0 (cycle symbol) ^{o}C.

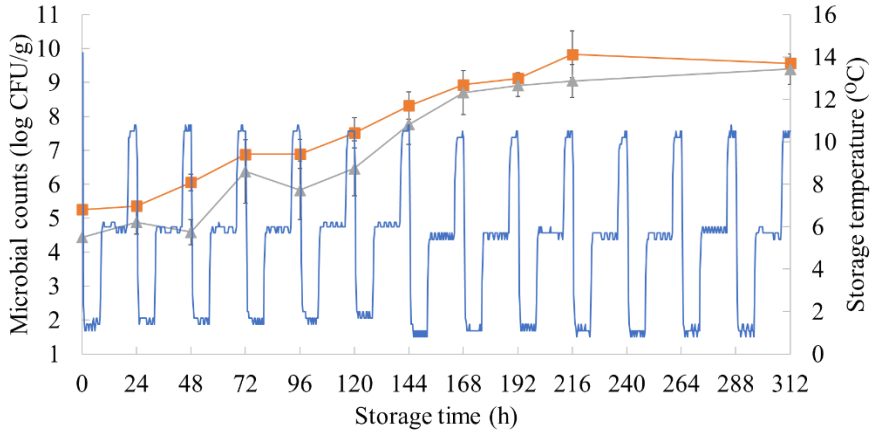

Figure 6.2: Mean (± SD, n=3) TVCs (square symbol) and *Pseudomonas* spp. counts (triangle symbol) in chicken marinated souvlaki samples and recorded temperature (^{o}C) (solid line) during storage at the dynamic temperature profile (12 h at 0 ^{o}C, 8 h at 5 ^{o}C and 4 h at 10 ^{o}C).

6.3.2 Predictive growth models for TVCs and Pseudomonas spp.

6.3.2.1 Two-step modeling: Primary growth models for TVCs and *Pseudomonas* spp. and secondary model growth-temperature for *Pseudomonas* spp.

The influence of temperature on the microbiota of chicken marinated souvlaki was further investigated and the growth kinetic parameters (μ_{max}, h^{-1}; λ: lag phase, h, y_{max} (log CFU/g) of TVCs and *Pseudomonas* spp. are presented in **Table 6.1**. The estimated lag phase of TVCs and *Pseudomonas* spp. was prolonged as storage temperature decreased, with the maximum value obtained for samples stored at 0 ^{o}C (TVCs: 80.09±14.95 h and *Pseudomonas* spp.: 93.49±10.67 h). Reversibly, μ_{max} parameter reached its lowest value for TVCs and *Pseudomonas* spp. for samples stored at 0 ^{o}C (TVCs: 0.035±0.002 h^{-1}, *Pseudomonas* spp.: 0.048±0.011 h^{-1}) and the highest one for samples stored at 10 ^{o}C (TVCs: 0.123±0.028 h^{-1}, *Pseudomonas* spp.: 0.310±0.343 h^{-1}). The kinetic parameters for TVCs and *Pseudomonas* spp. obtained in this work are in agreement with previous studies on stored chicken products (Gospavic et al., 2008; Lytou et al., 2016). Moreover, *Pseudomonas* spp. growth followed similar behavior as TVCs population, demonstrating once more *Pseudomonas* spp. dominant role in poultry's spoilage under aerobic conditions (Bruckner et al., 2013; Raab et al., 2018). Further on, the Ratkowsky model was fitted to the abovementioned μ_{max} values of *Pseudomonas* spp. and the respective parameters of b and T_{min} values were calculated at 0.013 and -16.44 ^{o}C, respectively. For this secondary model fitting, the value of RMSE was 0.054 log CFU/g and the coefficient of determination (R^2) was 0.811.

Table 6.1: Baranyi and Roberts (1994) model parameters (lag phase: λ, h; maximum specific growth: μ_{max}, h^{-1}; maximum number of counts: y_{max}, log CFU/g) and performance metrics (standard error of fitting: se(fit); coefficient of determination: R^2) obtained from DMFIT fitting to TVCs and *Pseudomonas* spp. counts in stored chicken marinated souvlaki.

Microbial group	Temperature (^{o}C)	λ, lag phase (h)	μmax (h^{-1})	ymax (log CFU/g)	se(fit) (Minimum-maximum)	R^2 (Minimum-maximum)
TVC	0	80.09±14.95	0.035±0.002	8.96±0.39	0.187-0.410	0.888-0.978
	5	38.26±1.28	0.090±0.022	9.49±0.23	0.218-0.350	0.953-0.980

	10	8.49±6.63	0.123±0.028	9.48±0.07	0.217-0.440	0.941-0.980
***Pseudomonas* spp.**	0	93.49±10.67	0.048±0.011	8.80±0.44	0.351-0.626	0.844-0.950
	5	27.99±23.40	0.079±0.042	9.70±0.19	0.333-0.491	0.920-0.968
	10	26.39±12.45	0.310±0.343	9.10±0.29	0.385-0.590	0.864-0.952

6.3.2.2 One step modeling approach

The estimated kinetic parameters of Huang full growth model (equations 6.2- 6.4) and Ratkowsky growth-temperature model (equation 6.1) via the IPMP-Global Fit software (USDA Agricultural Research Service, Eastern, Regional Research Center, Wyndmoor, PA) are available in **Table 6.2**, while the calculated μ_{max} and lag phase parameters of *Pseudomonas* spp. are provided in **Table 6.3**. RMSE value for this one-step approach was 0.341 log CFU/g while the degrees of freedom were 28. Specifically, *Pseudomonas* spp.μ_{max} parameter via one step modeling presented its maximum value at 10 ^{o}C (0.138 h^{-1}) and the minimum value at 0 ^{o}C (0.038 h^{-1}). *Pseudomonas* spp. lag phase was extended for the samples at 0 ^{o}C (84.4 h) while for samples at 10 ^{o}C lag phase decreased to 13.81 h. These values are in compliance with the existing literature for stored chicken products (Dominquez & Shaffner, 2007). Concerning b coefficient and T_{min} (or a and T_o for one step modeling) of Ratkowsky model, their values were established at 0.02±0.01 ^{o}C and -11±5.67 ^{o}C.

Table 6.2: Kinetic parameters estimated and statistics by Huang full growth primary model and the Ratkowsky growth model for temperatures.

Parameters	**Value**	**Std-Error**	**t-value**	**p-value**
a	0.02	0.01	2.39	2.40E-02
T0	-11.00	5.67	-1.94	6.21E-02
A	-0.15	4.33	-0.03	9.73E-01
m	1.40	1.47	0.95	3.49E-01
y0, T0.0	4.87	0.50	9.83	1.40E-10
y0, T5.0	4.95	0.49	10.04	8.89E-11
y0, T10.0	4.86	0.76	6.37	6.73E-07
ymax	9.24	0.36	25.88	4.29E-21

Table 6.3: Lag phase (λ) and μ_{max} values estimated by Huang full growth primary model for *Pseudomonas* spp. growth on chicken marinated souvlaki at 0, 5 and 10 °C.

Storage temperature (°C)	μ_{max} (h^{-1})	λ (h)
0	0.038	84.4
5	0.080	29.6
10	0.138	13.8

6.3.2.3 Model's external validation

Pseudomonas spp. observations from the dynamic temperature profile were fitted to the Baranyi and Roberts (1994) dynamic growth model, where y_o, y_{max} and h_o were defined based on the results of the two-step and the one step modeling process separately. For the two-step model evaluation, the initial and the final *Pseudomonas* spp. counts were 4.92 ± 0.16 log CFU/g and 9.19 ± 0.49 log CFU/g, respectively, while the h_o parameter (μ_{max} × lag phase) was calculated at 3.12. For the one-step modeling validation, y_o and y_{max} were established at the same values as of two-step modeling whereas h_o was defined at 3.75. The predictive versus the observed *Pseudomonas* spp. counts for the dynamic temperature profile are provided in **Figure 6.3** for the two modeling procedures. According to **Figure 6.3**, none of the two models seemed to over or under estimate *Pseudomonas* spp. counts, within the ± 10 % limit area, during storage at this dynamic temperature profile. The efficacy of the two models is demonstrated by the RMSE of prediction (**Table 6.4**) that reached values below the microbial criterion of ± 1.0 log CFU/g (Two step approach: 0.702 log CFU/g, One step approach: 0.653 log CFU/g). In addition, the calculated value of the bias factors (B_f) was within the range of 0.96-1.1 for both models indicating satisfactory prediction (Lianou et al., 2020) of *Pseudomonas* spp. counts, where only 7.8 % and 8.8 % of predictions through the two and the one step model being inaccurate (**Table 6.4**).

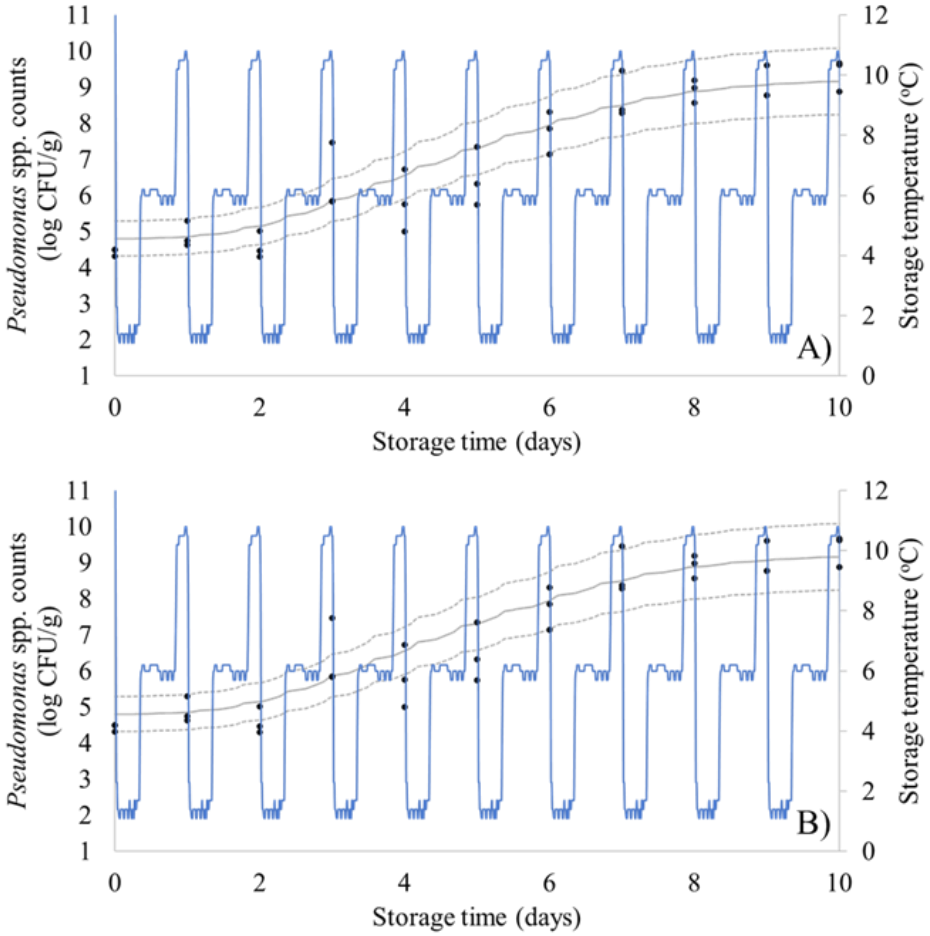

Figure 6.3: Observed *Pseudomonas* spp. counts (cycles) at chicken marinated souvlaki samples stored aerobically at a dynamic temperature profile. Solid line corresponds to the predictive model, dashed lines correspond to the ± 10 % limit area and solid blue line corresponds to temperature alterations during storage.

Table 6.4: Performance metrics (Root Mean Squared Error, RMSE; Bias factor, B_f; Accuracy factor, A_f) of the evaluation of the two-step and one-step model predicting *Pseudomonas* spp. growth in stored chicken marinated souvlaki.

Model	**Performance metrics**		
	RMSE (log CFU/g)	B_f	A_f
Two-step model	0.702	0.959	1.088
One-step model	0.653	0.967	1.078

6.3.3 Spectra and E-nose signals

E-nose signal response (intensity) per sensor is shown in **Figure 6.4A** for a fresh (0h) and a spoiled (240h) sample of chicken marinated souvlaki stored at 5°C. Differences in the intensity between fresh and spoiled samples also occurred in **Figure 6.4B** for the six sensors, namely: PA/2, T30/1, P10/1, P10/2, P40/1 and T70/2. The first sensor is linked with changes in ethanol, ammonia and organic amines (Lin et al., 2013) which are due to *Pseudomonas* spp. proteolytic activity during meat spoilage (Nychas et al., 2008). P40/1 sensor is related to the presence of fluorine (Wang et al., 2012; Xu et al., 2014). The remaining sensors T30/1, P10/1, P10/2, T70/2 could be associated with organic solvents, hydrocarbons, methane and aromatic compounds, respectively (Xu et al., 2014) and subsequently to *Pseudomonas* spp. biofilm formation during meat spoilage (Wang et al., 2012; Wickramasinghe et al., 2019).

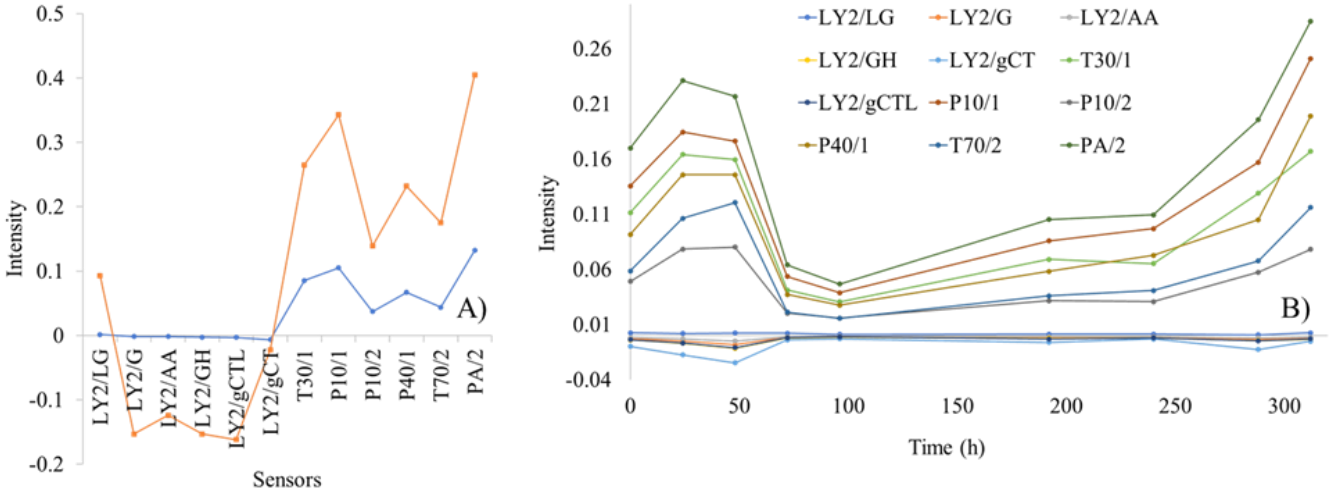

Figure 6.4: Signal (intensity) from E-nose analysis for fresh (blue line: 0 h) and spoiled (orange line: 240 h at 5ºC) chicken marinated souvlaki sample (A); Signal from each sensor array during spoiled samples (240 h at 5ºC) acquisition (B).

FT-IR and MSI spectra for fresh (0 h at 0 ºC) and spoiled (240 h at 5 ºC) chicken marinated souvlaki are represented in **Figure 6.5**. Regarding MSI spectra (**Figure 6.5B**), reflectance (mean intensity in pixels) between fresh and spoiled samples differed at 660, 700, 850, 870, 890, 910 and 940 nm, where the region of 660 to 700 nm is related to myoglobin in meat color as described elsewhere (Spyrelli et al., 2020). From FT-IR results (**Figure 6.5A**), the absorption bands showing variations between fresh and spoiled samples

were located in the areas of 1,000.87-1,150 cm^{-1} and 1,476.24-1,692.2 cm^{-1}. Specifically, absorption bands at 1,541.81 and 1,629.55 cm^{-1} were attributed to the metabolic products (amide I and II) associated with spoilage microorganisms as *Pseudomonas* spp. and their metabolic activity on the surface of meat during spoilage (Böcker et al., 2007; Alexandrakis et al., 2012).

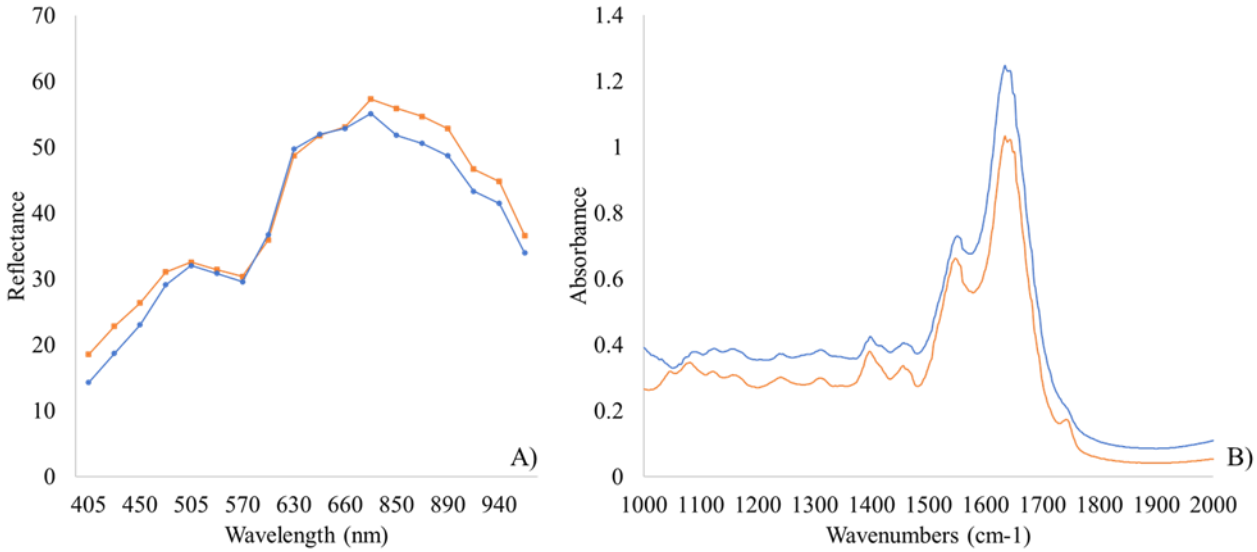

Figure 6.5: Reflectance from MSI spectra (405– 970 nm) (A) and absorbance from FT-IR spectra (1,000- 2,000 cm^{-1}) (B) for fresh (blue line: 0h) and spoiled (orange line: 240h) chicken marinated souvlaki at 5 ºC.

6.3.4 Regression Models assessing microbial loads in chicken marinated souvlaki

6.3.4.1 PLS-R models

PLS-R model parameters (slope, offset) and their performance metrics (r, RMSE) are presented in **Table 6.5** for model optimization (full cross-validation) and evaluation (prediction) for each sensor separately and in combination. MSI models exhibited the highest performance during prediction with RMSE value of 0.998 log CFU/g which was within the acceptable microbial prediction zone of ± 1.0 log CFU/g. Likewise, FT-IR model showed RMSE of prediction values of 1.025 log CFU/g. On the contrary, E-nose model poorly predicted TVCs with a RMSE of prediction value being 1.921 log CFU/g. These findings confirmed the suitability of MSI and FT-IR sensors for the quantitative assessment of TVCs in poultry products. Nevertheless, these non-invasive methods in

tandem with PLS-R models have been proposed as rapid and efficient tools for the detection of spoilage/freshness in meat and poultry (Kamruzzaman et al., 2013; Fengou et al., 2019; Rahman et al., 2018). Regarding E-nose model, its performance was not in full agreement with other studies where this sensor combined with PLS-R model successfully predicted the microbial population on chicken stored in modified atmospheres (Rajamäki et al., 2006) and the quality changes due to chicken fat oxidation (Song et al., 2013). This discrepancy could be attributed to the marination treatment performed in this study and the of organic acids such as ascorbic acid, sodium acetate and chloride in the headspace injected to the instrument.

Table 6.5: PLS-R model parameters (slope, offset) and performance metrics (correlation coefficient, r; Root Mean Squared Error, RMSE) for the estimation of TVCs in chicken marinated souvlaki samples via MSI, FT-IR, E-nose analyses.

Sensor	Process	Observations	Slope	Offset	Correlation coefficient, r	Root Mean Squared Error, RMSE (log CFU/g)
MSI	FCV	169	0.776	1.698	0.868	0.815
	Prediction	40	0.511	3.419	0.803	0.998
FT-IR	FCV	169	0.62	2.87	0.746	1.099
	Prediction	40	0.374	4.902	0.497	1.627
E-nose	FCV	169	0.576	3.232	0.757	1.12
	Prediction	40	0.044	6.145	0.245	1.921
MSI/FT-IR	FCV	169	0.687	2.363	0.818	0.941
	Prediction	40	0.592	2.689	0.783	0.983
FT-IR/E-nose	FCV	169	0.598	3.055	0.758	1.131
	Prediction	40	0.171	6.245	0.222	1.757
MSI/E-nose	FCV	169	0.596	3.061	0.75	1.149
	Prediction	40	0.503	3.498	0.727	1.373
3-sensors	FCV	169	0.596	3.056	0.751	1.148
	Prediction	40	0.474	3.821	0.722	1.367

From the combined 2 sensor models, the combination of FT-IR/MSI outperformed all the others (RMSE: 0.983 log CFU/g), followed by MSI/E-nose sensor. This outcome confirmed that HSI and/or MSI sensor data inclusion could improve E-nose prediction for meat freshness assessment (Khulal et al., 2017; Weng et al., 2020). These methods

combined with NIR have been reported as a reliable and alternative approach for the estimation of Total Volatile Basic Nitrogen (TVB-N) in pork (Huang et al., 2014). The combined 3 sensors model demonstrated a RMSE value of 1.367 during prediction while for E-nose/FT-IR model this value was 1.757 log CFU/g. Additionally, correlation coefficient (r) values ranged from 0.722 to 0.803, except E-nose that presented very low value for this performance index (r= 0.245). The predicted versus observed TVCs for the most efficient models, namely MSI and FT-IR/MSI, as well as for the combined 3 sensor model are illustrated in **Figure 6.6**. According to **Figure 6.6A** and **6.6B**, MSI and FT-IR/MSI models could estimate TVCs within the acceptable area of ± 1 log CFU/g, while underestimation of TVCs was evident for samples exceeding 8 log CFU/g for the combined 3 sensor model (**Figure 6.6C**).

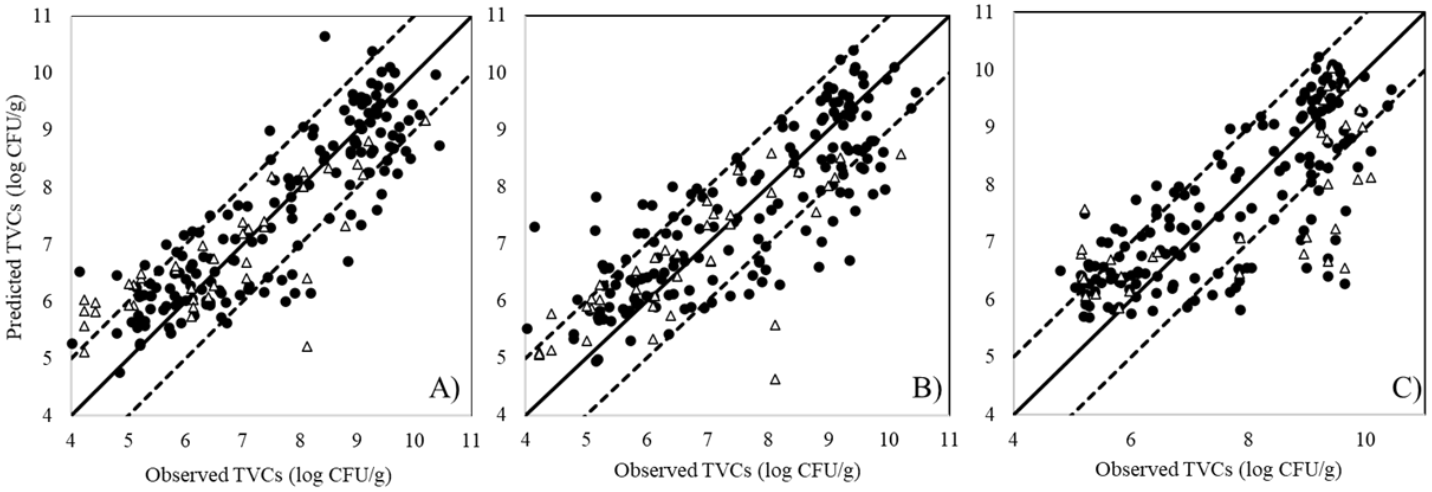

Figure 6.6: Predicted versus observed TVCs resulted from PLS-R model development based on data from: MSI (A), FT-IR/MSI (B) and combination of the 3 sensors (C). Solid symbols correspond to FCV process and open symbols to prediction process. Solid line represents the line of equity (y=x) while dashed lines indicate the limit area of ± 1.0 log CFU/g.

The beta coefficients for the PLS-R models via MSI, FT-IR/MSI and the combined 3 sensors are provided in the linear equations 6.6-6.8. Likewise, the contribution of each sensor to the estimation of TVCs via FT-IR/MSI model is presented in equation 6.7, where the scores of the first 6 PCs from MSI data and PC1 scores from FT-IR, obtaining values between 0.0991 to 14.800, were considered as significant based of Martens Uncertainty test. On the other hand, for the combined 3 sensor model (equation 6.8), b coefficients corresponding to PC4 scores from FT-IR data PCA analysis and to PC1, PC3 and PC4 scores from E-nose data PCA analysis, demonstrated significant contribution to models' development and prediction performance.

$$Y_{TVCs/MSI} = 13.984 + 9.529 \times X_{mean,405nm} - 6.481 \times X_{mean,505nm} + 13.632 \times X_{mean,570nm} - 6.533 \times X_{mean,630nm} + 5.323 \times X_{mean,645nm} + 9.131 \times X_{mean,660nm} - 8.421 \times X_{mean,700nm} - 4.695 \times X_{mean,850nm} + 4.261 \times X_{mean,890nm} - 6.315 \times X_{SD,405nm} - 4.904 \times X_{SD,435nm} + 9.588 \times X_{SD,470nm} + 5.172 \times X_{SD,505nm} + 3.452 \times X_{SD,525nm} - 8.106 \times X_{SD,570nm} - 3.473 \times X_{SD,850nm} + 4.979 \times X_{SD,940nm} \quad (6.6)$$

$$Y_{TVCs/FT\text{-}IR/MSI} = 7.374 - 1.606 \times X_{PC1/MSI} - 3.963 \times X_{PC2/MSI} + 2.914 \times X_{PC3/MSI} + 2.794 \times X_{PC4/MSI} + 7.930 \times X_{PC5/MSI} + 14.800 \times X_{PC6/MSI} - 0.091 \times X_{PC1/FT\text{-}IR} \quad (6.7)$$

$$Y_{TVCs/3\ sensors} = 7.548 - 0.274 \times X_{PC4/FT\text{-}IR} + 2.068 \times X_{PC1/E\text{-}nose} - 6.201 \times X_{PC3/E\text{-}nose} + 2.198 \times X_{PC4/E\text{-}nose} \quad (6.8)$$

6.3.4.2 SVM-R models

The values of RMSE of prediction for the developed SVM-R models assessing TVCs in chicken marinated souvlaki samples, calculated by k-cross validation (k-CV, k=10), are presented in **Table 6.6**. From single sensor models, MSI achieved the most efficient assessment of TVCs with a RMSE value of cross-validation and prediction of 0.832 and 0.973 log CFU/g, respectively. Similarly, the combination of PCA scores derived from FT-IR and MSI data demonstrated an acceptable linear SVM-R model with RMSE value of prediction close to 1.0 log CFU/g. On the contrary, E-nose/FT-IR and MSI/E-nose models showed RMSE values of prediction over 1.5 log CFU/g and therefore they were considered not acceptable. The same outcome was observed for the 3-sensors model where RMSE of prediction was 1.938 log CFU/g. E-nose and FT-IR individual models failed to accurately predict TVCs providing RMSE values exceeding 1.921 log CFU/g. Even though E-nose analysis provides the lowest data size among the other two spectroscopic methods (Kutsanedzie et al., 2019), it seemed that microbial spoilage could be described more thoroughly by the other two techniques. In general, the obtained results indicated that SVM-R models performed similarly to PLS-R models, with the exception of FT-IR model, where the SVM-regression approach presented higher RMSE values through k-CV and prediction.

Table 6.6: SVM-R model performance (RMSE of cross-validation and prediction) from MSI, FT-IR and E-nose sensors (individual and combined).

	Sensor					
	E-nose		FT-IR		MSI	
Step	k-CV	Prediction	k-CV	Prediction	k-CV	Prediction
RMSE (log CFU/g)	1.311	1.921	1.846	3.583	0.832	0.973
	E-nose/FT-IR		FT-IR/MSI		MSI/E-nose	
Step	k-CV	Prediction	k-CV	Prediction	k-CV	Prediction
RMSE (log CFU/g)	1.06	1.579	0.953	0.999	1.134	1.658
	3- sensors					
Step	k-CV			Prediction		
RMSE (log CFU/g)	1.022			1.938		

The correlation between predicted and observed TVCs derived from SVM-R models developed on MSI and FT-IR/MSI data is demonstrated in **Figures 6.7** and **6.8,** respectively. In the case of MSI, model optimization (**Figure 6.7A**) did not show differences between observed and predicted TVCs, whereas there was clear overestimation for TVCs between 4 to 6 log CFU/g during prediction (**Figure 6.7B**). In addition, for both MSI and FT-IR/MSI models, an underestimation of the predicted TVCs occurred for samples with TVCs load of 8 log CFU/g (**Figure 6.7B** and **6.8B**). In addition, the SVM-regression beta coefficients for MSI and FTI-IR/MSI models are documented in **Figures 6.9** and **6.10,** respectively. Similar to PLS-R model via MSI implementation, the beta coefficients corresponding to the reflectance from 570-700 nm indicated their important contribution in the prediction of spoilage in chicken samples. Regarding FT-IR/MSI model, the scores from PC1, PC2, PC5 and PC6 from MSI analysis had a greater impact on TVCs prediction, while the scores from PC1 from FT-IR data analysis seemed to influence models' performance.

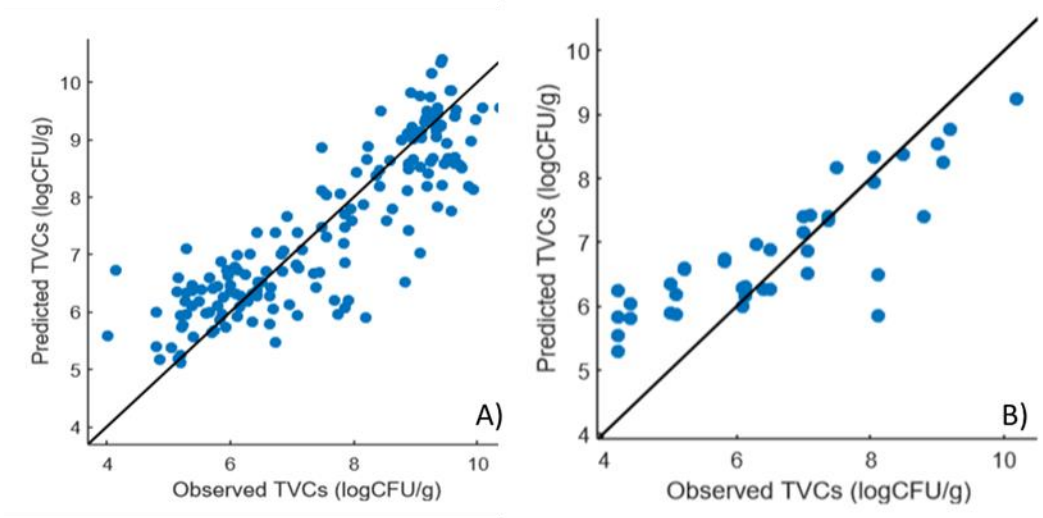

Figure 6.7: Predicted versus observed TVCs resulted from SVM-R model of MSI data for k-CV process (A) and prediction (B). Solid line represents the line of equity (y=x).

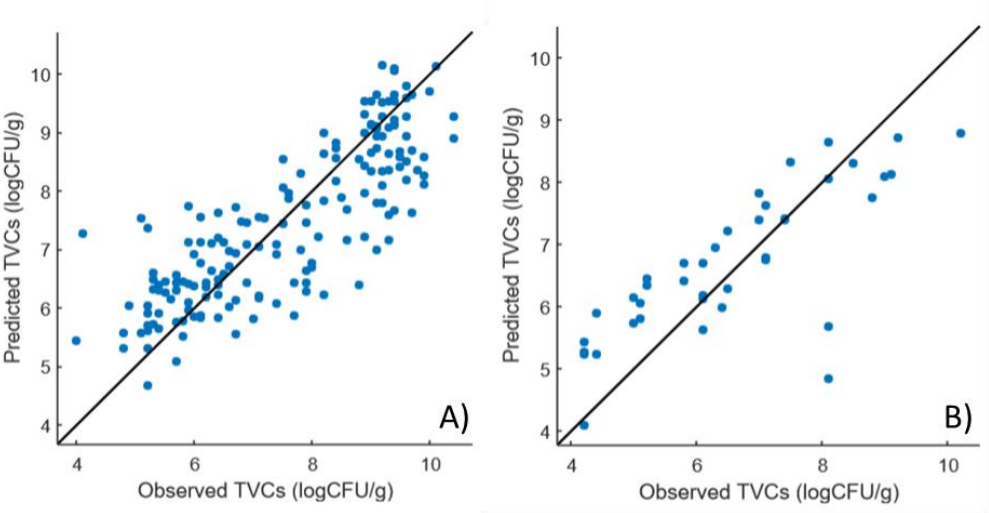

Figure 6.8: Predicted versus observed TVCs resulted from SVM-R model of FT-IR/MSI data for k-CV process (A) and prediction (B). Solid line represents the line of equity (y=x).

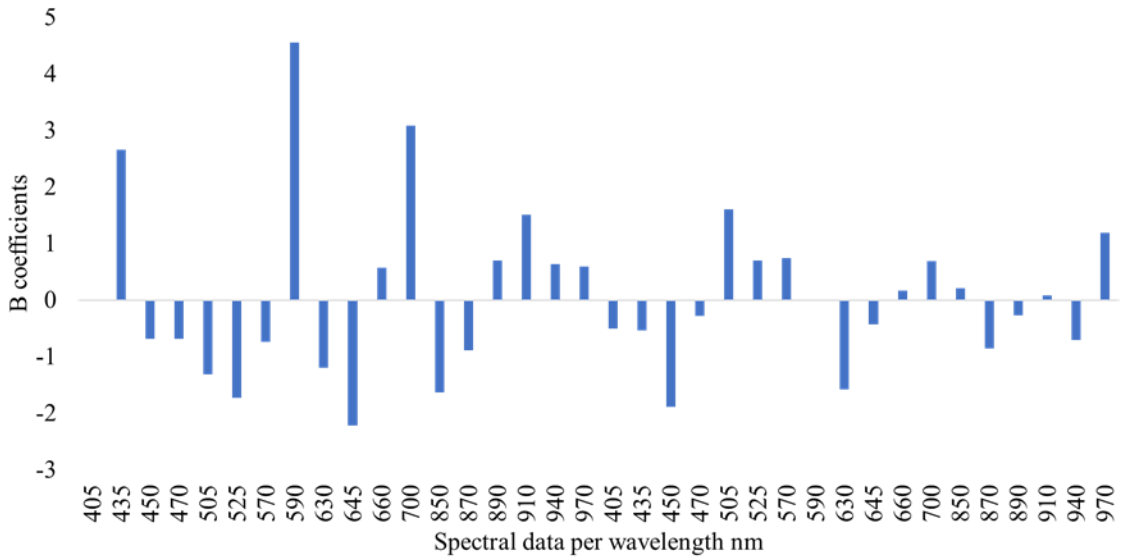

Figure 6.9: Beta (B) coefficients of the SVM-R model developed on MSI spectral data (mean intensity of pixels per wavelength) for chicken marinated souvlaki.

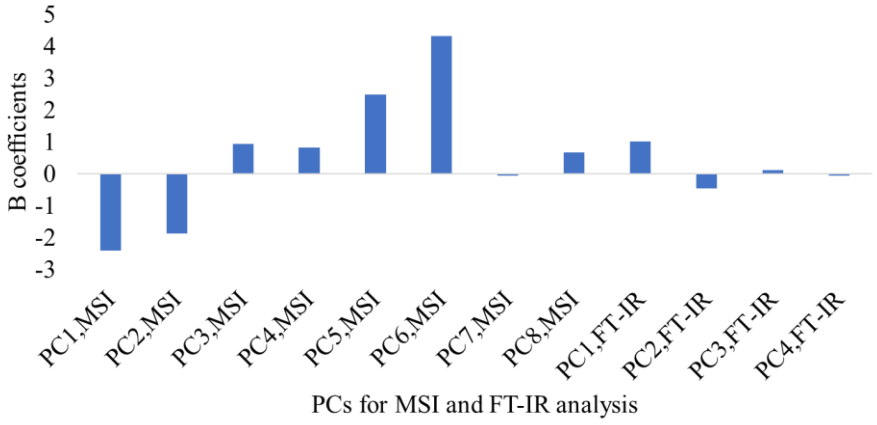

Figure 6.10: Beta (B) coefficients of the SVM-R model developed on FT-IR/MSI data (PCA scores) for chicken marinated souvlaki.

In an attempt to improve SVM-R model performance and find the appropriate kernel function, Bayesian optimization process was employed and the resulted parameter and function combination (with the minimum MSE) is provided in **Table 6.7**. It is worth noticed that linear kernel function reached the minimum MSE values, where in another research SVM Gaussian kernel function (RBF) combined to PLS-R and E-nose were suggested as feasible rapid methods for the estimation of pork's microbiota (Wang et al.,

2012). Likewise, SVM (RBF) regression model coupled to E-nose could successfully predict the spoilage microorganisms in beef meat (Papadopoulou et al., 2013).

Table 6.7: SVM-R optimized parameters and kernel function combinations (for each sensor model) indicating the minimum MSE.

	Box of constraction, c	**epsilon, e**	**Kernel function**
FT-IR	2.5095	0.00566	Linear
MSI	1.2616	0.0023	Linear
E-nose	0.0976	0.3806	Linear
FT-IR/MSI	16.322	0.2407	Linear
E-nose/FT-IR	0.0157	0.0342	Linear
MSI/E-nose	216.512	0.0031	Linear
3-sensors	0.0289	0.0315	Linear

6.3.5 Classification models assessing spoilage in chicken marinated souvlaki

The overall accuracy (%) of prediction for the 3-class classification models was less than 60 % (**Figure 6.11**). From the use of single sensors, the LSVM model developed on MSI spectral data reached an overall accuracy of 52.5 %. The same LSVM algorithm developed on FT-IR/MSI data demonstrated more accurate classification performance compared to LDA and CSVM models (overall accuracy: 52.5%). The superiority of LSVM model coupled to MSI data has been reported in similar studies for quality assessment in meat (Wang et al., 2012; Papadopoulou et al., 2013; Fengou et al., 2021a) and specifically in chicken thigh fillets (Spyrelli et al., 2021). Another combination that exhibited overall accuracy close to 60 % was LDA coupled to MSI/E-nose data (overall accuracy, 55.0 %), which was the most accurate classification model containing E-nose data. This improved performance among the other combinations of 2-sensor models highlighted the positive synergetic role of MSI and E-nose signals to the generation of models assessing meat quality (Kutsanedzie at al., 2019; Weng et al., 2020). The inclusion of E-nose data to FT-IR and to FT-IR/MSI data could not improve the discrimination potential among the different classes.

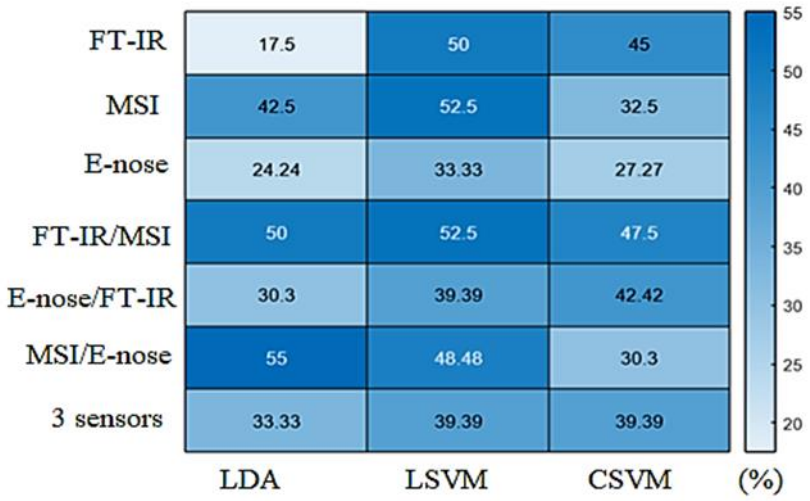

Figure 6.11: Heatmap presenting the performance (overall accuracy %) of LDA, LSVM and CSVM models developed on each sensor separately and in combination for the classification of chicken marinated samples in 3 quality classes.

The performance (confusion matrix) of the 3 most accurate models (MSI and LSVM, FT-IR/MSI and LSVM, MSI/E-nose and LDA) classifying chicken samples in 3 quality classes, as well as the performance metrics of sensitivity (%) and precision (%) per class are demonstrated in **Table 6.8**. For the MSI model, 123 out of 169 samples and 21 out of 40 samples were correctly classified in the 3 quality classes during model development (k-CV) and prediction, respectively. LSVM model developed on MSI data provided sensitivity for class 1, 2 and 3 of 69.23%, 28.13% and 88.78 %, respectively, during training (using k-CV), whereas for model prediction the respective sensitivity was 28.57%, 12.50% and 88.89%. For the same model, precision ranged from 40.91 to 87.00 % and from 10.00 to 80 % during model development (using k-CV) and prediction, respectively, with the lowest percentages obtained for class 2 (semi-fresh). For the combined FT-IR/MSI model, 130 out of 169 samples and 21 out of 40 samples were classified correctly during model development (using k-CV) and prediction, respectively. Per class sensitivity varied from 31.25 to 92.93 % and from 21.43 to 88.89 % during model development and prediction, respectively, while the corresponding precision was estimated between 55.56 to 84.40 % and 13.33 to 84.21 % for model development and prediction, respectively. For the combined MSI/E-nose model, 127 out of 169 samples and 22 out of 40 samples were correctly classified during model training and prediction, respectively.

Sensitivity and precision percentages were calculated in the range of 42.33-87.85% and 50-84.68% during model development, respectively, whereas for prediction these performance indexes gradually decreased at 12.50-78.95% and 11.11-85.71%, respectively. It is worth noticing that sensitivity for class 3 (spoiled samples) demonstrated the highest percentages for both model development and prediction in all model combinations. The majority of class 1 (fresh) samples were misclassified as class 2 (semi-fresh) in most cases while models could not identify correctly class 2 (sensitivity ranged from 12.50 to 25.00 %) mainly because of the low number of observations corresponding to this class in the training data.

Table 6.8: Confusion matrix and performance metrics of the developed models (LDA, LSVM, CSVM) for the classification of samples in 3 quality classes, via MSI, FT-IR/MSI and MSI/E-nose data.

Sensor	**Model**	**Step**	**Confusion Matrix**				**Performance metrics**	
MSI	LSVM	k-CV	o/p	Class 1	Class 2	Class 3	Sensitivity (%)	Precision (%)
			Class 1	27	9	3	69.23	57.45
			Class 2	13	9	10	28.13	40.91
			Class 3	7	4	87	88.78	87.00
		Prediction	o/p	Class 1	Class 2	Class 3	Sensitivity (%)	Precision (%)
			Class 1	4	8	2	28.57	40.00
			Class 2	5	1	2	12.50	10.00
			Class 3	1	1	16	88.89	80.00
FT-IR/MSI	Model	Step	Confusion Matrix				Performance metrics	
	CSVM	k-CV	o/p	Class 1	Class 2	Class 3	Sensitivity (%)	Precision (%)
			Class 1	28	5	5	73.68	66.67
			Class 2	10	10	12	31.25	55.56
			Class 3	4	3	92	92.93	84.40
		Prediction	o/p	Class 1	Class 2	Class 3	Sensitivity (%)	Precision (%)
			Class 1	3	11	0	21.43	50.00
			Class 2	3	2	3	25.00	13.33
			Class 3	0	2	16	88.89	84.21
MSI/E-nose	Model	Step	Confusion Matrix				Performance metrics	
	CSVM	k-CV	o/p	Class 1	Class 2	Class 3	Sensitivity (%)	Precision (%)
			Class 1	22	7	7	61.11	61.11
			Class 2	5	11	10	42.31	50.00

	Class 3	9	4	94	87.85	84.68
Prediction	o/p	Class 1	Class 2	Class 3	Sensitivity (%)	Precision (%)
	Class 1	6	4	3	46.15	85.71
	Class 2	1	1	6	12.50	11.11
	Class 3	0	4	15	78.95	62.50

In order to improve the performance of the models, it was considered necessary to employ a two-class scheme (fresh vs. spoiled) by combining the samples of class 1 and 2 together and thus increase the number of training cases in class 1. The performance of the 2-class models in terms of overall accuracy was improved compared to the 3-class models as illustrated in **Figure 6.12**. For spectroscopic sensor models (MSI, FT-IR, FT-IR/MSI) the overall accuracy of prediction exceeded 60 % in most cases, with the highest percentages obtained for FT-IR/MSI (LDA: 85%, LSVM: 82.5%, CSVM: 87.5%), followed by MSI and SVM models (LSVM: 80 % and QSVM: 77.5%). The combination of SVM models with the above-mentioned spectroscopic techniques as well as the use of LDA with FT-IR data has been recommended in recent studies as an effective approach for the quality assessment of meat freshness (Candŏgan et al., 2021). The high overall accuracy of all FT-IR/MSI models confirmed that the combination of these nondestructive techniques could assess more effectively the quality of meat (Huang et al., 2014).

Overall accuracy performance was improved for the 2-class FT-IR models compared to the 3-class FT-IR models, however their performance was below 60 % which cannot be considered satisfactory. Improved overall accuracy was observed for E-nose models but it could not exceed 39.4%. Moreover, the performance of MSI/E-nose models could not be improved by the exclusion of the third (semi-fresh) class, where the highest percentage of overall accuracy was calculated at 48.48 % for the LDA model. In contrast, the CSVM model developed on the combined FT-IR and E-nose data identified the correct class of the samples satisfactorily with overall accuracy of 63.63 %. Concerning the 3 sensor models, the use of CSVM exhibited the most accurate discrimination between samples with overall accuracy of 72.73%.

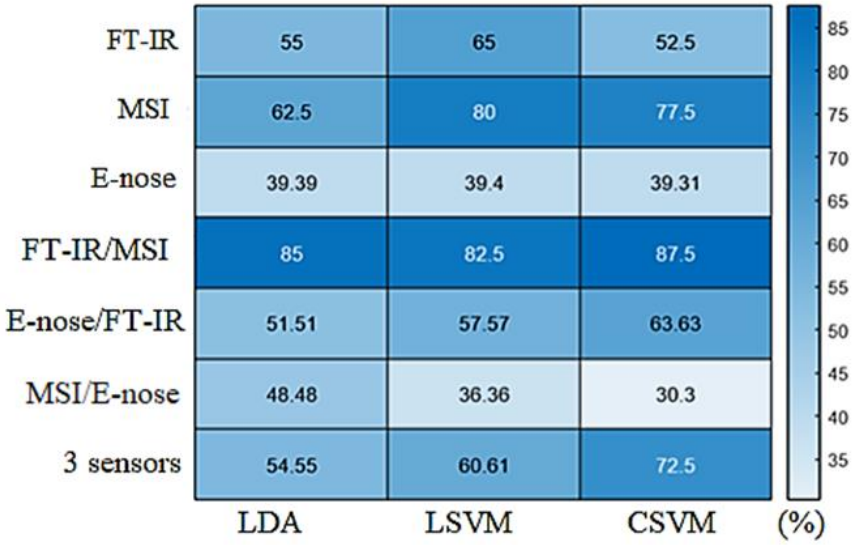

Figure 6.12: Heatmap presenting the performance (overall accuracy %) of LDA, LSVM and CSVM models developed on each sensor separately and in combination for the classification of chicken marinated samples in 2 quality classes.

The improved performance of the MSI (combined with LSVM and CSVM models) is demonstrated in the confusion matrix (**Table 6.9**) where the per class sensitivity (%) and precision (%) is presented. For the MSI and LSVM model, 149 out of 169 samples and 32 out of 40 samples were accurately classified in their respective class during model development and prediction, respectively. Sensitivity and precision for class 1 (fresh samples) reached 90.14 % and 83.12 % for model development, respectively, while for model prediction the respective percentages were 83.12 % and 85.0 %. The CSVM model developed on MSI data classified 127 out of 169 samples and 31 out of 40 samples in their correct class for model development and prediction, respectively. For this model, sensitivity for class 1 (fresh) was calculated at 74.65% and 88.89% for cross validation and prediction, respectively, whereas precision ranged from 68.83 to 72.41%. In both MSI models, sensitivity for class 2 (spoiled) was approximately the same as for class 1 during cross validation, with the exception of the prediction of the CSVM model where one spoiled sample was misclassified as fresh.

Table 6.9: Confusion matrix and performance metrics of the developed models (LSVM, CSVM) for the classification of samples in 2 quality classes via MSI data.

Sensor	**Model**	**Step**	**Confusion Matrix**			**Performance metrics**	
MSI	LSVM	k-CV	o/p	Class 1*	Class 2**	Sensitivity (%)	Precision (%)
			Class 1	64	7	90.14	83.12
			Class 2	13	85	86.75	
		Prediction	o/p	Class 1	Class 2	Sensitivity (%)	Precision (%)
			Class 1	17	5	77.27	85
			Class 2	3	15	83.33	
	Model	Step	Confusion Matrix			Performance metrics	
	CSVM	k-CV	o/p	Class 1	Class 2	Sensitivity (%)	Precision (%)
			Class 1	53	18	74.65	68.83
			Class 2	24	74	75.51	
		Prediction	o/p	Class 1	Class 2	Sensitivity (%)	Precision (%)
			Class 1	21	1	95.45	72.41
			Class 2	8	10	55.55	

*Class 1: fresh
**Class 2: spoiled

For the 2-sensors and 3-sensors models, the respective confusion matrix and the performance indexes of sensitivity and precision are represented in **Table 6.10**. For the LDA model developed on combined FT-IR/MSI data, 141 out of 169 samples and 34 out of 40 samples were correctly classified during model cross validation and prediction, respectively. The calculated sensitivity for class 1 and precision were amounted to 80 % and 86.36 % for model cross validation and prediction, respectively. The LSVM model identified correctly 143 out of 169 samples and 33 out of 40 samples during cross validation and prediction, respectively. Moreover, the LSVM model developed on FT-IR/MSI data provided sensitivity for class 1 and precision of 87.14 % and 78.20 % for cross validation, respectively and 77.27 % and 89.47% for prediction, respectively. For CSVM model, 135 out of 169 samples and 35 out of 40 samples were classified in their correct class during cross validation and prediction, respectively. Sensitivity for class 1 and precision was 77.14 % and 75 % for model cross validation, respectively and 90% and 86.95% for model prediction, respectively. For the 3 sensors model, 154 out of 169 samples and 29 out of 40 samples were properly classified during cross validation and prediction, respectively. Sensitivity for class 1 reached 90.77% and 88.23 % for cross validation and prediction,

while the respective values for precision were 86.76% and 68.18%. Sensitivity values for class 2 were in most cases similar to sensitivity values for class 1, exceeding 80% with the exception of the 3 sensors model where the sensitivity for class 2 was calculated at 66.67%. This outcome indicated the potential of the developed models to accurately identify and categorize both fresh (class 1) and spoiled (class 2) samples.

Table 6.10: Confusion matrix and performance metrics of the developed models (LSVM, CSVM) for the classification of samples in 2 quality classes via FT-IR/MSI and 3-sensors data.

Sensor	**Model**	**Step**	**Confusion Matrix**			**Performance metrics**	
FT-IR/MSI	LDA	k-CV	o/p	Class 1	Class 2	Sensitivity (%)	Precision (%)
			Class 1	56	14	80	80
			Class 2	14	85	85.86	
		Prediction	o/p	Class 1	Class 2	Sensitivity (%)	Precision (%)
			Class 1	19	3	86.36	86.36
			Class 2	3	15	83.33	
	Model	Step	Confusion Matrix			Performance metrics	
	LSVM	k-CV	o/p	Class 1	Class 2	Sensitivity (%)	Precision (%)
			Class 1	61	9	87.14	78.20
			Class 2	17	82	82.83	
		Prediction	o/p	Class 1	Class 2	Sensitivity (%)	Precision (%)
			Class 1	17	5	77.27	89.47
			Class 2	2	16	88.89	
	Model	Step	Confusion Matrix			Performance metrics	
	CSVM	k-CV	o/p	Class 1	Class 2	Sensitivity (%)	Precision (%)
			Class 1	54	16	77.14	75
			Class 2	18	81	81.82	
		Prediction	o/p	Class 1	Class 2	Sensitivity (%)	Precision (%)
			Class 1	20	2	90	86.95
			Class 2	3	15	83.33	
3 sensors	Model	Step	Confusion Matrix			Performance metrics	
	CSVM	k-CV	o/p	Class 1	Class 2	Sensitivity (%)	Precision (%)
			Class 1	59	6	90.77	86.76
			Class 2	9	95	91.34	

	Prediction	o/p	Class 1	Class 2	Sensitivity (%)	Precision (%)
		Class 1	15	2	88.23	68.18
		Class 2	7	14	66.67	

Chapter 7: Quality and safety assessment of marinated chicken souvlaki

Abstract

Campylobacteriosis is the most frequent reported zoonosis transmitted to humans through the food chain. *Campylobacter* spp. have been isolated from poultry meat as well as from marinated poultry products. Under this scope, the objective of this research was the investigation of *Campylobacter* spp. behavior after inoculation of six *Campylobacter* strains in chicken souvlaki under different storage temperatures. Moreover, the microbial growth of the indigenous microbiota of the inoculated and non-inoculated chicken marinated souvlaki was examined. In brief, chicken marinated souvlaki samples were inoculated by a multiple-strain inoculum (6 strains of *C. coli* and *C. jejuni*) and stored aerobically at three different isothermal conditions (0, 5 and 10 ^{o}C) and a dynamic temperature profile (12 h at 0 ^{o}C, 8 h at 5 ^{o}C and 4 h at 10 ^{o}C). At regular time intervals, inoculated and non-inoculated samples were microbiologically analyzed for the enumeration of Total Viable Counts (TVCs), *Pseudomonas* spp., anaerobic bacteria and *Campylobacter* spp. count. TVCs and *Pseudomonas* spp. counts were fitted to a one-step predictive model for chicken marinated souvlaki (inoculated and non-inoculated) and the obtained models were validated with the available independent data from the dynamic temperature profile storage experiment. Furthermore, survival models determining *Campylobacter* spp. counts during storage at isothermal conditions were developed and assessed. Molecular analysis via Random amplified polymorphic DNA PCR (RAPD-PCR) was conducted with isolates from three time points during the experiments. The developed models for the spoilage microbiota (TVCs and *Pseudomonas* spp.) in inoculated and non-inoculated samples demonstrated RMSE values lower than 1 log CFU/g (below 0.941 log CFU/g), while B_f and A_f indices were considered acceptable (B_f: 0.90- 1.05, A_f: 1.100). *Campylobacter* spp. could survive despite the low storage temperature presenting a decline of 1.5 log CFU/g from the initial population. From the developed survival models, the highest accuracy was achieved for the modified Weibull model at 5 ^{o}C storage with RSME, and R^2 values of 0.112 log CFU/g, and 0.909 respectively. Molecular analysis showed that both *Campylobacter coli* and *jejuni* strains could survive during low storage temperatures, with the exception of 5 ^{o}C where only *Campylobacter coli* was detectable in the samples.

7.1 Introduction

Since 2005, campylobacteriosis has been reported as the most commonly reported zoonosis (over 70 % of documented pathogens infections) in the EU and all around the world (World Health Organization, 2013; EFSA/ECDC, 2019). This severe disease is manifested in the majority of cases as gastroenteritis with acute non-inflammatory or grossly bloody diarrhea (i.e., dysentery), fever and abdominal pain or cramps lasting for one week or more, whereas in some cases there are evident symptoms such as bacteremia, Guillain-Barré syndrome, reactive arthritis, miscarriages and depression (Gharst et al., 2013; Bolton & Robertson, 2016). *Campylobacter* spp. are transmitted through the food chain and affects humans mainly through food and water consumption (Codex Alimentarius Commission, 2011; Dogan et al., 2019). The highest detection of *Campylobacter* in foods was reported on fresh meat from broilers which was also linked to strong evidence outbreaks of campylobacteriosis (EFSA/ECDC, 2019). In this context, in 2011 the Codex Alimentarius Commission and EU as well published guidelines for the control of *Campylobacter* spp. in chicken meat implemented at one or more steps in the farm to table chain (Codex Alimentarius Commission, 2011; EFSA Panel on Biological Hazards (BIOHAZ), 2011). Moreover, a supplementary regulation of the EU 2073/2005 regulation for the microbial criteria in food was considered appropriate and thus in the amended EU 2017/1495 regulation the limit of detection of *Campylobacter* spp. in raw poultry slaughters was limited to 1,000 CFU/g (EU, 2017).

Campylobacter spp. is a Gram-negative, microaerophilic, spiral shaped rod inhabiting in high populations the gastrointestinal tract of predominantly birds (chicken and turkey). This bacterium could be also found in red meat products (bovine, sheep, cattle and pigs) and it can survive in the water and even sand (Lanzl et al., 2020). Poultry meat could be contaminated with this pathogen from the caeca via the water supply system, inadequate hygiene practices, contaminated surfaces in the slaughter house and/or the chilling procedure after evisceration (Demirok et al., 2012; Seliwiorstow et al., 2016; Rouger et al., 2017, McCarthy et al., 2019). Additionally, humans could be infected by *Campylobacter* spp. due to the consumption of contaminated raw or undercooked chicken products (Silva et al., 2011; Skarp et al., 2015; Huang et al., 2019; Andritsos et al., 2020). Until now, two species of *Campylobacter*, *C. jejuni* and *C. coli* have been reported in approximately 90 %

of campylobacteriosis cases in humans (Solow et al., 2003; Gharst et al., 2013; Repérant et al., 2016). Likewise, these two species have been isolated most frequently from broiler meat during prevalence surveys in the last decade (Torralbo et al., 2015; Stella et al., 2017; EFSA/ECDC, 2019; Andritsos et al., 2020; Lytou et al., 2020).

For the reduction and elimination of *Campylobacte*r spp. in raw or stored chicken meat several studies have been undertaken to investigate the effect of temperature on the growth and/or survival of *Campylobacter* strains (Blankenship & Craven, 1982; Hazeleger et al., 1998; Duffy & Dukes, 2006). Specifically, the potential of *Campylobacter* spp. to survive in poultry for long periods at chilling temperatures (4°C) has been reported (Silva et al., 2011). Furthermore, certain *Campylobacter* strains could remain viable even at low concentration in chicken matrix after the exposure and maintenance at freezing temperatures (below -20 ^{o}C) (Lee at al., 1998; Zhao et al., 2003; Yun et al., 2016; Lanzl et al., 2020). Several survival/inactivation models (log-linear models, Weibull and modified Weibull) of *Campylobacter* have been developed to describe the reduction of this pathogen via chilling process in chicken products (Ritz et al., 2006; González et al., 2009; Membré et al., 2013; Duqué et al., 2019). Nevertheless, the influence of marination and o chemical decontaminants (mainly acids) combined with refrigeration storage temperatures has been also evaluated for the reduction of *Campylobacter* spp. in chicken, where this pathogen was characterized as acid tolerant (Chaveerach et al., 2003; Björkroth, 2005; Meredith et al., 2013; Lytou et al., 2020).

The aim of this work was firstly to investigate the behavior of *Campylobacter* strains, isolated previously from chicken marinated samples (during a survey in the Greek poultry market), after inoculation on chicken samples marinated with functional acid marinade (commercial product) and storage at three chilling conditions. Survival models of *Campylobacter* spp. were developed at each storage temperature and validated via independent data obtained through a dynamic temperature profile experiment. In parallel, the growth of the indigenous spoilage microbiota (TVCs and *Pseudomonas* spp.) was monitored during storage of the inoculated and non-inoculated samples and a one-step predictive growth model was developed and externally validated for each microbial group individually. Further on, RAPD-PCR was performed to isolates obtained at the beginning,

middle and final time points of storage in order to elucidate the impact of temperature and marinade on the initial inoculum.

7.2 Materials and Methods

7.2.1 Inoculum preparation

Five *Campylobacter* spp. strains obtained during a previous survey in chicken marinated souvlaki (Lytou et al., 2020) were used for the inoculum formulation as follows: 9D (*C. coli*, pH: 5.6), 7L (*C. coli*, pH: 5.5), 6Z (*C. coli*, pH: 6.4), 1H (*C. coli*, pH: 5.8) and 6A (*C. jejuni*, pH: 5.9). Moreover, one *Campylobacter* strain from the collection of the Laboratory of Microbiology and Biotechnology of Foods (LMBF) of the Agricultural University of Athens (AUA) was used as inoculum in the present study, namely B-450 (*Campylobacter jejuni* subsp. *jejuni*, ATCC 29428). The acid tolerance of the above-mentioned strains has been reported by Lytou et al. (2020). The strains were revived from a stock culture (-20 ^{o}C), cultured in 10 ml Bolton Broth (Campylobacter Enrichment Broth, NCM0094A, Neogen Culture Media, UK) with lysed horse blood (Lysed horse blood, HB036, TCS Biosciences Lted) and incubated for 48 hours at 41.5 ± 0.5 ^{o}C in anaerobic conditions (Microbiology Anaerocult C: for the generation of an oxygen- depleted and CO_2 – enriched atmosphere in an anaerobic jar, 1.32383.0001, Millipore, USA). A volume of 10 μl of each revived culture was transferred to 10 ml of sterilized Bolton Broth and incubated in anaerobic conditions for 48 h at 41.5 ± 0.5 ^{o}C. The obtained cultures were transferred in separate sterile falcons and the bacterial cells were separated from the broth medium by centrifugation (5,000 g for 10 min at 4^{o}C) and washed twice with 10 ml sterile Bolton Broth. The derived pellets were resuspended in the same Bolton Broth volume (10 ml). Further on, equal volumes of each bacterial suspension were mixed in a sterile Duran bottle resulting in a composite *Campylobacter* spp. inoculum of 7.99-8.27 log CFU/ml as assessed by plate counting. The composite inoculum was further diluted with the same diluent to achieve a final inoculum of 10^3 CFU/ml that was used for all experiments.

7.2.2 Sample preparation and storage

Chicken marinated souvlaki (chicken thigh fillet, sodium chloride, sodium acetate, sodium citrate, enzyme tenderizer and ascorbic acid) with pH values from 6.2 to 6.5 was transferred to the laboratory within 30 min under refrigeration. Samples were weighted

(20.41 ± 0.13 g) and placed aseptically in styrofoam dishes (two portions per dish). Each sample was inoculated with 100 μl of the strain mixture by dispersing it with a pipette and spreading it with a sterile spatula over the surface of chicken. Further on, samples were maintained at 4 ºC for 30 min to ensure inoculum attachment and afterwards the same procedure was repeated on the other side of the sample. The styrofoam dishes containing the inoculated samples were wrapped with cling film (household food wrap) and stored at three different isothermal conditions (0, 5 and 10 ºC) in high precision incubators (MIR-153, Sanyo Electric Co., Osaka, Japan). After inoculation, control (non-inoculated) samples were also stored at the same conditions, in order to compare the growth behavior of the indigenous microbiota of untreated chicken marinated souvlaki with the inoculated samples, and simultaneously detect the presence of *Campylobacter* spp. in this poultry product. Two independent experiments were undertaken with duplicate samples analyzed in each experiment (n=4), whereas the same experimental procedure was performed with samples stored at a dynamic temperature profile (12 h at 0 ºC, 8 h at 5 ºC and 4 h at 10 ºC) in order to investigate the influence of temperature changes on the indigenous microbiota as well as on the dynamics of *Campylobacter* spp. strains.

7.2.3 Microbiological analysis

Each sample (20 g) was subjected to microbiological analysis for the enumeration of the indigenous microbiota and the inoculated pathogen counts at the beginning of storage as well as at pre-determined time intervals. For this reason, the 20 g sample was added aseptically in 180 ml of sterile Bolton Broth (Campylobacter Enrichment Broth, NCM0094A, Neogen Culture Media, UK) in a stomacher bag (Seward Medical, London, UK) and homogenized in a stomacher device (Lab Blender 400, Seward Medical, London, UK) for 60 s at room temperature. For the enumeration of TVCs, *Pseudomonas* spp., anaerobic bacteria and *Campylobacter* spp., serial decimal dilutions were performed in the same diluent and spread on the following media: a) Plate Count Agar (Tryptic Glucose Yeast Agar PCA, Ref.4021452, Biolife, Italiana S.r.l, Milano, Italy) for the estimation of TVCs after incubation at 25 ºC for 72 h; b) Pseudomonas Agar Base (LAB108, LABM., U.K.) supplemented with Cetrimide-Fusidin-Cephaloridine (Modified C.F.CX108, LABM, UK) for the estimation of the presumptive *Pseudomonas* spp. after incubation at 25 ºC for 48 h; c) Columbia Blood Agar (Campylobacter Selective Agar CBA, LAB001,

UK) with 5% lysed horse blood for the estimation of the anaerobic bacteria after inoculation at 41.5 ^{o}C for 48 h under anaerobic conditions; d) Columbia Blood Agar (Campylobacter Selective Agar CBA, LAB112, UK) with 5% lysed horse blood supplemented with Skirrow medium (Skirrow supplement, LABM 214, UK), for the estimation of *Campylobacter* spp. after inoculation at 41.5 ^{o}C for 48 h under anaerobic conditions; e) Campylobacter Blood Free Selective Medium (Modified CCDA, LAB112, UK) supplemented with Ceroperazone/Amphotericin (Ref.X112, LAB M, UK), for the estimation of *Campylobacter* spp. after inoculation at 41.5 ^{o}C for 48 h under anaerobic conditions. After incubation, counts were logarithmically transformed and expressed as log CFU/g.

7.2.4 Predictive models

7.2.4.1 Growth predictive models for TVCs and *Pseudomonas* spp.

One-step modeling (Huang et al., 2016) was applied to TVCs and *Pseudomonas* spp. counts from the isothermal conditions of storage for the determination of the primary and secondary kinetic parameters for TVCs and *Pseudomonas* spp. on inoculated and non-inoculated chicken marinated souvlaki. The Huang full growth primary model (Huang, 2013) (equations 7.1-7.3) and the secondary Ratkowsky sub-optimal growth-temperature model (Ratkowsky, 1983) (equation 7.4) were fitted to TVCs and *Pseudomonas* spp. counts using IPMP-Global Fit software (USDA Agricultural Research Service, Eastern, Regional Research Center, Wyndmoor, PA).

$$\boldsymbol{Y(t) = Y_0 + Y_{max} - ln\,[e^{Y0} + (e^{Ymax} - e^{Y0})\,e^{-\mu max\,B(t)}]} \quad (7.1)$$

$$\boldsymbol{B(t) = t + \frac{1}{4}\,ln\frac{1+e^{-4(t-\lambda)}}{1+e^{4\lambda}}} \quad (7.2)$$

$$\boldsymbol{\lambda = \frac{e^{A}}{\mu max^{m}}} \quad (7.3)$$

where: Y(t) is the base-10 logarithms (log10) of the real time microbial counts (log CFU/g) at the respective storage time t (h), y_o is the initial base-10 logarithms (log_{10}) of the microbial counts (log CFU/g), y_{max} is the final base-10 logarithms (log_{10}) of the microbial counts (log CFU/g), μmax is the specific growth rate of the microbial group (h^{-1}), b, A and m are regression coefficients, λ is the lag phase (h) and B(t) is the transition function.

$$\sqrt{\mu_{max}} = b\ (T-T_{min})\quad (7.4)\ \text{(Ratkowsky, 1983)}$$

Model performance of the model developed under isothermal conditions was validated against observed growth of *Pseudomonas* spp. (n=33, different batch) under a dynamic temperature profile (12 h at 0 ^{o}C, 8 h at 5 ^{o}C and 4 h at 10 ^{o}C) using the differential equations of the Baranyi and Roberts model (Baranyi & Roberts, 1994) that were numerically integrated in Microsoft® Excel. The accuracy of the prediction was estimated by the RMSE value, the bias factor (B_f) and the accuracy factor (A_f) (Ross, 1996).

7.2.4.2 Survival/ Inactivation models for *Campylobacter* spp.

The influence of the chilling storage temperatures on the kinetic behavior of *Campylobacter* spp. on chicken marinated souvlaki was assessed via survival/inactivation models developed by GInaFiT Version 1.6 add-in software for Excel Microsoft® (available at https://cit.kuleuven.be/biotec/software/GinaFit, KULeuven, Belgium). This free software has been implemented in a variety of experimental data for the development of linear and non-linear survival/inactivation curves of spoilage and pathogenic bacteria (Geeraerd et al., 2005.) In this study, the Weibull model (equation 7.5) (Mafart et al., 2002) and the modified Weibull model (equation 7.6) (Albert & Mafart, 2005) were employed to determine the kinetic parameters of *Campylobacter* spp. at 0, 5, and 10 ^{o}C.

$$\frac{N}{N0} = 10^{-(\frac{t}{\delta})^p}\quad (7.5)$$

$$N = (N_0 - N_{res}) \times 10^{-(\frac{t}{\delta})^p} + N_{res}\quad (7.6)$$

where, N is the number of surviving bacterial after a certain time of refrigerated storage (log CFU/g), N_0 is the initial bacterial populations (log CFU/g), t is the duration of the treatment (in this case the storage time in hours), δ is the scale factor denoting the time for the first decimal reduction (h), p is the shape factor of the curve (dimensionless) ($p > 1$ indicates convex curves whereas $p < 1$ denotes concave curves) and N_{ref} is the residual bacterial populations (log CFU/g) (Mafart et al., 2002, Albert & Mafart, 2005).

7.2.5 Molecular analysis

Campylobacter spp. colonies were isolated from Skirrow and mCCDA agar plates for chicken marinated souvlaki samples at the beginning (0 h), middle (0 ^{o}C: 120 h, 5 ^{o}C: 96 h, 10 ^{o}C: 72 h) and final (0 ^{o}C: 312 h, 5 ^{o}C: 240 h, 10 ^{o}C: 216h, dynamic temperature profile: 312h) time of storage. The isolates (44) were verified for their purity via confirmation tests, namely (a) by streaking on Columbia Blood agar and incubated aerobically at 41.5 ^{o}C for 48 h, (b) by streaking on Columbia Blood agar and incubated micro-aerobically at 25 ^{o}C for 48 h, (c) by oxidase test, and (d) by microscopic observation, according to ISO 10272-1:2006. Pure colonies from the initial composite inoculum were also isolated in order to compare their profile to the obtained profiles from storage experiments and hence elucidate the survival of each strain according to the storage temperature. The isolates were maintained at -20 ^{o}C in 1.5 mL Bolton broth with 20% glycerol and 2 % horse blood.

DNA extraction was performed using the total genomic DNA extraction protocol for bacteria (Doulgeraki et al., 2011), while the extracted DNA was qualitatively and quantitatively evaluated by nanophotometer (Implen, Germany) measurements at wavelengths of 260, 280, and 230 nm. Random amplified polymorphic DNA (RAPD)-PCR analysis was performed with a M13 primer (5′-GAGGGTGGCGGTTCT-3′) (Hanjilouka et al., 2014; Tzamourani et al., 2021). Volume of 50 μl from PCR amplifications were consisted based on Lytou et al. (2021) publication: PCR-buffer (10 × PCR buffer B with 1.5 mM $MgCl_2$, Kapa Biosystems, Wilmington, MA, USA), additional 0.2 mM $MgCl_2$, 0.8 mM dNTPs, 4 μM primer M13, 1 U Taq DNA polymerase (Kapa Biosystems, USA), DNA (100 ng) and sterile distilled water. PCR reaction was conducted as described elsewhere (Lytou et al., 2021). Briefly, an initial denaturation step at 95 ^{o}C for 3 min, 3 cycles of denaturation at 95 ^{o}C for 3 min, primer annealing at 35 ^{o}C for 5 min and primer elongation 72 ^{o}C for 5 min, followed by 32 cycles of denaturation at 95 ^{o}C for 1 min, primer annealing at 55 ^{o}C for 2 min and primer elongation 72 ^{o}C for 3 min, and a final elongation step at 72 ^{o}C for 7 min (Lytou et al., 2021). Aliquots of PCR products were separated via electrophoresis on a 1.5% agarose gel in 1 × TAE (40 mM Tris–acetate, 1 mM EDTA, pH 8.2) buffer at 100 V for 75 min. Gels were stained with ethidium bromide and visualized under UV light in a Bio-Rad GelDoc 2000 system (Bio-Rad Laboratories

Inc., Hercules, CA, USA) using the analysis software Quantity-One (Bio-Rad, Hercules, CA, USA). The resulted gel images were analyzed using the Jaccard/Dice coefficient and the unweighted pair group method with arithmetic mean (UPGMA) cluster analysis, via the BioNumerics software version 6.1 (Applied Maths, Sint-Martens-Latem, Belgium).

7.3 Results and Discussion

7.3.1 Microbiological results

The microbiological results for each microbial group (TVCs, *Pseudomonas* spp., anaerobic microorganisms on Columbia Agar, *Campylobacter* spp. on mCCDA and Skirrow agar) during the storage of the inoculated chicken marinated souvlaki are presented in **Figure 7.1**. Chilling temperatures influenced the population of the indigenous spoilage microbiota, with 0 ^{o}C demonstrating the highest inhibitory effect on chickens' spoilage. Moreover, TVCs and *Pseudomonas* spp. followed similar growth pattern at all storage temperatures indicating that *Pseudomonas* spp. was the dominant spoilage microorganism responsible for chicken meat deterioration under aerobic conditions (Gospavic et al., 2008; Belak et al., 2011; Bruckner et al., 2013; Remenant et al., 2015). The initial TVCs and *Pseudomonas* spp. counts were 5.36 ± 0.59 and 4.46 ± 0.12 log CFU/g, respectively, for the isothermal storage conditions, as well as 6.96 ± 0.07 and 6.28 ± 0.13 log CFU/g, respectively, for the dynamic temperature profile. At 0 ^{o}C (**Figure 7.1A**), these two microbial groups reached the spoilage threshold of marinated poultry (7.0 log CFU/g) (Gospavic et al., 2008; Lytou et al., 2018) after 168 h (7.13 ± 0.30 log CFU/g) and 192 h (7.0 ± 0.43 log CFU/g), respectively. On the contrary, the anaerobic populations on Columbia agar presented a slight increase from 3.87 ± 0.15 log CFU/g to 4.21 ± 0.36 log CFU/g. *Campylobacter* spp. results obtained from Skirrow agar and mCCDA did not differ as both media are selective for the enumeration of this pathogen (ISO 10272-1:2006). Specifically, for Skirrow agar the initial and final counts were documented at 3.45 ± 0.16 log CFU/g and 2.57 ± 0.28 log CFU/g respectively. For mCCDA, the initial population of *Campylobacter* spp. was estimated at 3.20 ± 0.20 log CFU/g and the final population at 2.63 ± 0.63 log CFU/g after 312 h of storage.

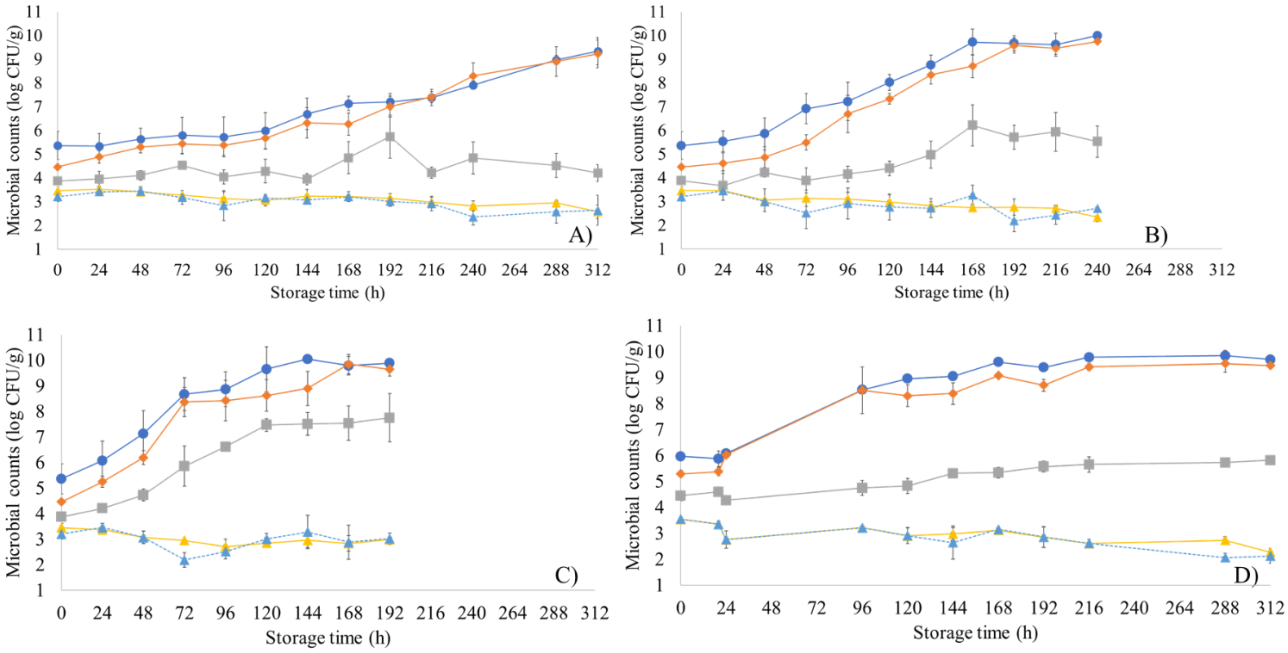

Figure 7.1: Microbial counts of TVCs (cycles), *Pseudomonas* spp. (diamonds), anaerobic bacteria on Columbia blood agar (squares), *Campylobacter* spp. on mCCDA (solid line with triangles) and on Skirrow (dashed line with triangles) in inoculated chicken marinated souvlaki stored at 0 ºC (A), 5 ºC (B), 10 ºC (C) and a dynamic temperature profile (D).

For samples stored at 5 ºC (**Figure 7.1B**), TVCs and *Pseudomonas* spp. counts exhibited values above the spoilage threshold of 7.0 log CFU/g in 96 h (7.21 ± 0.81 log CFU/g) and 120 h (7.33 ± 0.22 log CFU/g) of storage respectively, while anaerobic counts on Columbia blood agar were at 5.53 ± 0.66 log CFU/g after 240 h. Furthermore, *Campylobacter* spp. counts on Skirrow and mCCDA media at the end of storage at 5 ºC (240 h) were estimated at 2.34 ± 0.20 and 2.70 ± 0.04 log CFU/g. Regarding samples stored at 10 ºC, TVCs and *Pseudomonas* spp. counts exceeded the spoilage threshold of 7.0 log CFU/g after 48 h (7.12 ± 0.90 log CFU/g) and 72 h (8.36 ± 0.57 log CFU/g) of storage. Columbia blood agar counts reached values greater than 7.0 log CFU/g only in the case of isothermal storage (7.47 ± 0.25 log CFU/g), while *Campylobacter* spp. counts at the end of storage (192 h) were 2.98 ± 0.07 log CFU/g in Skirrow agar and 3.01 ± 0.22 log CFU/g in mCCDA. For the dynamic temperature profile, TVCs and *Pseudomonas* spp. counts were recorded at 7.01 ± 0.1 log CFU/g and at 7.5 ± 0.89 log CFU/g in 24 h, respectively. At the end of the dynamic temperature profile experiment (312 h), counts on Columbia blood agar were 5.81 ± 0.07 log CFU/g, while *Campylobacter* spp. counts were estimated at 2.27 ± 0.16 log CFU/g in Skirrow agar and 2.12 ± 0.27 log CFU/g in mCCDA. The

survival of *Campylobacter* spp. at freezing and chilling temperatures as well as its acid tolerance on marinated matrices and modified broths has been well documented in the literature (Fletcer et al., 1983; Chaveerach et al., 2003; Zhao et al., 2003; Ritz et al., 2006; Lanzl et al., 2020; Lytou et al., 2020).

In addition, microbiological analysis was performed to non- inoculated samples and the obtained results are provided in **Figure 7.2**. For the isothermal conditions of storage, TVCs, *Pseudomonas* spp. counts and anaerobic populations on Columbia blood agar showed similar growth behavior with the ones observed in inoculated samples, with their initial counts being 5.06 ± 0.28, 4.99 ± 0.26 and 4.67 ± 0.33 log CFU/g, respectively. In the case of the dynamic temperature profile, TVCs, *Pseudomonas* spp. counts and anaerobic counts on Columbia blood agar were 5.63 ± 0.14, 5.09 ± 0.03 and 3.74 ± 0.34 log CFU/g respectively. TVCs and *Pseudomonas* spp. loads in control (non- inoculated) samples presented a similar growth pattern as in the inoculated samples and reached the spoilage threshold of 7.0 log CFU/g one day later compared with the inoculated samples. Specifically, TVCs and *Pseudomonas* spp. counts exceeded 7.0 log CFU/g in 216 h at 0 ºC (TVCs:7.66 ± 0.63 log CFU/g, *Pseudomonas* spp. counts: 7.29 ± 0.79 log CFU/g), in 96 h at 5 ºC (TVCs: 7.22 ± 0.88 log CFU/g, *Pseudomonas* spp. counts: 6.49 ± 0.48 log CFU/g) and in 72 h at 10 ºC (TVCs: 7.52 ± 0.29 log CFU/g, *Pseudomonas* spp. counts: 6.03 ± 0.28 log CFU/g). For the dynamic temperature profile, spoilage was evident after 24 h of storage with TVCs values of 7.03 ± 0.15 log CFU/g. For the samples stored at 0 ºC, the anaerobic counts on Columbia blood agar were estimated at 6.80 ± 0.65 log CFU/g in 312 h, while at 5 ºC were 7.29 ± 0.55 log CFU/g in 144 h. Finally, at 10°C and in the dynamic temperature profile, counts on Columbia blood agar were 7.02 ± 0.78 log CFU/g (in 120 h) and 6.02 ± 0.31 log CFU/g (in 312 h).

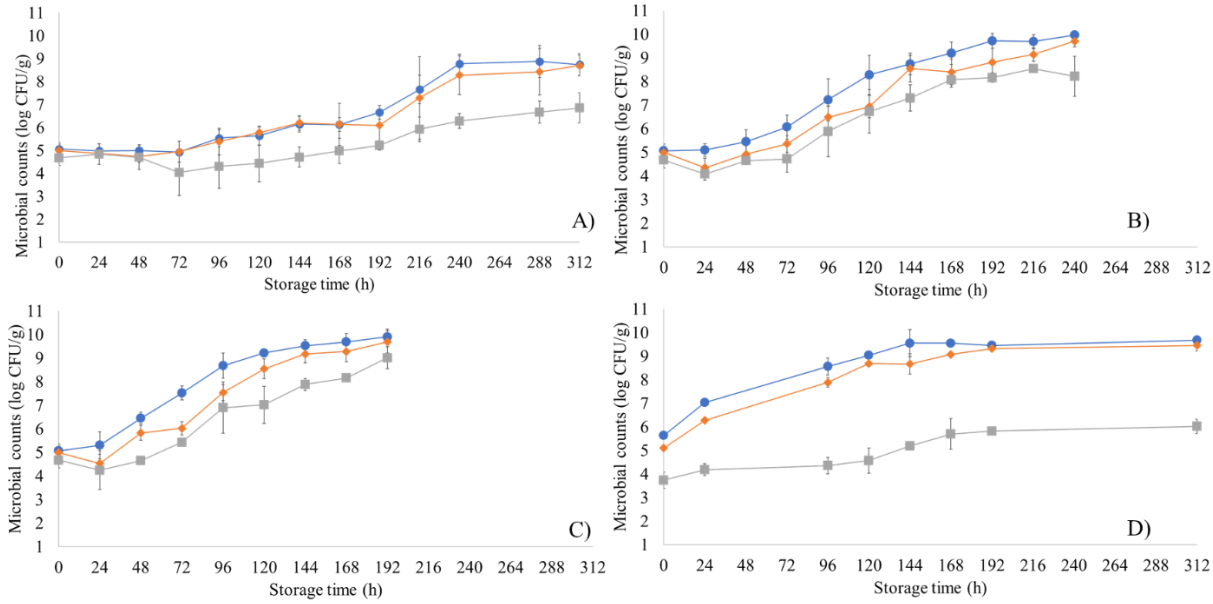

Figure 7.2: Microbial counts of TVCs (cycles), *Pseudomonas* spp. (diamonds) and anaerobic bacteria on Columbia blood agar (squares) in non-inoculated chicken marinated souvlaki stored at 0 ºC (A), 5 ºC (B), 10 ºC (C) and a dynamic temperature profile (D).

7.3.2 Growth models for the determination of TVCs and Pseudomonas spp. in chicken marinated souvlaki

The parameters for the primary full growth model of Huang full growth model (Huang, 2016) and the secondary Ratkowsky sub-optimal growth-temperature model (Ratkowsky, 1983) estimated by IPMP Global Fit software to TVCs and *Pseudomonas* spp. counts from inoculated and non-inoculated chicken marinated souvlaki samples are shown in **Tables 7.1** and **7.2**. TVCs could be associated with the determination of the shelf life of poultry products stored aerobically (Dominquez & Shaffner, 2011; Galarz et al., 2016; Lytou et al., 2016) whereas *Pseudomonas* spp. has been identified as the dominant microbial group responsible for the aerobic spoilage of white muscle food such as poultry and fish (Koutsoumanis et al., 2000; Bruckner et al., 2013; Raab et al., 2018). The secondary Ratkowsky model parameters a and T_0 of inoculated and non- inoculated samples for TVCs prediction demonstrated similar values that ranged from 0.010 to 0.013 and from -15 to -16 ºC. The same outcome was occurred for *Pseudomonas* spp. where the estimated values of a and T_0 parameters were 0.012 and -16.80 ºC for the inoculated samples, and 0.013 and -20.50 ºC for the non- inoculated ones. The negative temperature could be associated to the psychotropic behavior of the indigenous chicken's microbiota

and more specifically to *Pseudomonas* spp. growth behavior (Huang et al., 2011). It has to be underlined that similar model parameters for TVCs and *Pseudomonas* spp. growth on muscle foods (red meat, poultry, fish) have been reported in other studies via squared root models (Koutsoumanis et al., 2006; Zang et al., 2011; Lytou et al., 2016) and demonstrated high variability due to differences in the experimental design, the food matrix as well as variability among batches.

Table 7.1: Parameters and statistics by Huang full growth primary model and the Ratkowsky secondary model for TVCs in chicken marinated souvlaki samples.

Samples	**Inoculated chicken marinated souvlaki**			**Non- Inoculated chicken marinated souvlaki**		
Parameters	Value[a]	Std-Error	p-value	Value	Std-Error	p-value
a	0.013	0.004	3.02E-04	0.010	0.002	8.49E-05
T_0	-15.000	4.740	1.96E-03	-16.00	4.66	7.94E-04
A	-1.740	3.750	6.43E-01	-0.69	2.90	8.13E-01
m	1.930	1.220	1.17E-01	1.61	0.99	1.05E-01
y_0, $T_{0.0}$	5.540	0.249	3.41E-45	4.98	0.25	7.87E-41
y_0, $T_{5.0}$	5.370	0.295	8.73E-37	5.16	0.28	5.79E-37
y_0, $T_{10.0}$	5.490	0.375	7.94E-29	4.95	0.39	6.05E-24
y_{max}	9.860	0.211	1.39E-80	9.75	0.22	3.18E-78

[a]Mean value (n=4)

Table 7.2: Parameters and statistics by Huang full growth primary model and the Ratkowsky secondary model for *Pseudomonas* spp. in chicken marinated souvlaki samples.

Samples	**Inoculated chicken marinated souvlaki**			**Non- Inoculated chicken marinated souvlaki**		
Parameters	Value[a]	Std-Error	p-value	Value	Std-Error	p-value
a	0.012	0.003	2.85E-04	0.013	0.01	1.53E-03
T_0	-16.80	5.33	2.05E-03	-20.50	7.22	5.22E-03
A	-1.62	3.41	6.35E-01	0.95	2.65	7.20E-01
m	1.99	1.18	9.55E-02	1.06	0.93	2.56E-01
y_0, $T_{0.0}$	5.03	0.25	3.96E-41	4.86	0.28	3.96E-35
y_0, $T_{5.0}$	4.41	0.29	1.16E-29	4.71	0.25	1.32E-38
y_0, $T_{10.0}$	4.66	0.38	2.05E-23	4.74	0.32	8.07E-29
y_{max}	9.44	0.21	9.44E-80	9.44	0.27	1.54E-65

[a]Mean value (n=4)

Based on the abovementioned parameters and equations 3 and 4, μ_{max} and lag phase (h) were calculated and their values at each storage temperature are provided in **Table 7.3**.

As expected, the values of μ_{max} for TVCs and *Pseudomonas* spp. in both inoculated and non-inoculated samples increased with increasing storage temperature. Specifically, the minimum μ_{max} values for TVCs were observed at 0°C in both inoculated and non-inoculated samples (0.039 and 0.042 h^{-1}). For *Pseudomonas* spp., μ_{max} values increased similarly to TVCs μ_{max} highlighting once more that *Pseudomonas* spp. was the dominant spoilage microorganism during storage in inoculated and non-inoculated chicken samples. Reversibly, the lag phase duration (λ) for the two microbial groups decreased with increasing storage temperature. As expected, the lowest λ values were observed in inoculated (13.05 h for TVCs and 13.99 h for *Pseudomonas* spp.) and non-inoculated samples (17.40 h for TVCs and 26.72 h for *Pseudomonas* spp.) stored at 10 ^{o}C. Finally, the calculated RMSE values were lower than 0.7 log CFU/g in all cases.

Table 7.3: Lag- phase and μ_{max} values estimated by the Huang full growth primary model for TVCs and *Pseudomonas* spp. growth on chicken marinated souvlaki stored at 0, 5 and 10 ^{o}C.

Samples	**Inoculated chicken marinated souvlaki**				**Non-inoculated chicken marinated souvlaki**			
Microbial group	TVCs		*Pseudomonas* spp.		TVCs		*Pseudomonas* spp.	
T ^{o}C	μ_{max} (h^{-1})	lag phase (h)	μ_{max} (h^{-1})	lag phase (h)	μ_{max} (h^{-1})	lag phase (h)	μ_{max} (h^{-1})	lag phase (h)
0	0.039	93.74	0.046	89.75	0.042	83.10	0.044	56.98
5	0.069	30.88	0.078	31.82	0.072	34.62	0.068	37.59
10	0.107	13.05	0.117	13.99	0.111	17.40	0.097	26.72
RMSE (log CFU/g)	0.57		0.54		0.44		0.68	

The μ_{max} and lag phase duration values for TVCs of aerobically stored chicken at isothermal conditions (4-20 ^{o}C) have been reported by previous researchers using the Baranyi and Roberts primary growth model (Lytou et al., 2016) and the modified Gompertz equation (Galarz et al., 2016). Furthermore, Dominquez and Schaffner (2007) reported that *Pseudomonas* spp. μ_{max} parameter on chicken stored at 0, 5, 10, 15, 20, and 25 ^{o}C was 0.03592 h^{-1}, 0.069077 h^{-1}, 0.113287 h^{-1}, 0.326736 h^{-1}, 0.41953 h^{-1} and 0.40111 h^{-1}, respectively, which are in good agreement with the values obtained in this work. Similar *Pseudomonas* spp. growth kinetic parameters at different storage temperatures were reported using the Baranyi and Roberts model, where the lag phase duration was 12.3 h,

6.2 h and 4 h for poultry stored at 10, 15, and 20 ^{o}C, respectively (Gospavic et al., 2008). Moreover, the estimated μ_{max} and lag phase duration values for *Pseudomonas* spp. did not differ from the respective parameters obtained by the modified Gompertz equation (Galarz et al., 2016; Raab et al., 2018).

For the prediction of TVCs and *Pseudomonas* spp. growth at the dynamic temperature profile for both inoculated and non-inoculated samples, the initial and final load (y_o and y_{max}), the parameters a and T_0, as well as the parameter h_o for the Baranyi and Roberts dynamic model, estimated as μ_{max} × lag phase (Lianou et al., 2020), were defined as follows: a) For TVCs in inoculated samples: y_o= 5.34 log CFU/g, y_{max}= 9.86 log CFU/g, ho= 2.37, a= 0.013, and T_0= -15.00 ^{o}C; b) For TVCs in non-inoculated samples: y_o=5.03 log CFU/g, y_{max}= 9.75 log CFU/g, ho= 2.63, a= 0.010, and T_0= -16.00 ^{o}C; c) For *Pseudomonas* spp. counts in inoculated samples: y_o=4.70 log CFU/g, y_{max}= 9.44 log CFU/g, ho= 2.78, a= 0.012, and T_0= -16.80 ^{o}C; d) For *Pseudomonas* spp. counts in non-inoculated samples: y_o=4.77, y_{max}=9.44, ho=2.54, a= 0.102, and T_0= -20.50 ^{o}C. The growth profiles of TVCs and *Pseudomonas* spp. under the dynamic temperature scenario are presented in **Figure 7.3**. It is characteristic that an under-estimation of both TVCs and *Pseudomonas* spp. counts was observed within the first 24 hours of storage. This could be attributed to the variability among the different batches used in this work (different initial microbial load), as well as to the different metabolic profile products of the microbiota caused by temperature shifts (Papadopoulou et al., 2011).

Furthermore, for TVCs model of inoculated samples, RMSE, B_f and A_f indices reached the values of 0.941 log CFU/g, 0.983 and 1.111 respectively. For the case of non-inoculated samples and TVCs predictive model, RMSE, B_f and A_f yielded 0.858 log CFU/g, 0.986 and 1.101, respectively. Based on the values of the A_f index, the average difference between predictions and observations were *ca.* 10 %. Model validation for *Pseudomonas* spp. on inoculated samples presented RMSE value of 0.778 log CFU/g, while B_f and A_f performance metrics were 0.995 and 1.100, respectively. Likewise, model validation for *Pseudomonas* spp. on non-inoculated samples, presented RMSE, B_f and A_f values of 0.839 log CFU/g, 1.018 and 1.100, respectively. In all cases, the performance metrics were considered acceptable and hence models' performances were evaluated as

good due to the low RMSE values (lower than 1 log CFU/g), the B_f values which were in the range 0.90- 1.05 (Mellefont et al., 2013) (within the fail- dangerous zone) and the A_f values indicating that the difference of predicted to observed values was within ± 11 %.

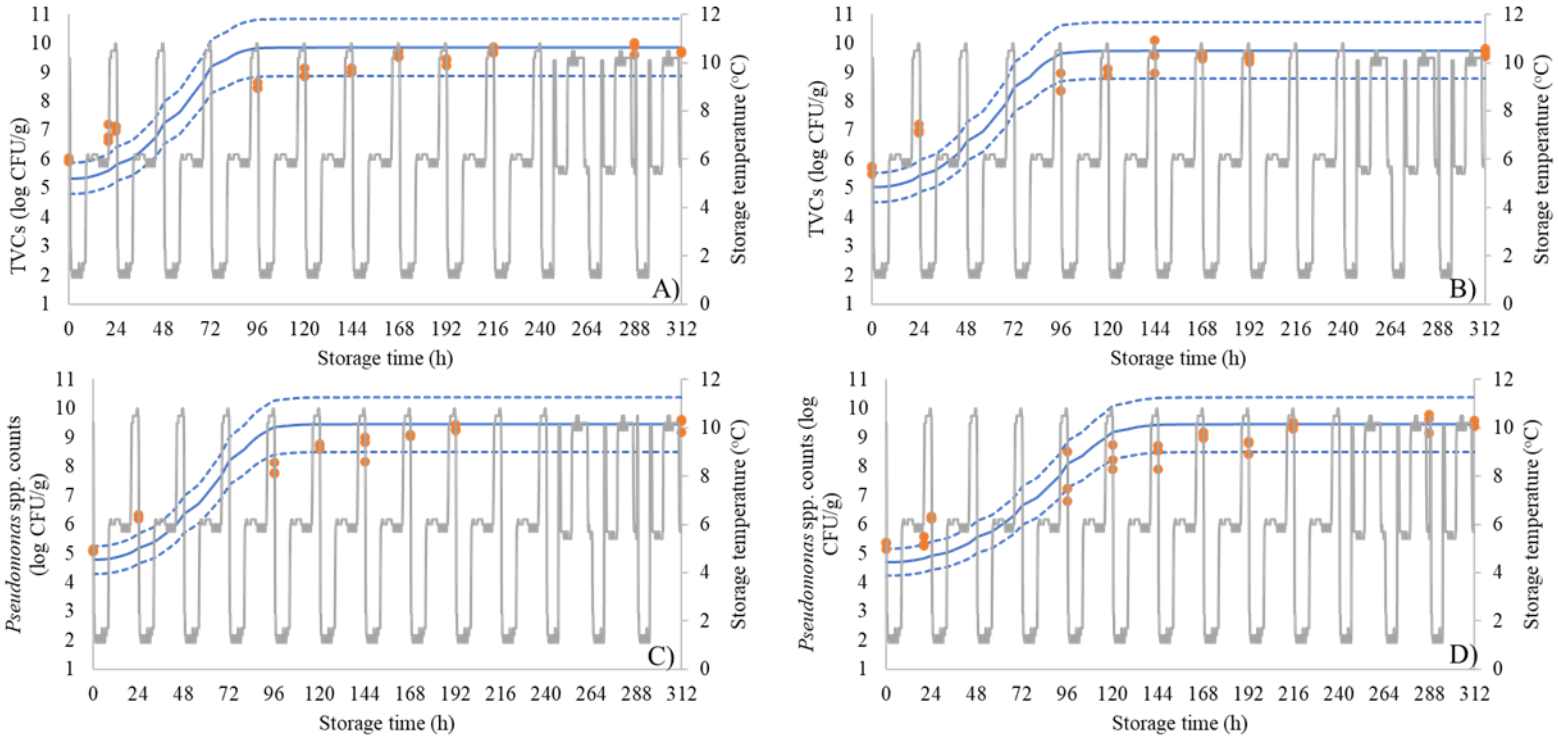

Figure 7.3: Comparison between observed (points) and predicted (lines) growth of TVCs and *Pseudomonas* spp. on inoculated (A, C) and non-inoculated (B, D) chicken marinated souvlaki samples stored aerobically under periodically changing temperature profile. Dashed lines correspond to the ± 10 % relative error zone.

7.3.3 Survival models of Campylobacter spp. in chicken marinated souvlaki

The calculated parameters for the inactivation Weibull and modified Weibull models for *Campylobacter* spp. in chicken marinated souvlaki during storage at isothermal conditions are presented in **Table 7.4**. As expected, the lowest storage temperature (0 ºC) presented the highest value for delta parameter (404.73 h) which is the time needed for the first decimal reduction of the pathogen, whereas at 10 ºC the lowest value for delta parameter was observed (59.52 h). In previous studies, different values of p and delta parameters for the Weibull model have been reported in order to describe the survival of *Campylobacter* spp. under chilling temperatures in chicken products (Ritz et al., 2006; González et al., 2009). The Weibull model was fitted adequately to the experimental data

as inferred by the values of RMSE (0.112- 0.215 log CFU/g), R^2 (> 0.824) and R^2 adjusted (> 0.788).

Table 7.4: Parameters and statistics for Weibull and modified Weibull inactivation models of *Campylobacter* spp. in stored chicken marinated souvlaki samples at isothermal conditions (0, 5 and 10 ºC).

Storage temperature (ºC)	Parameters	Estimated Parameter value	Standard Error	RMSE (log CFU/g)	R^2	R^2 adjusted
0	Delta (h)	404.73	58.39	0.122	0.824	0.788
	p	1.14	0.41			
	$log_{10}(N_0)$ (CFU/g)	3.46	0.09			
5	Delta (h)	250.12	29.67	0.112	0.909	0.886
	p	0.96	0.27			
	$log_{10}(N_0)$ (CFU/g)	3.45	0.10			
10	$Log_{10}(N_{res})$ (CFU/g)	2.87	0.05	0.215	0.890	0.825
	Delta (h)	59.52	13.53			
	p	2.15	1.51			
	$Log_{10}(N_0)$ (CFU/g)	3.45	0.10			

The fitted inactivation models at each storage temperature condition are also graphically illustrated in **Figure 7.4**. It needs to be noted that the population of the pathogen was reduced by *ca.* 1.0 log CFU/g throughout storage. This finding is in good agreement with other studies reporting pathogen reduction varied from 0.51 to 1.57 log CFU/g in chicken during chilling and frozen storage (Bhaduri & Cottrell, 2004; Huang et al., 2012).

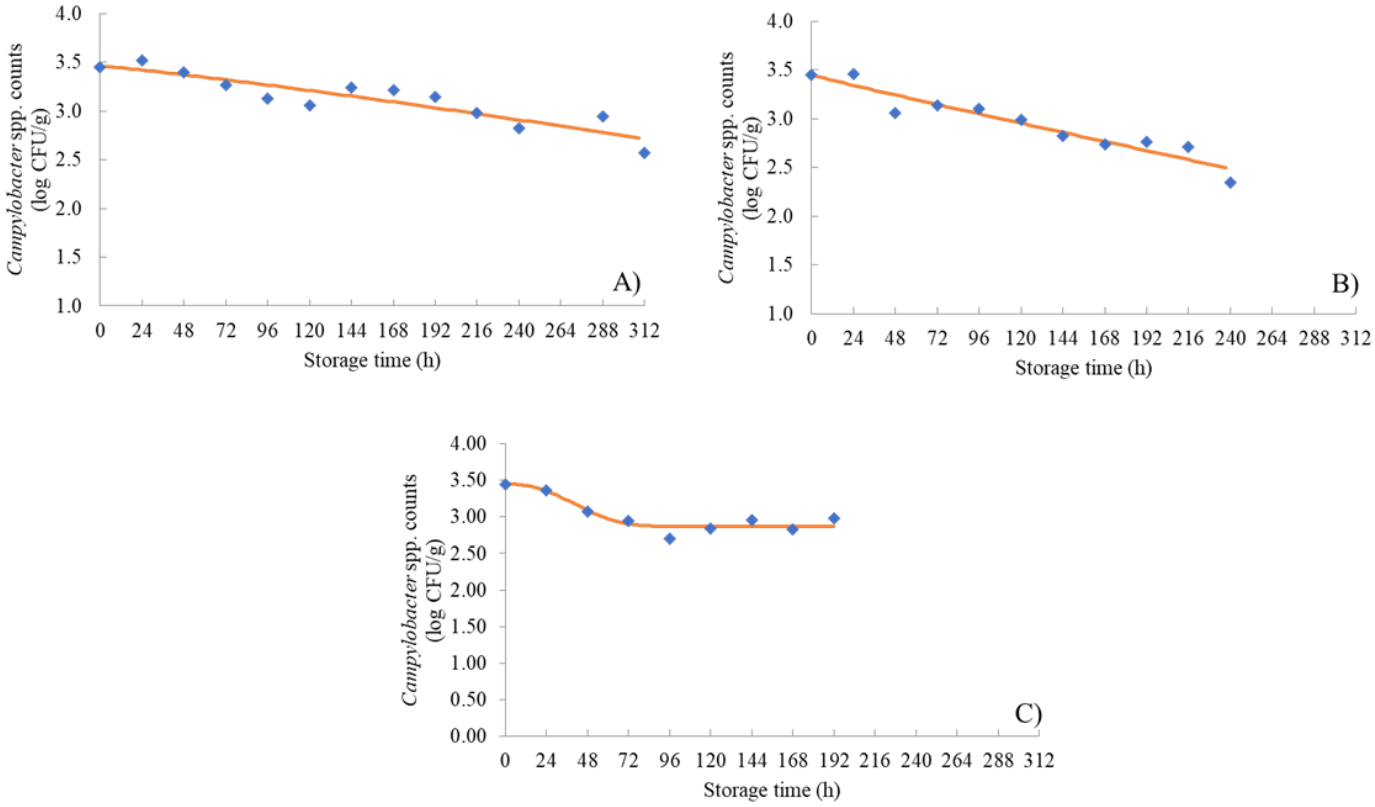

Figure 7.4: Survival curves of *Campylobacter* spp. in chicken marinated souvlaki during storage stored at 0 ºC (A), 5 ºC (B) and 10 ºC (C). Data points are mean (± standard error) of two independent experiments with two replications each (n =4).

7.3.4 Molecular analysis results

The results from RAPD-PCR products via electrophoresis are presented in **Figure 7.5A,** whereas the relative abundance for the six *Campylobacter* strains, namely *C. jejuni* (R450 and 6A) and *C. coli* (9D, 7L, 6Z, and 1H), assembling the composite inoculum for selected time points at the three storage temperatures is shown in **Figure 7.5B**. At the beginning of storage experiments (0 h), all the inoculated *Campylobacter* strains were recovered, with *C. coli* 1H and 7L representing 45.45 % and 18.18 % of the relative abundance, respectively. After 120 h of storage at 0 ºC, *C. coli* 6Z could not be recovered, whereas the relative abundances of *C. coli* 9D and *C. jejuni* 6A were 28.57 %. On the other hand, *C. coli* 6Z was recovered at the end of storage (312 h) at 0 ºC and dominated all the other strains (7L, 1H, 6A), while *C. jejuni* R450 and *C. coli* 9D could not be detected. Regarding storage at 5 ºC, four strains (1H, R450, 9D and 6Z) were recovered after 96 h, with *C. coli* 6Z presenting the highest abundance (40%). At the end of storage at 5 °C, the

strains *C. coli* 7L, 6Z and 9D strains were recovered in the same abundance (20 %), whereas 40 % of the isolates presented similar profile to *C. coli* 1H. After storage for 72 h at 10 ºC, *C. coli* 6Z was the only strain that could not be detected while the presence of the remaining 5 strains was equal amounting to 20 %. At the end of storage (216 h) at 10 °C, three (9D, R450, 6Z) out of six strains could be recovered, with *C. coli* 9D presenting the highest abundance (50 %) followed by *C. jejuni* R450 (33.33%). The abovementioned findings demonstrated that both *C. jejuni* and *C. coli* could survive under the chilling temperatures until the end of storage, with the exception of 5ºC where *C. coli* strains were only detectable at the end of storage (240 h). This observation is in line with previous studies reporting that *C. coli* is more frequently isolated from poultry industries where temperatures are with the range of 4-7 ºC (Membré et al., 2013).

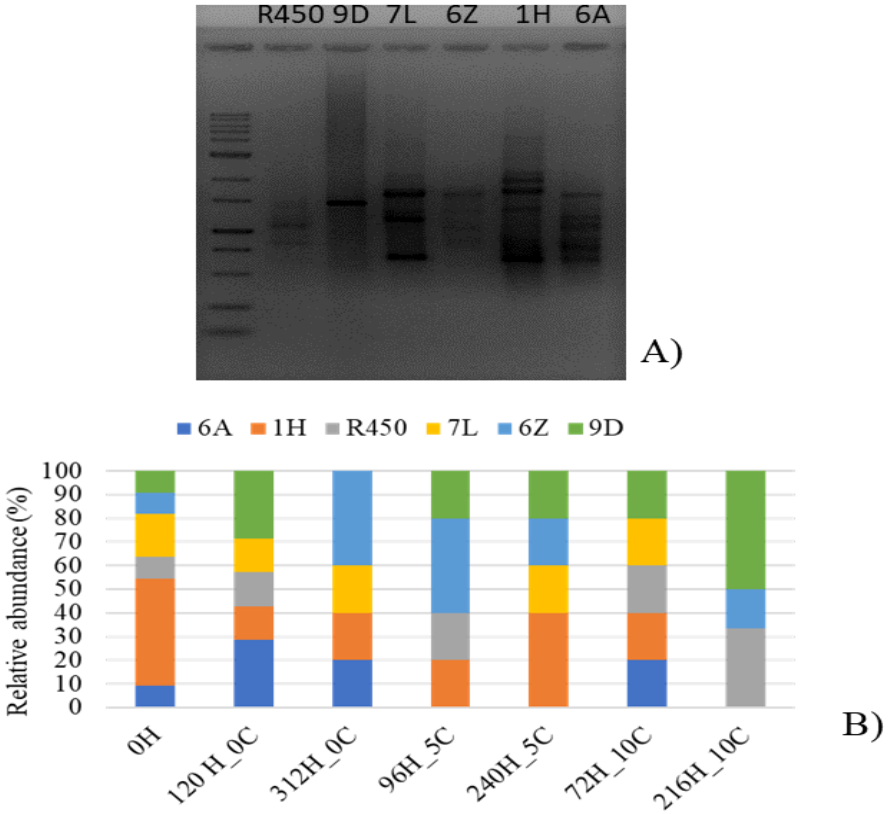

Figure 7.5: A) RAPD-PCR profiles of the 6 *Campylobacter* strains (R450, 6A, 9D, 7L, 6Z and 1H) assembling the composite inoculum for the experiments; B) Relative abundance (%) of the 6 *Campylobacter* strains in the isolates from different time points during storage at 0, 5, and 10 ºC.

Chapter 8: Conclusions and Future Perspectives

In the present thesis, non- destructive spectroscopic and biomimetic sensors (MSI, FTIR, E-nose) were implemented at- line or off- line in raw and stored (under isothermal conditions and dynamic temperature profiles) chicken products, namely chicken breast fillet, chicken thigh fillet, chicken marinated souvlaki (using two types of marinade) and chicken burger. Machine learning methods (PLS-R, SVM-R, LDA, QDA, SVM classification), ensemble methods and data fusion were employed for the development and validation of quantitative and qualitative models estimating the microbial load on the product's surface, the time from slaughter and their spoilage level.

The findings from the performance of MSI and FT-IR methods in different food matrices (chapters 2, 3, 4, 5, 6) illustrated that each sensor and developed model was muscle specific and not only food specific. According to chapter 2, the food matrix (muscle type, spices and marinade) had a great impact on the prediction of the "time from slaughter" parameter. Specifically, chicken thigh fillet and chicken burger models with MSI data predicted more accurately the "time from slaughter parameter" mainly due to their composition.

In chapters 2, 3 and 4, MSI and FT-IR sensors were employed for the assessment of quality in chicken breast fillets. Chicken breast spoilage was detected by MSI analysis and PLS-R model; however, the performance metrics during the external validation were not satisfactory (RMSE values above ± 1 log CFU/cm^2). RMSE values decreased when nonlinear machine learning models (nnet) with MSI data were developed for the estimation of TVCs (chapter 3). In contrast, FT-IR coupled with PLS-R models provided more accurate predictions of TVCs. This outcome is in good agreement with other reports where the successful determination of microbial loads in chicken meat by FT-IR was attributed to the absorbance in the area 1,550- 1,650 cm^{-1} corresponding to the proteolytic activity of the microbiota during meat spoilage. Further on, in chapter 4, classification models were investigated for their efficacy to assess spoilage levels on the surface of chicken breast samples, whereas additional measurements were acquired via these sensors from four different batches stored at isothermal and dynamic conditions and coupled to microbiological and sensory analysis data. Linear, nonlinear and ensemble models were employed for the classification of the samples in quality classes. Results showed that MSI

analysis combined with an ensemble model classified stored chicken breast fillets in their correct class by 64.8 %. The low performance of MSI analysis could be explained due to the low concentration of myoglobin in this muscle. FT-IR data analysis with PLS-DA model exhibited higher overall accuracy (69.7 %) compared to the other developed models and therefore this method could be proposed as an alternative for the assessment of quality in chicken breast fillets. It is worth noting that the overall accuracy percentages in all cases did not exceed 70 % due to the variability of the samples used in external validation, which came from different seasons of the year and stored at dynamic temperature conditions (different metabolic activity of the microbiota). In order to further ameliorate model performance, data from dynamic temperature conditions could be used during model optimization, while MSI and FT-IR features could be fused for the development of qualitative models for chicken breast fillets.

In chapter 5, the potential of MSI analysis for quality assessment in chicken thigh fillets was further confirmed. Similar to chapter 2, MSI data in tandem with PLS-R models could satisfactorily estimate TVCs and *Pseudomonas* spp. on the surface of chicken thigh. Likewise, MSI and FT-IR spectral data analyzed by SVMs and QDA models, respectively, could successfully classify stored samples in their proper sensory classes (fresh vs. spoiled), whereas the combination of MSI and SVMs excelled with overall prediction accuracy of 94.4%. These encouraging results are in line with other studies where MSI data combined with SVM provided robust models for quality assessment in meat, while FT-IR spectral data analyzed by LDA efficiently discriminated stored meat during spoilage. Further optimization of the developed models should be based on batches from different seasons of the year or storage conditions in order to enhance the database concerning spoilage phenomena in chicken thigh.

In chapter 6, MSI, FT-IR and E-nose were evaluated for their potential to assess the quality of marinated chicken souvlaki via data fusion using a variety of linear/nonlinear quantitative and qualitative models. In accordance with the previous chapters, the importance of choosing the appropriate machine learning model depending on the sensors' features, as well as the synergetic effect of data fusion from different sensors was highlighted. For the assessment of TVCs via PLS-R models, MSI data provided the most

accurate predictions followed by FT-IR/MSI model and the combined three sensors model. Likewise, SVM-R models developed on MSI and FT-IR/MSI data exhibited the most satisfactory determination of TVCs. The classification models for the categorization of stored chicken marinated souvlaki into three classes (fresh, semi-fresh, spoiled) did not provide acceptable results (low overall accuracy), with MSI-LSVM model and MSI/E-nose-CSVM model showing the highest values of overall accuracy compared to the other models. The exclusion of the semi-fresh class seemed to improve classification performance with MSI-LSVM, FT-IR/MSI- LSVM and FT-IR/MSI-LDA models for two quality classes presenting good overall accuracy, sensitivity and precision. The performance of the models was further confirmed by external validation using data from independent meat batches and different analysts. Even though quantitative and qualitative models developed on E-nose data could not classified accurately the samples at their correct quality class, the fused model of MSI/E-nose provided improved performance metrics. E-nose weakness could be attributed to the existence of organic acids in the marinade that could influence MOS signals. Overall, MSI data and the fusion of FT-IR and MSI data were proved effective for the assessment of the microbiological quality in chicken marinated souvlaki regardless of product batch, storage conditions or analyst.

Concerning the safety in poultry (chapter 7), chilling temperatures (0, 5, and 10 °C) inhibited as expected *Campylobacter* spp. growth in marinated chicken souvlaki; however, the population of the pathogen declined by only 1.5 log CFU/g. The developed Weibull survival models could be efficiently fitted to *Campylobacter* spp. counts with the model developed with data from the 5 ^{o}C storage condition providing the lowest RMSE value (0.112 log CFU/g). Regarding TVCs and *Pseudomonas* spp. on the inoculated samples, their population dynamics were not affected by the presence of *Campylobacter* spp. inoculum, as inferred by the comparison of μ_{max} and lag phase values in inoculated and non-inoculated samples. Molecular analysis revealed that both *C. coli* and *C. jejuni* were present during chicken marinated souvlaki storage at chilling temperatures, with the exception of 5 ^{o}C where only *C. coli* strains could be recovered from the samples at the end of storage. These findings illustrated the ability of *Campylobacter* spp. to survive during refrigerated storage of poultry meat and even its presence in low populations (2.0 log CFU/g) could be extremely hazardous to humans due to cross-contamination.

The overall findings of this thesis for the assessment of the quality of poultry products by the implementation of rapid and non-destructive analytical methods such as MSI and FT-IR are encouraging. These two environmentally friendly methods could efficiently detect the microbiological quality and hence spoilage in a variety of poultry products stored at different storage temperatures, seasons of the year and packaging conditions. The validation of the developed models with different meat batches, seasons of slaughter, storage conditions and analysts illustrated their potential to assess successfully spoilage in these products.

Further on, the developed predictive models from this research could be validated with data collected from poultry product oriented by different producers. Moreover, the proposed models (developed off- line at the laboratory) in tandem with FT-IR and MSI techniques could be performed for the assessment of quality on-line or at-line on an industrial scale similarly to the successful implementation of MSI analysis described in Chapter 2. Nevertheless, the continuous update of data from these techniques (different storage temperatures, packaging conditions, season of slaughter, producers or suppliers) and model optimization could result in the development of reliable models predicting spoilage in poultry meat and hence contribute in the reduction of food waste.

References

Al-Nehlawi, A., Saldo, J., Vega, L. F. and Guri, S., 2013. Effect of high carbon dioxide atmosphere packaging and soluble gas stabilization pre-treatment on the shelf-life and quality of chicken drumsticks. Meat Science, 94(1), 1-8. https://doi.org/10.1016/j.meatsci.2012.12.008.

Alamprese, C., Casale, M., Sinelli, N., Lanteri, S. and Casiraghi, E. 2013. Detection of minced beef adulteration with turkey meat by UV–vis, NIR and MIR spectroscopy. LWT-Food Science and Technology, 53(1), 225-232. https://doi.org/10.1016/j.lwt.2013.01.027

Alamprese, C., Amigo, J. M., Casiraghi, E. and Engelsen, S. B., 2016. Identification and quantification of turkey meat adulteration in fresh, frozen-thawed and cooked minced beef by FT-NIR spectroscopy and chemometrics. Meat Science, 121, 175-181. https://doi.org/10.1016/j.meatsci.2016.06.018

Albert, I. and Mafart, P., 2005. A modified Weibull model for bacterial inactivation. International Journal of Food Microbiology, 100(1-3), 197-211. doi:10.1016/j.ijfoodmicro.2004.10.016

Alexandrakis, D., Downey, G. and Scannell, A.G., 2012. Rapid non-destructive detection of spoilage of intact chicken breast muscle using near-infrared and Fourier transform mid-infrared spectroscopy and multivariate statistics. Food Bioprocess Technology 5 (1), 33–65. https://doi.org/10.1007/s11947-009-0298-4.

Alomar, D., Gallo, C., Castaneda, M. and Fuchslocher, R., 2003. Chemical and discriminant analysis of bovine meat by near infrared reflectance spectroscopy (NIRS). Meat Science, 63(4), 441-450. https://doi.org/10.1016/S0309-1740(02)00101-8

Amorim, A., Rodrigues, S., Pereira, E., Valentim, R. and Teixeira, A., 2016. Effect of caponisation on physicochemical and sensory characteristics of chickens. Animal, 10(6), 978-986. https://doi.org/10.1017/S1751731115002876

Andritsos, N.D., Tzimotoudis, N. and Mataragas, M., 2020. Estimating the performance of four culture media used for enumeration and detection of Campylobacter species in chicken meat. LWT, 118, 108808. https://doi.org/10.1016/j.lwt.2019.108808

Arafat, M.Y., Hoque, S., Xu, S. and Farid, D.M., 2019. Machine learning for mining imbalanced data. IAENG International Journal of Computer Science, 46(2), 332-348.

Argyri, A.A., Panagou, E.Z., Tarantilis, P.A., Polysiou, M. and Nychas, G.J., 2010. Rapid qualitative and quantitative detection of beef fillets spoilage based on Fourier transform infrared spectroscopy data and artificial neural networks. Sensors and Actuators B: Chemical, 145(1), 146-154. https://doi.org/10.1016/j.snb.2009.11.052

Argyri, A.A., Jarvis, R.M., Wedge, D., Xu, Y., Panagou, E.Z. and Goodacre, R., G-J, E., 2013. A comparison of Raman and FT-IR spectroscopy for the prediction of meat spoilage. Food Control. 29 (2), 461–470. https://doi.org/10.1016/j.foodcont.2012.05.040.

Argyri, A.A., Panagou, E.Z. and Nychas, G.-J.E., 2014. Monitoring microbial spoilage of foods by vibrational spectroscopy (FTIR and Raman). In: Boziaris, I.S. (Ed.), Novel Food Preservation and Microbial Assessment Techniques. CRC Press, Boca Raton, 386–434.

Arredondo, T., Oñate, E., Santander, R., Tomic, G., Silva, J.R., Sánchez, E. and Acevedo, C.A., 2014. Application of neural networks and meta-learners to recognize beef from OTM cattle by using volatile organic compounds. Food and Bioprocess Technology, 7(11), 3217-3225. https://doi.org/10.1007/s11947-014-1289-7

Asuero, A.G., Sayago, A. and Gonzalez, A.G., 2006. The correlation coefficient: an overview. Critical Reviews in Analytical Chemistry. 36 (1), 41–59. https://doi.org/10.1080/10408340500526766.

Balabin, R.M. and Lomakina, E.I., 2011. Support vector machine regression (LS-SVM)—an alternative to artificial neural networks (ANNs) for the analysis of quantum chemistry data? Physical Chemistry Chemical Physics, 13(24), 11710-11718. DOI: 10.1039/C1CP00051A

Balamatsia, C.C., Patsias, A., Kontominas, M.G. and Savvaidis, I.N., 2007. Possible role of volatile amines as quality-indicating metabolites in modified atmosphere-packaged chicken fillets: Correlation with microbiological and sensory attributes. Food Chemistry, 104(4), 1622-1628. https://doi.org/10.1016/j.foodchem.2007.03.013

Balasubramanian, S., Panigrahi, S., Logue, C.M., Marchello, M., Doetkott, C., Gu, H., Sherwood, J. and Nolan, L., 2004. Spoilage identification of beef using an electronic nose system. Transactions of the ASAE, 47(5), 1625.

Balasubramanian, S., Panigrahi, S., Logue, C.M., Marchello, M. and Sherwood, J.S., 2005. Identification of salmonella-inoculated beef using a portable electronic nose system. Journal of Rapid Methods & Automation in Microbiology, 13(2), 71-95. https://doi.org/10.1111/j.1745-4581.2005.00011.x

Balasubramanian, S., Panigrahi, S., Logue, C.M., Gu, H. and Marchello, M., 2009. Neural networks-integrated metal oxide-based artificial olfactory system for meat spoilage identification. Journal of Food Engineering, 91(1), 91-98. doi:10.1016/j.jfoodeng.2008.08.008

Baltic, T., Ciric, J., Lazic, I.B., Pelic, D.L., Mitrovic, R., Djordjevic, V. and Parunovic, N., 2019. Packaging as a tool to improve the shelf life of poultry meat. In IOP Conference Series: Earth and Environmental Science (Vol. 333, No. 1, p. 012044). IOP Publishing. doi:10.1088/1755-1315/333/1/012044

Baranyi, J. and Roberts, T.A. 1994. A dynamic approach to predicting bacterial growth in food. International journal of food microbiology, 23(3-4), 277-294. https://doi.org/10.1016/0168-1605(94)90157-0.

Barker, M. and Rayens, W. 2003. Partial least squares for discrimination. Journal of Chemometrics: A Journal of the Chemometrics Society, 17(3), 166-173. https://doi.org/10.1002/cem.785

Barni, M., Cappellini, V. and Mecocci, A., 1997. Colour-based detection of defects on chicken meat. Image and Vision Computing, 15(7), 549-556. https://doi.org/10.1016/S0262-8856(97)01138-4

Baston, O. and Barna, O., 2010. Raw chicken leg and breast sensory evaluation. Food Science and Technology, 11(1), 25-30. https://www.researchgate.net/publication/49613866

Baston, O., Barna, O. and Vasile, A., 2017. Freshness evaluation of chicken meat using microbiota and biogenic amine index. Food and Environment Safety Journal, 9(2), 61-66. http://fia-old.usv.ro/fiajournal/index.php/FENS/article/view/410

Belák, Á., Kovács, M., Hermann, Z., Holczman, Á., Márta, D., Stojakovič, S., Bajcsi, N. and Maráz, A., 2011. Molecular analysis of poultry meat spoiling microbiota and heterogeneity of their proteolytic and lipolytic enzyme activities. Acta Alimentaria, 40(Supplement-1), 3-22. DOI: 10.1556/AAlim.40.2011.Suppl.2

Berrueta, L.A., Alonso-Salces, R.M. and Héberger, K., 2007. Supervised pattern recognition in food analysis. Journal of chromatography A, 1158(1-2), 196-214. https://doi.org/10.1016/j.chroma.2007.05.024

Bhaduri, S. and Cottrell, B., 2004. Survival of cold-stressed Campylobacter jejuni on ground chicken and chicken skin during frozen storage. Applied and Environmental Microbiology, 70(12), 7103-7109. https://doi.org/10.1128/AEM.70.12.7103-7109.2004

Björkroth, J., 2005. Microbiological ecology of marinated meat products. Meat Science, 70(3), 477-480. doi:10.1016/j.meatsci.2004.07.018

Bi, Y., Yuan, K., Xiao, W., Wu, J., Shi, C., Xia, J., Chu, G., Zhang, G. and Zhou, G. 2016. A local pre-processing method for near-infrared spectra, combined with spectral segmentation and standard normal variate transformation. Analytica Chimica Acta, 909, 30–40. https://doi.org/10.1016/j.aca.2016.01.010.

Blankenship, L.C. and Craven, S.E., 1982. Campylobacter jejuni survival in chicken meat as a function of temperature. Applied and Environmental Microbiology, 44(1), 88-92. https://doi.org/10.1128/aem.44.1.88-92.1982

Bolton, D.J. and Robertson, L.J., 2016. Mental health disorders associated with foodborne pathogens. Journal of Food Protection, *79*(11), 2005-2017. https://doi.org/10.4315/0362-028X.JFP-15-587

Borràs, E., Ferré, J., Boqué, R., Mestres, M., Aceña, L. and Busto, O., 2015. Data fusion methodologies for food and beverage authentication and quality assessment–A review. Analytica Chimica Acta, 891, 1-14. https://doi.org/10.1016/j.aca.2015.04.042

Boulesteix, A.L. and Strimmer, K., 2007. Partial least squares: a versatile tool for the analysis of high-dimensional genomic data. Briefings in bioinformatics, 8(1), 32-44. https://doi.org/10.1093/bib/bbl016

Bouzembrak, Y., Klüche, M., Gavai, A. and Marvin, H.J., 2019. Internet of Things in food safety: Literature review and a bibliometric analysis. Trends in Food Science & Technology, 94, 54-64. https://doi.org/10.1016/j.tifs.2019.11.002

Böcker, U., Ofstad, R., Wu, Z., Bertram, H.C., Sockalingum, G.D., Manfait, M., Kohler, A., 2007. Revealing covariance structures in Fourier transform infrared and Raman microspectroscopy spectra: a study on pork muscle fiber tissue subjected to different processing parameters. Applied Spectroscopy. 61 (10), 1032–1039. https://doi.org/10.1366/000370207782217707

Breiman, L., 2001. Random forrest. Machine Learning 45, 5–32. https://doi.org/10.1023/A:1010933404324.

Brereton, R.G. and Lloyd G.R. 2014. Partial least squares discriminant analysis: taking the magic away. Journal of Chemometrics. 28, 213-225. https://doi.org/10.1002/cem.2609

Bruckner, S., Albrecht, A., Petersen, B. and Kreyenschmidt, J., 2013. A predictive shelf life model as a tool for the improvement of quality management in pork and poultry chains. Food Control, *29*(2), 451-460. https://doi.org/10.1016/j.foodcont.2012.05.048

Cai, J., Chen, Q., Wan, X. and Zhao, J., 2011. Determination of total volatile basic nitrogen (TVB-N) content and Warner–Bratzler shear force (WBSF) in pork using Fourier transform near infrared (FT-NIR) spectroscopy. Food Chemistry, 126(3), 1354-1360. https://doi.org/10.1016/j.foodchem.2010.11.098

Candoğan, K., Altuntas, E.G. and İğci, N., 2021. Authentication and quality assessment of meat products by fourier-transform infrared (FTIR) spectroscopy. Food Engineering Reviews, 13(1), 66-91. https://doi.org/10.1007/s12393-020-09251-y

Carstensen, J.M. and Hansen, J.F. An Apparatus and a Method of Recording an Image of an Object. Patent family EP1051660, Patent 17, 198, 15 November 2003

Chao, K., Yang, C.C., Chen, Y.R., Kim, M.S. and Chan, D.E., 2007. Hyperspectral-multispectral line-scan imaging system for automated poultry carcass inspection applications for food safety. Poultry Science, 86(11), 2450-2460. https://doi.org/10.3382/ps.2006-00467

Chaveerach, P., Ter Huurne, A.A.H.M., Lipman, L.J.A. and Van Knapen, F., 2003. Survival and resuscitation of ten strains of Campylobacter jejuni and Campylobacter coli under acid conditions. Applied and Environmental Microbiology, 69(1), 711-714. https://doi.org/10.1128/AEM.69.1.711-714.2003

Chen, Q., Cai, J., Wan, X. and Zhao, J., 2011. Application of linear/non-linear classification algorithms in discrimination of pork storage time using Fourier transform near infrared (FT-NIR) spectroscopy. LWT-Food Science and Technology, 44(10), 2053-2058. https://doi.org/10.1016/j.lwt.2011.05.015

Chen, Q., Hui, Z., Zhao, J. and Ouyang, Q., 2014. Evaluation of chicken freshness using a low-cost colorimetric sensor array with AdaBoost–OLDA classification algorithm. LWT-Food Science and Technology, 57(2), 502-507. http://dx.doi.org/10.1016/j.lwt.2014.02.031

Chen, R.Y., 2015. Autonomous tracing system for backward design in food supply chain. Food Control, 51, 70-84. https://doi.org/10.1016/j.foodcont.2014.11.004

Chmiel, M. and Słowiński, M., 2018. Effect of storage in display cases on the sensory quality of chicken breast meat (m. pectoralis). Brazilian Journal of Poultry Science, 20, 91-98.https://doi.org/10.1590/1806-9061-2017-0628
Cho, B.K., Chen, Y.R. and Kim, M.S., 2007. Multispectral detection of organic residues on poultry processing plant equipment based on hyperspectral reflectance imaging technique. Computers and Electronics in Agriculture, 57(2), 177-189. https://doi.org/10.1016/j.compag.2007.03.008

Chung, S. and Yoon, S.C., 2021. Detection of Foreign Materials on Broiler Breast Meat Using a Fusion of Visible Near-Infrared and Short-Wave Infrared Hyperspectral Imaging. Applied Sciences, 11(24), 11987. https://doi.org/10.3390/app112411987

Codex Alimentarius Commission (CAC), 2011. Guidelines for the control of Campylobacter and Salmonella in chicken meat. CAC/GL 78-2011. *Food and Agriculture Organization (FAO), Rome*.

Collins, K.E., Kiepper, B.H., Ritz, C.W., McLendon, B.L., Wilson, J.L., 2014. Growth, livability, feed consumption, and carcass composition of the Athens Canadian Random Bred 1955 meat-type chicken versus the 2012 high-yielding Cobb 500 broiler. Poultry Science. 93 (12), 2953–2962. https://doi.org/10.3382/ps.2014-04224.

Cortes, C. and Vapnik, V., 1995. Support-vector networks. Machine learning, 20(3), 273-297. https://doi.org/10.1007/BF00994018

Cover, T. and Hart, P. 1967. Nearest neighbor pattern classification. IEEE transactions on information theory, 13(1), 21-27. DOI: 10.1109/TIT.1967.1053964

Cozzolino, D. and Murray, I., 2004. Identification of animal meat muscles by visible and near infrared reflectance spectroscopy. LWT-Food Science and Technology, 37(4), 447-452. https://doi.org/10.1016/j.lwt.2003.10.013

Cullen, P.J., O'Donnell, C.P. and Fagan, C.C., 2014. Benefits and challenges of adopting PAT for the food industry. In Process analytical technology for the food industry (1-5). Springer, New York, NY. https://doi.org/10.1007/978-1-4939-0311-5_1

Dalgaard, P. 1995. Modelling of microbial activity and prediction of shelf life for packed fresh fish. International Journal of Food Microbiology, 26(3), 305-317. https://doi.org/10.1016/0168-1605(94)00136-T.

Daugaard, S.B., Adler-Nissen, J. and Carstensen, J.M., 2010. New vision technology for multidimensional quality monitoring of continuous frying of meat. Food Control, 21(5), 626-632. https://doi.org/10.1016/j.foodcont.2009.09.007

Dawson, P.L., Chaves, B.D., Northcutt, J.K. and Han, I.Y., 2013. Quality and shelf life of fresh chicken breasts subjected to crust freezing with and without skin. Journal of Food Quality, 36(5), 361-368. https://doi.org/10.1111/jfq.12046

De Marchi, M., Riovanto, R., Penasa, M. and Cassandro, M., 2012. At-line prediction of fatty acid profile in chicken breast using near infrared reflectance spectroscopy. Meat science, 90(3), 653-657. https://doi.org/10.1016/j.meatsci.2011.10.009

Demirok, E., Veluz, G., Stuyvenberg, W.V., Castaneda, M.P., Byrd, A. and Alvarado, C.Z., 2013. Quality and safety of broiler meat in various chilling systems. Poultry Science, 92(4), 1117-1126. https://doi.org/10.3382/ps.2012-02493

Deniz, E., Güneş Altuntaş, E., Ayhan, B., İğci, N., Özel Demiralp, D. and Candoğan, K., 2018. Differentiation of beef mixtures adulterated with chicken or turkey meat using FTIR spectroscopy. Journal of Food Processing and Preservation, 42(10), e13767. https://doi.org/10.1111/jfpp.13767

Dey, S., Saha, S., Singh, A.K. and McDonald-Maier, K., 2021. FoodSQRBlock: Digitizing food production and the supply chain with blockchain and QR code in the cloud. Sustainability, 13(6), 3486. https://doi.org/10.3390/su13063486

Di Rosa, A.R., Leone, F., Cheli, F. and Chiofalo, V., 2017. Fusion of electronic nose, electronic tongue and computer vision for animal source food authentication and quality assessment–A review. Journal of Food Engineering, 210, 62-75. https://doi.org/10.1016/j.jfoodeng.2017.04.024

Dissing, B.S., Papadopoulou, O.S., Tassou, C., Ersbøll, B.K., Carstensen, J.M., Panagou, E.Z. and Nychas, G.J. 2013. Using multispectral imaging for spoilage detection of pork meat. Food Bioprocess Technology. 6, 2268–2279. https://doi.org/10.1007/s11947-012-0886-6.

Dixit, Y., Casado-Gavalda, M.P., Cama-Moncunill, R., Cama-Moncunill, X., Markiewicz-Keszycka, M., Cullen, P.J., & Sullivan, C. 2017. Developments and challenges in online NIR spectroscopy for meat processing. Comprehensive Reviews in Food Science and Food Safety, 16, 1172–1187. https://doi.org/10.1111/1541-4337.12295.

Dogan, O.B., Clarke, J., Mattos, F. and Wang, B., 2019. A quantitative microbial risk assessment model of Campylobacter in broiler chickens: Evaluating processing interventions. Food Control, 100, 97-110. https://doi.org/10.1016/j.foodcont.2019.01.003
Dominguez, S.A. and Schaffner, D.W., 2007. Development and validation of a mathematical model to describe the growth of Pseudomonas spp. in raw poultry stored under aerobic conditions. International Journal of Food Microbiology, 120(3), 287-295. https://doi.org/10.1016/j.ijfoodmicro.2007.09.005

Doulgeraki, A.I., Paramithiotis, S. and Nychas, G.J.E., 2011. Characterization of the Enterobacteriaceae community that developed during storage of minced beef under aerobic or modified atmosphere packaging conditions. International journal of food microbiology, 145(1), 77-83. https://doi.org/10.1016/j.ijfoodmicro.2010.11.030

Doulgeraki, A.I., Ercolini, D., Villani, F. and Nychas, G.J.E., 2012. Spoilage microbiota associated to the storage of raw meat in different conditions. International Journal of Food Microbiology, 157(2), 130-141. https://doi.org/10.1016/j.ijfoodmicro.2012.05.020

Dourou, D., Grounta, A., Argyri, A.A., Froutis, G., Tsakanikas, P., Nychas, G.J.E., Doulgeraki, A.I., Chorianopoulos, N.G. and Tassou, C.C., 2021. Rapid microbial quality assessment of chicken liver inoculated or not with Salmonella Using FTIR spectroscopy

and machine learning. Frontiers in Microbiology, 3573. https://doi.org/10.3389/fmicb.2020.623788

Duda, R.O.; Hart, P.E.; Stork, D.G. Pattern Classification, 2nd ed.; Wiley-Interscience: New York, NY, USA, 2000; ISBN: 978-0-468 471-05669-0.

Duffy, L. and Dykes, G.A., 2006. Growth temperature of four Campylobacter jejuni strains influences their subsequent survival in food and water. Letters in Applied Microbiology, 43(6), 596-601. https://doi.org/10.1111/j.1472-765X.2006.02019.x

Duque, B., Haddad, N., Rossero, A., Membré, J.M. and Guillou, S., 2019. Influence of cell history on the subsequent inactivation of Campylobacter jejuni during cold storage under modified atmosphere. Food Microbiology, 84, 103263. https://doi.org/10.1016/j.fm.2019.103263

EFSA Panel on Biological Hazards (BIOHAZ), 2011. Scientific Opinion on Campylobacter in broiler meat production: control options and performance objectives and/or targets at different stages of the food chain. EFSA Journal, 9(4):2105. [141 pp.]. doi:10.2903/j.efsa.2011.2105. Available online: www.efsa.europa.eu/efsajournal
EFSA Panel on Biological Hazards (BIOHAZ), 2016. Growth of spoilage bacteria during storage and transport of meat. EFSA Journal, 14(6), e04523. https://doi.org/10.2903/j.efsa.2016.4523

EFSA/ECDC, 2019. Scientific report on the European Union One Health 2018 Zoonoses Report. EFSA J., 17, 5926. DOI: 10.2903/j.efsa.2019.5926

EFSA/ECDC, 2021. he European Union One Health 2020 Zoonoses Report. EFSAJournal 2021;19(12):6971, 324 pp. DOI: https://doi.org/10.2903/j.efsa.2021.6971

Ellis, D. I., Broadhurst, D., Kell, D. B., Rowland, J. J. and Goodacre, R. 2002. Rapid and quantitative detection of the microbial spoilage of meat by Fourier transform infrared spectroscopy and machine learning. Applied and Environmental Microbiology, 68(6), 2822-2828. DOI: 10.1128/AEM.68.6.2822-2828.2002.

Engel, J., Gerretzen, J., Szymańska, E., Jansen, J.J., Downey, G., Blanchet, L. and Buydens, L.M., 2013. Breaking with trends in pre-processing?. TrAC Trends in Analytical Chemistry, 50, 96-106. https://doi.org/10.1016/j.trac.2013.04.015

Estelles-Lopez, L., Ropodi, A., Pavlidis, D., Fotopoulou, J., Gkousari, C., Peyrodie, A., Panagou, E.Z., Nychas, G.-J.E. and Mohareb, F., 2017. An automated ranking platform for machine learning regression models for meat spoilage prediction using multispectral imaging and metabolic profiling. Food Research International. 99, 206–215. https://doi.org/10.1016/j.foodres.2017.05.013.

EU, 2017. Commission Regulation (EU) 2017/1495 of 23 August 2017 amending Regulation (EC) No 2073/2005 as regards Campylobacter in broiler carcasses. Available online: https://eur-lex.europa.eu/legal-content/EN/TXT/?uri=CELEX%3A32017R1495
Falkovskaya, A. and Gowen, A., 2020. Literature review: spectral imaging applied to poultry products. Poultry Science, 99(7), 3709-3722. https://doi.org/10.1016/j.psj.2020.04.013

FAO, 2019. The State of Food and Agriculture 2019. Moving Forward on Food Loss and

Waste Reduction. Licence: CC BY-NC-SA 3.0 IGO, Rome

FAO, 2022. Technical Platform on the Measurement and Reduction of Food Loss and Waste. Available online: http://www.fao.org/platform-food-loss-waste/en/ (accessed on 12 February 2022).

FAO, 2022. Gateway to Poultry Production and Products. Available online: http://www.fao.org/poultry-production-products/en/ (accessed on 12 February 2022).

Feng, Y. Z. and Sun, D. W. 2013a. Determination of total viable count (TVC) in chicken breast fillets by near-infrared hyperspectral imaging and spectroscopic transforms. Talanta, 105, 244-249. https://doi.org/10.1016/j.talanta.2012.11.042

Feng, Y. Z. and Sun, D. W. 2013b. Near-infrared hyperspectral imaging in tandem with partial least squares regression and genetic algorithm for non-destructive determination and visualization of Pseudomonas loads in chicken fillets. Talanta, 109, 74-83. https://doi.org/10.1016/j.talanta.2013.01.057

Feng, Y.Z., ElMasry, G., Sun, D.W., Scannell, A.G., Walsh, D. and Morcy, N., 2013. Near-infrared hyperspectral imaging and partial least squares regression for rapid and reagentless determination of Enterobacteriaceae on chicken fillets. Food Chemistry, 138(2-3), 1829-1836. https://doi.org/10.1016/j.foodchem.2012.11.040

Feng, C.H., Makino, Y., Oshita, S. and Martín, J.F.G., 2018. Hyperspectral imaging and multispectral imaging as the novel techniques for detecting defects in raw and processed meat products: Current state-of-the-art research advances. Food Control, 84, 165-176. https://doi.org/10.1016/j.foodcont.2017.07.013

Fengou, L.C., Spyrelli, E., Lianou, A., Tsakanikas, P., Panagou, E.Z. and Nychas, G.-J.E., 2019. Estimation of minced pork microbiological spoilage through fourier transform infrared and visible spectroscopy and multispectral vision technology. Foods 8 (7), 238. https://doi.org/10.3390/foods8070238.

Fengou, L.C., Mporas, I., Spyrelli, E., Lianou, A. and Nychas, G.J., 2020. Estimation of the microbiological quality of meat using rapid and non-invasive spectroscopic sensors. IEEE Access, 8, pp.106614-106628. DOI: 10.1109/ACCESS.2020.3000690

Fengou, L.C., Tsakanikas, P. and Nychas, G.J.E., 2021a. Rapid detection of minced pork and chicken adulteration in fresh, stored and cooked ground meat. Food Control, 125, p.108002. https://doi.org/10.1016/j.foodcont.2021.108002

Fengou, L.C., Lianou, A., Tsakanikas, P., Mohareb, F. and Nychas, G.J.E., 2021b. Detection of meat adulteration using spectroscopy-based sensors. Foods, 10(4), 861. https://doi.org/10.3390/foods10040861

Fletcher, R.D., Albers, A.C., Chen, A.K. and Albertson Jr, J.N., 1983. Ascorbic acid inhibition of Campylobacter jejuni growth. Applied and Environmental Microbiology, 45(3), 792-795. https://doi.org/10.1128/aem.45.3.792-795.1983

Fraqueza, M.J. and Barreto, A.S., 2011. Gas mixtures approach to improve turkey meat shelf life under modified atmosphere packaging: The effect of carbon monoxide. Poultry science, 90(9), 2076-2084. https://doi.org/10.3382/ps.2011-01366

Friedman, J.H., Hastie, T., Tibshirani, R., and Friedman, J.H., 2009. The elements of statistical learning: data mining, inference, and prediction (Vol. 2, pp. 1-758). New York: springer.

Galarz, L.A., Fonseca, G.G. and Prentice, C., 2016. Predicting bacterial growth in raw, salted, and cooked chicken breast fillets during storage. Food Science and Technology International, 22(6), 461-474. https://doi.org/10.1177/1082013215618519

Geeraerd, A.H., Valdramidis, V.P. and Van Impe, J.F., 2005. GInaFiT, a freeware tool to assess non-log-linear microbial survivor curves. International Journal of Food Microbiology, 102(1), 95-105. https://doi.org/10.1016/j.ijfoodmicro.2004.11.038
Geladi, P., 1986. Kowalski BR. Partial least-squares regression–a tutorial. Analytica Chimica. Acta 185, 1–17. https://doi.org/10.1016/0003-2670(86)80028-9.

Georgnaras, I., Kunene, N.F., von Holy, A. and Hastings, J.W., 1999. Amplified fragment length polymorphism fingerprinting of Pseudomonas strains from a poultry processing plant. Applied and Environmental Microbiology, 65(9), 3828-3833. https://doi.org/10.1128/AEM.65.9.3828-3833.1999

Gharst, G., Oyarzabal, O.A. and Hussain, S.K., 2013. Review of current methodologies to isolate and identify Campylobacter spp. from foods. Journal of Microbiological Methods, 95(1), 84-92. https://doi.org/10.1016/j.mimet.2013.07.014

Ghasemi-Varnamkhasti, M., Mohtasebi, S.S., Siadat, M. and Balasubramanian, S., 2009. Meat quality assessment by electronic nose (machine olfaction technology). Sensors, 9(8), 6058-6083. https://doi.org/10.3390/s90806058

Ghasemi-Varnamkhasti, M., Mohtasebi, S.S. and Siadat, M., 2010. Biomimetic-based odor and taste sensing systems to food quality and safety characterization: An overview on basic principles and recent achievements. Journal of Food Engineering, 100(3), 377-387. https://doi.org/10.1016/j.jfoodeng.2010.04.032

Gomes, J.F.S. and Leta, F.R., 2012. Applications of computer vision techniques in the agriculture and food industry: a review. European Food Research and Technology, 235(6), 989-1000. https://doi.org/10.1007/s00217-012-1844-2

González, M., Skandamis, P.N. and Hänninen, M.L., 2009. A modified Weibull model for describing the survival of Campylobacter jejuni in minced chicken meat. International Journal of Food Microbiology, 136(1), 52-58. doi:10.1016/j.ijfoodmicro.2009.09.022

Gospavic, R., Kreyenschmidt, J., Bruckner, S., Popov, V. and Haque, N. 2008. Mathematical modelling for predicting the growth of Pseudomonas spp. in poultry under variable temperature conditions. International Journal of Food Microbiology, 127(3), 290-297. https://doi.org/10.1016/j.ijfoodmicro.2008.07.022

Gram, L., Ravn, L., Rasch, M., Bruhn, J.B., Christensen, A.B. and Givskov, M., 2002. Food spoilage—interactions between food spoilage bacteria. International Journal of Food Microbiology, 78(1-2), 79-97. https://doi.org/10.1016/S0168-1605(02)00233-7

Grassi, S. and Alamprese, C., 2018. Advances in NIR spectroscopy applied to process analytical technology in food industries. Current Opinion in Food Science, 22, 17-21. https://doi.org/10.1016/j.cofs.2017.12.008

Grewal, M.K., Jaiswal, P. and Jha, S.N., 2015. Detection of poultry meat specific bacteria using FTIR spectroscopy and chemometrics. Journal of Food Science and Technology, 52(6), 3859-3869. https://doi.org/10.1007/s13197-014-1457-9

Gromski, P.S., Muhamadali, H., Ellis, D.I., Xu, Y., Correa, E., Turner, M.L. and Goodacre, R., 2015. A tutorial review: Metabolomics and partial least squares-discriminant analysis–a marriage of convenience or a shotgun wedding. Analytica Chimica Acta, 879, 10-23. https://doi.org/10.1016/j.aca.2015.02.012

Grouven, U., Bergel, F. and Schultz, A., 1996. Implementation of linear and quadratic discriminant analysis incorporating costs of misclassification. Computer methods and programs in biomedicine, 49(1), 55-60. https://doi.org/10.1016/0169-2607(95)01705-4

Grunert, T., Stephan, R., Ehling-Schulz, M. and Johler, S., 2016. Fourier transform infrared spectroscopy enables rapid differentiation of fresh and frozen/thawed chicken. Food Control, 60, 361-364. https://doi.org/10.1016/j.foodcont.2015.08.016

Hazeleger, W.C., Wouters, J.A., Rombouts, F.M. and Abee, T., 1998. Physiological activity of Campylobacter jejuni far below the minimal growth temperature. Applied and Environmental Microbiology, 64(10), 3917-3922. https://doi.org/10.1128/AEM.64.10.3917-3922.1998

Hadjilouka, A., Andritsos, N.D., Paramithiotis, S., Mataragas, M. and Drosinos, E.H., 2014. Listeria monocytogenes serotype prevalence and biodiversity in diverse food products. Journal of Food Protection, 77(12), 2115-2120. https://doi.org/10.4315/0362-028X.JFP-14-072

Hesterberg, T., Choi, N.H., Meier, L. and Fraley, C., 2008. Least angle and ℓ1 penalized

regression: a review. Statistics Survey. 2, 61–93. https://doi.org/10.1214/08-ss035.

Ho, T. K. 1998. The random subspace method for constructing decision forests. IEEE transactions on pattern analysis and machine intelligence, 20(8), 832-844. DOI: 10.1109/34.709601.

Hoerl, A.E. and Kennard, R.W., 1970. Ridge regression: biased estimation for nonorthogonal problems. Technometrics 12 (1), 55–67. https://doi.org/10.1080/00401706.1970.10488634.

Höll, L., Behr, J. and Vogel, R. F. 2016. Identification and growth dynamics of meat spoilage microorganisms in modified atmosphere packaged poultry meat by MALDI-TOF MS. Food Microbiology, 60, 84-91. https://doi.org/10.1016/j.fm.2016.07.003.

Hu, F., Liu, X., Dai, J. and Yu, H. 2014. A novel algorithm for imbalance data classification based on neighborhood hypergraph. The Scientific World Journal, 2014. http://dx.doi.org/10.1155/2014/876875.

Huang, L., Hwang, C.A. and Phillips, J., 2011. Evaluating the Effect of Temperature on Microbial Growth Rate—The Ratkowsky and a Bělehrádek-Type Models. Journal of Food Science, 76(8), M547-M557. DOI: 10.1111/j.1750-3841.2011.02345.x

Huang, J., Jiang, F., Hu, Y., Zhou, X., Gu, S. and Jiao, X.A., 2012. An inactivation kinetics model for Campylobacter jejuni on chicken meat under low-temperature storage. Foodborne Pathogens and Disease, 9(6), 513-516. DOI: 10.1089/fpd.2011.1070

Huang, L., 2013. Optimization of a new mathematical model for bacterial growth. Food Control, 32(1), 283-288. http://dx.doi.org/10.1016/j.foodcont.2012.11.019

Huang, L., Zhao, J., Chen, Q. and Zhang, Y., 2014. Nondestructive measurement of total volatile basic nitrogen (TVB-N) in pork meat by integrating near infrared spectroscopy, computer vision and electronic nose techniques. Food Chemistry, 145, 228-236. https://doi.org/10.1016/j.foodchem.2013.06.073

Huang, L., 2016. Mathematical modeling and validation of growth of Salmonella Enteritidis and background microorganisms in potato salad–One-step kinetic analysis and model development. Food Control, 68, 69-76. http://dx.doi.org/10.1016/j.foodcont.2016.03.039

Huang, J., Zang, X., Zhai, W., Guan, C., Lei, T. and Jiao, X., 2018. Campylobacter spp. in chicken-slaughtering operations: A risk assessment of human campylobacteriosis in East China. Food Control, 86, 249-256. https://doi.org/10.1016/j.foodcont.2017.11.026

Huffman, B., Mazrouei, R., Bevelheimer, J. and Shavezipur, M., 2017, August. Three-Dimensional Biomimetic Biosensors for Food Safety Applications. In International Design Engineering Technical Conferences and Computers and Information in Engineering Conference (Vol. 58165, p. V004T09A002). American Society of Mechanical Engineers.

https://doi.org/10.1115/DETC2017-67446

Hutchison, M.L., Walters, L.D., Avery, S.M., Reid, C.A., Wilson, D., Howell, M., Johnston, A.M. and Buncic, S., 2005. A comparison of wet-dry swabbing and excision sampling methods for microbiological testing of bovine, porcine, and ovine carcasses at red meat slaughterhouses. Journal of Food Protection, 68(10), 2155-2162. https://doi.org/10.4315/0362-028X-68.10.2155

Jaafreh, S., Valler, O., Kreyenschmidt, J., Günther, K. and Kaul, P., 2019. In vitro discrimination and classification of Microbial Flora of Poultry using two dispersive Raman spectrometers (microscope and Portable Fiber-Optic systems) in tandem with chemometric analysis. Talanta, 202, 411-425. https://doi.org/10.1016/j.talanta.2019.04.082

Jain, A.K., Mao, J. and Mohiuddin, K.M., 1996. Artificial neural networks: a tutorial. Computer 29 (3), 31–44. https://doi.org/10.1109/2.485891.

Jiménez-Carvelo, A. M., González-Casado, A., Bagur-González, M. G. and Cuadros-Rodríguez, L. 2019. Alternative data mining/machine learning methods for the analytical evaluation of food quality and authenticity–A review. Food Research International, 122, 25-39. https://doi.org/10.1016/j.foodres.2019.03.063

Jolliffe, I.T., 1982. A note on the use of principal components in regression. J. Roy. Stat.

Soc.: Series C (Applied Statistics) 31 (3), 300–303.

i Furnols, M.F. and Gispert, M., 2009. Comparison of different devices for predicting the lean meat percentage of pig carcasses. Meat Science, 83(3), 443-446. https://doi.org/10.1016/j.meatsci.2009.06.018

Indahl, U. G., Martens, H. and Næs, T. 2007. From dummy regression to prior probabilities in PLS-DA. Journal of Chemometrics: A Journal of the Chemometrics Society, 21(12), 529-536. https://doi.org/10.1002/cem.1061.

Iulietto, M.F., Sechi, P., Borgogni, E. and Cenci-Goga, B.T., 2015. Meat spoilage: a critical review of a neglected alteration due to ropy slime producing bacteria. Italian Journal of Animal Science, 14(3), 4011. https://doi.org/10.4081/ijas.2015.4011

Kamble, S.S., Gunasekaran, A., Parekh, H. and Joshi, S., 2019. Modeling the internet of things adoption barriers in food retail supply chains. Journal of Retailing and Consumer Services, 48, 154-168. https://doi.org/10.1016/j.jretconser.2019.02.020

Kamruzzaman, M., Sun, D.W., ElMasry, G. and Allen, P., 2013. Fast detection and visualization of minced lamb meat adulteration using NIR hyperspectral imaging and multivariate image analysis. Talanta, 103, 130-136. https://doi.org/10.1016/j.talanta.2012.10.020

Kamruzzaman, M., Makino, Y. and Oshita, S., 2015. Non-invasive analytical technology for the detection of contamination, adulteration, and authenticity of meat, poultry, and fish: A review. Analytica Chimica Acta, 853, 19-29. https://doi.org/10.1016/j.aca.2014.08.043

Kamruzzaman, M., Makino, Y. and Oshita, S. 2016. Rapid and non-destructive detection of chicken adulteration in minced beef using visible near-infrared hyperspectral imaging and machine learning. Journal of Food Engineering, 170, 8-15. https://doi.org/10.1016/j.jfoodeng.2015.08.023

Keshavarzi, Z., Barzegari Banadkoki, S., Faizi, M., Zolghadri, Y. and Shirazi, F.H., 2020. Comparison of transmission FTIR and ATR spectra for discrimination between beef and chicken meat and quantification of chicken in beef meat mixture using ATR-FTIR combined with chemometrics. Journal of Food Science and Technology, 57(4), 1430-1438. https://doi.org/10.1007/s13197-019-04178-7

Khulal, U., Zhao, J., Hu, W. and Chen, Q., 2017. Intelligent evaluation of total volatile basic nitrogen (TVB-N) content in chicken meat by an improved multiple level data fusion model. Sensors and Actuators B: Chemical, 238, 337-345. https://doi.org/10.1016/j.snb.2016.07.074

Kim, K.S., Choi, H.H., Moon, C.S. and Mun, C.W., 2011. Comparison of k-nearest neighbor, quadratic discriminant and linear discriminant analysis in classification of

electromyogram signals based on the wrist-motion directions. Current Applied Physics, 11(3), 740-745. https://doi.org/10.1016/j.cap.2010.11.051

Kouma, J.P. and Liu, L., 2011, October. Internet of food. In 2011 International Conference on Internet of Things and 4th International Conference on Cyber, Physical and Social Computing (pp. 713-716). IEEE. DOI: 10.1109/iThings/CPSCom.2011.120

Koutsoumanis, K.P., Taoukis, P.S., Drosinos, E.H. and Nychas, G.J.E., 2000. Applicability of an Arrhenius model for the combined effect of temperature and CO2 packaging on the spoilage microflora of fish. Applied and Environmental Microbiology, 66(8), 3528-3534. https://doi.org/10.1128/AEM.66.8.3528-3534.2000

Koutsoumanis, K., Stamatiou, A., Skandamis, P. and Nychas, G.J., 2006. Development of a microbial model for the combined effect of temperature and pH on spoilage of ground meat, and validation of the model under dynamic temperature conditions. Applied and Environmental Microbiology, 72(1), 124-134. https://doi.org/10.1128/AEM.72.1.124-134.2006

Koutsoumanis, K. P., Stamatiou, A. P., Drosinos, E. H. and Nychas, G. J. 2008. Control of spoilage microorganisms in minced pork by a self-developed modified atmosphere induced by the respiratory activity of meat microflora. Food microbiology, 25(7), 915-921. https://doi.org/10.1111/j.1472-765X.2004.01546.x.

Koutsoumanis, K., 2009. Modeling food spoilage in microbial risk assessment. Journal of food protection, 72(2), 425-427. https://doi.org/10.4315/0362-028X-72.2.425

Koutsoumanis, K., Tsaloumi, S., Aspridou, Z., Tassou, C. and Gougouli, M., 2021. Application of Quantitative Microbiological Risk Assessment (QMRA) to food spoilage: Principles and methodology. Trends in Food Science & Technology, 114, 189-197. https://doi.org/10.1016/j.tifs.2021.05.011

Kumar, Y. and Karne, S.C., 2017. Spectral analysis: A rapid tool for species detection in meat products. Trends in Food Science & Technology, 62, 59-67. http://dx.doi.org/10.1016/j.tifs.2017.02.008

Kumar, J., Akhila, K. and Gaikwad, K.K., 2021. Recent developments in intelligent packaging systems for food processing industry: a review. Journal of Food Processing and Technology, 12, 895.

Kucheryavskiy, S. 2018. Analysis of NIR spectroscopic data using decision trees and their ensembles. Journal of Analysis and Testing, 2(3), 274-289. https://doi.org/10.1007/s41664-018-0078-0

Kutsanedzie, F.Y., Guo, Z. and Chen, Q., 2019. Advances in nondestructive methods for meat quality and safety monitoring. Food Reviews International, 35(6), 536-562. https://doi.org/10.1080/87559129.2019.1584814

Lanzl, M.I., Zwietering, M.H., Hazeleger, W.C., Abee, T. and den Besten, H.M.W., 2020. Variability in lag-duration of Campylobacter spp. during enrichment after cold and

oxidative stress and its impact on growth kinetics and reliable detection. Food Research International, 134, 109253. https://doi.org/10.1016/j.foodres.2020.109253

Lee, A., Smith, S.C. and Coloe, P.J., 1998. Survival and growth of Campylobacter jejuni after artificial inoculation onto chicken skin as a function of temperature and packaging conditions. Journal of Food Protection, 61(12), 1609-1614. https://doi.org/10.4315/0362-028X-61.12.1609

Lee, H.S., Kwon, M., Heo, S., Kim, M.G. and Kim, G.B., 2017. Characterization of the biodiversity of the spoilage microbiota in chicken meat using next generation sequencing and culture dependent approach. Korean Journal for Food Science of Animal Resources, 37(4), 535. doi: 10.5851/kosfa.2017.37.4.535

Li, H., Chen, Q., Zhao, J. and Ouyang, Q., 2014. Non-destructive evaluation of pork freshness using a portable electronic nose (E-nose) based on a colorimetric sensor array. Analytical Methods, 6(16), 6271-6277. DOI: 10.1039/C4AY00014E

Li, T. and Messer, K.D., 2019. To scan or not to scan: the question of consumer behavior and QR codes on food packages. Journal of Agricultural and Resource Economics, 44(1835-2019-1549), 311-327. DOI: 10.22004/ag.econ.287977

Liang, R., Yu, X., Wang, R., Luo, X., Mao, Y., Zhu, L. and Zhang, Y., 2012. Bacterial diversity and spoilage-related microbiota associated with freshly prepared chicken products under aerobic conditions at 4 C. Journal of Food Protection, 75(6), 1057-1062.

https://doi.org/10.4315/0362-028X.JFP-11-439

Lianou, A., Panagou, E.Z. and Nychas, G.J., 2016. Microbiological spoilage of foods and beverages. In The stability and shelf life of food (pp. 3-42). Woodhead Publishing. https://doi.org/10.1016/B978-0-08-100435-7.00001-0

Lianou, A., Moschonas, G., Nychas, G. J. E. and Panagou, E. Z. 2018. Growth of Listeria monocytogenes in pasteurized vanilla cream pudding as affected by storage temperature and the presence of cinnamon extract. Food Research International, 106, 1114-1122. https://doi.org/10.1016/j.foodres.2017.11.027

Lianou, A., Raftopoulou, O., Spyrelli, E. and Nychas, G.J.E., 2021. Growth of Listeria monocytogenes in Partially Cooked Battered Chicken Nuggets as a Function of Storage Temperature. Foods, 10(3), 533. https://doi.org/10.3390/foods10030533

Lin, M., Al Holy, M., Mousavi Hesary, M., Al Qadiri, H., Cavinato, A.G. and Rasco, B.A., 2004. Rapid and quantitative detection of the microbial spoilage in chicken meat by diffuse reflectance spectroscopy (600–1100 nm). Letters in Applied Microbiology. 39 (2), 148–155. https://doi.org/10.1111/j.1472-765X.2004.01546.x.

Lin, C.Y., Lin, L.C. and Hsu, J.C., 2011. Effect of caponization on muscle composition, shear value, ATP related compounds and taste appraisal in Taiwan country chicken cockerels. Asian-Australasian Journal of Animal Sciences, 24(7), 1026-1030. https://doi.org/10.5713/ajas.2011.10068

Lin, H., Yan, Y., Zhao, T., Peng, L., Zou, H., Li, J., Yang, X., Xiong, Y., Wang, M. and Wu, H., 2013. Rapid discrimination of Apiaceae plants by electronic nose coupled with

multivariate statistical analyses. Journal of Pharmaceutical and Biomedical Analysis, 84, 1-4. https://doi.org/10.1016/j.jpba.2013.05.027
Lindblad, M., 2007. Microbiological sampling of swine carcasses: a comparison of data obtained by swabbing with medical gauze and data collected routinely by excision at Swedish abattoirs. International Journal of Food Microbiology, 118(2), 180-185. https://doi.org/10.1016/j.ijfoodmicro.2007.07.009

Liu, D., Sun, D.W. and Zeng, X.A., 2014. Recent advances in wavelength selection techniques for hyperspectral image processing in the food industry. Food and Bioprocess Technology, 7(2), 307-323. https://doi.org/10.1007/s11947-013-1193-6

Liu, Y.J., Xie, J., Zhao, L.J., Qian, Y.F., Zhao, Y. and Liu, X., 2015. Biofilm formation characteristics of Pseudomonas lundensis isolated from meat. Journal of Food Science. 80 (12), M2904–M2910. https://doi.org/10.1111/1750-3841.13142

Loh, W. Y. 2011. Classification and regression trees. Wiley interdisciplinary reviews: data mining and knowledge discovery, 1(1), 14-23 https://doi.org/10.1002/widm.8

Loubes, J.M. and Massart, P., 2004. Discussion of" Least angle regression. Ann. Stat. 32 (2), 460–465. https://doi.org/10.1214/009053604000000067.

Loutfi, A., Coradeschi, S., Mani, G.K., Shankar, P. and Rayappan, J.B.B., 2015. Electronic noses for food quality: A review. Journal of Food Engineering, 144, 103-111. https://doi.org/10.1016/j.jfoodeng.2014.07.019

Luts, J., Ojeda, F., Van de Plas, R., De Moor, B., Van Huffel, S. and Suykens, J.A., 2010. A tutorial on support vector machine-based methods for classification problems in chemometrics. Analytica Chimica Acta, 665(2), 129-145. doi:10.1016/j.aca.2010.03.030

Lytou, A., Panagou, E. Z. and Nychas, G. J. E. 2016. Development of a predictive model for the growth kinetics of aerobic microbial population on pomegranate marinated chicken breast fillets under isothermal and dynamic temperature conditions. Food Microbiology, 55, 25-31. https://doi.org/10.1016/j.ijfoodmicro.2017.12.023

Lytou, A. E., Nychas, G. J. E. and Panagou, E. Z. 2018. Effect of pomegranate-based marinades on the microbiological, chemical and sensory quality of chicken meat: A metabolomics approach. International Journal of Food Microbiology, 267, 42-53. https://doi.org/10.1016/j.ijfoodmicro.2017.12.023

Lytou, A.E., Renieri, C.T., Doulgeraki, A.I., Nychas, G.J.E. and Panagou, E.Z., 2020. Assessment of the microbiological quality and safety of marinated chicken products from Greek retail outlets. International Journal of Food Microbiology, 320, 108506. https://doi.org/10.1016/j.ijfoodmicro.2019.108506

Lytou, A.E., Schoina, E., Liu, Y., Michalek, K., Stanley, M.S., Panagou, E.Z. and Nychas, G.J.E., 2021. Quality and safety assessment of edible seaweeds Alaria esculenta and Saccharina latissima cultivated in Scotland. Foods, 10(9), 2210. https://doi.org/10.3390/foods10092210

Macé, S., Joffraud, J.J., Cardinal, M., Malcheva, M., Cornet, J., Lalanne, V., Chevalier, F., Sérot, T., Pilet, M.F. and Dousset, X., 2013. Evaluation of the spoilage potential of bacteria

isolated from spoiled raw salmon (Salmo salar) fillets stored under modified atmosphere packaging. International journal of food microbiology, 160(3), 227-238. https://doi.org/10.1016/j.ijfoodmicro.2012.10.013

Mafart, P., Couvert, O., Gaillard, S. and Leguérinel, I., 2002. On calculating sterility in thermal preservation methods: application of the Weibull frequency distribution model. International Journal of Food Microbiology, 72 (1-2), 107-113. https://doi.org/10.1016/S0168-1605(01)00624-9

Manthou, E., Lago, S.L., Dagres, E., Lianou, A., Tsakanikas, P., Panagou, E.Z., Anastasiadi, M., Mohareb, F. and Nychas, G.J.E., 2020. Application of spectroscopic and multispectral imaging technologies on the assessment of ready-to-eat pineapple quality: A performance evaluation study of machine learning models generated from two commercial data analytics tools. Computers and Electronics in Agriculture, 175, 105529. https://doi.org/10.1016/j.compag.2020.105529

Marcato, S.M., Sakomura, N.K., Kawauchi, I.M., Barbosa, N.A.A., Freitas, E.C., 2006. Growth of body parts of two broiler chicken strain. In: XII European Poultry Conference, 10–14. https://doi.org/10.1590/S1516-635X2008000200007.

Márquez, C., López, M.I., Ruisánchez, I. and Callao, M.P., 2016. FT-Raman and NIR spectroscopy data fusion strategy for multivariate qualitative analysis of food fraud. Talanta, 161, 80-86. https://doi.org/10.1016/j.talanta.2016.08.003

Marini, F., 2009. Artificial neural networks in foodstuff analyses: Trends and perspectives A review. Analytica Chimica Acta, 635(2), 121-131. doi:10.1016/j.aca.2009.01.009

McCarthy, Z., Smith, B., Fazil, A., Ryan, S.D., Wu, J. and Munther, D., 2019. An individual-carcass model for quantifying bacterial cross-contamination in an industrial three-stage poultry scalding tank. Journal of Food Engineering, 262, 142-153. https://doi.org/10.1016/j.jfoodeng.2019.05.013

Mellefont, L.A., McMeekin, T.A. and Ross, T., 2003. Performance evaluation of a model describing the effects of temperature, water activity, pH and lactic acid concentration on the growth of Escherichia coli. International journal of food microbiology, 82(1), 45-58. https://doi.org/10.1016/S0168-1605(02)00253-2

Membré, J.M., Laroche, M. and Magras, C., 2013. Meta-analysis of Campylobacter spp. survival data within a temperature range of 0 to 42° C. Journal of Food Protection, 76(10), 1726-1732. doi:10.4315/0362-028X.JFP-13-042

Meredith, H., Walsh, D., McDowell, D.A. and Bolton, D.J., 2013. An investigation of the immediate and storage effects of chemical treatments on Campylobacter and sensory characteristics of poultry meat. International Journal of Food Microbiology, 166(2), 309-315. http://dx.doi.org/10.1016/j.ijfoodmicro.2013.07.005

Mohareb, F., Papadopoulou, O., Panagou, E., Nychas, G. J., and Bessant, C. 2016. Ensemble-based support vector machine classifiers as an efficient tool for quality assessment of beef fillets from electronic nose data. Analytical Methods, 8(18), 3711-3721. DOI: 10.1039/c6ay00147e

Morales, P.A., Aguirre, J.S., Troncoso, M.R. and Figueroa, G.O., 2016. Phenotypic and genotypic characterization of Pseudomonas spp. present in spoiled poultry fillets sold in retail settings. LWT, 73, 609-614. https://doi.org/10.1016/j.lwt.2016.06.064

Nakariyakul, S. and Casasent, D.P., 2009. Fast feature selection algorithm for poultry skin tumor detection in hyperspectral data. Journal of Food Engineering, 94(3-4), 358-365. https://doi.org/10.1016/j.jfoodeng.2009.04.001

Nychas, G.J. and Tassou, C.C., 1997. Spoilage processes and proteolysis in chicken as detected by HPLC. Journal of the Science of Food and Agriculture, 74(2), 199-208. https://doi.org/10.1002/(SICI)1097-0010(199706)74:2<199::AID-JSFA790>3.0.CO;2-4

Nychas, G.-J.E., Skandamis, P.N., Tassou, C.C., Koutsoumanis, K.P., 2008. Meat spoilage during distribution. Meat Sci. 78 (1–2), 77–89. https://doi.org/10.1016/j.meatsci.2007.06.020.

Nychas, G.J.E.; Panagou, E.Z. and Mohareb, F., 2016. Novel approaches for food safety management and communication. Current Opinion in Food Science, 12, 13–20. https://doi.org/10.1016/j.cofs.2016.06.005

Osuna, E., Freund, R. and Girosi, F. (1997, September). An improved training algorithm for support vector machines. In Neural networks for signal processing VII. Proceedings of the 1997 IEEE signal processing society workshop (pp. 276-285). IEEE. DOI: 10.1109/NNSP.1997.622408

Panagou, E.Z., Papadopoulou, O., Carstensen, J.M. and Nychas, G.J.E. 2014. Potential of multispectral imaging technology for rapid and non-destructive determination of the microbiological quality of beef filets during aerobic storage. International Journal of Food Microbiology, *174*, 1–11. https://doi.org/10.1016/j.ijfoodmicro.2013.12.026.

Panov, P. and Džeroski, S., 2007, September. Combining bagging and random subspaces to create better ensembles. In International Symposium on Intelligent Data Analysis (pp. 118-129). Springer, Berlin, Heidelberg. https://doi.org/10.1007/978-3-540-74825-0_11

Papadopoulou, O., Panagou, E. Z., Tassou, C. C. and Nychas, G. J. 2011. Contribution of Fourier transform infrared (FTIR) spectroscopy data on the quantitative determination of minced pork meat spoilage. Food Research International, *44*(10), 3264-3271. https://doi.org/10.1016/j.foodres.2011.09.012

Papadopoulou, O.S., Panagou, E.Z., Mohareb, F.R. and Nychas, G.J.E., 2013. Sensory and microbiological quality assessment of beef fillets using a portable electronic nose in tandem with support vector machine analysis. Food Research International, 50(1), 241-249. https://doi.org/10.1016/j.foodres.2012.10.020

Park, B., Lawrence, K.C., Windham, W.R., Chen, Y.R. and Chao, K., 2002. Discriminant analysis of dual-wavelength spectral images for classifying poultry carcasses. Computers and Electronics in Agriculture, 33(3), 219-231. https://doi.org/10.1016/S0168-1699(02)00010-8

Park, B., Lawrence, K.C., Windham, W.R. and Smith, D.P., 2006. Performance of hyperspectral imaging system for poultry surface fecal contaminant detection. Journal of Food Engineering, 75(3), 340-348. https://doi.org/10.1016/j.jfoodeng.2005.03.060

Patsias, A., Badeka, A.V., Savvaidis, I.N. and Kontominas, M.G., 2008. Combined effect of freeze chilling and MAP on quality parameters of raw chicken fillets. Food Microbiology, 25(4), 575-581. https://doi.org/10.1016/j.fm.2008.02.008

Pintelas, P. and Livieris, I. E., 2020. Special issue on ensemble learning and applications.

Algorithms 2020, 13(6), 140; https://doi.org/10.3390/a13060140

Polikar, R., 2006. Ensemble based systems in decision making. IEEE Circuits and systems magazine, 6(3), 21-45. DOI: 10.1109/MCAS.2006.1688199

Porep, J. U., Kammerer, D. R. and Carle, R. 2015. On-line application of near infrared (NIR) spectroscopy in food production. Trends in Food Science & Technology, 46(2), 211-230. https://doi.org/10.1016/j.tifs.2015.10.002

Prieto, N., Roehe, R., Lavín, P., Batten, G. and Andrés, S. 2009. Application of near infrared reflectance spectroscopy to predict meat and meat products quality: A review. Meat science, 83(2), 175-186. https://doi.org/10.1016/j.meatsci.2009.04.016.

Pu, H., Kamruzzaman, M. and Sun, D.W., 2015. Selection of feature wavelengths for developing multispectral imaging systems for quality, safety and authenticity of muscle foods-a review. Trends in Food Science Technology, 45, 86–104. https://doi.org/10.1016/j.tifs.2015.05.006.

Qin, J., Chao, K., Kim, M.S., Lu, R. and Burks, T.F., 2013. Hyperspectral and multispectral imaging for evaluating food safety and quality. Journal of Food Engineering, 118(2), 157-171. https://doi.org/10.1016/j.jfoodeng.2013.04.001

Raab, V., Bruckner, S., Beierle, E., Kampmann, Y., Petersen, B. and Kreyenschmidt, J. 2008. Generic model for the prediction of remaining shelf life in support of cold chain management in pork and poultry supply chains. Journal on Chain and Network Science, *8*(1), 59-73. https://doi.org/10.3920/JCNS2008.x089

Rahman, U., Sahar, A., Pasha, I., Rahman, S. and Ishaq, A., 2018. Assessing the capability of Fourier transform infrared spectroscopy in tandem with chemometric analysis for predicting poultry meat spoilage. PeerJ. 6, e5376. DOI: 10.7717/peerj.5376

Rajamäki, T., Alakomi, H.L., Ritvanen, T., Skyttä, E., Smolander, M. and Ahvenainen, R., 2006. Application of an electronic nose for quality assessment of modified atmosphere packaged poultry meat. Food Control, 17(1), 5-13. https://doi.org/10.1016/j.foodcont.2004.08.002

Ratkowsky, D.A., Lowry, R.K., McMeekin, T.A., Stokes, A.N. and Chandler, R., 1983. Model for bacterial culture growth rate throughout the entire biokinetic temperature range. Journal of Bacteriology, 154(3), 1222-1226. https://doi.org/10.1128/jb.154.3.1222-1226.1983

Remenant, B., Jaffrès, E., Dousset, X., Pilet, M.F. and Zagorec, M., 2015. Bacterial spoilers of food: behavior, fitness and functional properties. Food Microbiology, 45, 45-53. http://dx.doi.org/10.1016/j.fm.2014.03.009

Reperant, E., Laisney, M.J., Nagard, B., Quesne, S., Rouxel, S., Le Gall, F., Chemaly, M. and Denis, M., 2016. Influence of enrichment and isolation media on the detection of Campylobacter spp. in naturally contaminated chicken samples. Journal of Microbiological Methods, 128, 42-47. http://dx.doi.org/10.1016/j.mimet.2016.06.028

Restaino, E., Fassio, A. and Cozzolino, D., 2011. Discrimination of meat patés according to the animal species by means of near infrared spectroscopy and chemometrics Discriminación de muestras de paté de carne según tipo de especie mediante el uso de la espectroscopia en el infrarrojo cercano y la quimiometria. CyTA-Journal of Food, 9(3), 210-213. https://doi.org/10.1080/19476337.2010.512396

Rinnan, Å., Van Den Berg, F. and Engelsen, S.B., 2009. Review of the most common pre-processing techniques for near-infrared spectra. TrAC Trends in Analytical Chemistry, 28(10), 1201-1222. https://doi.org/10.1016/j.trac.2009.07.007

Ritz, M., Nauta, M.J., Teunis, P.F.M., Van Leusden, F., Federighi, M. and Havelaar, A.H., 2007. Modelling of Campylobacter survival in frozen chicken meat. Journal of Applied Microbiology, 103(3), 594-600. doi:10.1111/j.1365-2672.2007.03284.x

Rokach, L. 2010. Ensemble-based classifiers. Artificial intelligence review, 33(1), 1-39.

https://doi.org/10.1007/s10462-009-9124-7

Ropodi, A.I., Pavlidis, D.E., Mohareb, F., Panagou, E.Z. and Nychas, G.J., 2015. Multispectral image analysis approach to detect adulteration of beef and pork in raw meats. Food Research International, 67, 12-18. http://dx.doi.org/10.1016/j.foodres.2014.10.032

Ropodi, A.I., Panagou, E.Z., Nychas, G.-J.E. 2016. Data mining derived from Food analyses using non-invasive/non-destructive analytical techniques; Determination of Food authenticity, quality & safety in tandem with Computer Science Disciplines. Trends in Food Science & Technology. 50: 11-15. https://doi.org/10.1016/j.tifs.2016.01.011

Ropodi, A. I., Panagou, E. Z. and Nychas, G. J. E. 2018. Rapid detection of frozen-then-thawed minced beef using multispectral imaging and Fourier transform infrared spectroscopy. Meat science, 135, 142-147. https://doi.org/10.1016/j.meatsci.2017.09.016

Ross, T., 1996. Indices for performance evaluation of predictive models in food microbiology. Journal of Applied Bacteriology, 81(5), 501-508. https://doi.org/10.1111/j.1365-2672.1996.tb03539.x

Rouger, A., Tresse, O. and Zagorec, M., 2017. Bacterial contaminants of poultry meat: sources, species, and dynamics. Microorganisms 5 (3), 50. https://doi.org/10.3390/microorganisms5030050.

Säde, E., Murros, A. and Björkroth, J., 2013. Predominant enterobacteria on modified-atmosphere packaged meat and poultry. Food microbiology, 34(2), 252-258. https://doi.org/10.1016/j.fm.2012.10.007

Sahar, A. and Dufour, É., 2014. Use of Fourier transform-infrared spectroscopy to predict spoilage bacteria on aerobically stored chicken breast fillets. LWT-Food Science and Technology, 56(2), 315-320. https://doi.org/10.1016/j.lwt.2013.12.009

Sakomura, N.K., Silva, E.P., Dorigam, J.C., Gous, R.M., St-Pierre, N., 2015. Modeling

amino acid requirements of poultry. Journal of Applied Poultry Research. 24 (2), 267–282.

Sant'Ana, A.S., Franco, B.D. and Schaffner, D.W., 2012. Modeling the growth rate and lag time of different strains of Salmonella enterica and Listeria monocytogenes in ready-to-eat lettuce. Food Microbiology, 30(1), 267-273. https://doi.org/10.1016/j.fm.2011.11.003

Sanz-Valero, J., Álvarez Sabucedo, L.M., Wanden-Berghe, C. and Santos Gago, J.M., 2016. QR codes: Outlook for food science and nutrition. Critical reviews in food science and nutrition, 56(6), 973-978. https://doi.org/10.1080/10408398.2012.742865

Seiffert, C., Khoshgoftaar, T. M., Van Hulse, J. and Napolitano, A. (2008, December). RUSBoost: Improving classification performance when training data is skewed. In 2008 19th international conference on pattern recognition (pp. 1-4). IEEE. DOI: 10.1109/ICPR.2008.4761297.

Seliwiorstow, T., Baré, J., Berkvens, D., Van Damme, I., Uyttendaele, M. and De Zutter, L., 2016. Identification of risk factors for Campylobacter contamination levels on broiler carcasses during the slaughter process. International Journal of Food Microbiology, 226, 26-32. http://dx.doi.org/10.1016/j.ijfoodmicro.2016.03.010

Shi, H., Zhang, M. and Adhikari, B., 2018. Advances of electronic nose and its application in fresh foods: A review. Critical Reviews in Food Science and Nutrition, 58(16), 2700-2710. https://doi.org/10.1080/10408398.2017.1327419

Silva, J., Leite, D., Fernandes, M., Mena, C., Gibbs, P.A. and Teixeira, P., 2011. Campylobacter spp. as a foodborne pathogen: a review. Frontiers in Microbiology, 2, 200. DOI: 10.3389/fmicb.2011.00200

Silva, F., Domingues, F.C. and Nerin, C., 2018. Trends in microbial control techniques for poultry products. Critical Reviews in Food Science and Nutrition, 58(4), 591-609. https://doi.org/10.1080/10408398.2016.1206845

Skarp, C.P.A., Hänninen, M.L. and Rautelin, H.I.K., 2016. Campylobacteriosis: the role of poultry meat. Clinical Microbiology and Infection, 22(2), 103-109. http://dx.doi.org/10.1016/j.cmi.2015.11.019

Smolander, M., Alakomi, H.L., Ritvanen, T., Vainionpää, J. and Ahvenainen, R., 2004. Monitoring of the quality of modified atmosphere packaged broiler chicken cuts stored in

different temperature conditions. A. Time–temperature indicators as quality-indicating tools. Food Control, 15(3), 217-229. https://doi.org/10.1016/S0956-7135(03)00061-6

Sokolova, M. and Lapalme, G. 2009. A systematic analysis of performance measures for classification tasks. Information Processing & Management, 45(4), 427-437. https://doi.org/10.1016/j.ipm.2009.03.002.

Solow, B.T., Cloak, O.M. and Fratamico, P.M., 2003. Effect of temperature on viability of Campylobacter jejuni and Campylobacter coli on raw chicken or pork skin. Journal of Food Protection, 66(11), 2023-2031. https://doi.org/10.4315/0362-028X-66.11.2023

Song, S., Yuan, L., Zhang, X., Hayat, K., Chen, H., Liu, F., Xiao, Z. and Niu, Y., 2013. Rapid measuring and modelling flavour quality changes of oxidised chicken fat by electronic nose profiles through the partial least squares regression analysis. Food Chemistry, 141(4), 4278-4288. https://doi.org/10.1016/j.foodchem.2013.07.009

Sørensen, K. M., Petersen, H. and Engelsen, S. B. 2012. An on-line near-infrared (NIR) transmission method for determining depth profiles of fatty acid composition and iodine value in porcine adipose fat tissue. Applied Spectroscopy, 66(2), 218-226. https://doi.org/10.1366/11-06396

Souza, V.G., Pires, J.R., Vieira, É.T., Coelhoso, I.M., Duarte, M.P. and Fernando, A.L., 2018. Shelf-life assessment of fresh poultry meat packaged in novel bionanocomposite of chitosan/montmorillonite incorporated with ginger essential oil. Coatings, 8(5), 177. doi:10.3390/coatings8050177

Spyrelli, E.D., Doulgeraki, A.I., Argyri, A.A., Tassou, C.C., Panagou, E.Z. and Nychas, G.J.E. 2020. Implementation of Multispectral Imaging (MSI) for Microbiological Quality Assessment of Poultry Products. Microorganisms, 8(4), 552. https://doi.org/10.3390/microorganisms8040552.

Spyrelli, E.D., Papachristou, C., Nychas, G.J.E. and Panagou, E.Z., 2021. Microbiological Quality Assessment of Chicken Thigh Fillets Using Spectroscopic Sensors and Multivariate Data Analysis. Foods, 10(11), 2723. https://doi.org/10.3390/foods10112723

Su, W.H. and Sun, D.W., 2018. Multispectral imaging for plant food quality analysis and visualization. Comprehensive Reviews in Food Science and Food Safety, 17(1), 220-239. https://doi.org/10.1111/1541-4337.12317

Sun, S. and Zhang, C. 2007. Subspace ensembles for classification. Physica A: Statistical Mechanics and its Applications, 385(1), 199-207. https://doi.org/10.1016/j.physa.2007.05.010

SuXia, X., Rui, W., JiuQing, W. and PeiYuan, G., 2018, June. Study on chicken quality classification method based on K-means-RBF multi-source data fusion. In *2018 Chinese Control And Decision Conference (CCDC)* (pp. 405-410). IEEE. **DOI:**10.1109/CCDC.2018.8407167

Teena, M., Manickavasagan, A., Mothershaw, A., El Hadi, S. and Jayas, D.S., 2013. Potential of machine vision techniques for detecting fecal and microbial contamination of food products: A review. Food and Bioprocess Technology, 6(7), 1621-1634. https://doi.org/10.1007/s11947-013-1079-7

Tian, H., Li, F., Qin, L., Yu, H. and Ma, X., 2014. Discrimination of chicken seasonings and beef seasonings using electronic nose and sensory evaluation. Journal of Food Science, 79(11), S2346-S2353. https://doi.org/10.1111/1750-3841.12675

Timsorn, K., Thoopboochagorn, T., Lertwattanasakul, N. and Wongchoosuk, C., 2016. Evaluation of bacterial population on chicken meats using a briefcase electronic nose. Biosystems Engineering, 151, 116-125. http://dx.doi.org/10.1016/j.biosystemseng.2016.09.005

Tompkin, R.B., 1994. HACCP in the meat and poultry industry. Food Control, 5(3), 153-161. https://doi.org/10.1016/0956-7135(94)90075-2

Torralbo, A., Borge, C., García-Bocanegra, I., Méric, G., Perea, A. and Carbonero, A., 2015. Higher resistance of Campylobacter coli compared to Campylobacter jejuni at chicken slaughterhouse. Comparative immunology, microbiology and infectious diseases, 39, 47-52. http://dx.doi.org/10.1016/j.cimid.2015.02.003

Tsakanikas, P., Pavlidis, D. and Nychas, G.J. 2015. High throughput multispectral image processing with applications in food science. PLoS ONE, 10, e0140122, https://doi.org/10.1371/journal.pone.0140122.

Tsakanikas, P., Pavlidis, D., Panagou, E. and Nychas, G.J., 2016. Exploiting multispectral imaging for non-invasive contamination assessment and mapping of meat samples. Talanta, 161, 606-614. https://doi.org/10.1016/j.talanta.2016.09.019

Tsakanikas, P., Fengou, L.C., Manthou, E., Lianou, A., Panagou, E.Z. and Nychas, G.J.E., 2018. A unified spectra analysis workflow for the assessment of microbial contamination of ready-to-eat green salads: Comparative study and application of non-invasive sensors. Computers and Electronics in Agriculture, 155, 212-219. https://doi.org/10.1016/j.compag.2018.10.025

Tsakanikas, P., Karnavas, A., Panagou, E.Z. and Nychas, G.J. 2020. A machine learning workflow for raw food spectroscopic classification in a future industry. Scientific Reports, 10(1), 1-11. https://doi.org/10.1038/s41598-020-68156-2

Tzamourani, A.P., Di Napoli, E., Paramithiotis, S., Economou-Petrovits, G., Panagiotidis, S. and Panagou, E.Z., 2021. Microbiological and physicochemical characterisation of green table olives of Halkidiki and Conservolea varieties processed by the Spanish method on industrial scale. International Journal of Food Science & Technology, 56(8), 3845-3857. https://doi.org/10.1111/ijfs.15000

UNEP, United Nations Environment Programme, 2021. Food Waste Index Report 2021. Nairobi. Available online at: https://www.fao.org/platform-food-loss waste/resources/detail/en/c/1378978/ (Accessed at 14/03/2022)

Vaikousi, H., Biliaderis, C.G. and Koutsoumanis, K.P., 2009. Applicability of a microbial Time Temperature Indicator (TTI) for monitoring spoilage of modified atmosphere packed minced meat. International Journal of Food Microbiology, 133(3), 272-278. https://doi.org/10.1016/j.ijfoodmicro.2009.05.030

van den Berg, F., Lyndgaard, C.B., Sørensen, K.M. and Engelsen, S.B., 2013. Process analytical technology in the food industry. Trends in Food Science & Technology, 31(1), 27-35. https://doi.org/10.1016/j.tifs.2012.04.007

Vasconcelos, H., Saraiva, C. and de Almeida, J. M. 2014. Evaluation of the spoilage of raw chicken breast fillets using Fourier transform infrared spectroscopy in tandem with chemometrics. Food and Bioprocess Technology, 7(8), 2330-2341. http://dx.doi.org/10.1016/j.lwt.2013.12.009

Verboven, S., Hubert, M., Goos, P., 2012. Robust preprocessing and model selection for

spectral data. Journal of Chemometrics. 26 (6), 282–289. https://doi.org/10.1002/cem.2446.

Verdouw, C.N., Wolfert, J., Beulens, A.J.M. and Rialland, A., 2016. Virtualization of food supply chains with the internet of things. Journal of Food Engineering, 176, 128-136. http://dx.doi.org/10.1016/j.jfoodeng.2015.11.009

Wang, D., Wang, X., Liu, T. and Liu, Y., 2012. Prediction of total viable counts on chilled pork using an electronic nose combined with support vector machine. Meat science, 90(2), 373-377. https://doi.org/10.1016/j.meatsci.2011.07.025

Weng, X., Luan, X., Kong, C., Chang, Z., Li, Y., Zhang, S., Al-Majeed, S. and Xiao, Y., 2020. A comprehensive method for assessing meat freshness using fusing electronic nose, computer vision, and artificial tactile technologies. Journal of Sensors, 2020. https://doi.org/10.1155/2020/8838535

Wickramasinghe, N.N., Ravensdale, J.T., Coorey, R., Dykes, G.A. and Scott Chandry, P. 2019. In situ characterisation of biofilms formed by psychrotrophic meat spoilage pseudomonads. Biofouling 35 (8), 840–855. https://doi.org/10.1080/08927014.2019.1669021.

Wickramasinghe, N.N., Hlaing, M.M., Ravensdale, J.T., Coorey, R., Chandry, P.S. and Dykes, G.A., 2020. Characterization of the biofilm matrix composition of psychrotrophic, meat spoilage pseudomonads. Scientific Reports. 10 (1), 1–16. https://doi.org/10.1038/s41598-020-73612-0.

Wojnowski, W., Majchrzak, T., Dymerski, T., Gębicki, J. and Namieśnik, J., 2017. Electronic noses: Powerful tools in meat quality assessment. Meat Science, 131, 119-131. https://doi.org/10.1016/j.meatsci.2017.04.240

Wojnowski, W., Kalinowska, K., Majchrzak, T., Płotka-Wasylka, J. and Namieśnik, J., 2019. Prediction of the biogenic amines index of poultry meat using an electronic nose. Sensors, 19(7), 1580. https://doi.org/10.3390/s19071580

Wold, S., Sjöström, M., Eriksson, L. 2001. PLS-regression: a basic tool of chemometrics. Chemometrics and Intelligent Laboratory Systems. 58:109-130. https://doi.org/10.1016/S0169-7439(01)00155-1

World Health Organization, 2013. The global view of campylobacteriosis: report of an expert consultation, Utrecht, Netherlands, 9-11 July 2012.

Xiaobo, Z., Jiewen, Z., Povey, M.J., Holmes, M. and Hanpin, M., 2010. Variables selection methods in near-infrared spectroscopy. Analytica Chimica Acta, 667(1-2), 14-32. https://doi.org/10.1016/j.aca.2010.03.048

Xiong, Z., Xie, A., Sun, D. W., Zeng, X. A. and Liu, D. 2015. Applications of hyperspectral imaging in chicken meat safety and quality detection and evaluation: a review. Critical Reviews in Food Science and Nutrition, 55(9), 1287-1301. https://doi.org/10.1080/10408398.2013.834875

Xu, Q.S. and Liang, Y.Z., 2001. Monte Carlo cross validation. Chemometrics and Intelligent Laboratory Systems. 56 (1), 1–11. https://doi.org/10.1002/cem.858.

Xu, G., Liao, C., Ren, X., Zhang, X., Zhang, X., Liu, S., Fu, X., Wu, H., Huang, L., Liu, C. and Wang, X., 2014. Rapid assessment of quality of deer antler slices by using an electronic nose coupled with chemometric analysis. Revista Brasileira de Farmacognosia, *24*, 716-721. https://doi.org/10.1016/j.bjp.2014.10.011

Yang, C. C., Chao, K., Chen, Y. R. and Early, H. L. 2005. Systemically diseased chicken identification using multispectral images and region of interest analysis. Computers and Electronics in Agriculture, 49(2), 255-271. https://doi.org/10.1016/j.compag.2005.05.002

Yang, C.C., Chao, K., Chen, Y.R., Kim, M.S. and Early, H.L., 2006. Simple multispectral image analysis for systemically diseased chicken identification. Transactions of the ASABE, 49(1), 245-257. doi:10.13031/2013.20223.

Yang, Y., Zhuang, H., Yoon, S.C., Wang, W., Jiang, H. and Jia, B. 2018. Rapid classification of intact chicken breast fillets by predicting principal component score of quality traits with visible/near-infrared spectroscopy. Food Chemistry, 244, 184-189. https://doi.org/10.1016/j.foodchem.2017.09.148

Ye, X., Iino, K. and Zhang, S., 2016. Monitoring of bacterial contamination on chicken meat surface using a novel narrowband spectral index derived from hyperspectral imagery data. Meat Science, 122, 25-31. https://doi.org/10.1016/j.meatsci.2016.07.015

Yun, J., Greiner, M., Höller, C., Messelhäusser, U., Rampp, A. and Klein, G., 2016. Association between the ambient temperature and the occurrence of human Salmonella and Campylobacter infections. Scientific Reports, 6(1), 1-7. DOI: 10.1038/srep28442

Zhang, Y., Mao, Y., Li, K., Dong, P., Liang, R. and Luo, X., 2011. Models of Pseudomonas growth kinetics and shelf life in chilled Longissimus dorsi muscles of beef. Asian-Australasian Journal of Animal Sciences, 24(5), 713-722. doi: 10.5713/ajas.2011.10404

Zhao, T., Ezeike, G.O., Doyle, M.P., Hung, Y.C. and Howell, R.S., 2003. Reduction of Campylobacter jejuni on poultry by low-temperature treatment. Journal of food protection, 66(4), 652-655. https://doi.org/10.4315/0362-028X-66.4.652

Appendix I

Supplementary material for Chapter 3

Table 3A: Kinetic parameters of the primary growth model of Baranyi and Roberts (1994) for TVC and *Pseudomonas* spp.

		lag (h)	μ_{max} (h^{-1})	y_o (log CFU/cm^2)	y_{max} (log CFU/cm^2)	se(fit)	R^2
	TVC	92.6	0.0382	2.7	5.5	0.433- 0.492	0.826- 0.879
0 ºC	*Pseudomonas* spp.	72.2	0.0356	2.1	5.2	0.497- 0.514	0.826- 0.877
	TVC	52.8	0.0570	3.0	6.6	0.429- 0.551	0.875- 0.937
5 ºC	*Pseudomonas* spp.	17.5	0.0610	2.0	6.1	0.304- 0.522	0.866- 0.944
	TVC	22.7	0.0903	3.1	6.8	0.279- 0.506	0.894- 0.964
10 ºC	*Pseudomonas* spp.	N/A	0.0991	2.3	6.4	0.242- 0.489	0.899- 0.979
	TVC	10.2	0.2141	2.9	6.8	0.224- 0.545	0.879- 0.982
15 ºC	*Pseudomonas* spp.	8.8	0.2410	1.9	6.7	0.282- 0.442	0.941- 0.978

N/A: not available; yo: initial microbial load in sample (log CFU/cm^2); ymax: maximum microbial load in sample (log CFU/cm^2); se(fit): standard error of fit;

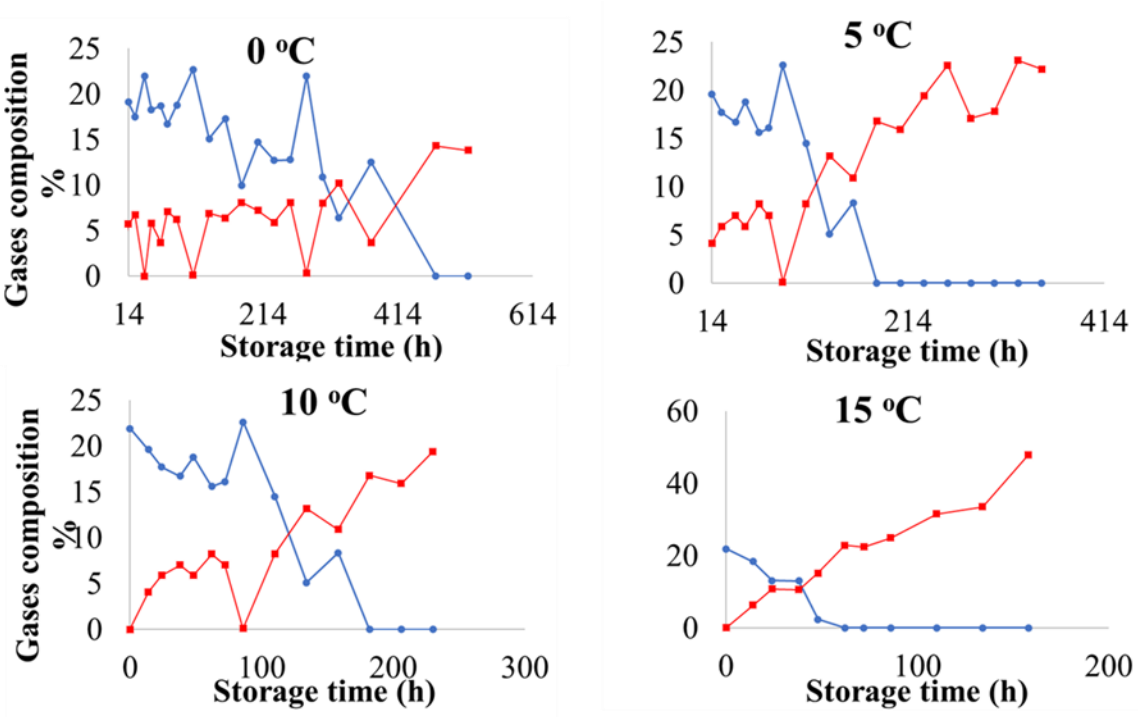

Figure 3A: Composition (%) of gases (O_2: blue line, CO_2: red line) in packaged chicken breast fillet samples during storage at 0, 5, 10, and 15 ºC.

Supplementary material for Chapter 4

Table 4A: Parameters for each machine learning algorithm developed for MSI and FT-IR sensors.

	Parameters	MSI	FT-IR
LSVM	c	1	1
	s	2.6225	16.4061
QSVM	c	1	1
	s	2.5673	17.3814
FineKNN	NumN	1	1
	Distance metric	euclidean	euclidean
	Distance Weight	equal	equal
	NSMethod	kdtree	exhaustive
	Bucketsize	50	[]
Subspace	NumL	30	30
	Lrate	0.1	1
SimpleTree	Nsplits	4	4
	MaxCat	10	9
	SplitsCr	gdi	gdi
rustBoosted	NumL	30	30
	Nsplits	20	20
	Lrate	0.1	0.1

Linear Support Vector Machines (LSVM); Quadratic Support Vector Machine, (QSVM); *k*-Nearest Neighbor classification **(**fineKNN); c: cost of constraints violation; s:scale parameter of the hypothesized (zero-mean) Laplace distribution estimated by maximum likelihood; NumN: number of Neighbors; NSMethod: Neighbors spliting method; NumL: number of learners; Lrate: learning rate; Nspilts: number of splits; MaxCat: maximum categories; SplitsCr: split criterion.

Table 4B: Functions performed for each machine learning algorithm developed for MSI and FT-IR sensors.

Algorithm/Ensemble	Function (m.file)
LDA	fitcdiscr
LSVM	fitcsvm (linear)
QSVM	fitcsvm (polynomial order:2)
FineKNN	fitcknn
Subspace	fitensemble/Subspace with Discriminant
SimpleTree	fitctree
rustBoosted	fitensemble/RUSBoost with Decision Tree learners

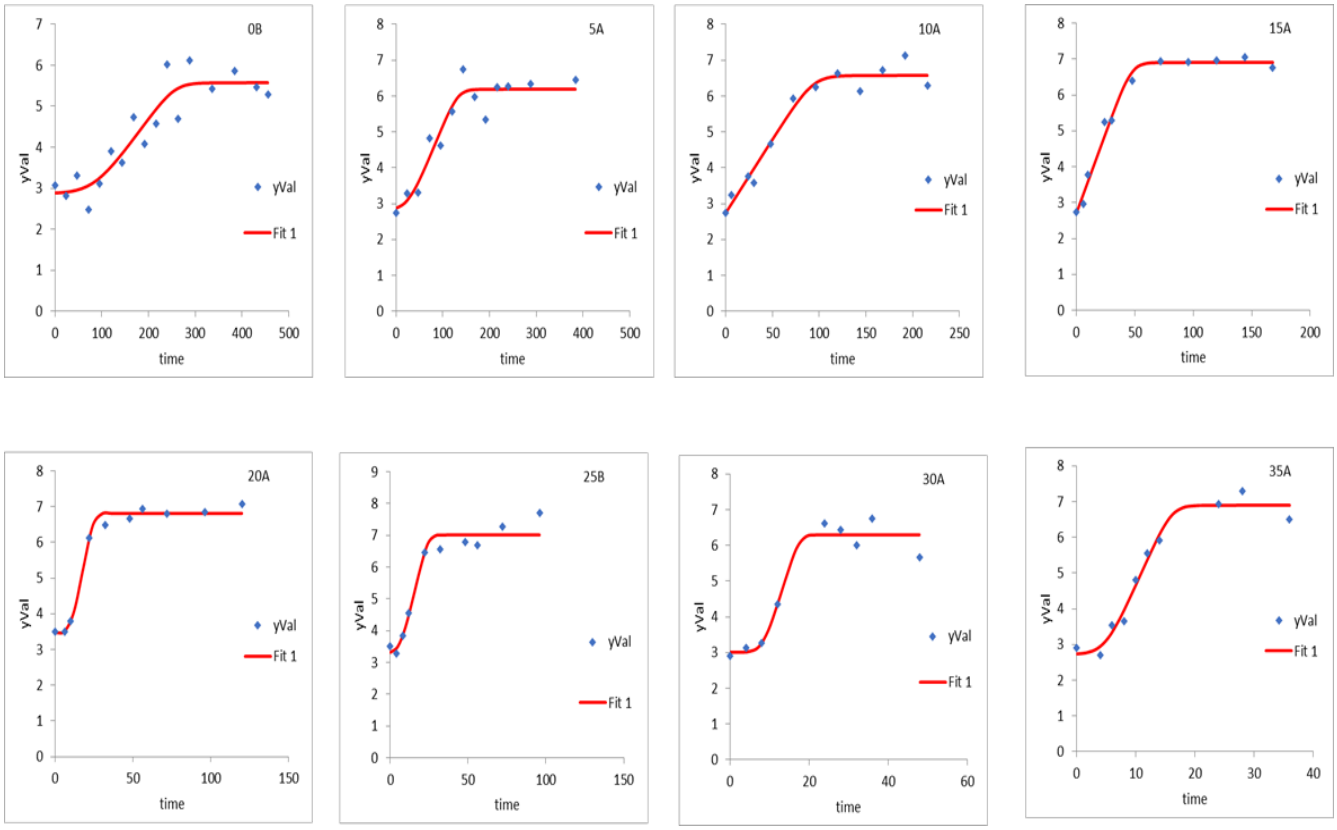

Figure 4A: Representative Baranyi and Roberts models for the prediction of TVCs at eight different storage conditions (0- 35 ºC) in chicken breast fillets via the implementation of DMFIT application.

Supplementary material for Chapter 5

Temperature (°C)	Source	SS	df	MS	F	p-value
15	Columns	0.652	3	0.21743	0.09	0.9672
	Error	100.915	40	2.52289		
	Total	11.568	43			
10	Columns	0.5359	3	0.17862	0.08	0.9691
	Error	95.0444	44	2.1601		
	Total	95.5803	47			
5	Columns	0.475	3	0.15833	0.08	0.9713
	Error	96.6625	48	2.0138		
	Total	97.1375	51			
0	Columns	0.4734	3	0.15782	0.1	0.9588
	Error	99.3133	64	1.55177		
	Total	99.7867	67			
20	Columns	0.208	3	0.6923	0.02	0.9957
	Error	129.93	40	3.24826		
	Total	130.138	43			
25	Columns	0.043	3	0.01431	0	0.9996
	Error	118.588	36	3.2941		
	Total	118.631	39			
30	Columns	0.0816	3	0.0272	0.01	0.9986
	Error	98.911	36	2.74753		
	Total	98.9926	39			
35	Columns	0.833	3	0.27767	0.1	0.957
	Error	85.1931	32	2.66228		
	Total	86.0261	35			
Dynamic 1	Columns	0.0029	2	0.00143	0	0.9993
	Error	63.5467	30	2.11822		
	Total	63.5495	32			
Dynamic 2	Columns	0.0703	2	0.03515	0.01	0.9871
	Error	81.139	30	2.70463		
	Total	81.2093	32			
Dynamic 1 and 2	Columns	3.385	5	0.67696	0.28	0.9219
	Error	144.686	60	2.41143		
	Total	148.07	65			

Table 5A: One way ANOVA for the TVCs of chicken thigh fillet samples at each isothermal storage temperature and dynamic temperature scenarios.

Table 5B: One way ANOVA for *Pseudomonas* spp. counts of chicken thigh fillet samples at each isothermal storage temperature and dynamic temperature scenarios.

Temperature (°C)	Source	SS	df	MS	F	p-value
15	Columns	0.216	3	0.07205	0.02	0.9948
	Error	118.162	40	2.95404		
	Total	118.378	43			
10	Columns	0.107	3	0.03552	0.01	0.9982
	Error	130.044	44	2.9554		
	Total	130.15	47			
5	Columns	0.736	3	0.24524	0.1	0.9569
	Error	103.108	44	2.34336		
	Total	103.844	47			
0	Columns	2.069	3	0.68962	0.4	0.7545
	Error	110.749	64	1.73045		
	Total	112.818	67			
20	Columns	0.756	3	0.25205	0.06	0.9808
	Error	169.741	40	4.24353		
	Total	170.497	43			
25	Columns	1.068	3	0.35598	0.09	0.9643
	Error	140.257	36	3.89602		
	Total	141.325	39			
30	Columns	3.4919	3	1.16398	0.44	0.7251
	Error	95.0259	36	2.63961		
	Total	98.5179	39			
35	Columns	0.8236	3	0.27453	0.14	0.9353
	Error	62.7508	32	1.96096		
	Total	63.5744	35			
Dynamic 1	Columns	0.0427	2	0.02133	0.01	0.9908
	Error	68.9284	30	2.29761		
	Total	68.971	32			
Dynamic 2	Columns	0.0775	2	0.03877	0.01	0.9873
	Error	91.2975	30	3.04325		
	Total	91.3751	32			
Dynamic 1 and 2	Columns	0.901	5	0.1802	0.07	0.9967
	Error	160.226	60	2.67043		
	Total	161.127	61			

Supplementary material for Chapter 6

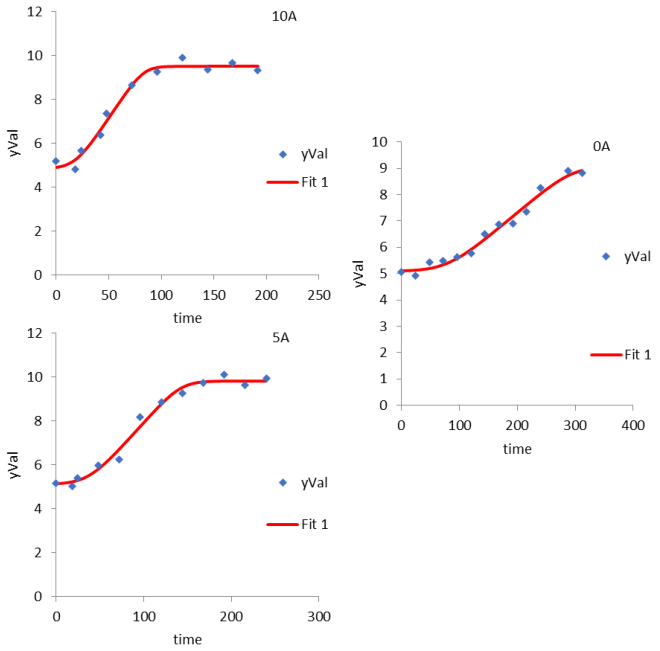

Figure 6A: Representative Baranyi and Roberts models for the prediction of TVCs at three different storage conditions (0, 5 and 10 ^{o}C) in marinated chicken souvlaki via the implementation of DMFIT application.

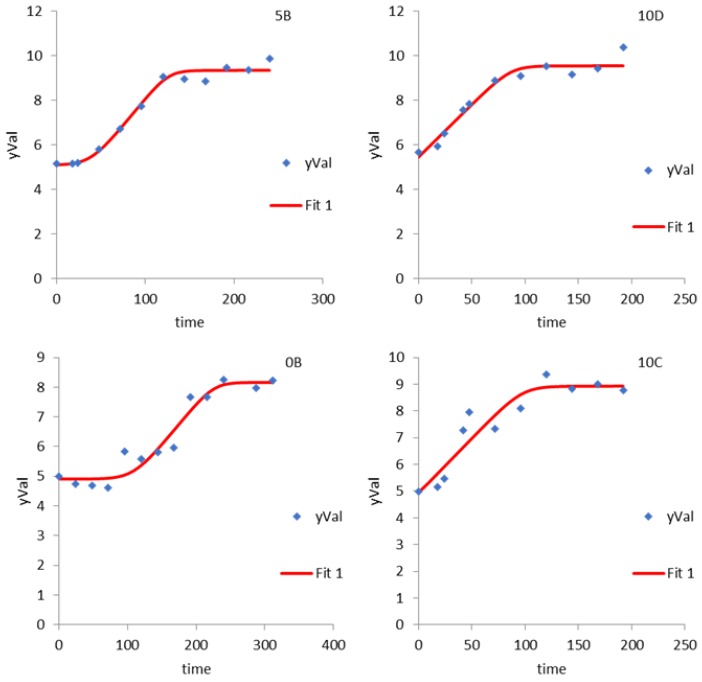

Figure 6B: Representative Baranyi and Roberts models for the prediction of *Pseudomonas* spp. at three different storage conditions (0, 5 and 10 ^{o}C) in marinated chicken souvlaki via the implementation of DMFIT application.

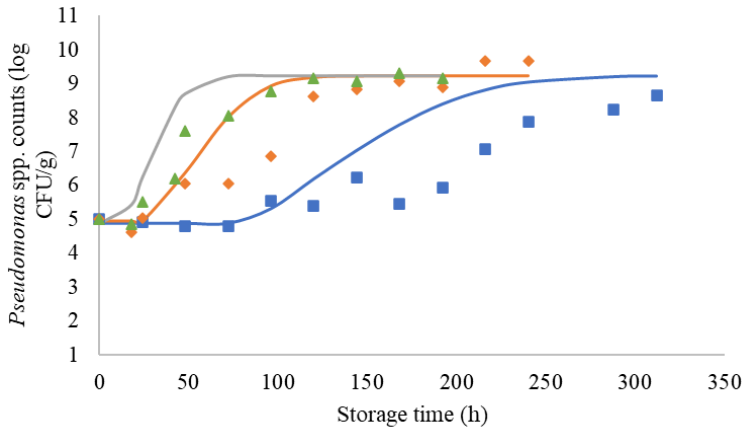

Figure 6C: *Pseudomonas* spp. predictive models (lines) and the corresponding observations (symbols) for marinated chicken souvlaki stored at 0 ºC (blue, square), 5 ºC (orange, diamond) and 10 ºC (green, triangle).

Supplementary material for Chapter 7

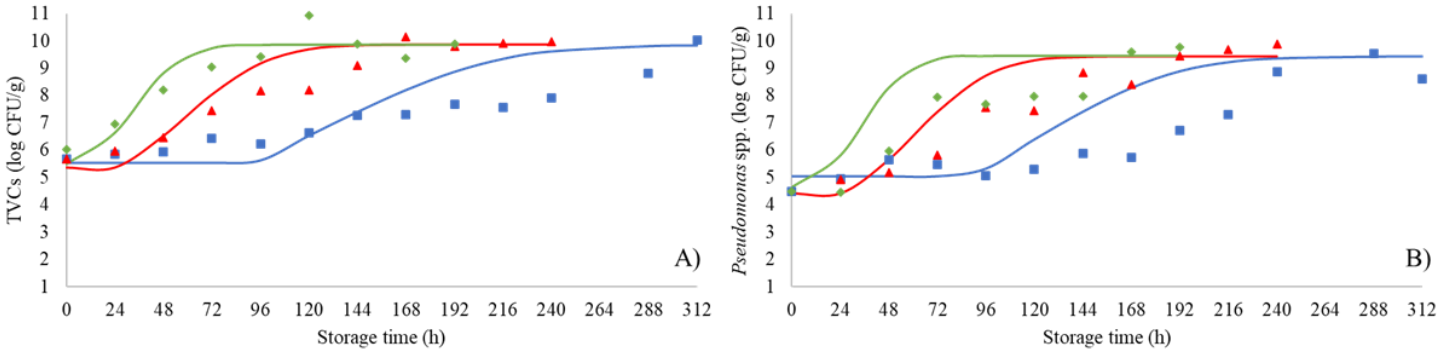

Figure 7A: TVCs (A) and *Pseudomonas* spp. (B) predictive models (lines) and the corresponding observations (symbols) for inoculated marinated chicken souvlaki stored at 0 ºC (blue, square), 5 ºC (red, diamond) and 10 ºC (green, triangle).

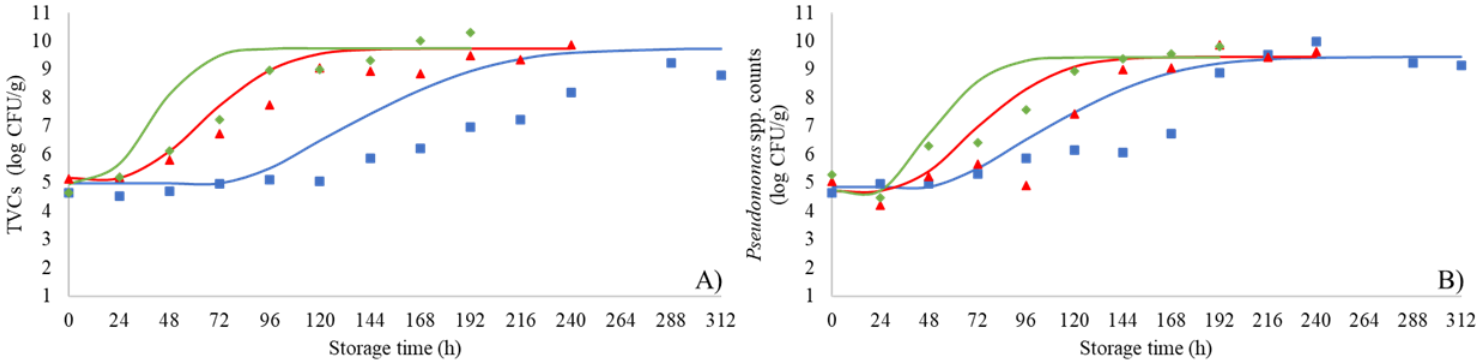

Figure 7B: TVCs (A) and *Pseudomonas* spp. (B) predictive models (lines) and the corresponding observations (symbols) for non-inoculated marinated chicken souvlaki stored at 0 ºC (blue, square), 5 ºC (red, diamond) and 10 ºC (green, triangle).

Appendix II

Published research from this PhD thesis

a) Evgenia D. Spyrelli, Agapi I. Doulgeraki, Anthoula A. Argyri, Chrysoula C. Tassou, Efstathios Z. Panagou and George- John E. Nychas Implementation of Multispectral Imaging (MSI) for Microbiological Quality Assessment of Poultry Products, microorganisms, 2020, 8, 552; doi:10.3390/microorganisms8040552
b) Spyrelli, E. D., Ozcan, O., Mohareb, F., Panagou, E. Z., & Nychas, G. J. E. (2021). Spoilage assessment of chicken breast fillets by means of fourier transform infrared spectroscopy and multispectral image analysis. Current research in food science, 4, 121-131. DOI: https://doi.org/10.1016/j.crfs.2021.02.007
c) Spyrelli, E.D., Papachristou, C.K., Nychas, G.J.E. and Panagou, E.Z., 2021. Microbiological Quality Assessment of Chicken Thigh Fillets Using Spectroscopic Sensors and Multivariate Data Analysis. Foods, 10(11), p.2723.

Conferences

- Evgenia D. Spyrelli, Efstathios Z. Panagou, George- John E. Nychas, Data fusion of three noninvasive methods for the quality assessment of chicken marinated souvlaki, (Accepted), IAFP European Symposium, 4- 6 May, Munich, Germany.
- Anastasia Lytou, Eirini Lariou, Evgenia Spyrelli, Athanasios Mallouchos, Efstathios Panagou, George-John NYCHAS, Volatilomics in tandem with machine learning for the quality assessment of chicken meat, (Accepted), IAFP European Symposium, 4- 6 May, Munich, Germany.
- E. D. Spyrelli, M. Choulioumi, E.Z. Panagou and G-J. E. Nychas, Rapid assessment of quality in marinated chicken souvlaki via data fusion of Fourier Transformed Infrared Spectroscopy (FT-IR), Multispectral Imaging (MSI) and electronic nose (e-nose), 9th Conference of MIKROBIOKOSMOS, 16- 18 December 2021, Athens, Greece
- Evgenia Spyrelli, Christina Papachristou, Valeriu Culcinschi, Anastasia Lytou, Efstathios Panagou and George-John Nychas, Multivariate Data Analysis for the Development of Classification Models Assessing Spoilage of Two Different Types of Poultry Meat (technical presentation), IAFP European Symposium 2021, Virtual Meeting, 27- 28 April 2021
- Evgenia Spyrelli, Christina Papachristou, Anastasia Lytou, Efstathios Panagou and George-John Nychas, Spoilage Assessment on Chicken Thighs Surface Via Non-Invasive Multispectral Image Analysis (MSI) (poster presentation), IAFP European Symposium 2021, Virtual Meeting, 27- 28 April 2021
- Doulgeraki A., Dourou D., Spyrelli E., Grounta A., Nychas G. J., Tassou C. 2020. NGS vs Cultural Methods to Map the Diversity of Spoilage Microbiota of Chicken Breast Fillets Under Different Storage Temperatures. (poster presentation) ASM virtual 2020.

- Lytou A., Spyrelli E., Schoina E., Researcher's night, 27 September 2019, National Technical University of Athens, Athens
- Spyrelli E.D., Kourkouli A., Skarpelos V., Lytou A., Panagou E.Z., Tassou C.C, Nychas G-J.E., Rapid assessment of chicken breast spoilage using Fourier transform infrared (FTIR) spectroscopy (poster presentation), 5th International Conference on Microbial Diversity, 25- 27 September 2019, Catania, Italy
- Evgenia Spyrelli, Agapi Doulgeraki, Anthoula Argyri, Chrysoula Tassou, Efstathios Panagou, George-John Nychas, NON-INVASIVE MULTISPECTRAL IMAGE ANALYSIS FOR THE ASSESSMENT OF SPOILAGE IN POULTRY PRODUCTS (poster presentation), 11th International Conference on Predictive Modelling in Foods, 17- 20 September 2019, Braganza, Portugal
- Evgenia Spyrelli, Agapi Doulgeraki, Anthoula Argyri, Chrysoula Tassou, Efstathios Panagou, George-John Nychas , RAPID QUALITY ASSESSMENT OF POULTRY PRODUCTS USING AT-LINE MULTISPECTRAL IMAGING (MSI) (poster presentation), 11th International Conference on Predictive Modelling in Foods, 17- 20 September 2019, Braganza, Portugal
- Ourania Raftopoulou, Evgenia Spyrelli, Efstathios Panagou, George-John Nychas, Alexandra Lianou, MODELLING OF LISTERIA MONOCYTOGENES GROWTH IN CHICKEN NUGGETS AS A FUNCTION OF TEMPERATURE (poster presentation), 11th International Conference on Predictive Modelling in Foods, 17- 20 September 2019, Braganza, Portugal
- Spyrelli E., Raftopoulou O., Tomara D., Choumi I., Panagou, E.Z., Nychas G-J.E, Rapid assessment of spoilage on the surface of stored chicken breast fillet via MSI (MULTISPECTRAL IMAGE ANALYSIS, MSI) (oral presentation), 12º Hellenic Scientific Conference in Chemical Engineering, 29-31 May 2019, Athens, Greece
- Spyrelli E. D., Doulgeraki A. I., Argyri A. A., Tassou C., Lianou A., Panagou E.Z., Nychas G-J.E., MSI analysis for the rapid estimation of quality at poultry products (oral presentation), 6ο Hellenic Conference "Meat and their products: From the farm to the plate", 1-2 February 2019, Thessaloniki, Greece